UNIVERSITÀ DEGLI STUDI DI UDINE
hic sunt futura

www.uniud.it

Corso di dottorato di ricerca in:

"Scienze e biotecnologie agrarie"

Ciclo 33°

Titolo della tesi

"Sieve-element specific responses to phytoplasma infection: new insights about the role of occlusion proteins and callose"

Dottorando
Chiara Bernardini

Supervisore
Prof.ssa Rita Musetti

Coordinatore
Prof. Francesco Nazzi

Anno 2021

To my family
my lighthouse

To remind me my classical roots
and to remind to everyone the
strict link between science and
philosophy, with the meaning of
love for the Knowledge
πάνει μάνος

SUMMARY

LIST OF THE FIGURES

LIST OF THE ACRONYMS USED IN THE THESIS

AAP Acquisition access period

ABA abscisic acid

AY Aster yellow

CALS7 callose synthase 7

CC companion cell

CES cellulose synthase

CWINV cell wall invertase

ETI effector triggered immunity

ER-PM CS endoplasmic reticulum-plasma membarane contact sites

FRU fructose

GLU glucose

GSL glucan synthase like (synonym of callose synthase

IAP Inoculation access period

IAA indole acetic acid

JA jasmonate

JA-Ile isoleucine-jasmonate

LP Latency period

MeJA Methyl jasmonate

NB-LRR nucleotide binding leucine rich repeats proteins

NET3C actin binding protein networked

PAMPs pathogen associated molecular patterns

PHY phytoplasma

PPC phloem parenchyma cell

PPU pore plasmodesmata unit

PTI PAMP triggered immunity

SAP secreted AY-WB proteins

SA salicylic acid

SE sieve element

SEO sieve element occlusion protein

SEOR sieve element occlusion-related proteins

SP sieve plate

STP sugar transporter proteins

SUC sucrose transporters

SUS sucrose synthase

SYT synaptotagmin

SWEET Sugar will eventually be exported transporter

TCBS tricalbins

VAMP vesicle associated membrane proteins

ABSTRACT

Phytoplasma are phloem-limited, wall-less, uncultivable prokaryotes. They affect several economically important crops and fruit trees. Actually, no efficient treatments are available to directly control the diseases associated to these pathogens. The study of the molecular interaction between plant and phytoplasma could provide, in a close future, knowledge about the mechanism of host colonization and plant counteract, which is important to actuate new control approaches. Plants face mechanically phytoplasma infection by sealing the sieve elements by phloem protein and/or callose accumulation at the sieve pores, and activating several pathways involved in defense process. We used different mutant lines of *Arabidopsis thaliana* and a strain of the '*Candidatus* Phytoplasma asteris' (the Chrysanthemum Yellows phytoplasma), as pathosystem, to give insight on the possible link occurring between mechanical site-specific plant responses and systemic defense signaling.

The first part of the study, dealing with the interaction between phytoplasmas and the sieve-element occlusion related (SEOR) proteins, underlined the involvement of AtSEOR2 protein with the pathway of phytohormones. Phytohormone accumulation (in particular jasmonic acid, indol-acetic acid and abscisic acid) was early activated at infection site in *Atseor1ko* mutants, an Arabidopsis line expressing the sole AtSEOR2 protein in the sieve tubes. The possible mechanism involved in the reduction of phytoplasma titre in *Atseor1ko* mutants was discussed.

The second part of the study regarded the role of phloem callose in the interaction. Also in this case, an important relation between the synthesis of callose at the sieve plate (by the phloem specific callose synthase 7) and the early activation of systemic defense responses, was shown. In particular, plant lacking the production of phloem callose, resulted able to unbalance sugar transport (at both the symplasmic and apoplasmic level) and metabolism, favoring the priming of sugar-related signaling processes. Taken together these results drive us to the conclusion that, in Arabidopsis following phytoplasma infection, site-specific mechanical responses trigger systemic signals, mediated by SEOR proteins and callose.

1. PHYTOPLASMA AND PHYTOPLASMA DISEASE: AN OVERVIEW

1.1 PHYTOPLASMA

The first hypothesis about plant diseases related to phytoplasmas (previously named Mycoplasma-like Organisms, MLOs) dates back to1926 (Kunkel, 1926). However, for a long time, symptoms as leaf yellows, plant stunting and witches' brooms had been considered virus-related, until Doi *et al.*, in 1967 (Doi *et al.*, 1967) reported the presence of pleomorphic bodies inside the sieve elements of symptomatic plants and they were described *Mycoplasma*-like organisms, MLOs (Doi *et al.*, 1967; McCoy *et al.*, 1989).. Despite our scarce knowledge, the importance of the study of phytoplasma disease is commonly recognized. Phytoplasmas, in fact, can cause important yield and quality losses on the major crops in the world (Bertaccini *et al.*, 2014).

Phytoplasmas are prokaryotic pathogens belonging to the class of Mollicutes, without cell wall and phloem-limited (McCoy *et al.*, 1989; Musetti and Pagliari, 2019; Weisburg *et al.*, 1989). Phytoplasmas are inoculated in plant hosts by vector insects (see below). Phytoplasma size varies from 200 to 800 nm *(*Lee *et al.*, 2000) and inside the infected plant, the colonization of the sieve elements seems to be related to the sugar flow, from the source to sink (Christensen *et al.*, 2004): from the site of inoculation, phytoplasmas reach the main stem, colonizing the apex and, subsequently, the lower leaves (Saracco *et al.*, 2005; Wei *et al.*, 2004). Phytoplasma genome is relatively small with only one chromosome and several other plastids (Firrao *et al.*, 2007) and with a low content of guanin and cytosine (Razin *et al.*, 1998). As mycoplasmas lack numerous metabolic pathways such as tricarboxylic cycle, sterol biosynthesis or fatty acids biosynthesis, as well phytoplasmas lack for several genes. It seems that phytoplasmas have lost much more genes than mycoplasmas during the evolutive process (Hoshi *et al.*, 2009).

To supply to these lacks, phytoplasmas require the trophic substances to the host cells: for these reasons, inside the genome, lot of genes, encoding for several transporters, and able to modify the biology of the hosts (both vector than plant) are present (Bai *et al.*, 2009; Oshima *et al.*, 2004). All these features do not

allow to phytoplasmas to live outside the host or the vector and they do not allow to the researchers the cultivation in vitro, thus they are considered as obligate parasites (Oshima *et al.*, 2004).

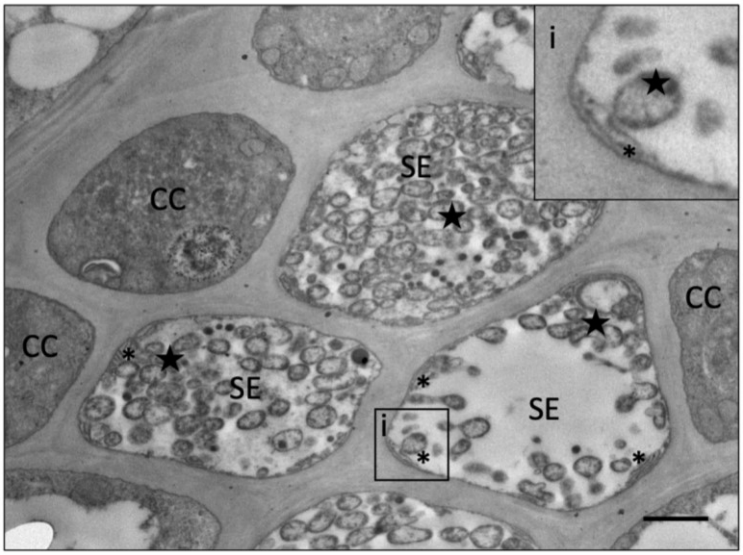

Figure 1.1 ***Phloem tissue colonized by phytoplasma.***

In the picture SE= sieve element cells, CC=companion cells, stars= phytoplasma and asterisks= sieve element reticula. In the insert (i) one phytoplasma interating with the membrane is shown.

Image adapted from van Bel and Musetti 2019.

1.2 TAXONOMY OF PHYTOPLASMA

Phytoplasmas belong to the class *Mollicutes* of the phylum *Tenericutes* (Brown, 2010) and evolved from a Gram-positive bacteria through a process of degenerative evolution (Oshima *et al.*, 2004). Phylogenetic analyses based on 16S rDNA revealed that they constitute a monophyletic clade with the most closely related microorganisms belonging to the genus *Acholeoplasma* within the class *Mollicutes* (Lim and Sears, 1992). The trivial name "phytoplasma", instead of MLOs, has been adopted only in the '90s by the Phytoplasma Working Team at the 10th Congress of International Organization of Mycoplasmology (Tully, 1993) with the aim to differentiate these plant pathogens from those infecting humans and animals. However, due to their inability to be cultured *in vitro*, except some successful experiences of axenic cultures (Contaldo *et al.*, 2012), they are currently classified under the provisional genus '*Candidatus* Phytoplasma' on the basis of 16S rDNA gene sequence analysis (The IRPCM Phytoplasma/Spiroplasma Working Team – Phytoplasma taxonomy group, 2004). Following the guidelines for naming a new '*Candidatus* Phytoplasma' species, two phytoplasma strains can be considered two different '*Candidatus* Phytoplasma' species when their 16S rRNA gene sequence similarity does not exceed 97.5%. In case of similarity higher than this conventional threshold, two strains are considered different when the following three criteria are satisfied: they have different plant host range, they are transmitted by different insect vectors and they can be distinguished by other molecular markers (The IRPCM Phytoplasma/Spiroplasma Working Team – Phytoplasma taxonomy group, 2004).

In the 90s a classification of phytoplasmas has been provided based on the 16S rRNA gene analyses. A classification in about 20 subclades (or phylogenetic groups) was proposed based on the phylogenetic study of the 16S rDNA by Seemüller *et al.* (1998). At the same time, another classification scheme in groups and subgroups has been provided based on the restriction fragment length polymorphism (RFLP) analysis with 17 endonucleases of PCR-amplified 16S rDNA (Lee *et al.*,1998; 2000). The 16Sr groups were consistent with subclades; thus, the phylogenetic interrelationships among subclades have formed a basis for phytoplasma classification. More information was subsequently provided by the in silico RFLP: with the virtual restriction the number of groups and subgroups became more than 32 and 100 respectively (Davis *et al.*, 2013; Nejat *et al.*, 2013; Quaglino *et al.*, 2009; Wei *et al.*, 2008, 2007; Wu *et al.*, 2012; Zhao *et al.*, 2013, 2009). Each of these subclades or 16S groups was proposed to be represented by at least one species of the provisional genus '*Candidatus* Phytoplasma' following the guidelines of the IRPCM (The IRPCM Phytoplasma/Spiroplasma Working Team – Phytoplasma taxonomy group, 2004).

During the following years, more insights about the phylogenetic relationships of phytoplasmas and the differentiation among very closely related phytoplasma strains, not distinguishable with the 16S rRNA gene, have been provided with the study of some genes less conserved than the 16S rRNA gene: *rpsV* (*rpl22*), *rpsC* (*rps3*), *tuf*, *secA* or *secY* or the spacer region 16S-23S, were used with the purpose to better discriminate phytoplasma strains (Hodgetts *et al.*, 2009, 2008; Lee *et al.*, 2010, 2007; Martini *et al.*, 2007).

1.3 SYMPTOMS AND RESPONSE FROM THE HOST

Symptoms causes can be ascribable to three reasons: the unbalance of the phytohormones following the infection (Dermastia, 2019), the altered mass flow and the deficiency of substances in the sink tissues (Ermacora and Osler, 2019). The symptoms appearance (Figure 1.2) varies depending on the environmental conditions on which the infected plant lives such as density between plants, phenological phase and season (Clements *et al.*, 2020). While some symptoms are peculiar of the phytoplasma-related disease, others are generalized but they concur to define the syndrome. One of the most common symptoms of phytoplasma colonization is the witches' brooms: with dwarfism it seems to be a symptom caused by the TENGU protein (see below) (Sugio, 2012). Other symptoms are the leaf yellowing and decrease of leaf size (Lepka *et al.*, 1999), the phyllody and the virescence of the flower, crinkled and rolled leaves with an abnormal development of the midribs, rosetting of the apex, proliferation of axillary buds, internode elongation and the uneven lignification (Zafari *et al.*, 2012). Sometimes with these symptoms, the generalized symptoms, as chlorosis, necrosis and decline can occur (Bertaccini *et al.*, 2014; Buoso *et al.*, 2019; Ermacora and Osler, 2019). In any case the symptomatology, and in particular when which one symptom appears in the infected plants, depends on the species of the host plant taken in consideration (Kaminska *et al.*, 2001).

Coming to the ultrastructural point of view (Figure 1.3), phytoplasmas may cause the necrosis of some area of the phloem (Braun and Sinclair, 1976), the plugging of the sieve plates and sieve element collapse

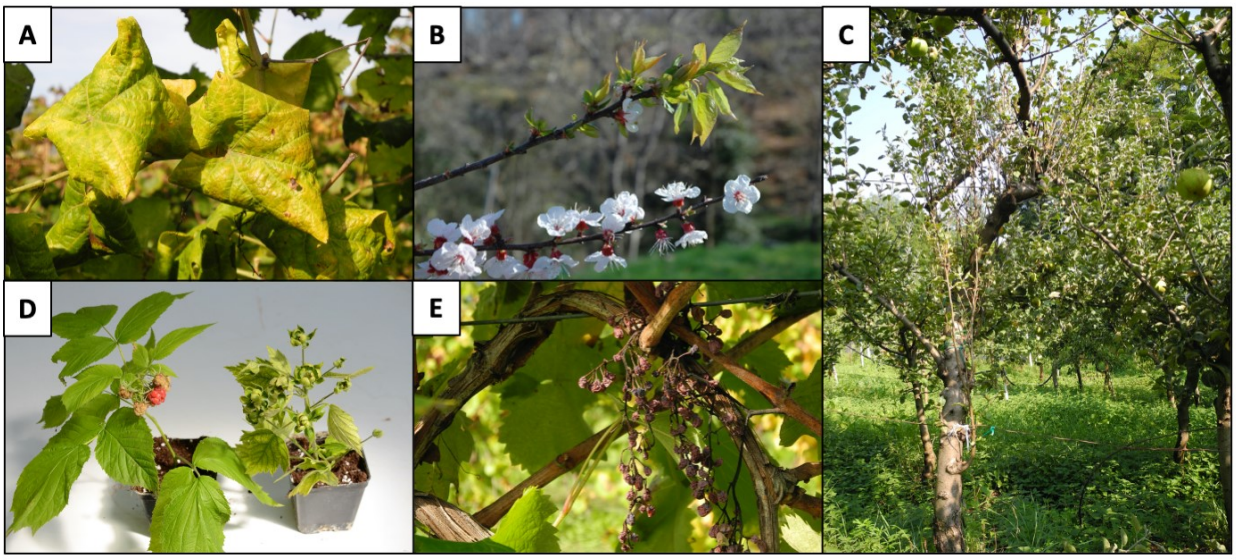

Figure 1.2 ***Symptoms caused by phytoplasmas****: chlorosis and crinckled leaves on grapevine (**A**), appearance of phenologic stage in the wrong time of the year (**B**), witches'brooms on apple tree (**C**), phyllody and general stunting in Rosaceae (**D**), dried rachis in grapevine after infection (**E**). Pictures were provided by P.A. Alberto Loschi, University of Udine.*

(Musetti *et al.*, 2004; Musetti and Favali, 2003), the phloem hyperplasia (Schneider, 1977) and a general decay of thylakoid system (Pagliari *et al.*, 2016). The plugging mechanism based presumably at the beginning of the infection on the Sieve Element Occlusion Related proteins (Anstead *et al.*, 2012; van Bel, 2019) and, subsequently on the callose deposition (van Bel, 2019, 2006), is required by the plant to try to isolate the infected region of the phloem. Contrarly to other defense mechanisms activated by the plant, the callose plugging can be reversible (Xie and Hong, 2011). Dealing with the hyperplasia, this symptom has been observed in several plants infected by phytoplasma but also by other phloem-limited pathogens: phytoplasma can cause an uncontrolled proliferation of the cells belonging to the infected tissue (De Marco *et al.*, 2016; Lv *et al.*, 2017; Pagliari *et al.*, 2017).

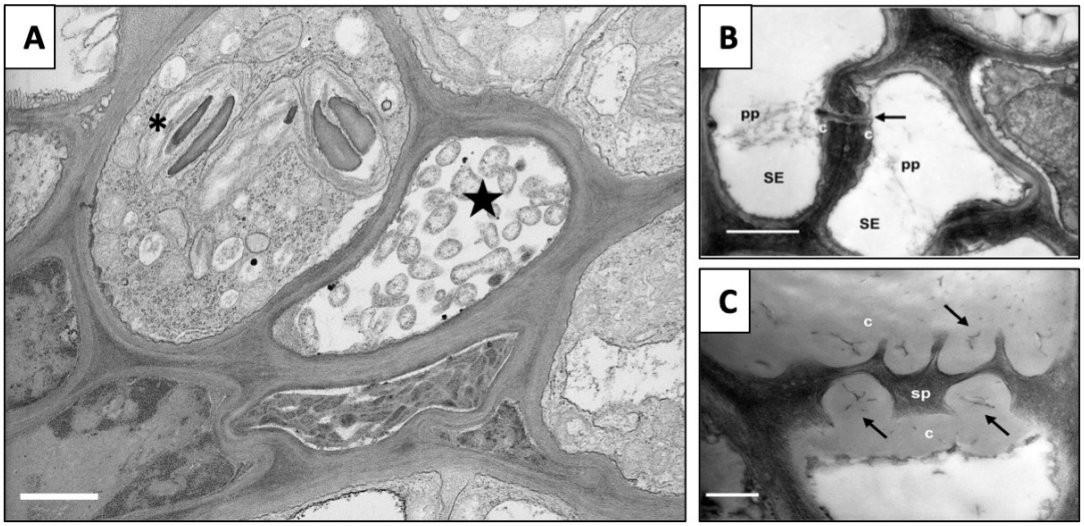

Figure 1.3 ***Cytological modifications in case of phytoplasma infection****. Chloroplast and thylakoid decay (**A**), phloem proteins and the plugging mechanism (**B**) and callose deposition (**C**). SE=sieve element, CC=companion cell, pp= phloem protein, c=callose, stars=phytoplasmas, asterisk=damaged thylakoids. Bar corresponds to 1µm. Pictures from Santi et al. 2013.*

1.4 PHYTOPLASMAS AFFECT PLANT-HOST METABOLISM

Plants face phytoplasmas and phytoplasmas handle the plants causing several modifications in several metabolic paths and producing chemical compounds with different functions. Studies on the RNA-seq and the gene expression revealed that many metabolic paths are modulated differently in case of infection (Albertazzi *et al.*, 2009; Snyman *et al.*, 2017; Zamharir *et al.*, 2011). These genes have been grouped by functions as follow: transcription factors and signaling transduction, carbohydrates metabolism and photosynthesis, cell

wall metabolism, protein and amino acid metabolism, secondary metabolism, protein synthesis (Albertazzi *et al.*, 2009; Zamharir *et al.*, 2011).

One of the most affected paths in plants following the infection is the sugar metabolism: phytoplasmas, requiring sugars and trophic substances, handle the plant metabolism to advantage themselves. Commonly it has been underlined the increase of sucrose in case of infection in the leaves and the accumulation of starch (Giorno *et al.*, 2013; Junqueira *et al.*, 2004; Lepka *et al.*, 1999; Maust *et al.*, 2003; Xue *et al.*, 2018; Zafari *et al.*, 2012) while in the roots no significative difference in the carbohydrate amount has been reported (Lepka *et al.*, 1999). About other sugars as glucose, fructose and sorbitol contrasting information are available (Giorno *et al.*, 2013; Lepka *et al.*, 1999). The altered sugar metabolism reflects the anomalous modulation of gene encoding for some key enzymes that require sucrose, and other sugars, as substrate for several other chemical reactions: is the case of sucrose phosphatase synthase, sucrose synthase or granule bound starch synthase or invertase that are upregulated in case of infection and that suggest the increase of the cleavage products in the cells (Giorno *et al.*, 2013; Hren *et al.*, 2009; Santi *et al.*, 2013b; Xue *et al.*, 2018). Nevertheless, phytoplasmas can affect not only sugar synthesis and cleavage but also their transport, causing a shift of the source-sink relation in the different plant organs (Santi *et al.*, 2013b).

RNA-seq analysis demonstrated that in phytoplasma-infected plants there is a general downregulation of the photosynthesis path (Buoso *et al.*, 2019; Hren *et al.*, 2009) and the consequent reduction of the chlorophyll production (Bertamini *et al.*, 2003, 2002; Junqueira *et al.*, 2004; Maust *et al.*, 2003).

Another aspect affected by the phytoplasmas is the phytohormone unbalance. The effect of infection on the concentration of phytohormone varies depending on the pathogen and the host plant: sometimes, the same host plant responds in different ways, depending on the inoculated phytoplasma and preferring one or other hormone cascade (Ahmad *et al.*, 2014). Phytoplasma can affect the path of jasmonate or salicylate, the cytokinins, the abscisic acid and the auxins (see chapter 2). It is commonly thought that the auxin unbalance is the mechanism which the symptoms based on: being the auxonic disorders, as the abnormal cell division and stem elongation, typical features of the development, they would cause the typical phytoplasma symptoms, as witches' brooms, stunting and reduction of stem elongation (Dermastia, 2019).

Phytoplasma infection causes the increase of Ca^{2+} level in the sieve element (Musetti *et al.*, 2013a; Musetti and Favali, 2003) that is probably the primary signal for the plugging mechanisms, (see chapter 3 and 4). The increase of Ca^{2+} concentration has been demonstrated in case of injury in *Vicia faba*, in which a distal stressful action comports a variation of calcium signature (Furch *et al.*, 2007) and the consequent restoration of the initial situation. Calcium is related with the maintenance of turgor, the management of several processes, but in case of infection, could be the signal on which all the mechanisms of defense, not only the well-known plugging, are based on (van Bel, 2019). One of these defenses could be the ROS production: it has been demonstrated, in fact, that calcium and ROS can be mutually influenced (Gilroy *et al.*, 2016, 2014). The fact

that phytoplasma and ROS production are related is clear since several years: it has been demonstrated the role of the H_2O_2 in case of recovery from phytoplasma (Musetti *et al.*, 2007, 2004) and the change of the ROS signature in case of infection (Kudla *et al.*, 2010). Moreover, in case of infection, some enzymes increase their activity, as the peroxidase, superoxide dismutase and the polyphenol oxidase (Zafari *et al.*, 2012), confirming the ROS production to face phytoplasma.

Others secondary modifications accompanied the ones reported above: generally infected plants have a decrease of soluble proteins (Zafari *et al.*, 2012), but an increase of proteins involved with the defense processes (Junqueira *et al.*, 2004) reflected by the higher expression level of the gene encoding for the PR proteins (Ahmad *et al.*, 2014). It has been demonstrated that the infected plants accumulate polyphenols as response to the infection (Junqueira *et al.*, 2004; Musetti *et al.*, 2000) or that they produce more alkaloids if compared the infected to the control condition (Favali *et al.*, 2004).

1.5 RECOVERY BY PHYTOPLASMA INFECTION

On fruit trees, many reports indicated cases of recovery on host plants (Constable, 2010; Musetti *et al.*, 2004; Pacifico *et al.*, 2019; Santi *et al.*, 2013a). Recovery has been defined as the remission of the symptoms on the canopy, which could be not even associated to the total disappearance of the pathogen (Schmid, 1965): the pathogen, in fact, remains detectable in the roots in apple trees (Musetti *et al.*, 2004) and grapevine (Landi *et al.*, 2019) and in leaves in apricot (Musetti *et al.*, 2005). Recovered plants show the accumulation of H2O2 in the sieve elements (Musetti *et al.*, 2004) and, moreover, a different regulation of some genes involved in the callose synthesis and the phloem protein codification (Musetti *et al.*, 2010). Dealing with the gene expression, pathogenesis related protein genes are not induced in case of phytoplasma infection in Malus, but the plants showed the increase of the genes involved in the jasmonate path (Musetti *et al.*, 2013b). It has been also demonstrated that the treatment with auxins induces this phenomenon in a species-specific way (depends both on the phytoplasma and the chemical kind of auxin used) (Ćurković Perica, 2008) revealing that probably all the phytohormone path intervenes in case of recovery.

1.6 TRANSMISSION AND INOCULATION

Phytoplasma can be transmitted by grafting or vector insects. It is well known since a long time that grafting is one source of inoculum of phytoplasmas for almost all the plants susceptible to phytoplasma (Buoso and Loschi, 2019). The grafting transmission resulted to be high efficient as several studies on fruit trees have

demonstrated (Carraro *et al.*, 2003; Kamihska and Korbin, 1999), but it must be considered that graft procedure can transmit several other pathogens (Roistacher, 1991). In experimental conditions, different kind of grafting can be carried out, depending on the host plant and the experimental settings that we choose: examples of grafts are the lateral graft (that has an high percentage of transmission), the apical graft, the leaf graft and the side graft (Buoso and Loschi, 2019).

For both field and experimental condition, another possible transmission is the vector-mediated transmission. All the vector insects of phytoplasmas are phloem-sucking and, the most successful, belong to the order of the *Hemiptera* and four superfamily: *Membracidea, Fulgoromorpha* and *Sternorrhynca* (Table 1) (Weintraub and Beanland, 2006).

Table 1.1 Superfamily and family of the major vectors of phytoplasma

Superfamily	Families or genera
Membracidea	*Cicadellidae*
Fulgoromorpha	*Cixiidae, Delphacidea, Derbidae and Flatidae*
Sternorrhynca	*2 Psyllidae genera*

The vector insects have some important features: they are hemimetabolous with nymphs and adults that live on the same host plant, they feed on a specific plant tissue, they have a strict relation with phytoplasma. This last one aspect is probably related with the similarity of phytoplasma with some obligate prokaryotes of the insect body (Weintraub and Beanland, 2006). The cycle of infection starts with the acquisition of the phytoplasma by the insect. This step, named Acquisition Access Period (AAP), varies from few minutes to hours or day and depends on the species involved in but also the primary titre of phytoplasma in the source plant. After the acquisition of phytoplasma, the pathogen inside the insect body replicates itself, circulates in the hemolymph and, at the end, it accumulates in high level in the posterior acrinar cells of the salivary gland. During this time, the vector is not infective: this period called latency period (LP) varies depending on species of insects and phytoplasma (Bosco *et al.*, 1997) but also on the growth stage of the insect (Palermo *et al.*, 2001). From here, trough the watery saliva, can be inoculated in an healthy plant with the feeding process: this step is called inoculation access period (IAP) (Weintraub and Beanland, 2006).

The phytoplasma-vector recognition is well-tuned and based on the presence of some attachment proteins (Lefol *et al.*, 1993; Suzuki *et al.*, 2006). It has been demonstrated that phytoplasma is able to modulate its gene expression pattern depending on the environment in order to adapt itself to the life inside host plant or insect vector (Oshima *et al.*, 2011). Several studies have demonstrated that a strict relation occurs between

phytoplasma and its vector: the pathogen is able, in fact, to vary the fitness of the vector (Beanland *et al.*, 2000), or the insect fecundity and the longevity (D'Amelio *et al.*, 2008) also depending on the number of different phytoplasma acquired by the insect at the same time (Rashidi *et al.*, 2014). Flavescence doreè phytoplasma showed to decrease drastically the fitness of *Scaphoideus titanus* and *Macrosteles quadripunctulatus* with a reduction of both longevity and fecundity (Bressan *et al.*, 2005a, 2005b). The same studies showed also that the decreased of fitness phytoplasma infection-related depends not only on the phytoplasma and species but also on the sex of the insect taken in consideration.

1.7 THE PERFECT HABITAT: THE PHLOEM

Phloem, and in particular the sieve elements, having several peculiar features, is the perfect habitat for phytoplasmas. Phloem is a tissue composed by sieve elements, companion cells, parenchyma cells and fibers (Esau, 1939; Parthasarathy, 1975). Sieve elements are lines of enucleated cells with a degenerate cytoplasm (Oparka and Turgeon, 1999). The process of degeneration of sieve elements is almost similar to the programmed cell death: a process of autolysis confers to the sieve elements the characteristic absence of organelles as the vacuole, the nucleus, the ribosomes and the Golgi bodies (Oparka and Turgeon, 1999; Van Bel, 2003). This process is acropetal: from the bases to the apical meristems. The remained cytoplasm is less dense comparing to the companion cells. Companion cells are the same of the sieve element cells if we consider the ontology: they both derive from an impartial division of a phloem mother cell. The difference is the absence of the autolysis in the companion cells (Oparka and Turgeon, 1999; Van Bel, 2003). Companion cells and sieve elements are connected by particular plasmodesmata that have a big size exclusion limit and they allow a quick exchange of solutes between the two kinds of cells: these plasmodesmata have an unicum pore at the companion cell side and a multiple pore at the sieve element side (Faulkner, 2018). Sieve elements are connected through sieve plates (SP): a zone reach of pores (sieve pores) bigger than the plasmodesmata. The formation of sieve plates is in phase of cellular division: the sieve pores are fulfilled of callose, subsequently hydrolized (Zavaliev *et al.*, 2011).

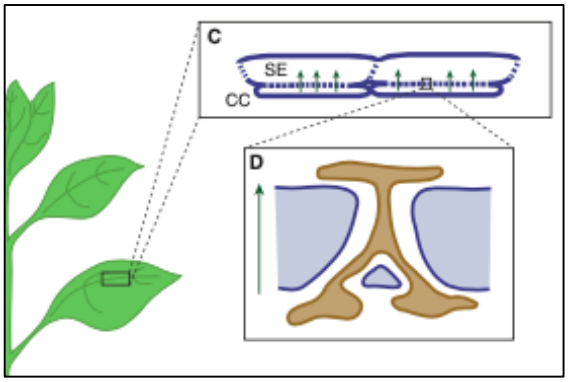

Figure 1.4 ***Plasmodesmata pore units in sieve element (PPU).*** *This particular kind of plasmodesmata has a multiple pore in the side of the companion cell. Image from Faulkner 2018.*

The transport of compounds inside the phloem complex is called "loading", because it is an energy-consuming process (Oparka and Turgeon, 1999). There are two kind of loading, the apoplasmic based on the membrane proteins and carriers, or the symplasmic through the plasmodesmata: depending on the preferred mechanism, a plants can be apoplasmic-loading prevalent or symplasmic loading prevalent (Rennie and Turgeon, 2009). The driving force inside the sieve tubes depends on a combination of pressure and turgor: in 1930, Munch described this phenomenon, providing the first equation to describe the mass flow (Munch, 1930). However transmission electron microscopy and further investigations on the phloem provided to the researchers different dark sides for this theory: the possible sealing of the phloem was only one aspect not kept in consideration by Munch (van Bel and Hafke, 2005). Therefore, it has been proposed a new model of the phloem, which was divided in regions: the collection phloem, where there are the source regions, the transport phloem, involved with the long-distance transport and the maintenance of the normal growth, and the release phloem, located in the sink tissues (van Bel and Hafke, 2005). Each one of these regions, having different features, concurs to demonstrate the inadequacy of the previous formula, even if, it was commonly recognized the role of the pressure and the turgor in the whole mechanism. The sieve plates play an important role on the regulation of the mass flow as demonstrated by Thompson and Holbrook' formula, based on the fluid dynamics' principles (Thompson and Holbrook, 2003): the diameter and the density of the pores can significantly affect the speed of the transport; thus, Mullendore *et al.*, (2010) performed a description of the sieve pores in order to obtain the physical parameters that can be used in the formula (Mullendore *et al.*, 2010).

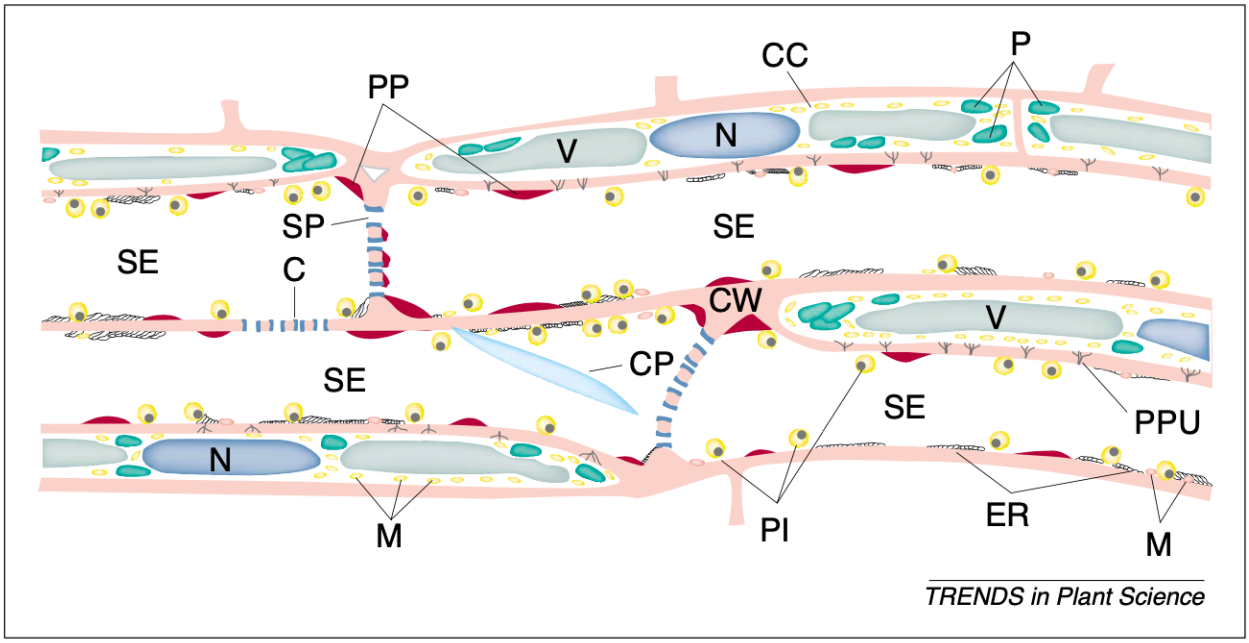

Figure 1.5 ***Structure of the sieve element in Vicia faba****. CC= companion cell, SE = sieve element, M=mitochondria, PI= plastids, ER=reticulum, SP = sieve plates, V= vacuole, CW= cell wall, N= nuclei, PPU=pore plasmodesmata units, C= callose. Image from van Bel et al., 2002*

Only in the second decade of the current century researchers have defined new formulae to describe the phloem transport, keeping in mind all the several points attacked in the Munch theory (Minchin and Lacointe, 2017; Pickard, 2012) and defining new strategies to have a direct measure of the mass flow (Vincent *et al.*, 2019).

The transport along the sieve tubes is a fine-tuned movement of various compounds necessary for the life. It has been reported that companion cells put into the sieve elements a broad range of compounds such as sucrose, several amino acids and ions as Ca^{2+}, Na^{+}, $Mg2^{+}$, K^{+}, NH_4^{+}, PO_4^{3-}, Cl^{-}, NO_3^{2-}, SO_4^{2-}, proteins and mRNA in solution in a watery matrix (Girousse *et al.*, 1991; Hayashi and Chino, 1986; Hijaz *et al.*, 2016; Ohshima *et al.*, 1990; van Dongen *et al.*, 2003; van Helden *et al.*, 1994; Weibull *et al.*, 1990). The circulating solution is poor in oxygen (van Dongen *et al.*, 2003) and the pH is slightly alkaline (7.0-8.0) (Hafke *et al.*, 2005), but very similar to the not-degenerated cells, and it can vary of some decimal units in case of sampling in different part of the plant (apical or basal) (Vreugdenhil and Koot-Gronsveld, 1989). Some similarities were shown comparing phloem sap to the homopterous insect haemolymph that is important considering their role in the maintenance cycle of the phytoplasmas (van Bel, 2019).

In this context, RNAs can have several function activating signaling cascades involved with the maintenance, the physiology or with the defense (Ham and Lucas, 2017) as well as sugars can be involved, besides their trophic role, with the signaling in case of stresses (Wind *et al.*, 2010).

Why is this environment suitable for phytoplasmas? Phytoplasmas are pleomorphic bacteria and they are able to pass through the sieve pores thanks to this characteristic (Pagliari *et al.*, 2016). Moreover their reduced genome (see above) confer them the need to depend to an habitat rich in trophic substances, as phloem sap is (van Bel, 2019). Phytoplasma, from an evolutionary point of view, have responded to the low amount of oxygen in the habitat with the use of the glycolysis as primary source of energy (Ohshima *et al.*, 1990). Taken together these considerations, lead to the conclusion that sieve element is the perfect habitat for pleomorphic pathogen, with a reduced genome and with high capability of adaptation to the environment.

1.8 THE PLANT IMMUNE SYSTEM

Plants have two way to recognize pathogens: the pathogen associated molecular patterns (PAMPs) and the effector triggered immunity (ETI) (Dodds and Rathjen, 2010).

PAMPs are particular molecules associated to a class of pathogens, such as the chitin or the flagellin. These are recognized by pattern recognition receptors (PRRs), transmembrane proteins of the plasma membrane of the host. the recognition of the PAMPs by the PRR leads to the PAMPs triggered immunity (PTI). The second kind of immunity is the effector triggered immunity: based on an intracellular recognition

of the proteins secreted by the pathogen (Dodds and Rathjen, 2010; Jones and Dangl, 2006). The effector, secreted with different secretion systems (Chang *et al.*, 2014), reaches a target in the host cell. Effectors are defined by Sugio *et al.*, as "small molecules secreted from the pathogen to facilitate the multiplication and the spread" (Sugio, 2012). The target is a nucleotide binding leucine rich repat protein, commonly called as NB-LRR, that are able to recognize the pathogen in a direct way, or with an indirect recognition, in which a third protein is a bridge between effector and NB-LRR (i.e. the RIN4 protein, see chapter 3). The theory on which this process is based on is the "guard theory": the NB-LRR is a guardee for the effector, for which the complex RIN4-RPM1/RPS2 seems to be the best example (Ray *et al.*, 2019). It has been proposed a zig zag model between PTI and ETI (Jones and Dangl, 2006). This model is divided in phases. In the first phase the PAMPs are recognized by a PRR activating the PTI. The pathogen starts to secrete effectors: in the phase two these effectors affect the response of the PTI reducing its strength. In the subsequent phase, the phase three, the effectors are recognized by a specific NB-LRR protein that activates the ETI response: ETI response, nevertheless similar, is stronger than the PTI and drives to a hypersensitive response (Jones and Dangl, 2006) reason for which the ETI response is not suitable for the necrotrophic pathogens (Glazebrook, 2005).

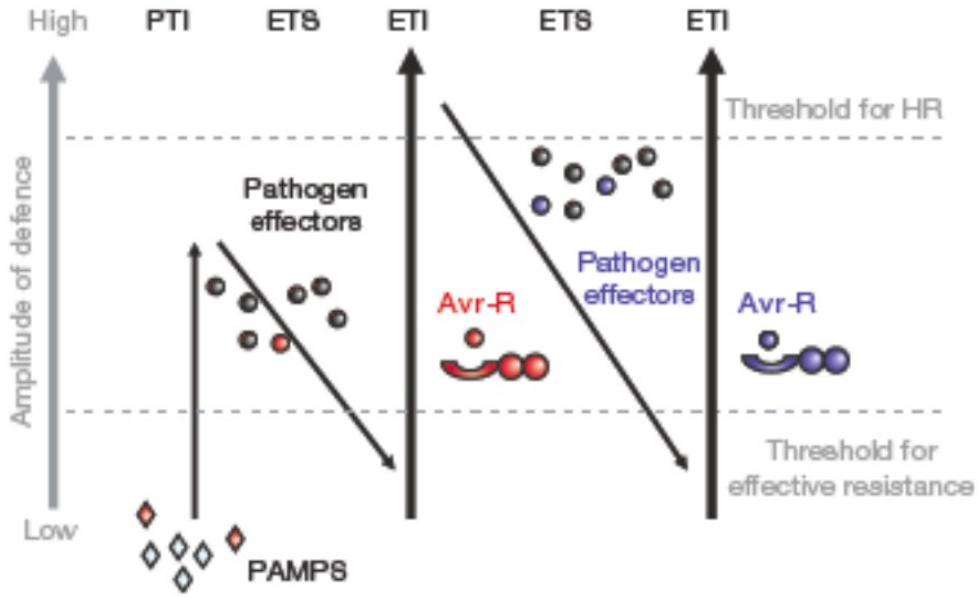

Figure 1.6 ***The zig-zag model.*** *The pathogen-associated molecular patterns (PAMPs) are recognized by the plant surface receptors (pattern recognition receptor) activating the PTI mechanism of defense. To overcome this mechanism, pathogens secrete effectors causing the ETS (effector triggered susceptibility). Effectors are recognized by R proteins and activating the ETI (effector triggered immunity). Image from Jones and Dangl, 2006.*

1.9 PHYTOPLASMA EFFECTORS

Like other microorganism, phytoplasma secreted effectors. As well as gene modulation is dependent on the environment in which phytoplasmas are (i.e. host plant or insect vector) (Oshima *et al.*, 2011), also the expression of the effectors is location-dependent (MacLean *et al.*, 2011). Effectors have been well studied in the bacterial, in which several different type of secretion systems are present (Chang *et al.*, 2014). However, it has been demonstrated that phytoplasmas have the SecA system (Kakizawa *et al.*, 2004; Oshima *et al.*, 2004), a common secretion system shared with all the domains of life (Chang *et al.*, 2014) and the YidC system for the integration of membrane proteins, a secretion system independent from the Sec (Serek *et al.*, 2004). SecA secretion system has been largely studied and described as an heterotrimeric channel complex formed by SecA, SecYEG and SecB subunits (Chang *et al.*, 2014). Instead, the YidC seems to be related with the insertion of membrane proteins rather than the exportation of proteins (Serek *et al.*, 2004).

Effectors have several functions as the facilitation of the effective penetration of the pathogen or its spread (Doehlemann *et al.*, 2009), the mimesis of some plant hormones and consequent effects on the path involved with the phytohormone unbalance (Sugio *et al.*, 2011), the inhibition of plant response (Pecher *et al.*, 2019), the circumvention of the PAMPs response (Hörger and van der Hoorn, 2013), the inhibition of some proteolytic activity or passive protection (for a review see (Toruño *et al.*, 2019).

Effectors interacts with a huge number of proteins belonging to several family and with different functions: Marrero et al demonstrated in a screening of 979 proteins that phytoplasma effectors interact with almost 28% of plant proteins (Marrero *et al.*, 2020).

1.10 THE USE OF MODEL SYSTEMS

Actually, the use of model systems is a key aspect in the research to describe in dept what could happen in the natural environment. With the model systems researchers are able to control all the conditions involved in the whole process. Here, we propose one model plant and one model phytoplasma fundamental for the study of plant-pathogen interaction.

Arabidopsis as model plant

At a certain point of scientific research, the need of a common use of a model plant was required. Among the putative plants taken in consideration, several plants with an agronomic interest were included (Koornneef and Meinke, 2010). Only at the end of the '70s and at the beginning of '80s, Arabidopsis affirmed itself as model plant (Somerville and Koornneef, 2002). *Arabidopsis thaliana* is a plant belonging to the family of *Brassicaceae* with a worldwide distribution, but without agronomical interest (Meinke, 1998). *A. thaliana* has several ecotypes, but two of them are commonly recognize as standards: Columbia and Landsberg (Meinke, 1998). Initially the choice of Arabidopsis was nearly imposed by laboratory exigences: it has, in fact, a short life cycle and is culturable in several conditions due to its small dimension (Koornneef and Meinke, 2010). With the beginning of the cloning epoque a new interest affected Arabidopsis: the small genome (2120 megabases) divided in five chromosomes was an interesting feature to make the cloning procedures easier (Meinke, 1998; Somerville and Koornneef, 2002). Moreover other features concurred to make Arabidopsis the perfect model plant: the self-pollinating flower, the number of seeds produces in one lifecycle and, at the end, the suitability to the transformation (Somerville and Koornneef, 2002). During the years following the '80s, the net of researchers working on Arabidopsis drastically increased and the genome has been completely sequenced with genetic linkage maps that indicate the position of the 20.000 genes (Rhee, 2003). Actually, mutants lines realized for Arabidopsis are more than 500.000 (Berardini *et al.*, 2015).

In this scenario, the role of Arabidopsis also in the plant-pathogen interaction is clear. Several studies has been carried out also in the phytoplasma-plant panorama, showing *A. thaliana* as a perfect model plant also for the phytoplasma-plant interaction (Cettul and Firrao, 2011; MacLean *et al.*, 2011; Pagliari *et al.*, 2016; Rossi *et al.*, 2018).

Aster yellow phytoplasmas as model in the plant-pathogen interaction

Chrysanthemum Yellows (CY) phytoplasma was reported in 1990, in Italy with *Catharantus roseus* and *Chrysanthemum carinatum* as host plants (Bertaccini *et al.*, 1990) and the strain is maintained in the host plants using *Macrosteles quadripunctulatus* as insect vector (Saracco *et al.*, 2005). CY-phytoplasma belongs

to the class of AY-phytoplasmas in particular to the 16SrI-B group (Saracco *et al.*, 2005). Symptoms caused by CY-phytoplasma have been identified by Marcone *et al.*, (1997) as stunting and yellowing, short internodes, with small leaves upward rolled. Several studies used CY-phytoplasma as model in a pathosystem that includes CY- phytoplasma/Arabidopsis for the study of the phytoplasma-plant interaction (Cettul and Firrao, 2011; Pacifico *et al.*, 2015; Pagliari *et al.*, 2018, 2017, 2016). Based on the 16S sequencing the AY group has been entirely classified as '*Candidatus* Phytoplasma asteris" (Lee *et al.*, 2004).

In Aster yellow (AY)-phytoplasma group more than 100 phytoplasmas are comprised, with a worldwide diffusion (McCoy *et al.*, 1989). AY-phytoplasma belongs to the 16SrI group and, during the years several subgroups have been identified: phytoplasma comprised in AY share more than 97.5% of similarity, threshold value in the common guidelines previously described (The IRPCM Phytoplasma/Spiroplasma Working Team – Phytoplasma taxonomy group, 2004), but they occupy different ecological niches (Lee *et al.*, 2004). Marcone and coauthors identified almost six subgroups based on the classification on the tuf gene (Marcone *et al.*, 2000) and to this number consequent studies added other four groups, based on the RFLP analysis (Lee *et al.*, 2004). Among the strains belonging to AY, two of them have been sequenced: AY-WB and OY (Bai *et al.*, 2009; Oshima *et al.*, 2004).

In AY phytoplasmas, 56 secreted by AY proteins have been identified, known with the acronym of SAP (Bai *et al.*, 2009). Trough the study of SAP11 the target in the nuclei has been underlined (Bai *et al.*, 2009). Among these effectors, the most studied molecules are SAP36 expressed when the phytoplasma is inside the vector insect, SAP11, TENGU and SAP54, all involved during infection of the plant (Sugio *et al.*, 2011). These last three effectors are the most studied: to identify which one effector causes symptoms on the plants, each effector has been individually expressed in Arabidopsis (MacLean *et al.*, 2011). SAP11 has been demonstrated to cause crinkled leaves and reduced stem production. A study underlined its relation with TCP factors in both AY-WB than in Maize bushy stunt phytoplasma (Pecher *et al.*, 2019; Sugio *et al.*, 2011), however demonstrated for other effectors (Marrero *et al.*, 2020). TENGU effector, another AY effector, is the responsible of the dwarfism and the witches' brooms, moreover it seems to affect the auxin metabolism having some effect or at the signaling level or on the biosynthesis pathway (Hoshi *et al.*, 2009).

SAP54 seems to interact with the floral development through the modulation of the MADS domain transcription factor family gene (MTF) (MacLean *et al.*, 2014) and it finds its homolog also in different phytoplasma strains (Fernández *et al.*, 2019; Singh and Lakhanpaul, 2020).

1.11 SETTING THE EXPERIMENTS

Checking the phytoplasma strain

In all the experiments described in this thesis, Chrysanthemum Yellows (CY)-phytoplasma was used. CY-phytoplasmas is a strain of the '*Candidatus* Phytoplasma asteris' (Lee *et al.*, 2004). CY-phytoplasma was maintained on *Chrysantemum carinatum* and *Catharanthus roseus* plants in a greenhouse at the University of Udine. Plants were maintained at temperature of 20°C.

Table 1.2 ***PCR reaction mix*** *for the primer pair R16F2/R16R2 (Lee et al., 2000)*

Component	Quantity
H2O	
DNTPs	200uM
Primer forward	0.4uM
Primer reverse	0.4uM
MgCl	1.5
Taq polymerase	0.625u
Template	40ng
Buffer	5x

To check the phytoplasma strain maintenance over the time, DNA was extracted from leaves of symptomatic *C. carinatum* and *C. roseus* using CTAB following the Doyle and Doyle protocol (Doyle and Doyle, 1990), modified by Martini *et al.* (Martini *et al.*, 2009). The quality of the extracted DNA eluted in 50um of TE buffer, was checked with the NanoDrop 1000 Spectrophotometer (Thermo Fisher Scientific, Wilmington, DE, USA). PCR was improved with the primer pair R16F2n/R16R2n with the PCR mix reported in **Errore. L'origine riferimento n on è stata trovata.**. And the PCR protocol reported in Table 1.4, according to (Pagliari *et al.*, 2016). PCR amplicons have been observed in a 1% agarose in TAE gel through electrophoresis stained with GelRedTM (10000x, Biotium, USA) and visualized with UV light.

Table 1.3 ***PCR reaction protocol***

Step	Features	
Initial denaturation	94°C for 2 min	
Denaturation	94°C for 1 min	40 cycles
Anealling	55°C for 1 min	
Extension	72°C for 2 min	
Final extension	72°C for 2 min	

The amplicons were digested with the TruI, AluI and HhaI enzymes in order to obtain the restriction fragment pattern for every strain collected and in order to discriminate different phytoplasma groups. The restriction conditions for all the enzymes are reported in the Table 1.5. The pattern of restriction has been visualized with a 2.5% agarose gel in TBE, stained with GelREdTM (Biotium, USA).

Table 1.4 ***Features of the restriction***

Enzyme	Restriction mix	Restriction protocol
TruI	Buffer 2ul, H2O 11.5 ul, template 6ul, enzyme 0.5ul	65°C overnight
AluI		37°C overnight
HhaI		

Infection cycle and healthy colonies maintenance

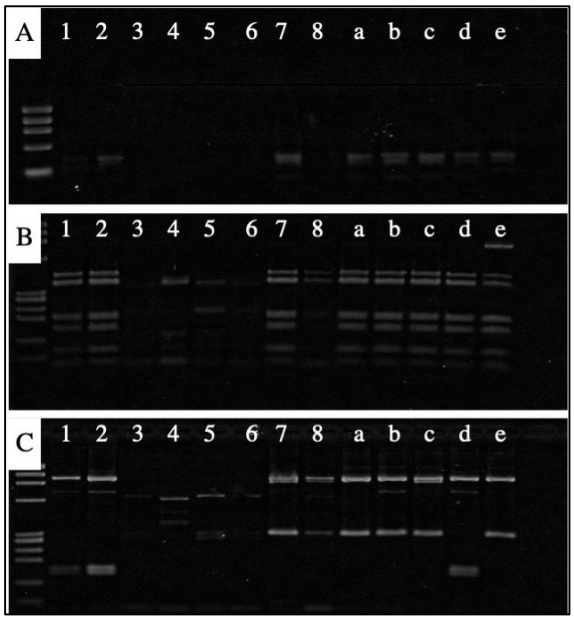

Figure 1.7 RFLP classification of the putative phytoplasma strains*. The PCR products of infected chrisanthemum and perivinkle plants were digested singly with the enzymes TruI (A), AluI (B) and HhaI (C). Putative strains (samples 1 to 8) were compared with positive controls a (NJAY = aster yellow witches' brooms), b (GD = grey dogwood stunt), c (AY Maryland aster yellow), d (SAY severe western aster yellow) and e (CPH Clover phyllody). The strain 2 had the same profile of the strain d, belonging to the 16Sr-IB.*

To transmit CY-phytoplasma to uninfected daisy or periwinkle plants, the vectors *Euscelidius variegatus* or *Macrosteles quadripunctulatus* were used. The insects grew under greenhouse conditions, with an average temperature of 20°C. For *E. variegatus*, the infection protocol indicated by Bosco *et al.*, (2007) was used (Bosco *et al.*, 2007; Pacifico *et al.*, 2015) with an AAP of 7 days, a LP of 40 days and IAP of 7 days. Instead, for *M. quadripunctulatus* an AAP of 7 days, a LP of 20 days and IAP of 7 days were used according to previous studies (Bosco *et al.*, 2007).

In daisy plants symptoms appearance occurs in an average of 15 days, depending on the individual. Before every infection cycle (for the strain maintenance and for the experiments) the infection status of daisy plants was checked with a real time PCR using the primer pairs R16F2n/R16R2n with the PCR conditions reported above.

To maintain the vector colonies, healthy insects, were reared on *Hordeum vulgare* (*E. variegatus*) or *Avena sativa* (*M. quadripunctulatus*) as previously reported (Pagliari *et al.*, 2017, 2016; Palermo *et al.*, 2001). The same plants were used for insect maintenance during latency period.

REFERENCES

Ahmad, J.N., Renaudin, J., Eveillard, S., 2014. Expression of defence genes in stolbur phytoplasma infected tomatoes, and effect of defence stimulators on disease development. Eur. J. Plant Pathol. 139, 39–51.

Albertazzi, G., Milc, J., Caffagni, A., Francia, E., Roncaglia, E., Ferrari, F., Tagliafico, E., Stefani, E., Pecchioni, N., 2009. Gene expression in grapevine cultivars in response to Bois Noir phytoplasma infection. Plant Sci. 176, 792–804.

Anstead, J.A., Froelich, D.R., Knoblauch, M., Thompson, G.A., 2012. Arabidopsis P-Protein Filament Formation Requires Both AtSEOR1 and AtSEOR2. Plant Cell Physiol. 53, 1033–1042.

Bai, X., Correa, V.R., Toruño, T.Y., Ammar, E.-D., Kamoun, S., Hogenhout, S.A., 2009. AY-WB Phytoplasma Secretes a Protein That Targets Plant Cell Nuclei. Mol. Plant-Microbe Interactions® 22, 18–30.

Beanland, L., Hoy, C.W., Miller, S.A., Nault, L.R., 2000. Influence of Aster Yellows Phytoplasma on the Fitness of Aster Leafhopper (Homoptera: Cicadellidae). Ann. Entomol. Soc. Am. 93, 271–276.

Berardini, T., Reiser, L., Li, D., Mezheritsky, Y., Muller, R., Strait, E., Huala, E., 2015. The arabidopsis information resource: Making and mining the "gold standard" annotated reference plant genome. genesis 53.

Bertaccini, A., Davis, E., Lee, I.-M., Conti, M., Dally, E., Douglas, S., 1990. Detection of chrysanthemum yellows mycoplasmalike organism by dot hybridization and Southern blot analysis. Plant Dis. 74, 40–43.

Bertaccini, A., Duduk, B., Paltrinieri, S., Contaldo, N., 2014. Phytoplasmas and Phytoplasma Diseases: A Severe Threat to Agriculture. Am. J. Plant Sci. 05, 1763–1788. 1

Bertamini, M., Grando, M.S., Nedunchezhian, N., 2003. Effects of phytoplasma infection on pigments, chlorophyll-protein complex and photosynthetic activities in field grown apple leaves. Biol. Plant. 47, 237–242.

Bertamini, M., Nedunchezhian, N., Tomasi, F., Grando, M., 2002. Phytoplasma [Stolbur-subgroup (Bois Noir-BN)] infection inhibits photosynthetic pigments, ribulose-1, 5-bisphosphate carboxylase and photosynthetic activities in field grown grapevine (Vitis vinifera L. cv. Chardonnay) leaves. Physiol. Mol. Plant Pathol. 61, 357–366.

Bosco, D., Galetto, L., Leoncini, P., Saracco, P., Raccah, B., Marzachì, C., 2007. Interrelationships Between "Candidatus Phytoplasma asteris" and Its Leafhopper Vectors (Homoptera: Cicadellidae). J. Econ. Entomol. 100, 1504–1511.

Bosco, D., Minucci, C., Boccardo, G., Conti, M., 1997. Differential acquisition of chrysanthemum yellows phytoplasma by three leafhopper species. Entomol. Exp. Appl. 83, 219–224.

Braun, E., Sinclair, W., 1976. Histopathology of phloem necrosis in. Ulmus Am. Phytopathol. 66, 598–607.

Bressan, A., Clair, D., Sémétey, O., Boudon-Padieu, É., 2005a. Effect of two strains of Flavescence dorée phytoplasma on the survival and fecundity of the experimental leafhopper vector Euscelidius variegatus Kirschbaum. J. Invertebr. Pathol. 89, 144–149.

Bressan, A., Girolami, V., Boudon-Padieu, E., 2005b. Reduced fitness of the leafhopper vector Scaphoideus titanus exposed to Flavescence doree phytoplasma. Entomol. Exp. Appl. 115, 283–290.

Brown, D.R., 2010. Phylum XVI. Tenericutes Murray 1984a, 356 VP (Effective Publication: Murray 1984b, 33.), in: Bergey's Manual of Systematic Bacteriology. Springer, pp. 567–723.

Buoso, S., Loschi, A., 2019. Micro-Tom Tomato Grafting for Stolbur-Phytoplasma Transmission: Different Grafting Techniques, in: Phytoplasmas. Springer, pp. 9–19.

Buoso, S., Pagliari, L., Musetti, R., Martini, M., Marroni, F., Schmidt, W., Santi, S., 2019. 'Candidatus Phytoplasma solani' interferes with the distribution and uptake of iron in tomato. BMC Genomics 20, 703.

Carraro, L., Ferrini, F., Ermacora, P., & Loi, N. (2003, July). Transmission of European stone fruit yellows phytoplasma to Prunus species by using vector and graft transmission. In XIX International Symposium on Virus and Virus-like Diseases of Temperate Fruit Crops-Fruit Tree Diseases 657 (pp. 449-453).

Cettul, E., Firrao, G., 2011. Development of phytoplasma-induced flower symptoms in Arabidopsis thaliana. Physiol. Mol. Plant Pathol. 76, 204–211.

Chang, J.H., Desveaux, D., Creason, A.L., 2014. The ABCs and 123s of Bacterial Secretion Systems in Plant Pathogenesis. Annu. Rev. Phytopathol. 52, 317–345.

Christensen, N.M., Nyskjold, H., Nicolaisen, M., 2004. Real-Time PCR for Universal Phytoplasma Detection and Quantification, in: Dickinson, M., Hodgetts, J. (Eds.), Phytoplasma, Methods in Molecular Biology. Humana Press, Totowa, NJ, pp. 245–252.

Clements, J., Bradford, B.Z., Garcia, M., Piper, S., Huang, W., Zwolinska, A., Lamour, K., Hogenhout, S., Groves, R.L., 2020. *Candidatus (Ca.)* phytoplasma asteris subgroups display distinct disease progression dynamics during the carrot growing season (preprint). Ecology.

Constable, F.E., 2010. Phytoplasma epidemiology: grapevines as a model. Phytoplasmas Genomes Plant Hosts Vectors 188212.

Contaldo, N., Bertaccini, A., PALTONIERI, S., M. WINDSOR, H., Windsor, G.D., 2012. Axenic culture of plant pathogenic phytoplasmas. Phytopathol. Mediterr. 607–617.

Ćurković Perica, M., 2008. Auxin-treatment induces recovery of phytoplasma-infected periwinkle. J. Appl. Microbiol. 105, 1826–1834.

D'Amelio, R., Palermo, S., Marzachi, C., Bosco, D., 2008. Influence of Chrysanthemum yellows phytoplasma on the fitness of two of its leafhopper vectors, Macrosteles quadripunctulatus and Euscelidius variegatus. Bull Insectol 61, 349–354.

Davis, R.E., Zhao, Y., Dally, E.L., Lee, M., Jomantiene, R., Douglas, S.M., 2013. 'Candidatus Phytoplasma pruni', a novel taxon associated with X-disease of stone fruits, Prunus spp.: multilocus characterization based on 16S rRNA, secY, and ribosomal protein genes. Int. J. Syst. Evol. Microbiol. 63, 766–776.

De Marco, F., Pagliari, L., Degola, F., Buxa, S.V., Loschi, A., Dinant, S., Hir, R.L., Morin, H., Santi, S., Musetti, R., 2016. Combined microscopy and molecular analyses show phloem occlusions and cell wall modifications in tomato leaves in response to ' *Candidatus* Phytoplasma solani'. J. Microsc. 263, 212–225.

Dermastia, M., 2019. Plant Hormones in Phytoplasma Infected Plants. Front. Plant Sci. 10, 477.

Dodds, P.N., Rathjen, J.P., 2010. Plant immunity: towards an integrated view of plant–pathogen interactions. Nat. Rev. Genet. 11, 539–548.

Doehlemann, G., Van Der Linde, K., Aßmann, D., Schwammbach, D., Hof, A., Mohanty, A., Jackson, D., Kahmann, R., 2009. Pep1, a secreted effector protein of Ustilago maydis, is required for successful invasion of plant cells. PLoS Pathog 5, e1000290.

Doi, Y., Teranaka, M., Yora, K., Asuyama, H., 1967. Mycoplasma-or PLT group-like microorganisms found in the phloem elements of plants infected with mulberry dwarf, potato witches' broom, aster yellows, or paulownia witches' broom. Jpn. J. Phytopathol. 33, 259–266.

Doyle, JJ, Doyle, JL, 1990. DNA extraction from Arabidopsis. Focus 12, 13–15.

Ermacora, P., Osler, R., 2019. Symptoms of phytoplasma diseases, in: Phytoplasmas. Springer, pp. 53–67.

Esau, K., 1939. Development and structure of the phloem tissue. Bot. Rev. 5, 373–432.

Faulkner, C., 2018. Plasmodesmata and the symplast. Curr. Biol. 28, R1374–R1378.

Favali, M.A., Musetti, R., Benvenuti, S., Bianchi, A., Pressacco, L., 2004. Catharanthus roseus L. plants and explants infected with phytoplasmas: alkaloid production and structural observations. Protoplasma 223, 45–51.

Fernández, F.D., Debat, H.J., Conci, L.R., 2019. Molecular characterization of effector protein SAP54 in Bellis virescence phytoplasma (16SrIII-J). Trop. Plant Pathol. 44, 392–397.

Firrao, G., Garcia-Chapa, M., Marzachì, C., 2007. Phytoplasmas: genetics, diagnosis and relationships with the plant and insect host. Front. Biosci. J. Virtual Libr. 12, 1353–1375.

Furch, A.C., Hafke, J.B., Schulz, A., van Bel, A.J., 2007. Ca2+-mediated remote control of reversible sieve tube occlusion in Vicia faba. J. Exp. Bot. 58, 2827–2838.

Gilroy, S., Białasek, M., Suzuki, N., Górecka, M., Devireddy, A.R., Karpiński, S., Mittler, R., 2016. ROS, calcium, and electric signals: key mediators of rapid systemic signaling in plants. Plant Physiol. 171, 1606–1615.

Gilroy, S., Suzuki, N., Miller, G., Choi, W.-G., Toyota, M., Devireddy, A.R., Mittler, R., 2014. A tidal wave of signals: calcium and ROS at the forefront of rapid systemic signaling. Trends Plant Sci. 19, 623–630.

Giorno, F., Guerriero, G., Biagetti, M., Ciccotti, A.M., Baric, S., 2013. Gene expression and biochemical changes of carbohydrate metabolism in in vitro micro-propagated apple plantlets infected by 'Candidatus Phytoplasma mali.' Plant Physiol. Biochem. 70, 311–317.

Girousse, C., Bonnemain, J.-L., Delrot, S., Bournoville, R., 1991. Sugar and amino acid composition of phloem sap of Medicago sativa: a comparative study of two collecting methods. Plant Physiol. Biochem. Paris 29, 41–48.

Glazebrook, J., 2005. Contrasting Mechanisms of Defense Against Biotrophic and Necrotrophic Pathogens. Annu. Rev. Phytopathol. 43, 205–227.

Hafke, J.B., van Amerongen, J.-K., Kelling, F., Furch, A.C., Gaupels, F., van Bel, A.J., 2005. Thermodynamic battle for photosynthate acquisition between sieve tubes and adjoining parenchyma in transport phloem. Plant Physiol. 138, 1527–1537.

Ham, B.-K., Lucas, W.J., 2017. Phloem-Mobile RNAs as Systemic Signaling Agents. Annu. Rev. Plant Biol. 68, 173–195.

Hayashi, H., Chino, M., 1986. Collection of Pure Phloem Sap from Wheat and its Chemical Composition. Plant Cell Physiol. 27, 1387–1393.

Hijaz, F., Manthey, J.A., Van der Merwe, D., Killiny, N., 2016. Nucleotides, micro-and macro-nutrients, limonoids, flavonoids, and hydroxycinnamates composition in the phloem sap of sweet orange. Plant Signal. Behav. 11, e1183084.

Hodgetts, J., Boonham, N., Mumford, R., Harrison, N., Dickinson, M., 2008. Phytoplasma phylogenetics based on analysis of secA and 23S rRNA gene sequences for improved resolution of candidate species of 'Candidatus Phytoplasma.' Int. J. Syst. Evol. Microbiol. 58, 1826–1837.

Hodgetts, J., Chuquillangui, C., Muller, G., Arocha, Y., Gamarra, D., Pinillos, O., Velit, E., Lozada, P., Boa, E., Boonham, N., 2009. Surveys reveal the occurrence of phytoplasmas in plants at different geographical locations in Peru. Ann. Appl. Biol. 155, 15–27.

Hörger, A.C., Van der Hoorn, R.A., 2013. The structural basis of specific protease–inhibitor interactions at the plant–pathogen interface. Curr. Opin. Struct. Biol. 23, 842–850.

Hoshi, A., Oshima, K., Kakizawa, S., Ishii, Y., Ozeki, J., Hashimoto, M., Komatsu, K., Kagiwada, S., Yamaji, Y., Namba, S., 2009. A unique virulence factor for proliferation and dwarfism in plants identified from a phytopathogenic bacterium. Proc. Natl. Acad. Sci. 106, 6416–6421.

Hren, M., Nikolić, P., Rotter, A., Blejec, A., Terrier, N., Ravnikar, M., Dermastia, M., Gruden, K., 2009. "Bois noir" phytoplasma induces significant reprogramming of the leaf transcriptome in the field grown grapevine. BMC Genomics 10, 460.

Jones, J.D.G., Dangl, J.L., 2006. The plant immune system. Nature 444, 323–329.

Junqueira, A., Bedendo, I., Pascholati, S., 2004. Biochemical changes in corn plants infected by the maize bushy stunt phytoplasma. Physiol. Mol. Plant Pathol. 65, 181–185.

Kakizawa, S., Oshima, K., Nishigawa, H., Jung, H.-Y., Wei, W., Suzuki, S., Tanaka, M., Miyata, S., Ugaki, M., Namba, S., 2004. Secretion of immunodominant membrane protein from onion yellows phytoplasma through the Sec protein-translocation system in Escherichia coli. Microbiology 150, 135–142.

Kamińska, M., & Korbin, M. 1999. Graft and dodder transmission of phytoplasma affecting lily to experimental hosts. Acta physiologiae plantarum, 21(1), 21-26.

Kaminska, M., Sliwa, H., Rudzinska-Langwald, A., 2001. The Association of Phytoplasma with Stunting, Leaf Necrosis and Witches' Broom Symptoms in Magnolia Plants. J. Phytopathol. 149, 719–724.

Koornneef, M., Meinke, D., 2010. The development of Arabidopsis as a model plant. Plant J. 61, 909–921.

Kudla, J., Batistič, O., Hashimoto, K., 2010. Calcium signals: the lead currency of plant information processing. Plant Cell 22, 541–563.

Kunkel, L., 1926. Studies on aster yellows. Am. J. Bot. 646–705.

Landi, L., Murolo, S., Romanazzi, G., 2019. Detection of 'Candidatus Phytoplasma solani'in roots from Bois noir symptomatic and recovered grapevines. Sci. Rep. 9, 1–12.

Lee, I. M., Gundersen-Rindal, D. E., & Bertaccini, A. (1998). Phytoplasma: ecology and genomic diversity. Phytopathology, 88(12), 1359-1366.

Lee, I.-M., Bottner-Parker, K., Zhao, Y., Davis, R., Harrison, N., 2010. Phylogenetic analysis and delineation of phytoplasmas based on secY gene sequences. Int. J. Syst. Evol. Microbiol. 60, 2887–2897.

Lee, I.-M., Davis, R.E., Gundersen-Rindal, D.E., 2000. Phytoplasma: Phytopathogenic Mollicutes. Annu. Rev. Microbiol. 54, 221–255.

Lee, I.-M., Gundersen-Rindal, D.E., Davis, R.E., Bottner, K.D., Marcone, C., Seemüller, E., 2004. 'Candidatus Phytoplasma asteris', a novel phytoplasma taxon associated with aster yellows and related diseases. Int. J. Syst. Evol. Microbiol. 54, 1037–1048.

Lee, I.-M., Zhao, Y., Davis, R.E., Wei, W., Martini, M., 2007. Prospects of DNA-based systems for differentiation and classification of phytoplasmas. Bull. Insectology 60, 239–244.

Lefol, C., Caudwell, A., Lherminier, J., Larrue, J., 1993. Attachment of the flavescence dorée pathogen (MLO) to leafhopper vectors and other insects. Ann. Appl. Biol. 123, 611–622.

Lepka, P., Stitt, M., Moll, E., Seemüller, E., 1999. Effect of phytoplasmal infection on concentration and translocation of carbohydrates and amino acids in periwinkle and tobacco. Physiol. Mol. Plant Pathol. 55, 59–68.

Lim, P., Sears, B., 1992. Evolutionary relationships of a plant-pathogenic mycoplasmalike organism and Acholeplasma laidlawii deduced from two ribosomal protein gene sequences. J. Bacteriol. 174, 2606–2611.

Lv, M.-F., Xie, L., Song, X.-J., Hong, J., Mao, Q.-Z., Wei, T.-Y., Chen, J.-P., Zhang, H.-M., 2017. Phloem-limited reoviruses universally induce sieve element hyperplasia and more flexible gateways, providing more channels for their movement in plants. Sci. Rep. 7, 1–13.

MacLean, A.M., Orlovskis, Z., Kowitwanich, K., Zdziarska, A.M., Angenent, G.C., Immink, R.G.H., Hogenhout, S.A., 2014. Phytoplasma Effector SAP54 Hijacks Plant Reproduction by Degrading MADS-box Proteins and Promotes Insect Colonization in a RAD23-Dependent Manner. PLoS Biol. 12, e1001835.

MacLean, Allyson M, Sugio, A., Heather, N., Grieve, V.M., Hogenhout, S.A., 2011. Arabidopsis thaliana as a model plant for understanding phytoplasma interactions with plant and insect hosts. Bull. Insectology 64, S173–S174.

MacLean, Allyson M., Sugio, A., Makarova, O.V., Findlay, K.C., Grieve, V.M., Tóth, R., Nicolaisen, M., Hogenhout, S.A., 2011. Phytoplasma Effector SAP54 Induces Indeterminate Leaf-Like Flower Development in Arabidopsis Plants. Plant Physiol. 157, 831–841.

Marcone, C., Ragozzino, A., & Seemuller, E. (1997). Dodder transmission of alder yellows phytoplasma to the experimental host Catharanthus roseus (periwinkle). European journal of forest pathology, 27(6), 347-350.

Marcone, C., Lee, I.M., Davis, R.E., Ragozzino, A., Seemüller, E., 2000. Classification of aster yellows-group phytoplasmas based on combined analyses of rRNA and tuf gene sequences. Int. J. Syst. Evol. Microbiol. 50, 1703–1713.

Marrero, M.C., Capdevielle, S., Huang, W., Busscher, M., Busscher-Lange, J., de Ridder, D., van Dijk, A.D., Hogenhout, S.A., Immink, R.G., 2020. Widespread targeting of

development-related host transcription factors by phytoplasma effectors. bioRxiv.

Martini, M., Lee, I.-M., Bottner, K.D., Zhao, Y., Botti, S., Bertaccini, A., Harrison, N.A., Carraro, L., Marcone, C., Khan, A.J., Osler, R., 2007. Ribosomal protein gene-based phylogeny for finer differentiation and classification of phytoplasmas. Int. J. Syst. Evol. Microbiol. 57, 2037–2051.

Martini, M., Musetti, R., Grisan, S., Polizzotto, R., Borselli, S., Pavan, F., Osler, R., 2009. DNA-Dependent Detection of the Grapevine Fungal Endophytes *Aureobasidium pullulans* and *Epicoccum nigrum*. Plant Dis. 93, 993–998.

Maust, B.E., Espadas, F., Talavera, C., Aguilar, M., Santamaría, J.M., Oropeza, C., 2003. Changes in carbohydrate metabolism in coconut palms infected with the lethal yellowing phytoplasma. Phytopathology 93, 976–981.

McCoy, R., Caudwell, A., Chang, C., Chen, T., Chiykowski, L., Cousin, M., Dale, J., De Leeuw, G., Golino, D., Hackett, K., 1989. Plant diseases associated with mycoplasma-like organisms. The Mycoplasmas (Whitcomb RF & Tully JG, eds).

Meinke, D.W., 1998. Arabidopsis thaliana: A Model Plant for Genome Analysis. Science 282, 662–682.

Minchin, P.E.H., Lacointe, A., 2017. Consequences of phloem pathway unloading/reloading on equilibrium flows between source and sink: a modelling approach. Funct. Plant Biol. 44, 507.

Mullendore, D.L., Windt, C.W., Van As, H., Knoblauch, M., 2010. Sieve Tube Geometry in Relation to Phloem Flow. Plant Cell 22, 579–593.

Munch, E., 1930. Stoffbewegungen in der Pflanze.

Musetti, R., Buxa, S.V., De Marco, F., Loschi, A., Polizzotto, R., Kogel, K.-H., van Bel, A.J.E., 2013a. Phytoplasma-Triggered Ca 2+ Influx Is Involved in Sieve-Tube Blockage. Mol. Plant-Microbe Interactions 26, 379–386.

Musetti, R., Paolacci, A., Ciaffi, M., Tanzarella, O. A., Polizzotto, R., Tubaro, F., … & Osler, R. 2010. Phloem cytochemical modification and gene expression following the recovery of apple plants from apple proliferation disease. Phytopathology, 100(4), 390-399.

Musetti, R., di Toppi, L.S., Ermacora, P., Favali, M.A., 2004. Recovery in Apple Trees Infected with the Apple Proliferation Phytoplasma: An Ultrastructural and Biochemical Study. Phytopathology 94, 203–208.

Musetti, R., di Toppi, L.S., Martini, M., Ferrini, F., Loschi, A., Favali, M.A., Osler, R., 2005. Hydrogen peroxide localization and antioxidant status in the recovery of apricot plants from European Stone Fruit Yellows. Eur. J. Plant Pathol. 112, 53–61.

Musetti, R., Farhan, K., De Marco, F., Polizzotto, R., Paolacci, A., Ciaffi, M., Ermacora, P., Grisan, S., Santi, S., Osler, R., 2013b. Differentially-regulated defence genes in Malus domestica during phytoplasma infection and recovery. Eur. J. Plant Pathol. 136, 13–19.

Musetti, R., Favali, M., Pressacco, L., 2000. Histopathology and polyphenol content in plants infected by phytoplasmas. CYTOBIOS-Camb.- 133–148.

Musetti, R., Favali, M.A., 2003. Cytochemical localization of calcium and X-ray microanalysis of Catharanthus roseus L. infected with phytoplasmas. Micron 34, 387–393.

Musetti, R., Marabottini, R., Badiani, M., Martini, M., Sanità di Toppi, L., Borselli, S., Borgo, M., Osler, R., 2007. On the role of H2O2 in the recovery of grapevine (Vitis vinifera cv. Prosecco) from Flavescence dorée disease. Funct. Plant Biol. 34, 750.

Musetti, R., Pagliari, L. (Eds.), 2019. Phytoplasmas: Methods and Protocols, Methods in Molecular Biology. Springer New York, New York, NY.

Nejat, N., Vadamalai, G., Davis, R.E., Harrison, N.A., Sijam, K., Dickinson, M., Abdullah, S.N.A., Zhao, Y., 2013. 'Candidatus Phytoplasma malaysianum', a novel taxon associated with virescence and phyllody of Madagascar periwinkle (Catharanthus roseus). Int. J. Syst. Evol. Microbiol. 63, 540–548.

Oparka, K.J., Turgeon, R., 1999. Sieve elements and companion cells—traffic control centers of the phloem. Plant Cell 11, 739–750.

Ohshima, T., Hayashi, H., Chino, M., 1990. Collection and chemical composition of pure phloem sap from Zea mays L. Plant Cell Physiol. 31, 735–737.

Oshima, K., Ishii, Y., Kakizawa, S., Sugawara, K., Neriya, Y., Himeno, M., Minato, N., Miura, C., Shiraishi, T., Yamaji, Y., Namba, S., 2011. Dramatic Transcriptional Changes in an Intracellular Parasite Enable Host Switching between Plant and Insect. PLoS ONE 6, e23242.

Oshima, K., Kakizawa, S., Nishigawa, H., Jung, H.-Y., Wei, W., Suzuki, S., Arashida, R., Nakata, D., Miyata, S., Ugaki, M., Namba, S., 2004. Reductive evolution suggested from the complete genome sequence of a plant-pathogenic phytoplasma. Nat. Genet. 36, 27–29.

Pacifico, D., Galetto, L., Rashidi, M., Abbà, S., Palmano, S., Firrao, G., Bosco, D., Marzachì, C., 2015. Decreasing Global Transcript Levels over Time Suggest that Phytoplasma Cells Enter Stationary Phase during Plant and Insect Colonization. Appl. Environ. Microbiol. 81, 2591–2602.

Pacifico, D., Margaria, P., Galetto, L., Legovich, M., Abbà, S., Veratti, F., Marzachì, C., Palmano, S., 2019. Differential gene expression in two grapevine cultivars recovered from "flavescence dorée." Microbiol. Res. 220, 72–82.

Pagliari, L., Buoso, S., Santi, S., Furch, A.C.U., Martini, M., Degola, F., Loschi, A., van Bel, A.J.E., Musetti, R., 2017. Filamentous sieve element proteins are able to limit phloem mass flow, but not phytoplasma spread. J. Exp. Bot. 68, 3673–3688.

Pagliari, L., Buoso, S., Santi, S., Van Bel, A.J.E., Musetti, R., 2018. What slows down phytoplasma proliferation? Speculations on the involvement of AtSEOR2 protein in plant defence signalling. Plant Signal. Behav. 13, e1473666.

Pagliari, L., Martini, M., Loschi, A., Musetti, R., 2016. Looking inside phytoplasma-infected sieve elements: A combined microscopy approach using Arabidopsis thaliana as a model plant. Micron 89, 87–97.

Palermo, S., Arzone, A., Bosco, D., 2001. Vector-pathogen-host plant relationships of chrysanthemum yellows (CY) phytoplasma and the vector leafhoppers *Macrosteles quadripunctulatus* and *Euscelidius variegatus*. Entomol. Exp. Appl. 99, 347–354.

Parthasarathy, M.V., 1975. Sieve-Element Structure, in: Zimmermann, M.H., Milburn, J.A. (Eds.), Transport in Plants I. Springer Berlin Heidelberg, Berlin, Heidelberg, pp. 3–38.

Pecher, P., Moro, G., Canale, M.C., Capdevielle, S., Singh, A., MacLean, A., Sugio, A., Kuo, C.-H., Lopes, J.R.S., Hogenhout, S.A., 2019. Phytoplasma SAP11 effector destabilization of TCP transcription factors differentially impact development and defence of Arabidopsis versus maize. PLOS Pathog. 15, e1008035.

Pickard, W.F., 2012. Münch without tears: a steady-state Münch-like model of phloem so simplified that it requires only algebra to predict the speed of translocation. Funct. Plant Biol. 39, 531.

Quaglino, F., Zhao, Y., Bianco, P., Wei, W., Casati, P., Durante, G., Davis, R., 2009. New 16Sr subgroups and distinct single nucleotide polymorphism lineages among grapevine Bois noir phytoplasma populations. Ann. Appl. Biol. 154, 279–289.

Rashidi, M., D'Amelio, R., Galetto, L., Marzachì, C., Bosco, D., 2014. Interactive transmission of two phytoplasmas by the vector insect. Ann. Appl. Biol. 165, 404–413.

Ray, S.K., Macoy, D.M., Kim, W.-Y., Lee, S.Y., Kim, M.G., 2019. Role of RIN4 in Regulating PAMP-Triggered Immunity and Effector-Triggered Immunity: Current Status and Future Perspectives. Mol. Cells 42.

Razin, S., Yogev, D., Naot, Y., 1998. Molecular biology and pathogenicity of mycoplasmas. Microbiol. Mol. Biol. Rev. 62, 1094–1156.

Rennie, E.A., Turgeon, R., 2009. A comprehensive picture of phloem loading strategies. Proc. Natl. Acad. Sci. 106, 14162–14167.

Rhee, S.Y., 2003. The Arabidopsis Information Resource (TAIR): a model organism database providing a centralized, curated gateway to Arabidopsis biology, research materials and community. Nucleic Acids Res. 31, 224–228.

Roistacher, C.N., 1991. Graft-transmissible diseases of citrus: Handbook for detection and diagnosis. Food & Agriculture Org.

Rossi, M., Pesando, M., Vallino, M., Galetto, L., Marzachì, C., Balestrini, R., 2018. Application of laser microdissection to study phytoplasma site-specific gene expression in the model plant Arabidopsis thaliana. Microbiol. Res. 217, 60–68.

Santi, S., De Marco, F., Polizzotto, R., Grisan, S., Musetti, R., 2013a. Recovery from stolbur disease in grapevine involves changes in sugar transport and metabolism. Front. Plant Sci. 4.

Santi, S., Grisan, S., Pierasco, A., De Marco, F., Musetti, R., 2013b. Laser microdissection of grapevine leaf phloem infected by stolbur reveals site-specific gene responses associated to sucrose transport and metabolism: LM of stolbur-infected grapevine phloem. Plant Cell Environ. 36, 343–355.

Saracco, P., Bosco, D., Veratti, F., Marzachì, C., 2005. Quantification over time of chrysanthemum yellows phytoplasma (16Sr-I) in leaves and roots of the host plant Chrysanthemum carinatum (Schousboe) following inoculation with its insect vector. Physiol. Mol. Plant Pathol. 67, 212–219.

Schmid, G., 1965. Five and more years of observations on the proliferation virus of apples in the field. Zast Bilja 16, 285–291.

Schneider, H., 1977. Indicator hosts for pear decline: symptomatology, histopathology, and distribution of mycoplasmalike organisms in leaf veins. Phytopathology 67, 592–601.

Seemüller, E., Marcone, C., Lauer, U., Ragozzino, A., Göschl, M., 1998. Current status of molecular classification of the phytoplasmas. J. Plant Pathol. 3–26.

Serek, J., Bauer-Manz, G., Struhalla, G., van den Berg, L., Kiefer, D., Dalbey, R., Kuhn, A., 2004. Escherichia coli YidC is a membrane insertase for Sec-independent proteins. EMBO J. 23, 294–301.

Singh, A., Lakhanpaul, S., 2020. Detection, characterization and evolutionary aspects of S54LP of SP (SAP54 Like Protein of Sesame Phyllody): a phytoplasma effector molecule associated with phyllody development in sesame (Sesamum indicum L.). Physiol. Mol. Biol. Plants 26, 445–458.

Snyman, M.C., Solofoharivelo, M.-C., Souza-Richards, R., Stephan, D., Murray, S., Burger, J.T., 2017. The use of high-throughput small RNA sequencing reveals differentially expressed microRNAs in response to aster yellows phytoplasma-infection in Vitis vinifera cv. 'Chardonnay.' PLOS ONE 12, e0182629.

Somerville, C., Koornneef, M., 2002. A fortunate choice: the history of Arabidopsis as a model plant. Nat. Rev. Genet. 3, 883–889.

Sugio, A., 2012. The genome biology of phytoplasma: modulators of plants and insects. Curr. Opin. Microbiol. 8.

Sugio, A., Kingdom, H.N., MacLean, A.M., Grieve, V.M., Hogenhout, S.A., 2011. Phytoplasma protein effector SAP11 enhances insect vector reproduction by manipulating plant development and defense hormone biosynthesis. Proc. Natl. Acad. Sci. 108, E1254–E1263.

Sugio, Akiko, MacLean, A.M., Kingdom, H.N., Grieve, V.M., Manimekalai, R., Hogenhout, S.A., 2011. Diverse Targets of Phytoplasma Effectors: From Plant Development to Defense Against Insects. Annu. Rev. Phytopathol. 49, 175–195.

Suzuki, S., Oshima, K., Kakizawa, S., Arashida, R., Jung, H.-Y., Yamaji, Y., Nishigawa, H., Ugaki, M., Namba, S., 2006. Interaction between the membrane protein of a pathogen and insect microfilament complex determines insect-vector specificity. Proc. Natl. Acad. Sci. 103, 4252–4257.

The IRPCM Phytoplasma/Spiroplasma Working Team – Phytoplasma taxonomy group, 2004. 'Candidatus Phytoplasma', a taxon for the wall-less, non-helical prokaryotes that colonize plant phloem and insects. Int. J. Syst. Evol. Microbiol. 54, 1243–1255.

Thompson, M.V., Holbrook, N.M., 2003. Scaling phloem transport: water potential equilibrium and osmoregulatory flow. Plant Cell Environ. 26, 1561–1577.

Toruño, T.Y., Shen, M., Coaker, G., Mackey, D., 2019. Regulated Disorder: Posttranslational Modifications Control the RIN4 Plant Immune Signaling Hub. Mol. Plant. Microbe Interact. 32, 56–64.

Tully, J., 1993. International Committee on Systematic Bacteriology Subcommittee on the Taxonomy of Mollicutes. Minutes of the interim meetings, 1 and 2 Aug. 1992, Ames, Iowa. Int J Syst Bacteriol 43, 394–397.

van Bel, A. J., & Musetti, R. (2019). Sieve element biology provides leads for research on phytoplasma lifestyle in plant hosts. Journal of experimental botany, 70(15), 3737-3755.

van Bel, A.J., 2019. Sieve Elements: The Favourite Habitat of Phytoplasmas, in: Phytoplasmas. Springer, pp. 255–277.

van Bel, A.J., 2006. Sieve-pore plugging mechanisms, in: Cell-Cell Channels. Springer, pp. 113–118.

van Bel, A. J., Ehlers, K., & Knoblauch, M. (2002). Sieve elements caught in the act. Trends in plant science, 7(3), 126-132.

van Bel, A.J.E., 2003. The phloem, a miracle of ingenuity. Plant Cell Environ. 26, 125–149.

van Bel, A.J.E., Hafke, J.B., 2005. Physiochemical Determinants of Phloem Transport, in: Vascular Transport in Plants. Elsevier, pp. 19–44.

van Dongen, J.T., Schurr, U., Pfister, M., Geigenberger, P., 2003. Phloem metabolism and function have to cope with low internal oxygen. Plant Physiol. 131, 1529–1543.

van Helden, M., Tjallingh, W.F., van Beek, T.A., 1994. Phloem sap collection from lettuce (Lactuca sativa L.): chemical comparison among collection methods. J. Chem. Ecol. 20, 3191–3206.

Vincent, C., Minchin, P.E.H., Liesche, J., 2019. Noninvasive Determination of Phloem Transport Speed with Carbon-14 (14C), in: Liesche, J. (Ed.), Phloem, Methods in Molecular Biology. Springer New York, New York, NY, pp. 153–162.

Vreugdenhil, D., Koot-Gronsveld, E.A., 1989. Measurements of pH, sucrose and potassium ions in the phloem sap of castor bean (Ricinus communis) plants. Physiol. Plant. 77, 385–388.

Wei, W., Davis, R.E., Jomantiene, R., Zhao, Y., 2008. Ancient, recurrent phage attacks and recombination shaped dynamic sequence-variable mosaics at the root of phytoplasma genome evolution. Proc. Natl. Acad. Sci. 105, 11827–11832.

Wei, W., Davis, R.E., Lee, I.-M., Zhao, Y., 2007. Computer-simulated RFLP analysis of 16S rRNA genes: identification of ten new phytoplasma groups. Int. J. Syst. Evol. Microbiol. 57, 1855–1867.

Wei, W., Kakizawa, S., Suzuki, S., Jung, H.-Y., Nishigawa, H., Miyata, S., Oshima, K., Ugaki, M., Hibi, T., Namba, S., 2004. In Planta Dynamic Analysis of Onion Yellows Phytoplasma Using Localized Inoculation by Insect Transmission. Phytopathology 94, 244–250.

Weibull, J., Ronquist, F., Brishammar, S., 1990. Free amino acid composition of leaf exudates and phloem sap: a comparative study in oats and barley. Plant Physiol. 92, 222–226.

Weintraub, P.G., Beanland, L., 2006. Insect vector of phytoplasmas. Annu. Rev. Entomol. 51, 91–111.

Weisburg, W., Tully, J., Rose, D., Petzel, J., Oyaizu, H., Yang, D., Mandelco, L., Sechrest, J., Lawrence, T., Van Etten, J., 1989. A phylogenetic analysis of the mycoplasmas: basis for their classification. J. Bacteriol. 171, 6455–6467.

Wind, J., Smeekens, S., Hanson, J., 2010. Sucrose: Metabolite and signaling molecule. Phytochemistry 71, 1610–1614.

Wu, W., Cai, H., Wei, W., Davis, R., Lee, I., Chen, H., Zhao, Y., 2012. Identification of two new phylogenetically distant phytoplasmas from S enna surattensis plants exhibiting stem fasciation and shoot proliferation symptoms. Ann. Appl. Biol. 160, 25–34.

Xie, B., Hong, Z., 2011. Unplugging the callose plug from sieve pores. Plant Signal. Behav. 6, 491–493.

Xue, C., Liu, Z., Dai, L., Bu, J., Liu, M., Zhao, Z., Jiang, Z., Gao, W., Zhao, J., 2018. Changing Host Photosynthetic, Carbohydrate, and Energy Metabolisms Play Important Roles in Phytoplasma Infection. Phytopathology® 108, 1067–1077.

Zafari, S., Niknam, V., Musetti, R., Noorbakhsh, S.N., 2012. Effect of phytoplasma infection on metabolite content and antioxidant enzyme activity in lime (Citrus aurantifolia). Acta Physiol. Plant. 34, 561–568.

Zamharir, M.G., Mardi, M., Alavi, S.M., Hasanzadeh, N., Nekouei, M.K., Zamanizadeh, H.R., Alizadeh, A., Salekdeh, G.H., 2011. Identification of genes differentially expressed during interaction of Mexican lime tree infected with "Candidatus Phytoplasma aurantifolia" 9.

Zavaliev, R., Ueki, S., Epel, B.L., Citovsky, V., 2011. Biology of callose (β-1,3-glucan) turnover at plasmodesmata. Protoplasma 248, 117–130.

Zhao, Y., Wei, W., Lee, M., Shao, J., Suo, X., Davis, R.E., 2013. The iPhyClassifier, an interactive online tool for phytoplasma classification and taxonomic assignment, in: Phytoplasma. Springer, pp. 329–338.

Zhao, Y., Wei, W., Lee, M., Shao, J., Suo, X., Davis, R.E., 2009. Construction of an interactive online phytoplasma classification tool, iPhyClassifier, and its application in analysis of the peach X-disease phytoplasma group (16SrIII). Int. J. Syst. Evol. Microbiol. 59, 2582.

2. AIMS

Sieve elements are the favorite habitat of phytoplasmas inside their plant hosts (van Bel and Musetti, 2019). Sieve elements are living cells, in which the nucleus, as well as the ribosomes, the tonoplast, and the Golgi system, has been degraded (van Bel, 2003). The plasma membrane remains intact and delimits a narrow parietal margin of cytoplasm (named mictoplasm; van Bel, 2003), containing smooth endoplasmic reticulum stacks, mitochondria, often degenerated and with a low degree of metabolism (van Bel and Kempers, 1991). Small plastids are located along the plasma membrane. All above cited organelles are tethered to each other and the plasma membrane by numerous connections (~7 nm long in *Vicia* and *Solanum* spp., Ehlers *et al.*, 2000). These little anchors, resembling EPCSs (ER–plasma membrane contact sites, Wang *et al.*, 2017), might prevent the organelles from being swept away by the mass flow in sieve tubes (Ehlers *et al.*, 2000; Van Bel, 2003). The presence of cytoskeleton components in sieve elements was also demonstrated (Hafke *et al.*, 2013). Finally, sieve elements contain a number of structural proteins of different shapes, many of these, fibrillar and disorganized in appearance (Anstead *et al.*, 2012; Batailler *et al.*, 2012; Rüping *et al.*, 2010).

As phytoplasmas are strictly dependent on sieve element resources, aims of my research was to give insight to the fine interaction established among phytoplasmas and some of the different sieve-element components.

In the Chapter 3 we explored the possibility that Sieve Element Occlusion-Related (SEOR) proteins in Arabidopsis, beside their role in sieve-plate plugging following phytoplasma infection, could be involved in plant-defense mechanisms related to phytohormone-mediated signaling. The results suggest that SEOR2 interferes with phytohormonal pathways in Arabidopsis midrib tissues in order to establish early defensive responses to phytoplasma infection.

In the chapter 4 we aimed to investigate about the synthesis, transport and metabolism of phloem callose and related soluble sugars in Arabidopsis during phytoplasma infection, in order to highlight how and to what extent callose and soluble sugars are involved in plant immune response and signaling.

The chapter 5 we presented preliminary results of a work still in progress: given the recent reports about the role(s) of synaptotagmins in plant-pathogen interaction, in particular in viral spread through the plasmodesmata (Lewis ad Lazarowiz, 2010; Uchiyama *et al.*, 2014; Levy *et al.*, 2015), we explored about the possible role of synaptotagmin A in the spread of phytoplasma in Arabidopsis.

The specific aims of the different works are reported in the introduction section of each chapter.

References

Anstead, J.A., Froelich, D.R., Knoblauch, M., Thompson, G.A., 2012. Arabidopsis P-Protein Filament Formation Requires Both AtSEOR1 and AtSEOR2. Plant Cell Physiol. 53, 1033–1042.

Batailler B, Lemaître T, Vilaine F, Sanchez C, Renard D, Cayla, T, Beneteau J, Dinant S, Bataillard (B), Dinant, S., 2012. Soluble and filamentous proteins in Arabidopsis sieve elements. Plant, Cell and Environment 35, 1258–1273.

Ehlers, K., Knoblauch, M., Van Bel, A., 2000. Ultrastructural features of well-preserved and injured sieve elements: minute clamps keep the phloem transport conduits free for mass flow. Protoplasma 214, 80–92.

Hafke, J.B., Höll, S.-R., Kühn, C., van Bel, A.J.E., 2013. Electrophysiological approach to determine kinetic parameters of sucrose uptake by single sieve elements or phloem parenchyma cells in intact Vicia faba plants. Front. Plant Sci. 4.

Rüping, B., Ernst, A.M., Jekat, S.B., Nordzieke, S., Reineke, A.R., Müller, B., Bornberg-Bauer, E., Prüfer, D., Noll, G.A., 2010. Molecular and phylogenetic characterization of the sieve element occlusion gene family in Fabaceae and non-Fabaceae plants. BMC Plant Biol. 10, 219.

Levy, A., Zheng, J. Y., & Lazarowitz, S. G. 2015. Synaptotagmin SYTA forms ER-plasma membrane junctions that are recruited to plasmodesmata for plant virus movement. Current Biology, 25(15), 2018-2025.

Lewis, J. D., & Lazarowitz, S. G. 2010. Arabidopsis synaptotagmin SYTA regulates endocytosis and virus movement protein cell-to-cell transport. Proceedings of the National Academy of Sciences, 107(6), 2491-2496.

Uchiyama, A., Shimada-Beltran, H., Levy, A., Zheng, J. Y., Javia, P. A., & Lazarowitz, S. G. 2014. The Arabidopsis synaptotagmin SYTA regulates the cell-to-cell movement of diverse plant viruses. Frontiers in plant science, 5, 584.

van Bel, A. J., & Musetti, R. (2019). Sieve element biology provides leads for research on phytoplasma lifestyle in plant hosts. Journal of experimental botany, 70(15), 3737-3755.

van Bel, A.J., Kempers, R., 1991. Symplastic isolation of the sieve element-companion cell complex in the phloem of Ricinus communis and Salix alba stems. Planta 183, 69–76.

van Bel, A.J.E., 2003. The phloem, a miracle of ingenuity: The phloem, a miracle of ingenuity. Plant Cell Environ. 26, 125–149.

Wang, X.-Q., Zheng, L.-L., Lin, H., Yu, F., Sun, L.-H., Li, L.-M., 2017. Grape hexokinases are involved in the expression regulation of sucrose synthase- and cell wall invertase-encoding genes by glucose and ABA. Plant Mol. Biol. 94, 61–78.

3. SPECIFIC RESPONSE OF THE SIEVE ELEMENTS TO PHYTOPLASMA INFECTION: SIEVE ELEMENT OCCLUSION-RELATED (SEOR) PROTEINS.

The purpose of this chapter was to give insight to the unexplored role of sieve-element occlusion related proteins in the interaction with phytoplasmas.

3.1 SIEVE ELEMENT PLUGGING MECHANISM AND SIGNALING: AN INTRODUCTION

The phloem structural proteins

The presence of proteins inside the angiosperms' sieve elements is known since a long time (Jekat *et al.*, 2013). Phloem proteins, or P- proteins, is a term used to indicate in general the whole amount of compounds in the phloem sap (Anstead *et al.*, 2012). In mature sieve element they form a complex with the organelles in the lumen, through clamp-like structures.

Several P-proteins have been found inside the sieve elements: soluble proteins, mesh proteins that are filamentous proteins in the lumina, proteins included in plastids, parietal proteins pressed against the membrane as PP1 and PP2 of the Cucurbitaceae, but only in the Fabaceae there are forisomes (Tuteja *et al.*, 2010).

Each one of these proteinaceous structures is specialized in a particular function (Anstead *et al.*, 2013): various P-proteins can play a role against biotic or abiotic stresses in response to JA, SA or ethylene (PR proteins), mirosinases, glucanases, dehydrin or dehydrogenases; P-proteins can play a role as structural proteins as actin and tubulin family or they can have marginal roles in some biological processes (Anstead *et al.*, 2013). One of their role, still pretty unknown, is during the phloem plugging, before the callose deposition: they can be considered as a quick response to injury and they act inasmuch the callose response may be too

slow to reduce the leak (van Bel, 2006). In this scenario, the first P-proteins characterized, involved in the sieve element plugging, were the forisomes of Fabaceae: forisomes are proteins with a crystalline structure encoded by Sieve Element Occlusion genes (SEO). Forisomes are composed with a variable number of forisomettes and, with changing in the concentration of calcium, swell radially and contract longitudinally, acting in this way to block SE stream. The result of their action is stopping the phloem sap flow in case of stress of the plant or in case of injury (Tuteja *et al.*, 2010).

Considering the absence of forisomes in the other botanical family, a similar function of sealing should be carried out by some other proteins: in this level Sieve Element Occlusion Related (SEOR) proteins play their role (Anstead *et al.*, 2012; Ernst *et al.*, 2012).

Sieve element occlusion related proteins (SEOR)

First of all, it is necessary to clarify that forisomes and SEOR proteins, nevertheless having something in common, belong two different gene family: SEO and SEOR respectively (Knoblauch *et al.*, 2014).

Rüping *et al.*, (2010) described the phylogenesis of these two families dividing them in 7 groups and identifying the group 5 as peculiar of dycots plants. The phylogenetic study has revealed that all the SEOR genes, belonging to the group 5, derived from a common SEOR ancestor. For some of the plants analyzed in the study, some pseudogenes were found: it is thought that these pseudogenes are involved in the regulation of the main genes (Rüping *et al.*, 2010) inasmuch they fail to amplify transcripts in RT-PCR. There is a basilar SEO(R) common structure among all the proteins belonging to the two family: SEO-N terminal domain, “potential thioredoxin fold” domain, calsequestrin and C-terminal motif M1 with conserved cysteine residues (Ernst *et al.*, 2012; Rüping *et al.*, 2010).

In Arabidopsis there are two genes belonging to the SEOR family, *AtSEOR1* (*At3g01680.1*) and *AtSEOR2* (*At3g01670.1*) and one pseudogene. The two proteins act together to assembly filaments, with a size of 2 nm and formed by the bound of 10-100 filaments scattered in the sieve element lumina. Anstead *et al.*, (2012) reported that, under confocal microscopy. GFP-tagged AtSEOR1 has filamentous appearance inside the SE lumen, otherwise the AtSEOR2 would remain as globular parietal fluorescent dots: it has been shown that plants lacking one of the two gene did not show the filaments in the phloem lumen (Anstead *et al.*, 2012; Pagliari *et al.*, 2017). The enhancement of the filament formation seems to be operated by calcium ions linked to the calsequestrin, a binding protein for these ions (Rüping *et al.*, 2010): the increase of the calcium concentration inside the SE results in the formation of the filaments.

It has been demonstrated that the function of the two SEOR proteins in Arabidopsis is related with the sieve element sealing: mutant lines lacking the two genes had a leak nine times higher of wild type plants in case of mechanical injury (Jekat *et al.*, 2013), but surprisingly, in case of infection by phytoplasma, the

filaments were found in the lumen of plants highly colonized also in the knockout lines (Pagliari *et al.*, 2017), even if they seem unable to block sieve-element mass flow.

Interestingly the mutant line lacking AtSEOR1 seems to be able to limit the pathogen spread in case of infection by phytoplasma, suggesting that AtSEOR2 'free' inside the sieve elements could have a role in the defense mechanism against the pathogen (Bernardini *et al.*, 2020; Pagliari *et al.*, 2017). Pagliari *et al.*, (2018) speculated a possible bound of AtSEOR2 protein with AtRIN4-RPS2 or RPM1 guardee proteins (Afzal *et al.*, 2011).

Plant immunity: the guard and the decoy model

Plants have essentially two mechanisms to recognize and face the pathogens. The first way is based on the pathogen-associated molecular patterns (PAMPs, see chapter 1), that are recognized by the pattern recognition receptors (PRR) located on the plasma membrane. This kind of recognizing is at the base of the so-called Pattern triggered immunity (PTI). The second way comprises the effectors released by the pathogens and it is called Effector triggered immunity (ETI) (Dodds and Rathjen, 2010). Even if the responses are similar, ETI and PTI have a different magnitude and the whole amount of the responses is controlled by the interaction between calcium and map kinases (MAPKs) that produce a cascade of responses inside the plant (Dodds and Rathjen, 2010; van der Hoorn and Kamoun, 2008).

Phytoplasmas and bacteria produce effectors stimulating in this way the ETI process of defense.

Type 3 bacterial effectors are recognized *in planta* following two different models. In the first model an internal receptor is bound by an effector and enhances the activity of a resistance (R) gene. The receptor acts as a guardee of the complex and this mechanism is called guard model. In the decoy model, which is the second way to recognize the pathogen, the effector binds a protein that mimics the real effector target. This binding can enhance the activity of a R protein (Khan *et al.*, 2016; van der Hoorn and Kamoun, 2008) and the decoy competes with the real target of the effector. In both the model the R protein activates several pathways involved in the effector triggered immunity. One of the examples of the guard model is given by RPM1-interacting protein 4, commonly known as RIN4 (Khan *et al.*, 2016; Ray *et al.*, 2019; van der Hoorn and Kamoun, 2008). RIN4 has a key role both in PTI, decreasing the plant response to the pathogen (Afzal *et al.*, 2011), than in ETI. In fact, it has been demonstrated that the effectors of *Pseudomonas syringae* AvrB, AvrRPM1, AvrRpt2 and at least HopF2, target the host protein RIN4 (Dodds and Rathjen, 2010) that is the guardee of two leucine-rich repeat receptors: RPM1 and RPS2 (NB-LRR). RIN4 is an intrinsically disordered proteins, that contains several molecular recognizing features, called MoRF, that give it the ability to bind different effectors (Toruño *et al.*, 2019). Afzal and coworkers (Afzal *et al.*, 2013) described the RIN4 protein: RIN4 has two NOI domains in N and C and C-terminal cysteine rich, only parts predictable of the entire protein. After the binding with the effector, in RIN4 posttranslational modifications take place (Toruño *et al.*,

2019). Depending on the kind of modification, RIN4 enhances or inhibits the activity of the NLR gene: in case of phosphorylation, the signal, mediated by RIPK, results as the inhibition of RPM1; otherwise, in case of proteolysis the signal result is the activation of RPS2 (Figure 3.1). Several other functions involved RIN4, for a review see Toruño *et al.*, (2019).

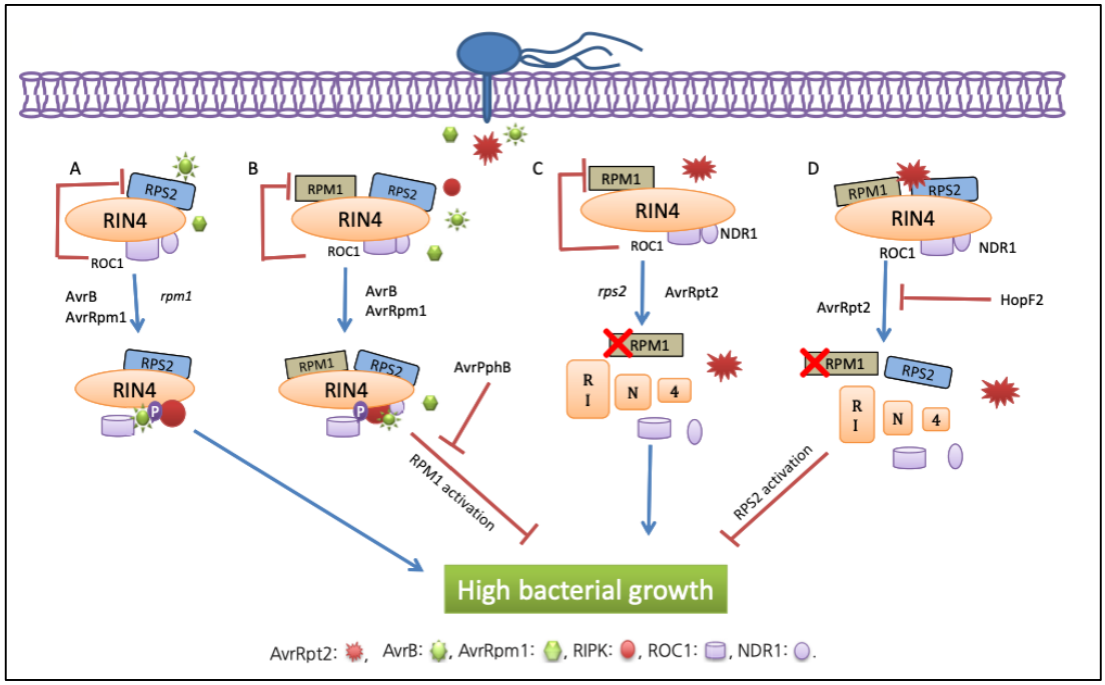

Figure 3.1 ***The activation of the R-proteins following the recognition of the effetors****. Depending on the kind of effector, RIN4 can be phosphorilated or degraded with the consequent activation of the RPM1 gene or the RPS2 gene. Image from Ray et al., 2019.*

Downstream from ETI and PTI: phytohormones and their relations with pathogens

From the ETI and PTI, the downstream to the major defense pathways is related in particular to the phytohormone response. Normally the main phytohormones involved in the process are salicylic acid and jasmonate-ethilene pathways (Dodds and Rathjen, 2010) to whom the other hormonal pathways are associated in different ways (Robert-Seilaniantz *et al.*, 2007). Salicylate, in fact is involved in the systemic acquired resistance resulting from the induction of the PR genes (Bari and Jones, 2009). The defense responses are strictly related with the fine-tuned salicylate-jasmonate ratio; several regulators intervene to maintain that ratio or to change it: some examples are given by NPR1, WRKY62, WRKY70, WRKY53, or the transcription factors JIN1 and MYC2, all having a key role in the antagonistic balance between the two phytohormones (Bari and Jones, 2009): several studies on different pathosystems had demonstrated the increase of one or the other hormone, depending on the relation of the pathogen with the plant: biotrophic or necrotrophic (Bari and Jones, 2009; Robert-Seilaniantz *et al.*, 2007). From a long time, the crosstalk between salicylate and jasmonate

has been reported as an antagonistic balance: the increase of one reduces the amount of the other (Robert-Seilaniantz *et al.*, 2011). Robert-Seilaniantz proposed a possible model of interaction in which auxins and cytokinins promotes the resistance enhancing the jasmonate pathway, while gibberellins promote the resistance enhancing the salicylate pathway. In this scenario ABA results as a player without a team and its role seems to be related with a general enhancement of the resistance through the abiotic stresses signaling (Robert-Seilaniantz *et al.*, 2007) (See 3.2).

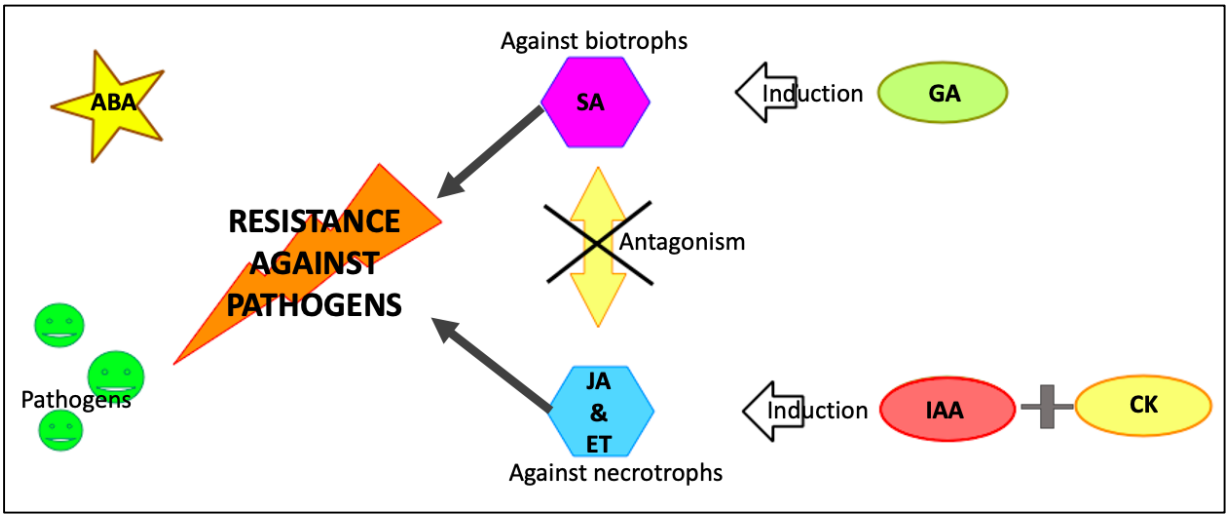

Figure 3.2 ***Possible model of interaction of phytohormones to face pathogen infection****. Adapted by Bernardini, from Robert-Seilaniantz 2007*

Phythohormone unbalance depends not only on the mechanism of action of the pathogens, and therefore on the possible defense available against them, but also on the kind of pathogen and its colonization tissue (Denancé *et al.*, 2013). In case of bacteria, infact, the Type III secretion system produces effectors (see chapter 1) that are able to create an hormone unbalance acting on different key gene regulating different paths (Denancé *et al.*, 2013) (Figure 3.3). As regards phytoplasmas, an example is given by the effector TENGU: it seems to act on the key genes of the auxin metabolism causing an alteration. In particular GH3.5 has been shown to act as a regulator of the SA pathway and IAA (Zhang *et al.*, 2007).

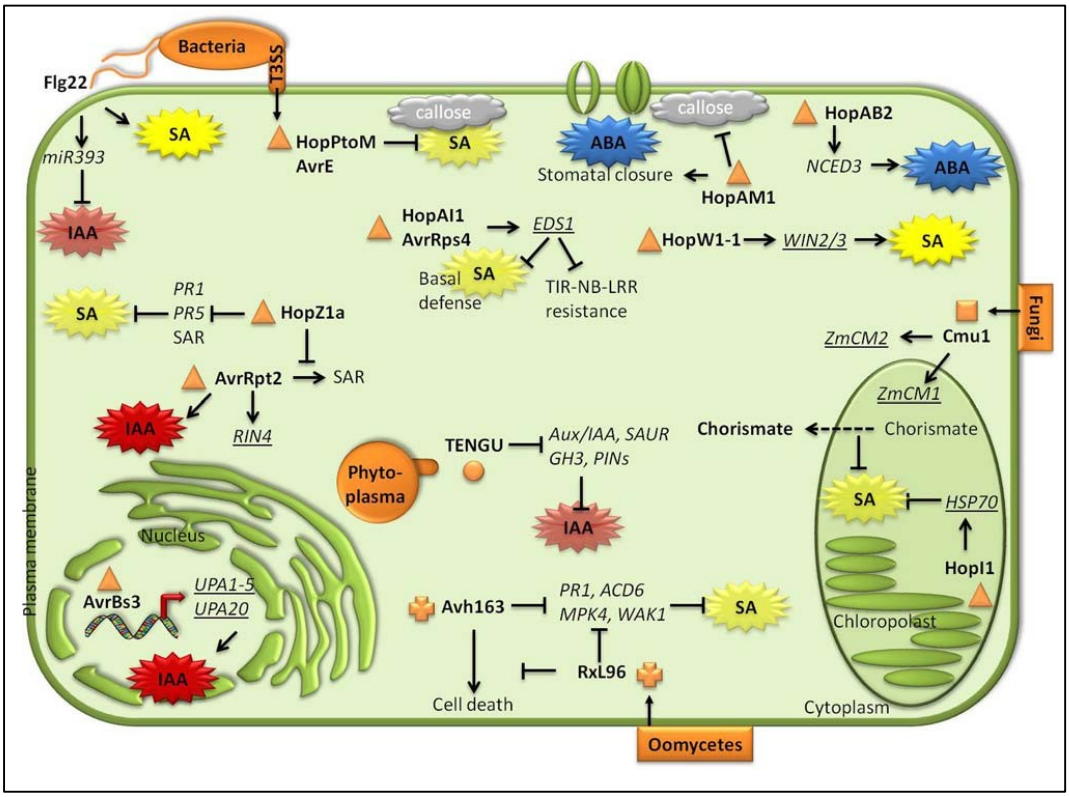

Figure 3.3 Strategies elaborated by pathogen and pests to interfere with the phytohormone synthesis and signaling. Image from Denancè et al., 2013.

References

Afzal, A.J., da Cunha, L., Mackey, D., 2011. Separable Fragments and Membrane Tethering of *Arabidopsis* RIN4 Regulate Its Suppression of PAMP-Triggered Immunity. Plant Cell 23, 3798–3811.

Afzal, A.J., Kim, J.H., Mackey, D., 2013. The role of NOI-domain containing proteins in plant immune signaling. BMC Genomics 14, 327.

Anstead, J.A., Froelich, D.R., Knoblauch, M., Thompson, G.A., 2012. Arabidopsis P-Protein Filament Formation Requires Both AtSEOR1 and AtSEOR2. Plant Cell Physiol. 53, 1033–1042.

Anstead, J.A., Hartson, S.D., Thompson, G.A., 2013. The broccoli (Brassica oleracea) phloem tissue proteome. BMC Genomics 14, 764.

Bari, R., Jones, J.D.G., 2009. Role of plant hormones in plant defence responses. Plant Mol. Biol. 69, 473–488.

Bernardini, C., Pagliari, L., De Rosa, V., Almeida-Trapp, M., Santi, S., Martini, M., Buoso, S., Loschi, A., Loi, N., Chiesa, F., Mithöfer, A., van Bel, A.J.E., Musetti, R., 2020. Pre-symptomatic modified phytohormone profile is associated with lower phytoplasma titres in an Arabidopsis seor1ko line. Sci. Rep. 10, 14770.

Denancé, N., Sánchez-Vallet, A., Goffner, D., Molina, A., 2013. Disease resistance or growth: the role of plant hormones in balancing immune responses and fitness costs. Front. Plant Sci. 4.

Dodds, P.N., Rathjen, J.P., 2010. Plant immunity: towards an integrated view of plant–pathogen interactions. Nat. Rev. Genet. 11, 539–548.

Ernst, A.M., Jekat, S.B., Zielonka, S., Muller, B., Neumann, U., Ruping, B., Twyman, R.M., Krzyzanek, V., Prufer, D., Noll, G.A., 2012. Sieve element occlusion (SEO) genes encode structural phloem proteins involved in wound

sealing of the phloem. Proc. Natl. Acad. Sci. 109, E1980–E1989.

Jekat, S.B., Ernst, A.M., Bohl, A. von, Zielonka, S., Twyman, R.M., Noll, G.A., Prüfer, D., 2013. P-proteins in Arabidopsis are heteromeric structures involved in rapid sieve tube sealing. Front. Plant Sci. 4.

Khan, M., Subramaniam, R., Desveaux, D., 2016. Of guards, decoys, baits and traps: pathogen perception in plants by type III effector sensors. Curr. Opin. Microbiol. 29, 49–55.

Knoblauch, M., Froelich, D.R., Pickard, W.F., Peters, W.S., 2014. SEORious business: structural proteins in sieve tubes and their involvement in sieve element occlusion. J. Exp. Bot. 65, 1879–1893.

Pagliari, L., Buoso, S., Santi, S., Furch, A.C.U., Martini, M., Degola, F., Loschi, A., van Bel, A.J.E., Musetti, R., 2017. Filamentous sieve element proteins are able to limit phloem mass flow, but not phytoplasma spread. J. Exp. Bot. 68, 3673–3688.

Pagliari, L., Buoso, S., Santi, S., Van Bel, A.J.E., Musetti, R., 2018. What slows down phytoplasma proliferation? Speculations on the involvement of AtSEOR2 protein in plant defence signalling. Plant Signal. Behav. 13, e1473666.

Ray, S.K., Macoy, D.M., Kim, W.-Y., Lee, S.Y., Kim, M.G., 2019. Role of RIN4 in Regulating PAMP-Triggered Immunity and Effector-Triggered Immunity: Current Status and Future Perspectives. Mol. Cells 42.

Robert-Seilaniantz, A., Grant, M., Jones, J.D.G., 2011. Hormone Crosstalk in Plant Disease and Defense: More Than Just JASMONATE-SALICYLATE Antagonism. Annu. Rev. Phytopathol. 49, 317–343. https://doi.org/10.1146/annurev-phyto-073009-114447

Robert-Seilaniantz, A., Navarro, L., Bari, R., Jones, J.D., 2007. Pathological hormone imbalances. Curr. Opin. Plant Biol. 10, 372–379.

Rüping, B., Ernst, A.M., Jekat, S.B., Nordzieke, S., Reineke, A.R., Müller, B., Bornberg-Bauer, E., Prüfer, D., Noll, G.A., 2010. Molecular and phylogenetic characterization of the sieve element occlusion gene family in Fabaceae and non-Fabaceae plants. BMC Plant Biol. 10, 219.

Toruño, T.Y., Shen, M., Coaker, G., Mackey, D., 2019. Regulated Disorder: Posttranslational Modifications Control the RIN4 Plant Immune Signaling Hub. Mol. Plant. Microbe Interact. 32, 56–64.

Tuteja, N., Umate, P., van Bel, A.J.E., 2010. Forisomes: calcium-powered protein complexes with potential as ‘smart’ biomaterials. Trends Biotechnol. 28, 102–110.

van Bel, A.J., 2006. Sieve-pore plugging mechanisms, in: Cell-Cell Channels. Springer, pp. 113–118.

van der Hoorn, R.A.L., Kamoun, S., 2008. From Guard to Decoy: A New Model for Perception of Plant Pathogen Effectors. Plant Cell 20, 2009–2017.

Zhang, Z., Li, Q., Li, Z., Staswick, P.E., Wang, M., Zhu, Y., He, Z., 2007. Dual regulation role of GH3. 5 in salicylic acid and auxin signaling during Arabidopsis-Pseudomonas syringae interaction. Plant Physiol. 145, 450–46

3.2 PRE-SYMPTOMATIC MODIFIED PHYTOHORMONE PROFILE IS ASSOCIATED WITH LOWER PHYTOPLASMA TITRE IN AN ARABIDOPSIS SEOR1KO LINE

CHIARA BERNARDINI[1], LAURA PAGLIARI[1], VALERIA DE ROSA[1], MARILIA ALMEIDA-TRAPP[2], SIMONETTA SANTI[1], MARTA MARTINI[1], SARA BUOSO[1], ALBERTO LOSCHI[1], NAZIA LOI[1], FIORELLA CHIESA[1], AXEL MITHÖFER[3], AART J. E. VAN BEL[4], RITA MUSETTI[1]*

[1]Department of Agricultural, Food, Environmental and Animal Sciences, University of Udine, via delle Scienze, 206 I-33100 Udine, Italy

[2]Department of Bioorganic Chemistry, Max Planck Institute for Chemical Ecology, Hans-Knöll-Straße 8, D-07745 Jena, Germany

[3]Research Group Plant Defense Physiology, Max Planck Institute for Chemical Ecology, Hans-Knöll-Straße 8, D-07745 Jena, Germany

[4]Institute of Phytopathology, Justus-Liebig University, Heinrich-Buff-Ring 26–32, D-35392 GIESSEN, GERMANY

* Correspondence: Prof. Rita Musetti rita.musetti@uniud.it

Keywords: *Arabidopsis thaliana*; AtSEOR1; AtSEOR2; phytohormones; phytoplasmas; plant defence; sieve element; sieve-element occlusion

One of the possible interactions of AtSEOR2 is with the phytohormone metabolism. In the following paper, published in September 2020, we study the phytohormone concentration in the pre-symptomatic stage and in the fully symptomatic stage. This paper is the result of a collaboration with the Max Planck Institute for Chemical Ecology in Jena.

www.nature.com/scientificreports

SCIENTIFIC REPORTS
nature research

OPEN

Pre-symptomatic modified phytohormone profile is associated with lower phytoplasma titres in an Arabidopsis *seor1ko* line

Chiara Bernardini[1], Laura Pagliari[1], Valeria De Rosa[1], Marilia Almeida-Trapp[2], Simonetta Santi[1], Marta Martini[1], Sara Buoso[1], Alberto Loschi[1], Nazia Loi[1], Fiorella Chiesa[1], Axel Mithöfer[3], Aart J. E. van Bel[4] & Rita Musetti[1]✉

The proteins AtSEOR1 and AtSEOR2 occur as conjugates in the form of filaments in sieve elements of *Arabidopsis thaliana*. A reduced phytoplasma titre found in infected defective-mutant *Atseor1ko* plants in previous work raised the speculation that non-conjugated SEOR2 is involved in the phytohormone-mediated suppression of Chrysanthemum Yellows (CY)-phytoplasma infection transmitted by *Euscelidius variegatus* (Ev). This early and long-lasting SEOR2 impact was revealed in *Atseor1ko* plants by the lack of detectable phytoplasmas at an early stage of infection (symptomless plants) and a lower phytoplasma titre at a later stage (fully symptomatic plants). The high insect survival rate on *Atseor1ko* line and the proof of phytoplasma infection at the end of the acquisition access period confirmed the high transmission efficiency of CY-phytoplasma by the vectors. Transmission electron microscopy analysis ruled out a direct role of SE filament proteins in physical phytoplasma containment. Time-correlated HPLC–MS/MS-based phytohormone analyses revealed increased jasmonate levels in midribs of *Atseor1ko* plants at an early stage of infection and appreciably enhanced levels of indole acetic acid and abscisic acid at the early and late stages. Effects of Ev-probing on phytohormone levels was not found. The results suggest that SEOR2 interferes with phytohormonal pathways in Arabidopsis midrib tissues in order to establish early defensive responses to phytoplasma infection.

Phytoplasmas affect hundreds of agronomically important plant species worldwide, including ornamentals, vegetables and fruit trees[1], causing profound alterations in plant cytology and physiology, by modulation of transcript and protein profiles[2,3] and changes in the hormonal balance (for a review see[4]).

Phytoplasmas are prokaryotic plant pathogens belonging to the class *Mollicutes*. In plant hosts, phytoplasmas are restricted to the sieve elements (SEs)[5], which are responsible for the translocation of nutrients and a broad spectrum of signals. Phloem-feeding insects act as vector hosts that contaminate healthy plants with phytoplasmas ingested during previous probing of infected plants[6].

In Arabidopsis, two non-redundant Sieve-Element Occlusion Related (SEOR) genes, *AtSEOR1* (At3g01680) and *AtSEOR2* (At3g01670)[7], were reported to be necessary for the formation of SE protein filaments through a heteromeric assemblage of the two SEOR proteins[8]. Studying the role of SEOR proteins following Chrysanthemum Yellows (CY)-phytoplasma infection in *Arabidopsis thaliana*, Pagliari et al.[9] noted that the *Atseor1ko* mutant line hosted a considerably lower number of phytoplasmas, even though the phloem flow (and thus the pathogen spread capability) is not affected[9]. This observation led to the hypothesis that an unknown SEOR2-associated mechanism assists the plant to combat the pathogen. It matches the idea that AtSEOR2 proteins, which are not

[1]Department of Agricultural, Food, Environmental and Animal Sciences, University of Udine, via delle Scienze, 206, 33100 Udine, Italy. [2]Department of Bioorganic Chemistry, Max Planck Institute for Chemical Ecology, Hans-Knöll-Straße 8, 07745 Jena, Germany. [3]Research Group Plant Defense Physiology, Max Planck Institute for Chemical Ecology, Hans-Knöll-Straße 8, 07745 Jena, Germany. [4]Institute of Phytopathology, Justus-Liebig University, Heinrich-Buff-Ring 26–32, 35392 Giessen, Germany. ✉email: rita.musetti@uniud.it

conjugated with SEOR1, as is the case in *Atseor1 ko* plants, may be involved in plant immune responses[10,11] or in phytohormone-mediated signalling pathways[12].

Phytohormones are key mediators in plant adaptation to environmental changes[13] and, hence, are also engaged in responses to beneficial[14] and pathogenic microorganisms[15]. In general, phytohormones sustain a dynamic network to optimize plant-responsive processes[16]. A number of studies addressed phytohormone levels in phytoplasma-infected plants (for a review see[4]). In accordance with this information, increased salicylic acid (SA) and abscisic acid (ABA) levels and a decreased indole-3-acetic acid (IAA) content are to be expected as responses to phytoplasma infection, while the picture for other phytohormones is unclear[4]. Simultaneous analyses of more than two phytohormones during phytoplasma infections are scarce[17,18] and give rise to contrasting conclusions. The conflicting results may be due to the use of diverse pathosystems (model plants[19]; field-grown woody plants[20]), different sampling methods (whole leaves[21]; leaf midribs[22]; seeds[23]; or phloem sap[24]), and dissimilar techniques (phytohormone quantification by HPLC analysis[21]; gene expression analyses[20,25]). All in all, the phytohormonal response(s) to phytoplasma infection remain(s) largely unclear thus far.

We investigated whether phytohormonal production is associated with the presence of free SEOR2 and, if so, which phytohormone levels at which stage are affected by phytoplasma infection. An attempt was made to localize the phytohormone production. To this end, phytohormone levels were monitored both in the midribs and laminar tissues of wild-type, *Atseor1ko* and *Atseor2ko* Arabidopsis lines at the beginning and at the end of the phytoplasma infection. As phytohormone synthesis could also have been activated by the leafhopper vector *Euscelidius variegatus*[26], Arabidopsis plants not infested by leafhoppers and plants infested by leafhoppers free from phytoplasmas were analysed in parallel. Furthermore, phytoplasma titre was quantified at the same infection stages and leafhopper survival rates were evaluated to exclude differences in insect-mediated transmission efficiency in the three Arabidopsis lines. As a structural element, transmission electron microscopy (TEM) analyses were performed to determine possible structural modifications brought about by phytoplasma infection.

Results

Phytoplasma transmission by *Euscelidius variegatus*. In this study, three treatment groups of the three Arabidopsis plant lines were investigated: (1) plants (no-Ev) not infested by *E. variegatus*, (2) plants (H-Ev) infested by *E. variegatus* from a healthy colony that never fed on phytoplasma-infected plants, and (3) plants (CY-Ev) infested by CY-infected *E. variegatus*. For each analysis plants were tested at two stages, i.e. 5 (T1) and 20 days (T2) after the end of the inoculation access period (IAP), which are referred to as the "early" and "late" stage of infection, respectively.

Three individuals of healthy *E. variegatus* or CY-infected *E. variegatus* were placed on wild-type, *Atseorko1* and *Atseor2ko* Arabidopsis plants. The insects were manually removed after 7 days (i.e. at the end of IAP) and the number of living individuals was counted. The survival rates of healthy *E. variegatus*, which ranged between 59 and 79% (Fig. S1), showed no statistically significant differences between the respective Arabidopsis lines. Yet there was a tendency for the healthy individuals to survive slightly better on the *Atseorko* mutants (Fig. S1). This tendency became statistically significant (Fig. S1) for CY-infected-*E. variegatus*, which suffered from decreased fitness on wild-type plants as compared to the mutants (with a lower survival rate, ranging from 19.5 to 38.9%).

Healthy and CY-infected *E. variegatus* were then pooled (as reported below) and processed for phytoplasma detection. PCR analysis, with a 1,250 bp amplicon as a final product, confirmed the presence of phytoplasmas in all pools from 3 insects having fed on CY-infected chrysanthemum. The success of the infection in CY-Ev plants was further confirmed by symptom development in each Arabidopsis line under investigation (100% plants were positive to CY phytoplasma following inoculation with vectors having fed on CY-infected chrysanthemum, with a transmission rate (p) of 1[27].

Five days after the IAP, no symptoms were visible in the lines exposed to the CY-infected *E. variegatus* (Fig. 1A,C,E). Initial symptoms (leaf chlorosis and petiole elongation) emerged starting from the 14th day after IAP and characteristic CY symptoms became fully discernible 20 days after IAP (Fig. 1B,D,F). In fact, at this time point, all infected plant lines showed reduced growth and shorter, yellowish leaves, with a thick main vein. Chlorosis progressed from the youngest leaves towards the others. The appearance of the symptoms in wild-type and mutant lines was similar at this stage of infection (Fig. 1B,D,F).

Phytoplasma quantification in Arabidopsis lines. To quantify the phytoplasma inside the CY-Ev Arabidopsis lines, qPCR was carried out using genomic DNA extracted from 12 plants for each infected Arabidopsis line.

At the early stage of infection (i.e. 5 days after IAP), none of the *Atseor1ko* plants tested positive for the presence of phytoplasma, while 58% of wild-type plants and 42% of *Atseor2ko* line did so (Fig. 2A). At this timepoint, the phytoplasma titre was lower in comparison to that found at the late stage of infection, and did not significantly differ among the Arabidopsis lines (Fig. 2B). The highest cycle quantification (Cq) value to detect phytoplasma DNA in 100 mg of plant tissue was 32.83 for wild-type, corresponding to 7.76E+03 genome units (GUs), 34.30 for *Atseor2ko*, corresponding to 2.73E+03 GUs, while none of *Atseor1ko* plants resulted positive for phytoplasma presence. At the late stage of infection (i.e. 20 days after IAP), 100% of the plants treated with CY-Ev tested positive for phytoplasmas (Fig. 2A), but the phytoplasma titre in the *Atseor1ko* line was significantly lower than in *Atseor2ko* or wild-type plants (Fig. 2B and[9]). The highest Cq value to detect phytoplasma DNA in 100 mg of plant tissue was 18.38 for wild-type, corresponding to 2.05E+08 GUs, 18.07 for *Atseor2ko*, corresponding to 2.70E+08 GUs, 20.17 for *Atseor1ko* corresponding to 6.62E+08 GUs.

Ultrastructural modifications in midrib phloem at the early and late stage of infection. Both *AtSEOR1* and *AtSEOR2*[8,28] are regarded as being necessary for the formation of SE protein filaments in Arabi-

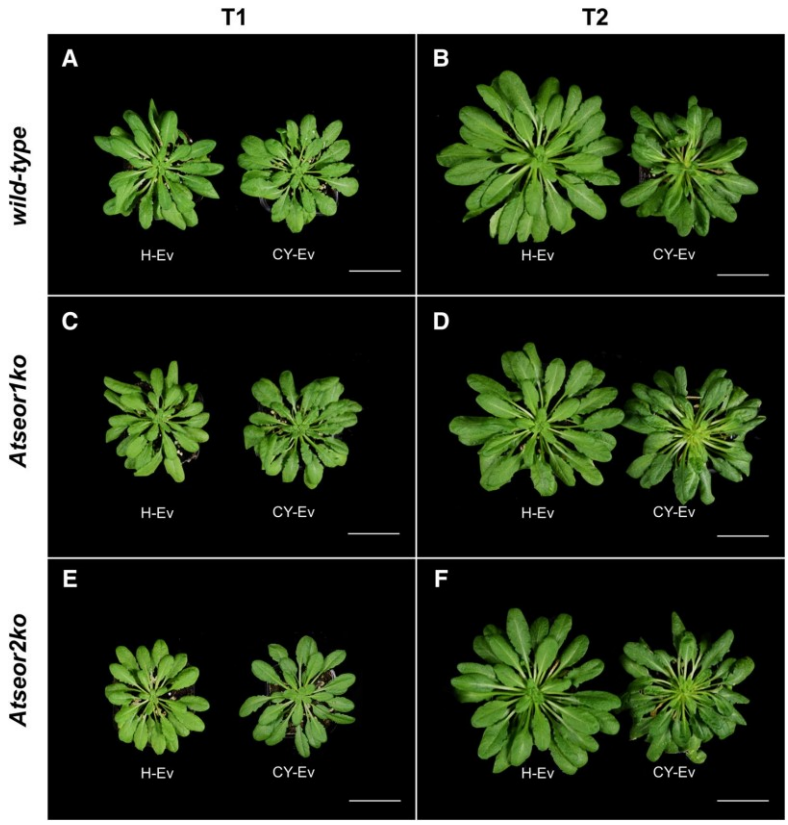

Figure 1. Phenotypes of *Arabidopsis thaliana* lines infested by healthy leafhoppers (H-Ev) or infested by CY-infected leafhoppers (CY-Ev) at the early (5 days after IAP, T1), and late stage (20 days after IAP, T2) of infection. The various conditions are indicated as follows: (**A**) and (**B**) wild-type, (**C**) and (**D**) *Atseor1ko* and **E** and **F** *Atseor2ko*, infested by healthy leafhoppers (H-Ev) or infested by CY-infected leafhoppers (CY-Ev). At an early infection stage (**A**,**C**,**E**) infected and healthy plants looked similar, symptoms manifested at the late (T2) stage (**B**,**D**,**F**), when chlorosis and leaf roll appeared. At both stages of infection, no differences between wild-type and the mutant lines were evident. Bars correspond to 5 cm.

dopsis. As expected[8], the SEs in the no-Ev wild-type line contained protein filaments, scattered throughout the SE lumen (Fig. 3A,G) and accumulated in the proximity of the sieve plates (Fig. 3D,J). On the contrary, the two no-Ev mutants, which are unable to form the respective SEOR partner proteins, showed no filaments in either the lumen (Fig. 3B,C,H,I) or near the sieve plates (Fig. 3E,F,K,L).

In order to examine leafhopper- or phytoplasma-induced ultrastructural modifications in SEs, 6 H-Ev and 6 CY-Ev plants of each line were sampled for TEM analysis and compared with the corresponding no-Ev plants at 5 and 20 days after IAP. Five days after IAP, the H-Ev plants (Fig. 4A–F) did not show ultrastructural changes as compared to the no-Ev plants (Fig. 3). The SEs in the wild-type Arabidopsis showed protein filaments both in SE lumen (Fig. 4A) and near the sieve plates (Fig. 4D). As in the no-Ev plants (Fig. 3), the H-Ev mutant plants did not show filaments in the lumen of SEs (Fig. 4B,C) or near the sieve plates (Fig. 4E,F).

At the early stage (5 days after IAP), the CY-Ev wild-type plants (Fig. 4G,J) did not differ from their controls (Fig. 4A,D), in that protein filaments had accumulated in SEs (Fig. 4G,J). At this stage, *Atseor1ko* and *Atseor2ko* CY-Ev plants did not show any ultrastructural alterations as well, because SE filaments were not detected (Fig. 4H,I,K,L) just as in their controls (Fig. 4B,C,E,F). At this time-point, phytoplasmas were not found in TEM pictures in any of the CY-Ev Arabidopsis lines (Fig. 4G–L).

Twenty days after IAP, the H-Ev plants (Fig. 5A–F) contained SE protein filaments only in the wild-type individuals (Fig. 5A,D) and not in the mutants (Fig. 5B,C,E,F) as in the no-Ev plants (Fig. 3). By contrast, SEs of all CY-Ev lines were characterized by the presence of filaments (Fig. 5G–L). Phytoplasmas were abundant throughout the entire SE, both in the SE lumen (Fig. 5G–I) and in proximity of the sieve plates (Fig. 5J–L).

A

Infection stage	Mutant line	Phytoplasma presence
T1	*Wild-type*	58,33%
	Atseor1ko	0,00%
	Atseor2ko	41,66%
T2	*Wild-type*	100%
	Atseor1ko	100%
	Atseor2ko	100%

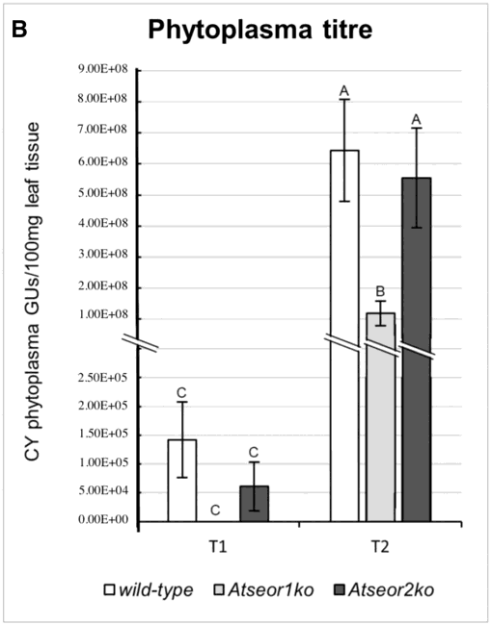

Figure 2. The CY phytoplasma titre and the percentage of infected plants at the early (5 days after IAP, T1) and late (20 days after IAP, T2) stage of infection. The percentage of infection (**A**) expresses the number of positive plants detected by real-time PCR out a total of 12 plants. Phytoplasma titre (**B**) is expressed as the number of CY phytoplasma genome units (GUs) per 100 mg of leaf sample to normalize the data. Different letters indicate different means according to the Holm-Sidak post hoc test, $P < 0.05$. Error bars indicate Standard Error of the Mean of 12 biological replicates for each condition.

Phytohormone quantification. To assess whether phytohormone-related defence mechanisms were activated in the Arabidopsis lines under investigation and to determine time and location of the activation, stress-related phytohormones were measured in extracts from no-Ev, H-Ev or CY-Ev plants, of wild-type, *Atseor1ko,* and *Atseor2ko* lines. For each condition, 6 plants were analysed and phytohormones were measured separately in laminae and midribs that were sampled at 5 days and 20 days after IAP (Tables 1, 2).

HPLC–MS/MS analysis revealed that the SA level was not affected by *E. variegatus* infestation at both time intervals in both tissues of H-Ev plants (Fig. 6A,B). SA levels in the laminar tissues of all CY-infected lines did not change significantly (Fig. 6A), with exception of *Atseor2ko* plants at the late stage of infection. In midribs, a significant increase in the SA levels only occurred in *Atseor2ko* CY-EV plants at the early stage of infection (Fig. 6B).

The JA and JA-Ile levels were not affected by *E. variegatus* infestation at both time intervals in laminae and midribs of H-Ev plants (Fig. 7A–D). This insensitivity contrasted the significant increase in JA levels in CY-Ev midribs of *Atseor1ko* line as compared to those of H-Ev and no-Ev plants at the early stage of infection (Fig. 7B). *Atseor2ko* line showed an opposite trend: both JA and JA-Ile levels decreased at the early stage of infection in

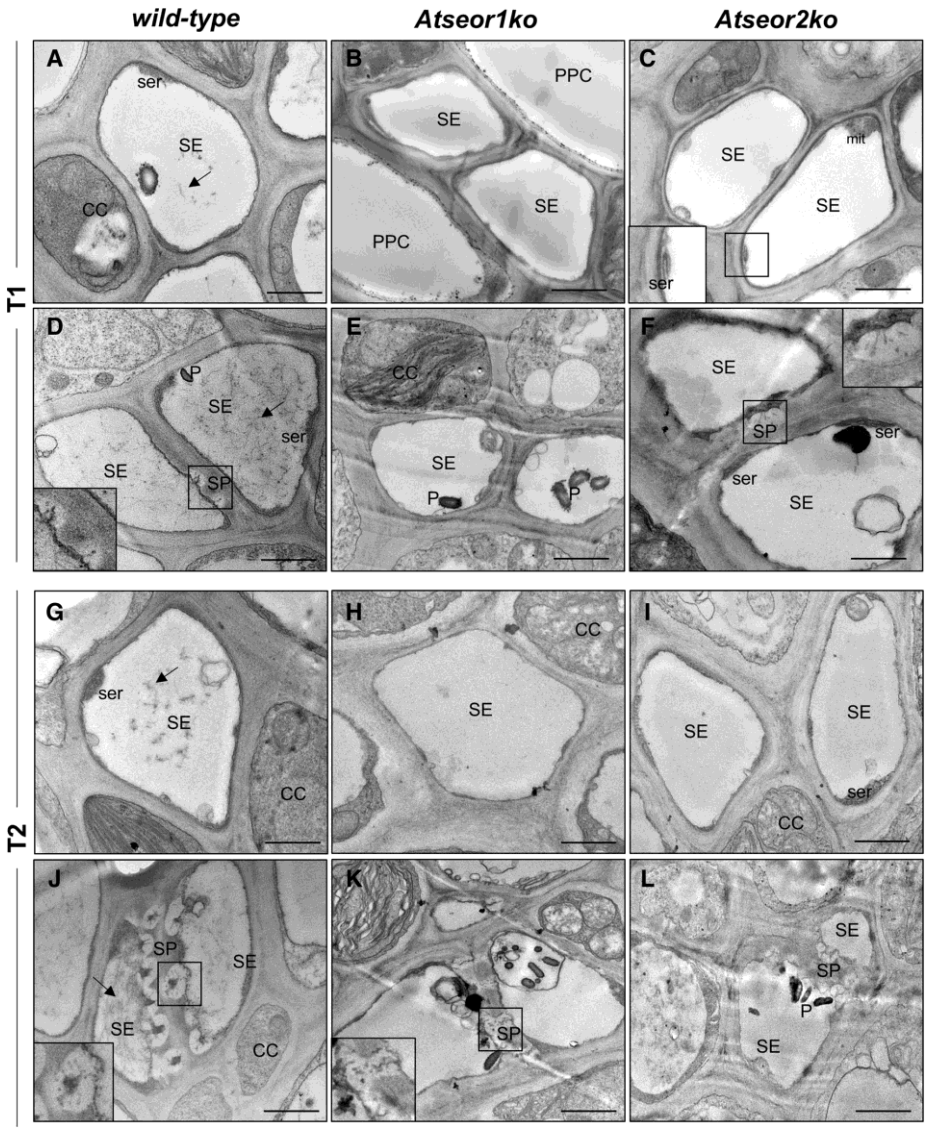

Figure 3. Ultrastructure of sieve elements in the three Arabidopsis lines not submitted to *Euscelidius variegatus* infestation (no-Ev plants). Phloem cross-sections were examined by TEM at T1 and T2s [i.e. respectively 5 (**A**–**F**) and 20 (**G**–**L**) days after the end of IAP] with the focus on structures in the SE lumen (**A**–**C**, **G**–**I**) and at the SPs (**D**–**F**, **J**–**L**). The wild-type line (**A**,**D**,**G**,**J**) contained SE protein filaments (black arrows). Both mutant lines, *Atseor1 ko* (**B**,**E**,**H**,**K**) and *Atseor2ko* (**C**,**F**,**I**,**L**), contained no protein filaments in either the SE lumen or in the SPs. *CC* companion cell, *mit* mitochondrion, *PPC* phloem parenchyma cell, *P* plastids, *SE* sieve element, *ser* sieve element reticulum, *SP* sieve plate. Bars correspond to 1 µm.

midribs. In laminae of all CY-infected lines JA and JA-Ile levels did not change in comparison with those of their controls (Fig. 7A,C).

The IAA levels were not affected by *E. variegatus* infestation at both time intervals in both tissues of H-Ev plants (Fig. 8A,B). The IAA concentrations in laminae decreased in the three CY-Ev lines 5 and 20 days after IAP (Fig. 8A), with a significant decrease in the two mutant lines at the early stage of infection. In midribs, the IAA concentration showed a statistically significant increase in wild-type CY-Ev samples, as compared to the

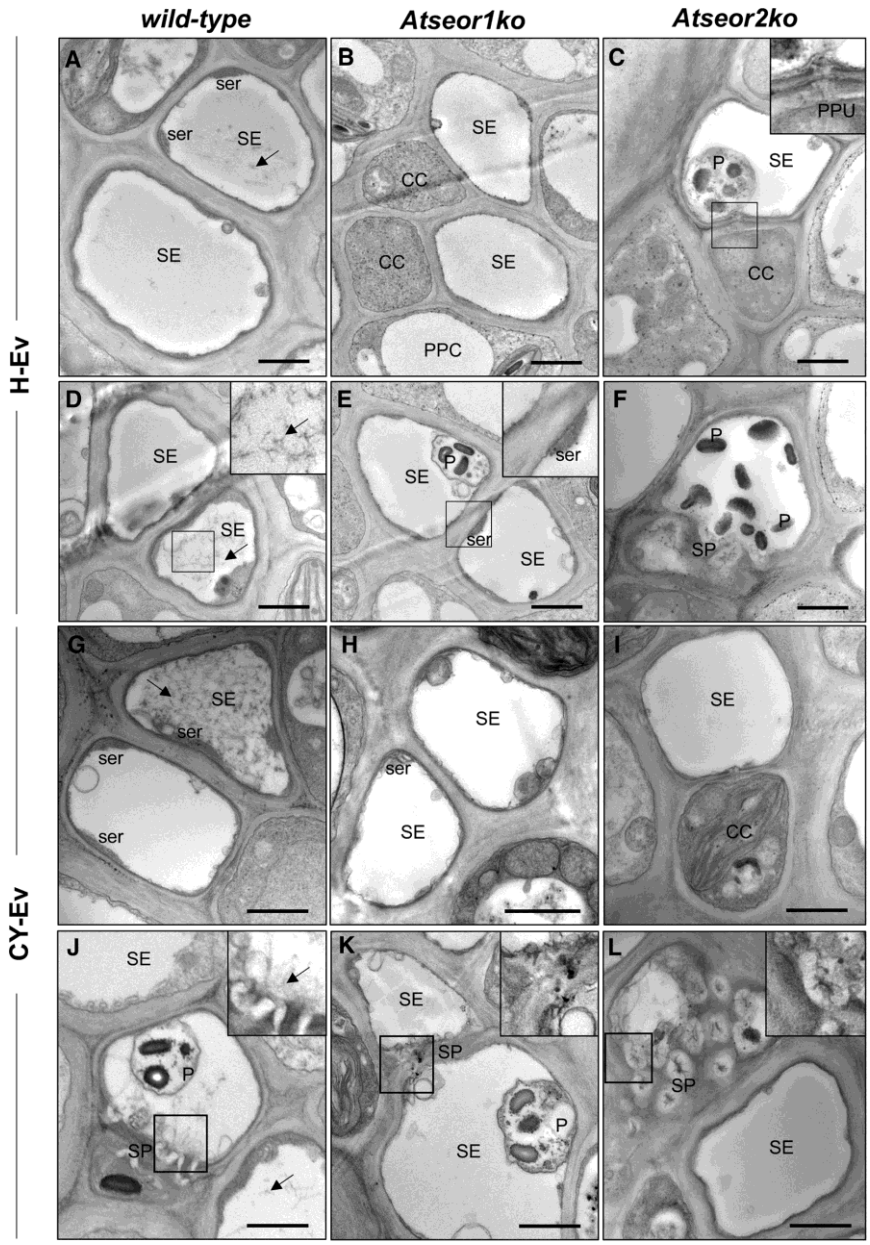

Figure 4. Ultrastructure of the sieve elements in three Arabidopsis lines at the early stage (5 days after IAP) of CY phytoplasma infection. Phloem cross-sections were examined by TEM in Arabidopsis lines infested by healthy leafhoppers (H-Ev, **A**–**F**) or infested by CY-infected leafhoppers (CY-Ev, **G**–**L**) with the focus on structures in the SE lumen (**A**–**C**, **G**–**I**) and at the SPs (**D**–**F**, **J**–**L**). The H-Ev (**A**,**D**) and CY-Ev (**G**,**J**) wild-type line contained SE protein filaments (black arrows). Mutant lines, both H-Ev (**B**,**C**,**E**,**F**) and CY-Ev (**H**,**I**,**K**,**L**), contained no protein filaments in either the SE lumen or in the SPs. In each Arabidopsis line, phytoplasmas were not detected. *CC* companion cell, *PPC* phloem parenchyma cell, *P* plastids, *PPU* pore-plasmodesma unit, *SE* sieve element, *ser* sieve element reticulum, *SP* sieve plate. Bars correspond to 1 µm.

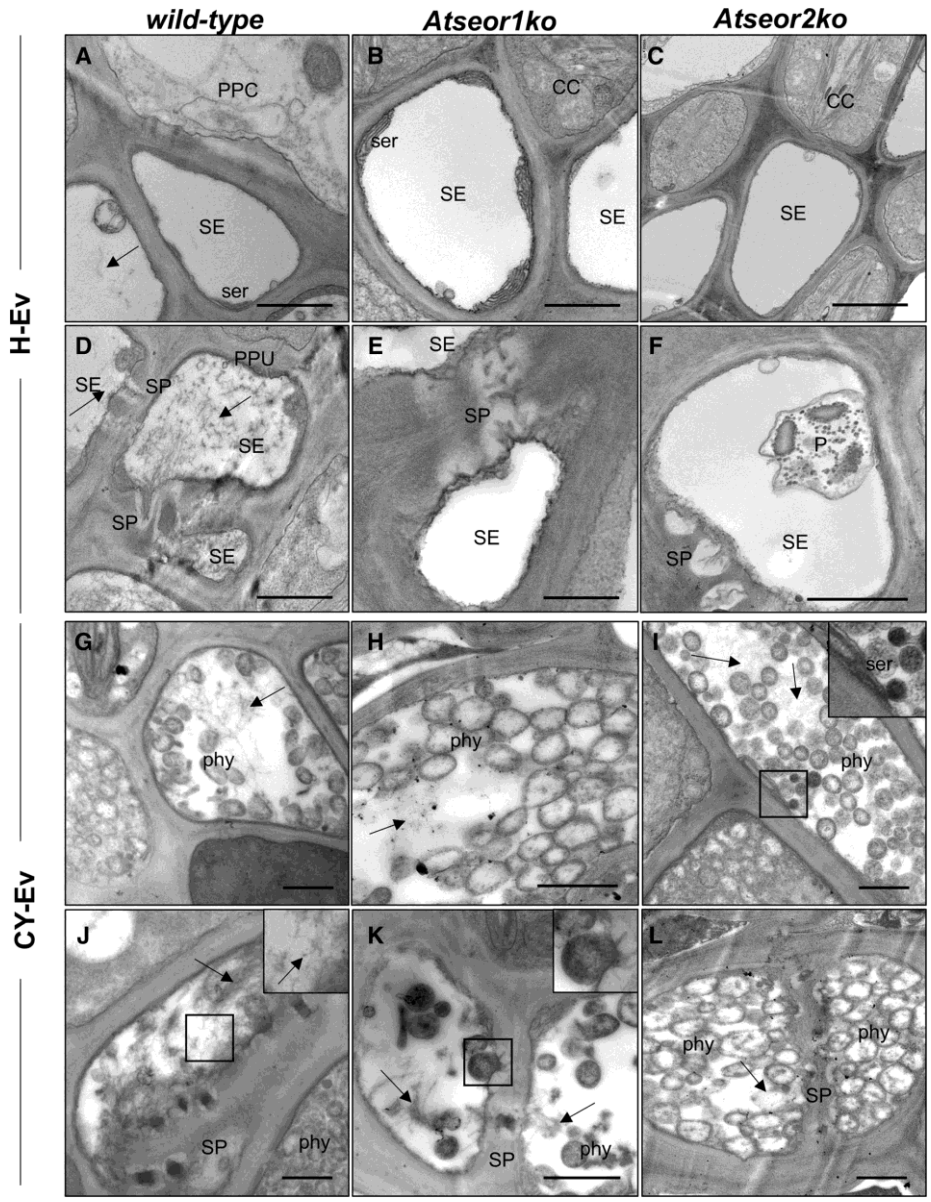

Figure 5. Ultrastructural modifications in three Arabidopsis lines at the late stage of infection. Phloem cross-sections of Arabidopsis lines infested by healthy leafhoppers (H-Ev, **A**–**F**) or infested by CY-infected leafhoppers (CY-Ev, **G**–**L**) were examined by TEM. SEs of H-Ev wild-type plants (**A**,**D**) contain protein filaments (black arrows) dispersed in the lumen (**A**) and accumulated at the SPs (**D**), while SEs of mutant lines (**B**,**C**,**E**,**F**) do not. They are visible in each CY-Ev Arabidopsis line (**G**–**L**, black arrows) as filamentous masses both in the SE lumen (**G**–**I**) and at the SPs (**J**–**L**) and numerous phytoplasmas are present in SEs (**G**–**I**) and at the SPs (**J**–**L**). *CC* companion cell, *PPC* phloem parenchyma cell, *phy* phytoplasmas, *P* plastids, *PPU* pore-plasmodesma unit, *SE* sieve element, *ser* sieve element reticulum, *SP* sieve plate. Bars correspond to 1 µm.

		SA lam	SA mid	JA lam	JA mid	JA-ile lam	JA-ile mid	IAA lam	IAA mid	ABA lam	ABA mid
T1	Wild type	=	=	=	=	=	=	–	=	=	=
	Atseor1ko	=	=	=	+	=	=	–	+	=	+
	Atseor2ko	=	+	=	–	=	–	–	=	=	+
T2	Wild type	=	=	=	=	=	=	–	+	=	=
	Atseor1ko	=	=	=	=	=	=	–	+	=	+
	Atseor2ko	+	=	=	=	=	=	–	=	=	=

Table 1. The table sums up the variations of phytohormone levels in the CY-Ev *Arabidopsis* lines during the infection compared to their respective H-Ev control plants. T1 and T2 indicate, respectively, 5 and 20 days after the end of IAP. = unchanged hormone level; + increased hormone level; – decreased hormone level.

		SA lam	SA mid	JA lam	JA mid	JA-ile lam	JA-ile mid	IAA lam	IAA mid	ABA lam	ABA mid
No-Ev *versus* CY-Ev	T1	=+	=+	==	+=	==	=–	–	++	–=	++
	T2	=+	==	==	==	==	==	==	+=	==	+=
H-Ev *versus* CY-Ev	T1	==	=+	==	+–	==	=–	–	+=	==	++
	T2	=+	==	==	==	==	==	–	+=	==	+=

Table 2. Responsiveness of *Atseor1ko* and *Atseor2ko* lines to phytoplasma infection (No-Ev, H-Ev or CY-Ev) at 5 (T1) and 20 (T2) days after the end of IAP. == (yellow): no significant differences in both *Atseor1ko* and *Atseor2ko*. ++ (yellow): significant increase in both *Atseor1ko* and *Atseor2ko*. –– (yellow): significant decrease in both *Atseor1ko* and *Atseor2ko*. =+ (light green): no significant differences in *Atseor1ko*, significant increase in *Atseor2ko*. =– (light red): no significant differences in *Atseor1ko*, significant decrease in *Atseor2ko*. += (light green): significant increase in *Atseor1ko*, no significant differences in *Atseor2ko*. –= (light red): significant decrease in *Atseor1ko*, no significant differences in *Atseor2ko*. +– (orange): significant increase in *Atseor1ko*, significant decrease in *Atseor2ko*.

H-Ev or no-Ev plants, 20 days after IAP (+190% was consistently enhanced). Interestingly, IAA level showed a significant increase at both time-points in the midribs of *Atseor1ko* plants (+93% at the early stage of infection and +357% at the late stage).

The ABA levels were not affected by *E. variegatus* infestation at both time intervals in both tissues of H-Ev plants (Fig. 8C,D). Following phytoplasma infection (CY-Ev plants), no significant changes were found in laminae of Arabidopsis lines at both time points (Fig. 8C). In the midribs, ABA levels remained unchanged in wild-type plants at both time points and in *Atseor2ko* at late stage of infection (Fig. 8D).

In comparison with the No-Ev or H-Ev samples, the ABA concentrations were significantly increased in CY-Ev in the midribs at both time-points in *Atseor1ko* plants (+177% at the early infection stage and +530% at the late infection stage) and at the early stage of infection in *Atseor2ko* plants (+242%).

All in all, infestation by *E. variegatus* does not seem to seriously affect the hormonal balance (Figs. 6, 7, 8), whereas CY infection is associated with changes on JA, IAA and ABA levels, in particular in the midribs of *Atseor1ko* plants during the pre-symptomatic early stage (Tables 1, 2).

Discussion

The *Atseor1ko* line limits phytoplasma replication from an early stage of infection onwards. In search for a role for SE protein filaments in response to phytoplasma infection[9], phytoplasma-infected *Atseor1ko* plants turned out to host a significantly lower phytoplasma titre in comparison to wild-type and *Atseor2ko* lines,

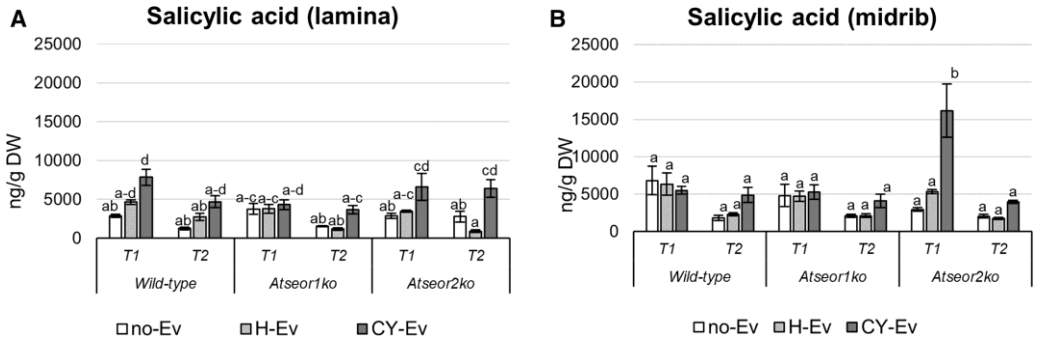

Figure 6. Salicylic acid levels in laminae and midribs of the three Arabidopsis lines non-infested by leafhoppers (no-Ev) or infested by healthy leafhoppers (H-Ev) or infested by CY-infected leafhoppers (CY-Ev), at the early (5 days after IAP, T1) and late (20 days after IAP, T2) stages of infection. The phytohormone levels are expressed as ng per g of tissue dry weight. Statistical analysis was performed using the Tukey HSD test as the post hoc test in a three-way ANOVA. Different letters (a, b, c) above the bars indicate significant differences, with $P < 0.05$; (a–c = abc, a–d = abcd). Error bars indicate the Standard Error of the Mean of 6 biological replicates for each condition.

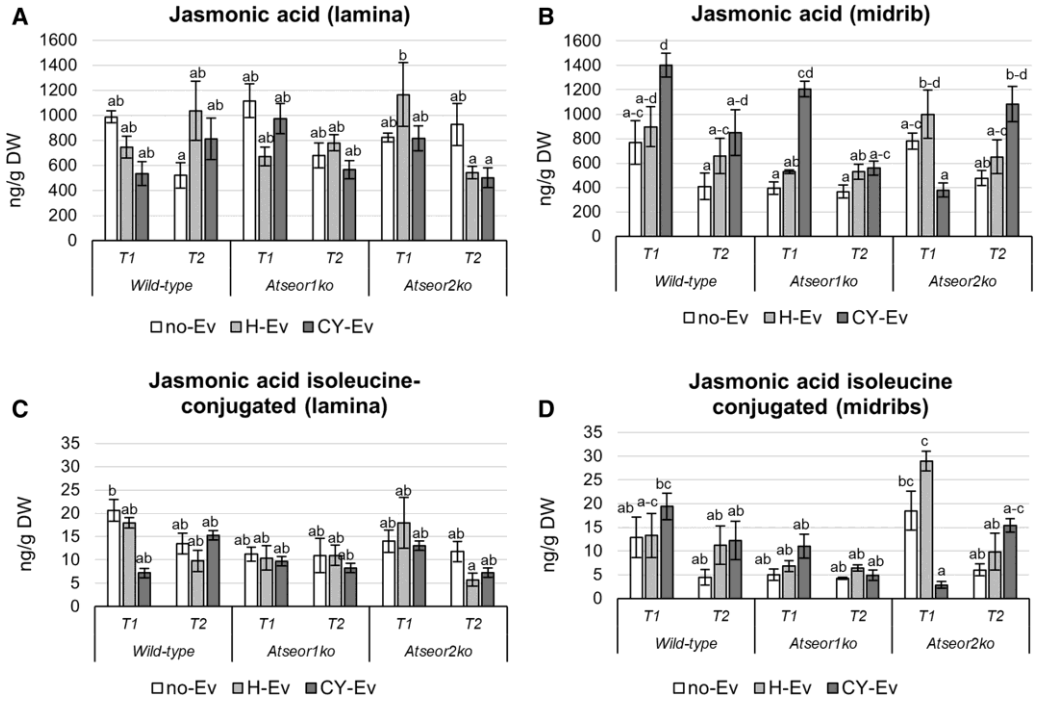

Figure 7. Jasmonic acid and jasmonate-isoleucine conjugate levels in laminae and midribs of the three Arabidopsis lines non-infested by leafhoppers (no-Ev) or infested by healthy leafhoppers (H-Ev) or infested by CY-infected leafhoppers (CY-Ev), at the early (5 days after IAP, T1) and late (20 days after IAP, T2) stages of infection. The phytohormone levels are expressed as ng per g of tissue dry weight. Statistical analysis was performed using the Tukey HSD test as the post hoc test in a three-way ANOVA. Different letters (a, b, c) above the bars indicate significant differences, with $P < 0.05$; (a–c = abc, a–d = abcd, b–d = bcd, c–e = cde). Error bars indicate the Standard Error of the Mean of 6 biological replicates for each condition.

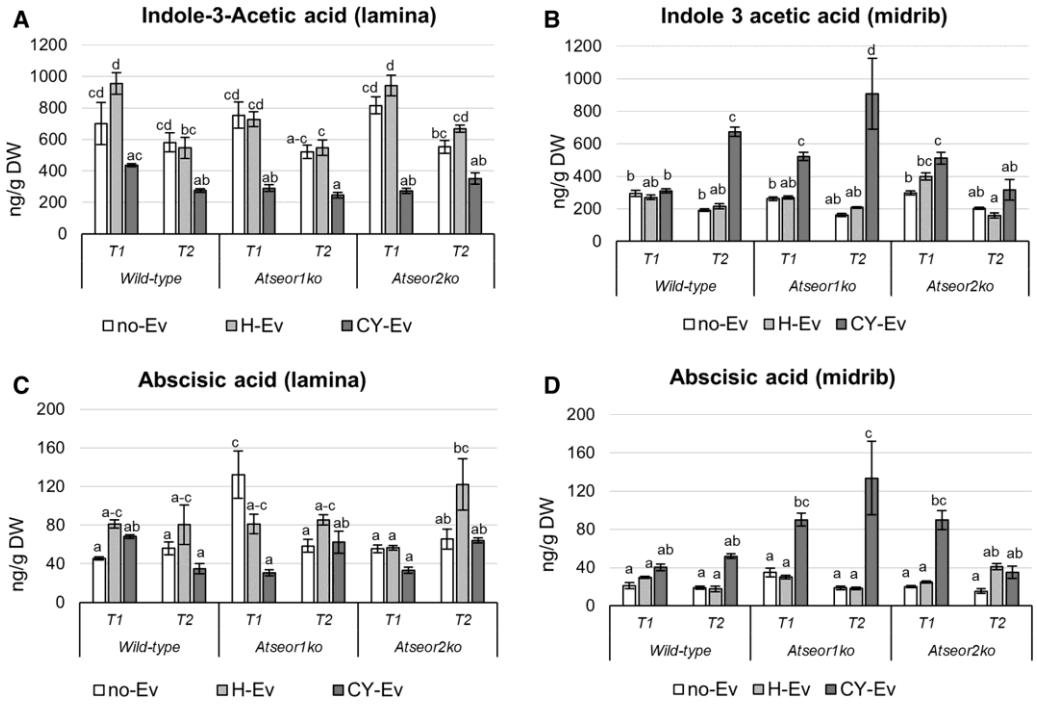

Figure 8. Indole acetic acid and abscisic acid levels in laminae and midribs of the three Arabidopsis lines non-infested by leafhoppers (no-Ev) or infested by healthy leafhoppers (H-Ev) or infested by CY-infected leafhoppers (CY-Ev), at the early (5 days after IAP, T1) and late (20 days after IAP, T2) stages of infection. The phytohormone levels are expressed as ng per g of tissue dry weight. Statistical analysis was performed using the Tukey HSD test as the post hoc test in a three-way ANOVA. Different letters (a, b, c, d) above the bars indicate significant differences, with $P < 0.05$; (a–c = abc). Error bars indicate the Standard Error of the Mean of 6 biological replicates for each condition.

but a satisfactory explanation was not evident. AtSEOR1 and AtSEOR2 are thought to be necessary for filament formation through their heterodimeric interaction[8]. Therefore, it was speculated that in the *Atseor1ko* line, the AtSEOR2 protein in its free form, i.e. not linked to AtSEOR1, is involved in immune signalling through an interaction with defence-related plant proteins[10,11]. In line with this conjecture, AtSEOR2 was found to interact with AtRIN4, a PRR plasma membrane-anchored protein in a matrix-based yeast two-hybrid assay[10]. Expression of *AtRIN4*, and the associated *AtRPM1* and *AtRPS2* genes in healthy and phytoplasma-infected wild-type and *Atseor1ko* lines revealed an upregulation in the mutant line as compared to the wild-type, which was suggestive of a role of AtSEOR2 in promoting defence mechanisms[11]. In this frame, interactions between AtSEOR2 and diverse transcription factors[29] as well as its intervention in the IAA and ABA signalling cascades were predicted[12,30].

In the present work, the relation between AtSEOR2 and phytohormone synthesis and the impact on phytoplasma titres was investigated in wild-type, *Atseor1ko* and *Atseor2ko* Arabidopsis lines. As the effectiveness of the defence processes is related to the readiness of plants to counter pathogens[31] and very little is known about the early response to phytoplasma infection, analyses were performed both at an early and a late time point of infection, i.e., respectively, at 5 days and 20 days after IAP. Up to 5 days after the end of IAP, the plant lines did not show any phenotypic differences (Fig. 1). As reported before[32], growth and development of infected plants at this stage were comparable to those of control plants exposed to non-infected insect vectors.

Real-time PCR analyses evidenced that at the early stage (Fig. 2), the average phytoplasma titres were low (Cq values ± SE wild-type: 29.11 ± 2.17; *Atseor1ko*: n.d.; *Atseor2ko*: 30.98 ± 3.71), which has been demonstrated previously[33]. Interestingly, none of the *Atseor1ko* individuals tested positive at all for the presence of phytoplasma at this stage (Cq value: n.d. and Fig. 2A). The very high transmission efficiency of *E. variegatus* under natural and experimental conditions[34–37] is confirmed in our experimental system (transmission rate 100%, p = 1[27]). Moreover, the higher vector survival rates on mutant lines (Fig. S1) together with the assumption that the vector fitness reflects the feeding capacity, infers that the lower phytoplasma titre in the *Atseor1ko* line is logically due to plant properties and not to reduced insect-mediated transmission efficiency.

The fact that insects showed higher survival rate on infected mutant lines than in wild-type, could be due to the complementary capability of AtSEOR proteins (both expressed in wild-type Arabidopsis) to aggregate in

presence of phytoplasmas [this work;[9]], reducing the phloem mass-flow and impairing stylet sucking-activity. Will et al.[38] demonstrated that SEOR-mediated plugging is induced by green peach aphid (Myzus persicae) feeding on Vicia faba and this mechanism impairs feeding in aphid-resistant varieties[39].

Phytoplasma titres at the early stage of infection showed trends similar to those 20 days after IAP (when the symptoms had become manifest): the phytoplasma titres in wild-type or *Atseor2ko* plants exceeded by far the titre in *Atseor1ko* plants (Fig. 2 and[9]). Therefore, phytoplasma multiplication was presumably impaired in the *Atseor1ko* line from the earliest stages of infection onwards.

Sieve-element protein filaments aggregate in sieve tubes of wild-type Arabidopsis line from the early stage of infection onward. We previously demonstrated that SE protein filaments play a role in the plant response to phytoplasma infection, even in the absence of genes that are considered necessary for their formation in healthy plants[8,9]. Nevertheless, the picture drawn at that time did not explain whether SE protein filaments per se are involved in some defence mechanisms, such as early pathogen containment. Ultrastructural analysis confirmed the presence, at the late stage of infection (i.e., 20 days after IAP, Fig. 5), of filamentous structures in each CY-Ev Arabidopsis line (wild-type, *Atseor1ko* and *Atseor2ko*) and revealed that, at the first stage of infection (5 days after IAP), SE protein filaments only aggregated in CY-Ev wild-type plants (Fig. 4). Their initial absence in the Arabidopsis line that is best equipped to suppress the pathogen invasion from the early stage of infection on (i.e. *Atseor1ko*), led us to exclude aggregation of SE protein filaments as a possible explanation for the better defence performance of the *Atseor1ko* line. Therefore, our investigations were further focused on the phytohormone levels, which are frequently related to defence mechanisms[15,16,40–43]. Since leaf midribs are rich in phloem tissues, where phytoplasmas and plants physically and chemically interact[5], plant responses were determined in leaf midribs and laminae separately.

Phytohormone levels in Arabidopsis lines are not affected by *E. variegatus* infestation at 5 and 20 days after the end of the IAP. Damage inflicted by insect feeding leads to the immediate activation of phytohormone-related signaling[26] and in particular to the synthesis and accumulation of JA in tissues both proximal and distal to injury sites[44].

As for the effects of leafhopper infestation, phytohormone levels were equal in the midribs or laminae of each line and at both time points (i.e. 5 and 20 days after the end of IAP) in H-Ev and no-Ev samples. Changes in phytohormonal balance following leafhopper infestation have been amply described[26], but the results were quite variable, probably owing to variations in infestation times[45]. In general, defense phytohormones are immediately induced in plant tissues after recognition of invaders, but the amounts tend to level off during persistent insect infestation[44]. Moreover, the effects of cutting, necessary to isolate midribs from laminae, may overshadow insect-induced responses[44].

The fact that the phytohormone levels are identical in H-Ev and no-Ev plants strongly supports the conclusion that the phytohormone modulation in CY-Ev plants is solely due to phytoplasma infection. This is in agreement with the observation that 6 days after *Scaphoideus titanus* infestation in grapevine, the expression level of genes involved in JA and ABA pathways were similar to those found in non-infested control leaves, while they had been upregulated 3 days after infestation[46].

Jasmonates, but not salicylic acid seem to be involved in the response of *Atseor1ko* line to phytoplasma infection. There are several indications for phytohormone involvement in diverse phytoplasma-plant interactions[4], but few studies have addressed plant responses at the early stage of infection[40,46].

The most frequently studied phytohormones in relation with phytoplasma infections are SA and JA, which both confer signal transduction leading to plant resistance. JA- and SA-mediated signalling pathways are presumed to be antagonistic[41,42]. Traditionally, SA signalling is deemed to activate resistance against biotrophic and hemibiotrophic pathogens, while JA is mainly thought to induce resistance against necrotrophic pathogens and wounding[44,47].

In CY-Ev wild-type and *Atseor1ko* lines SA levels did not change significantly in all tissues examined (Fig. 6). SA increased in the midribs of *Atseor2ko line* at the early stage of infection, followed by a drop at the late stage (Fig. 6). Enhanced amounts of SA resulted from different plant–phytoplasma interactions in whole leaves[18,40,48], in midribs[22] and phloem sap[49]. On the other hand, cases, which showed reduced SA levels in response to phytoplasma infection were also described[17,50]. The reason why SA level was significantly higher in *Atseor2ko* line compared to the other lines is unknown. It has to be noted that SA levels depend on many factors, such as the developmental stage of the vegetative cycle[17], varying environmental conditions[20], the phytoplasma strain in question[51], and distinct sets of virulence factors[49].

With regard to the JA concentration, the levels of both jasmonates were virtually unaffected in laminae. In midribs of all *Arabidopsis* lines JA showed a non-significant increment, apart from the *Atseor1ko* line, which showed significantly higher jasmonate levels at an early stage of infection (Fig. 7B). An increase of JA levels during the early stages of infection process, followed by decrease at symptom appearance, was described in different plant–phytoplasma interactions[14,17,20,24,52].

Sugio et al.[53] found that *Arabidopsis* plants infected with the '*Ca*. P. asteris' strain AY-WB produced more JA in old asymptomatic leaves (as well as in uninfected plants) as compared to young symptomatic leaves. The authors also demonstrated that reduced JA levels affected plant development, leading to symptom appearance and increasing insect-vector fitness[53]. Decreased JA levels were also reported in Arabidopsis expressing phytoplasma virulence factors (i.e. TENGU[14] or SAP11[53]), indicating that phytoplasma effectors were involved in host hormonal changes.

Janik et al.[17] hypothesized a relationship between an increased phytoplasma titre, the activity of phytoplasma effectors and the decrease of JA levels over the growth season. Interestingly, in perennial plants, increased JA synthesis was correlated to the phenomenon of recovery[40,48], a resilience status characterized by the loss of disease symptoms in plants which previously showed them[54,55]. Hence, the higher content of JA in *Atseor1ko* line could be related to failing phytoplasma detection (and to the absence of activity by their effectors) at the first stage of infection.

A JA–SA antagonism[41,42] may be visible in *Atseor1ko* and *Atseor2ko* lines at the early stage of infection, because at the high JA levels in the one correspond the low SA content in the other and vice versa at the same time point (Figs. 6B, 7B).

IAA- and ABA-synthesis are activated in the midribs of the phytoplasma-infected *Atseor1ko* line. As for the IAA variations in phytoplasma-infected plants, expression analyses of IAA-related genes in whole leaves[56,57], buds[58], or leaf midribs[59] infer a downregulation in several infected hosts. On the other hand, IAA levels were reported to increase in phloem sap[49], whole leaves[60] and leaf midribs[59] of phytoplasma-infected plants as compared to the respective control samples.

Here, phytoplasma infection induced a decrease in IAA levels in the laminae and an increase in the midribs in each *Arabidopsis* line (Fig. 8). This indicates a positive response of IAA synthesis, located in the midribs as reported previously[59]. The increase in IAA was statistically significant in infected midribs of *Atseor1ko* mutants at both time points, i.e. at 5 and 20 days after IAP (Fig. 8).

Previous studies evidenced an increase in ABA levels and the upregulation of ABA-related genes in all tissues of phytoplasma-infected plants[17,18,49,58,61]. In our study, a tissue-dependent ABA response was observed in wild-type plants; the ABA level decreased in laminae, while it increased in midribs. Variations in the expression of genes related to ABA biosynthesis have been associated with symptom expression[61]. ABA-promoted stomatal closure could induce pre-invasive defence by inhibiting the entry of pathogens through passive ports[62,63]. Furthermore, ABA signalling would initiate events such as callose accumulation and antagonize the signalling cascades of other phytohormones at an advanced state of infection[64,65]. It is worth noting that *Atseor1ko* was the only line, in which ABA is significantly enhanced in the midrib from the early infection stage on, and the higher level was maintained throughout the entire measurement period.

Potential modes of involvement of AtSEOR2. Thus far, the relationship between free AtSEOR2 and phytohormone synthesis is a mystery. Yet, there is a wide range of possibilities.

According to the COACH platform[66], AtSEOR2 protein (but not AtSEOR1) may have Ca^{2+} binding sites, which suggests a possible role for AtSEOR2 in the lowering of Ca^{2+} levels as does the sequestration of Ca^{2+} ions by SEOR-based forisomes in legumes[67]. The subsequent modification of Ca^{2+} signatures may promote ABA and IAA synthesis[68–72] in *Atseor1ko* infected plants. This hypothesis seemingly makes a logical connection between AtSEOR2 and the low phytoplasma titre owing to enhanced IAA and ABA synthesis.

In addition or alternatively, AtSEOR2 may effect on the IAA and ABA signalling pathways. To the best of our knowledge, the number of reports about possible interaction of AtSEOR2 protein with components of IAA- or ABA-signalling cascade is scarce. Yeast two-hybridization experiments demonstrated that AtSEOR2 is able to interact with the At4g04950 gene product, a monothiol glutaredoxin that is a key component involved in ROS accumulation and IAA signalling[73]. The role of AtSEOR2 in ABA-cascade signalling has also hardly been explored thus far. Some evidence has recently been presented for an interaction between AtSEOR2 and SUA (SUPPRESSOR OF ABI3-5), a main component of the ABA signalling pathway[74], and its involvement in the increased sensitivity to ABA[74]. Moreover, Nakashima and co-workers[30] demonstrated that *AtSEOR2* is one of the many genes whose expression changes in *A. thaliana* knock-out mutants of three SnRK2 kinases involved in ABA signalling. Interestingly, AtSEOR2 has been reported to interact with the At1G31280.1 gene product[12], an ABA-regulated protein that controls plant response against virus infections[75].

Furthermore, it is not excluded that AtSEOR2 directly interacts with receptor(s) in the SE-CC complex to elicit defence responses. SEOR proteins are characterized by a conserved C-terminal M1 motif, containing several conserved cysteine residues[28] characteristic of the so-called peptide ligands[76], which are engaged in the regulation of developmental processes and defence mechanisms against pathogens[77]. Interestingly, in mulberry infected by yellow dwarf disease, a phytoplasma-responsive gene encoding a protein that shows structural similarity to peptide ligands, was identified. This gene is involved in signaling and metabolism of IAA, ABA and JA[78].

In conclusion, AtSEOR2 indirectly manipulates plant response via increased phytohormone synthesis and phytohormone signalling and perhaps via interaction with membrane receptors. These responses emerge very early in the infection process, long before the appearance of infection symptoms.

Methods

Plant material and insect vectors. The seeds of wild-type, *Atseor1ko* (SALK_081968C), and *Atseor2ko* (SALK_148614C) lines of *A. thaliana* plants ecotype Columbia[9] were obtained from the Nottingham Arabidopsis Stock Centre (NASC). Wild-type and mutant lines (72 plants of each line) were grown at 20/22 °C under short-day conditions (9 h L/15 h D). Before the experiment, plants were cultivated for 45 days on a 5:1 mixture of soil substrate and perlite and fertilized twice a month with an N–P–K liquid fertilizer.

Healthy colonies of the insect vector *E. variegatus* were reared on *Avena sativa* in vented plexiglass cages at 20/22 °C, under short-day conditions (9 h L/15 h D). Fourth and fifth instar nymphs were transferred to *Chrysanthemum carinatum* plants infected with a phytoplasma strain related to '*Candidatus* Phytoplasma asteris' ('*Ca.* P. asteris', 16SrI-B subgroup), called Chrysanthemum yellows (CY) phytoplasma[9] as the source of inoculum for a 7-day phytoplasma acquisition-access period (AAP). After the AAP, the insects were fed again on *A. sativa* for

the 35-day latency period (LP) after which they have become infectious. Twelve 45-day-old *A. thaliana* plants per line were then each exposed to three infectious insects (CY-infected *E. variegatus*, CY-Ev plants) for a 7-day phytoplasma inoculation-access period (IAP), after which the insects were manually removed. Twelve Arabidopsis plants per line, treated with three healthy leafhoppers (H-Ev plants) were used as a healthy control. Healthy leafhoppers have been collected from healthy colonies and were as old as the infected ones.

For microscopy and phytohormone analyses, 12 plants per line not subjected to insect feeding (non-infested plants, no-Ev plants), were included as additional negative controls. For ultrastructural observations and phytohormone quantification, 6 H-Ev and 6 CY-Ev plants from each line (i.e. 6 independent biological replicates) were used, for the phytoplasma titre analyses12 H-Ev and 12 CY-Ev plants (i.e. 12 independent biological replicates) were used.

Evaluation of insect survival rate and phytoplasma detection. To ascertain successful phytoplasma transmission to the Arabidopsis plants, survival rates and the presence of phytoplasma were checked in leafhoppers that were removed from Arabidopsis plants at the end of the IAP. The survival rate was calculated using 12 biological replicates (i.e. 12 *Arabidopsis* plants) for each condition (i.e. various Arabidopsis lines and infection times). For phytoplasma detection, the 3 insects used on each Arabidopsis were pooled, to obtain 72 pools per condition. Total DNA was extracted as described[79] and the presence of phytoplasmas in each pool was assayed by conventional PCR using the primer pair R16F2/R2, as described by Pagliari and co-authors[9].

Phytoplasma transmission by leafhoppers was evaluated on the basis of the number of Arabidopsis plants showing symptoms 20 days after the end of IAP. To estimate the proportion of infectious insects in our experiment, the maximum likelihood estimator of p, $p = 1 - Q^{1/k}$ was used[27], where Q is the observed fraction of non-infected plants and k is the number of insects per plant, assuming that the vectors acted independently[27]. The formula can be applied when transmission trials are carried out using groups of insects[35].

Statistical analysis was performed using SigmaPlot 12.0 software (Systat Software, Inc., San Jose, CA, USA). The normal distribution of the data was checked with the Shapiro–Wilk normality test. A three-way ANOVA of the means (from 12 biological replicates and 3 technical replicates) followed by the Holm-Sidak test as the post hoc test for multiple comparisons demonstrated the significance for $p < 0.05$.

Phytoplasma quantification in Arabidopsis. Total DNA was extracted from 200 mg of whole-leaf tissue of H-Ev and CY-Ev plants according to Martini et al.[80]. The amount of CY phytoplasmas was quantified according to a real-time PCR protocol described in detail by Pagliari and co-authors[9]. Briefly, the ribosomal protein gene *rplV* (*rpl22*) was the target for amplification of CY phytoplasma DNA using the primer pair rp(I-B) F2/rp(I-B)R2[9]) and a CFX96 real-time PCR detection system (Bio-Rad Laboratories, Richmond, CA, USA). A standard curve was established by tenfold serial dilutions of plasmid DNA containing the 1,260 bp ribosomal protein fragment from CY phytoplasma, amplified with the primer pair rpF1C/rp(I)R1A. Real-time PCR mixture and cycling conditions were as previously described[9]. The phytoplasma concentration was expressed as the number of CY phytoplasma genome units (GUs) per mg of leaf sample to normalize the data. Differences among the means were calculated using SigmaPlot 12.0 software (Systat Software). The normal distribution of the data was checked with the Shapiro–Wilk normality test. A two-way ANOVA of the means (obtained from 12 biological replicates and 3 technical replicates) followed by the Holm-Sidak test as post hoc test for multiple comparisons demonstrated the significance for $p < 0.05$.

Transmission electron microscopy. To preserve the damage-sensitive sieve-element ultrastructure, a gentle preparation method was adopted following Pagliari et al.[9]. From each plant a 25 mm-long midrib portion was excised from rosette leaves. The midrib segments were submerged in MES buffer and then fixed with 3% paraformaldehyde and 4% glutaraldehyde solutions. Samples were rinsed, post-fixed overnight with 2% (w/v) OsO4, dehydrated in a graded ethanol series and then transferred to propylene oxide. From the central part of each midrib, 6–7 mm long segments were excised and embedded in Epon/Araldite epoxy resin (Electron Microscopy Sciences, Fort Washington, PA, USA).

Ultrathin sections (60–70 nm in thickness) were cut, stained with UAR-EMS (uranyl acetate replacement stain) (Electron Microscopy Sciences), and observed under a PHILIPS CM 10 (FEI, Eindhoven, The Netherlands) transmission electron microscope (TEM), operated at 80 kV, and equipped with a Megaview G3 CCD camera (EMSIS GmbH, Münster, Germany). Five non-serial cross-sections from each sample were analysed.

Phytohormone analyses. We adopted a validated HPLC–MS/MS method[81], optimized for *A. thaliana* and the low concentrations (nM to µM) of the phytohormones of interest. Phytohormone extraction was performed using 6 plants per experimental condition.

For each sample, roughly 250 mg of midribs and 250 mg of laminae were collected for phytohormone analysis, immersed immediately in liquid nitrogen and then stored at − 80 °C, as described by Pommerrenig et al.[82].

After freeze-drying, the samples were homogenized in a Geno/Grinder 2010 (SPEXSample Prep, München, Germany) at 1,100 rpm for 60 s. After homogenization, the phytohormones salicylic acid (SA), abscisic acid (ABA), jasmonic acid (JA), jasmonic acid- isoleucine conjugate (JA-Ile) and indole acetic acid (IAA) were extracted from 10–20 mg of dried plant tissue using 1 mL of extraction solution containing 20 ng/mL d6-ABA, 10 ng/mL d5-IAA, 20 ng/mL d6-JA and 10 ng/mL d4-SA as internal standards. After mixing and centrifugation, the supernatants were evaporated in a Speed Vac at 45 °C and the pellets resuspended in 100 µL of methanol:water 1:1.

The extracts were analysed using an HPLC–MS/MS method[81] on an Agilent 1,100 HPLC system (Agilent Technologies, Böblingen, Germany) connected to a LTQ Ion Trap mass spectrometer (Thermo Scientific, Bremen,

Germany). Chromatographic separation was carried out in a Luna phenyl-hexyl column (150 × 4.6 mm, 5 µm; Phenomenex, Aschaffenburg, Germany). Formic acid (0.05%, v/v) and MeOH with 0.05% (v/v) formic acid were used as mobile phases A and B, respectively. The elution profile was: 0–10 min, 42–55% B in A; 10–13 min, 55–100% B; 13–15 min 100% B; 15–15.1 min 100–42% B in A; 15.1–20 min 42% B in A. The mobile phase flow rate was 1.1 mL/min. The injection volume was 20 µL.

Phytohormone quantifications were based on calibration curves, and the data obtained from each sample were subsequently analysed with XCalibur software (Thermo Fisher Scientific). Statistical differences between the means obtained from 6 individuals exposed to the different conditions (i.e. various Arabidopsis lines and infection times) were evaluated using R Studio 1.1.456 software (Northern Ave, Boston, MA, USA) using three-way ANOVA and the Tukey HSD test as post hoc test for pairwise multiple comparisons, with $p < 0.05$. The normal distribution of the data was checked with the Shapiro–Wilk normality test.

Received: 15 April 2020; Accepted: 17 August 2020
Published online: 08 September 2020

References

1. Lee, I. M., Davis, R. E. & Gundersen-Rindal, D. Phytoplasma: phytopathogenic mollicutes. *Annu. Rev. Microbiol.* **54**, 221–255 (2000).
2. Albertazzi, G. *et al.* Gene expression in grapevine cultivars in response to Bois Noir phytoplasma infection. *Plant Sci.* **176**, 792–804 (2009).
3. Buoso, S. *et al.* '*Candidatus* Phytoplasma solani' interferes with the distribution and uptake of iron in tomato. *BMC Genomics* **20**(1), 703 (2019).
4. Dermastia, M. Plant hormones in phytoplasma infected plants. *Front. Plant Sci.* **10**, 477 (2019).
5. van Bel, A. J. E. & Musetti, R. Sieve-element biology provides leads for research on phytoplasma lifestyle in plant hosts. *J. Exp. Bot.* **70**, 3737–3755 (2019).
6. Alma, A., Lessio, F. & Nickel, H. Insects as phytoplasma vectors: ecological and epidemiological aspects. In *Phytoplasmas: Plant Pathogenic Bacteria-II* (eds Bertaccini, A. *et al.*) (Springer, Singapore, 2019).
7. Jekat, S. *et al.* P-proteins in Arabidopsis are heteromeric structures involved in rapid sieve tube sealing. *Front. Plant Sci.* **4**, 225 (2013).
8. Anstead, J., Froelich, D., Knoblauch, M. & Thompson, G. Arabidopsis P-protein filament formation requires both AtSEOR1 and AtSEOR2. *Plant Cell Physiol.* **53**, 1033–1042 (2012).
9. Pagliari, L. *et al.* Filamentous sieve element proteins are able to limit phloem mass flow but not phytoplasma spread. *J. Exp. Bot.* **13**, 3673–3688 (2017).
10. Afzal, A., Kim, J. & Mackey, D. The role of NOI-domain containing proteins in plant immune signaling. *BMC Genomics* **14**, 327 (2013).
11. Pagliari, L., Buoso, S., Santi, S., van Bel, A. J. E. & Musetti, R. What slows down phytoplasma proliferation? Speculations on the involvement of AtSEOR2. *Plant Signal. Behav.* **13**, e1473666 (2018).
12. Braun, P. *et al.* Evidence for network evolution in an Arabidopsis interactome map. *Science* **333**, 601–607 (2011).
13. van Wallendael, A. *et al.* A molecular view of plant local adaptation: incorporating stress-response networks. *Annu. Rev. Plant Biol.* **70**, 559–583 (2019).
14. Bedini, A., Mercy, L., Schneider, C., Franken, P. & Lucic-Mercy, E. Unravelling the initial plant hormone signalling, metabolic mechanisms and plant defense triggering the endomycorrhizal symbiosis behavior. *Front. Plant Sci.* **9**, 1800 (2018).
15. Verma, V., Ravindran, P. & Kumar, P. Plant hormone-mediated regulation of stress responses. *BMC Plant Biol.* **16**, 86. https://doi.org/10.1186/s12870-016-0771-y (2016).
16. Hillmer, R. A. *et al.* The highly buffered Arabidopsis immune signaling network conceals the functions of its components. *PLoS Genet.* **13**(5), e1006639 (2017).
17. Janik, K. *et al.* An effector of apple proliferation phytoplasma targets TCP transcription factors—a generalized virulence strategy of phytoplasma?. *Mol. Plant Pathol.* **18**, 435–442 (2017).
18. Wang, X., Hou, Q. & Liu, Y. Insights into the decarboxylative hydroxylation of salicylate catalyzed by the Flavin-dependent monooxygenase salicylate hydroxylase. *Theor. Chem. Acc.* **137**, 89 (2018).
19. Lazar, A. Prevalence of Phytoplasmas in UK. *Graduation Thesis: University Studies* (Doctoral dissertation, A. Lazar) (2010).
20. Hren, M. *et al.* "Bois noir" phytoplasma induces significant reprogramming of the leaf transcriptome in the field grown grapevine. *BMC Genomics* **10**, 460 (2009).
21. Youssef, S. A., Safwat, G., Shalaby, A. B. A. & El-Beltagi, H. S. Effect of phytoplasma infection on plant hormones, enzymes and their role in infected sesame. *Fresen. Environ. Bull.* **27**, 5727–5735 (2018).
22. Prezelj, N. *et al.* Metabolic consequences of infection of grapevine (*Vitis vinifera* L.) cv. "Modra frankinja" with Flavescence Dorée phytoplasma. *Front. Plant Sci.* **7**, 711 (2016).
23. Wei, W., Zhao, Y. & Davis, R. E. Phytoplasma inoculum titre and inoculation timing influence symptom development in newly infected plants. *Phytopathog. Mollicutes* **9**, 115–116 (2019).
24. Gai, Y. P. *et al.* Metabolomic analysis reveals the potential metabolites and pathogenesis involved in mulberry yellow dwarf disease. *Plant Cell Environ.* **37**, 1474–2149 (2014).
25. Snyman, M. C. *et al.* The use of high-throughput small RNA sequencing reveals differentially expressed microRNAs in response to aster yellows phytoplasma-infection in *Vitis vinifera* cv. 'Chardonnay'. *PLoS ONE* **12**(8), e0182629 (2017).
26. Zhang, L., Zhang, F., Melotto, M., Yao, J. & He, S. Y. Jasmonate signaling and manipulation by pathogens and insects. *J. Exp. Bot.* **68**(6), 1371–1385 (2017).
27. Swallow, W. H. Group testing for estimating infection rates and probabilities of disease transmission. *Phytopathology* **75**, 882 (1985).
28. Rüping, B. *et al.* Molecular and phylogenetic characterization of the sieve element occlusion gene family in Fabaceae and non-Fabaceae plants. *BMC Plant Biol.* **10**, 219 (2010).
29. Vainonen, J. *et al.* RCD1–DREB2A interaction in leaf senescence and stress responses in *Arabidopsis thaliana*. *Biochem. J.* **442**, 573–581 (2012).
30. Nakashima, K. *et al.* Three Arabidopsis SnRK2 protein kinases SRK2D/SnRK2.2 SRK2E/SnRK2.6/OST1 and SRK2I/SnRK2.3 involved in ABA signaling are essential for the control of seed development and dormancy. *Plant Cell Physiol.* **50**, 1345–1363 (2009).
31. de Wit, P. How plants recognize pathogens and defend themselves. *Cell. Mol. Life Sci.* **64**, 2726–2732 (2007).
32. Cettul, E. & Firrao, G. Development of phytoplasma-induced flower symptoms in *Arabidopsis thaliana*. *Physiol. Mol. Plant Pathol.* **76**, 204–211 (2011).

33. Pacifico, D. *et al.* Decreasing global transcript levels over time suggest that phytoplasma cells enter stationary phase during plant and insect colonization. *Appl. Environ. Microbiol.* **81**, 2591–2602 (2015).
34. Palermo, S., Arzone, A. & Bosco, D. Vector-pathogen-host plant relationships of chrysanthemum yellows (CY) phytoplasma and the vector leafhoppers *Macrosteles quadrupunctulatus* and *Euscelidius variegatus*. *Entomol. Exp. Appl.* **99**, 347–354 (2001).
35. Bosco, D. & Tedeschi, R. *Insect Vector Transmission Assays. Phytoplasma* 73–85 (Humana Press, Totowa, 2013).
36. Galetto, L. *et al.* Two phytoplasmas elicit different responses in the insect vector *Euscelidius variegatus* Kirschbaum. *Inf. Immun.* **86**(5), e0004218 (2018).
37. Rashidi, M., D'Amelio, R., Galetto, L., Marzachì, C. & Bosco, D. Interactive transmission of two phytoplasmas by the vector insect. *Ann. Appl. Biol.* **165**(3), 404–413 (2014).
38. Will, T., Kornemann, S. R., Furch, A. C., Tjallingii, W. F. & van Bel, A. J. Aphid watery saliva counteracts sieve-tube occlusion: a universal phenomenon?. *J. Exp. Biol.* **212**(20), 3305–3312 (2009).
39. Medina-Ortega, K. J. & Walker, G. P. Does aphid salivation affect phloem sieve element occlusion in vivo?. *J. Exp. Bot.* **64**(18), 5525–5535 (2013).
40. Paolacci, A. *et al.* Jasmonate-mediated defence responses unlike salicylate-mediated responses are involved in the recovery of grapevine from bois noir disease. *BMC Plant Biol.* **17**, 118 (2017).
41. Loake, G. & Grant, M. Salicylic acid in plant defence-the players and protagonists. *Curr. Opin. Plant Biol.* **10**, 466–472 (2007).
42. Vidhyasekaran, P. *Plant Hormone Signaling Systems in Plant Innate Immunity* (Springer, Dordrecht, 2015).
43. Pieterse, C. M., Van der Does, D., Zamioudis, C., Leon-Reyes, A. & van Wees, S. C. Hormonal modulation of plant immunity. *Annu. Rev. Cell Dev. Biol.* **28**, 489–521 (2012).
44. Glauser, G. *et al.* Spatial and temporal dynamics of jasmonates synthesis and accumulation in Arabidopsis in response to wounding. *J. Biol. Chem.* **283**, 16400–16407 (2008).
45. Yang, H. *et al.* Transcriptomic and phytochemical analyses reveal root-mediated resource-based defense response to leaf herbivory by *Ectropis oblique* in tea plant (*Camellia sinensis*). *J. Agric. Food Chem.* **67**, 5465–5476. https://doi.org/10.1021/acs.jafc.9b00195 (2019).
46. Bertazzon, N. *et al.* Grapevine comparative early transcriptomic profiling suggests that Flavescence doreè phytoplasma represses plant responses induced by vector feeding in susceptible varieties. *BMC Genomics* **20**, 526 (2019).
47. Kazan, K. & Lyons, R. Intervention of phytohormone pathways by pathogen effectors. *Plant Cell* **26**, 2285–2309 (2014).
48. Patui, S. *et al.* Involvement of plasma membrane peroxidases and oxylipin pathway in the recovery from phytoplasma disease in apple (*Malus domestica*). *Physiol. Plantarum.* **148**, 200–213 (2013).
49. Zimmermann, M. *et al.* Implications of '*Candidatus* Phytoplasma mali' infection on phloem function of apple trees. *J. Endocytob. Cell Res.* **26**, 67–75 (2015).
50. Lu, Y. T. *et al.* Transgenic plants that express the phytoplasma effector SAP11 show altered phosphate starvation and defense responses. *Plant Physiol.* **164**(3), 1456–1469 (2014).
51. Ahmad, J. *et al.* Effects of stolbur phytoplasma infection on DNA methylation processes in tomato plants. *Plant Pathol.* **62**, 205–216 (2013).
52. Minato, N. *et al.* The phytoplasmal virulence factor TENGU causes plant sterility by downregulating of the jasmonic acid and auxin pathways. *Sci. Rep.* **4**, 7399 (2014).
53. Sugio, A., MacLean, A., Grieve, V. & Hogenhout, S. A. Phytoplasma protein effector SAP11 enhances insect vector reproduction by manipulating plant development and defense hormone biosynthesis. *Proc. Natl. Acad. Sci. U.S.A.* **108**, E1254–E1263 (2011).
54. Musetti, R., Sanità di Toppi, L., Ermacora, P. & Favali, M. A. Recovery in apple trees infected with the apple proliferation phytoplasma: an ultrastructural and biochemical study. *Phytopathology.* **94**(2), 203–208 (2004).
55. Musetti, R. *et al.* On the role of H_2O_2 in the recovery of grapevine (*Vitis vinifera* cv. Prosecco) from Flavescence dorée disease. *Funct. Plant Biol.* **34**(8), 750–758 (2007).
56. Ehya, F. *et al.* Phytoplasma-responsive microRNAs modulate hormonal nutritional and stress signalling pathways in Mexican lime trees. *PLoS ONE* **8**, e66372 (2013).
57. Mardi, M., Farsad, L., Gharechahi, J. & Salekdeh, G. In-depth transcriptome sequencing of Mexican lime trees infected with '*Candidatus* Phytoplasma aurantifolia'. *PLoS ONE* **10**, e0130425 (2015).
58. Fan, G., Cao, X., Zhao, Z. & Deng, M. Transcriptome analysis of the genes related to the morphological changes of *Paulownia tomentosa* plantlets infected with phytoplasma. *Acta Physiol. Plant.* **37**, 202 (2015).
59. Alves, M. *et al.* Differential expression and phytohormone unbalance in *Citrus aurantifolia* plants during 'sudden decline of lime' a new phytoplasma disease in citrus. *Trop. Plant Pathol.* **43**, 520–532 (2018).
60. Pertot, I., Musetti, R., Pressacco, L. & Osler, R. Changes in indole-3-acetic acid level in micropropagated tissues of *Catharanthus roseus* infected by the agent of the clover phyllody and effect of exogenous auxins on phytoplasma morphology. *Cytobios* **95**, 13–23 (1998).
61. Mou, H. *et al.* Transcriptomic analysis of Paulownia infected by Paulownia Witches'-broom Phytoplasma. *PLoS ONE* **8**, e77217 (2013).
62. Ton, J., Flors, V. & Mauch-Mani, B. The multifaceted role of ABA in disease resistance. *Trends Plant Sci.* **14**, 310–317 (2009).
63. Flors, V., Ton, J., Jakab, G. & Mauch-Mani, B. Abscisic acid and callose: team players in defence against pathogens?. *J. Phytopathol.* **153**, 377–383 (2005).
64. Le Noble, M., Spollen, W. & Sharp, R. Maintenance of shoot growth by endogenous ABA: genetic assessment of the involvement of ethylene suppression. *J. Exp. Bot.* **55**, 237–245 (2004).
65. Staswick, P., Su, W. & Howell, S. Methyl jasmonate inhibition of root growth and induction of leaf protein are decreased in an *Arabidopsis thaliana* mutant. *Proc. Natl. Acad. Sci. U.S.A.* **89**, 6837–6840 (1992).
66. Yang, J., Roy, A. & Zhang, Y. BioLiP: a semi-manually curated database for biologically relevant ligand-protein interactions. *Nucleic Acids Res.* **41**, D1096–D1103 (2013).
67. Tuteja, N., Umate, P. & van Bel, A. J. Forisomes: calcium-powered protein complexes with potential as 'smart' biomaterials. *Trends biotechnol.* **28**(2), 102–111 (2010).
68. Larkindale, J. & Knight, M. R. Protection against heat stress-induced oxidative damage in Arabidopsis involves calcium, abscisic acid, ethylene & salicylic acid. *Plant Physiol.* **128**(2), 682–695 (2002).
69. Pandey, S. C. The gene transcription factor cyclic AMP-responsive element binding protein: role in positive and negative affective states of alcohol addiction. *Pharmacol. Ther.* **104**, 47–58 (2004).
70. Kudla, J. *et al.* Advances and current challenges in calcium signaling. *New Phytol.* **218**(2), 414–431 (2018).
71. Bürstenbinder, K. *et al.* The IQD family of calmodulin-binding proteins links calcium signaling to microtubules, membrane subdomains, and the nucleus. *Plant Physiol.* **173**(3), 1692–1708 (2017).
72. Li, J. *et al.* Assessment and application of phosphorus/calcium-cottonseed protein adhesive for plywood production. *J. Clean Prod.* **229**, 454–462 (2019).
73. Cheng, N. *et al.* Arabidopsis monothiol glutaredoxin AtGRXS17 is critical for temperature-dependent postembryonic growth and development via modulating auxin response. *J. Biol. Chem.* **286**, 20398–20406 (2011).
74. Szklarczyk, D. *et al.* STRING v11: protein–protein association networks with increased coverage supporting functional discovery in genome-wide experimental datasets. *Nucleic Acids Res.* **47**, D607-613 (2019).

75. Alazem, M., He, M., Moffett, P. & Lin, N. Abscisic acid induces resistance against bamboo mosaic virus through Argonaute 2 and 3. *Plant Physiol.* **174**, 339–355 (2017).
76. Olsson, V. *et al.* Look closely, the beautiful may be small: precursor-derived peptides in plants. *Annu. Rev. Plant Biol.* **70**, 153–186 (2019).
77. Murphy, E., Smith, S. & De Smet, I. Small signalling peptides in Arabidopsis development: how cells communicate over a short distance. *Plant Cell* **24**, 3198–3217 (2012).
78. Gai, Y. P. *et al.* MiRNA-seq-based profiles of miRNAs in mulberry phloem sap provide insight into the pathogenic mechanisms of mulberry yellow dwarf disease. *Sci. Rep.* **8**(1), 1–19 (2018).
79. Bosco, D. *et al.* DNA-based methods for the detection and the identification of phytoplasmas in insect vector extracts. *Mol. Biotechnol.* **22**, 9–18 (2002).
80. Martini, M. *et al.* DNA-dependent detection of the grapevine fungal endophytes *Aureobasidium pullulans* and *Epicoccum nigrum*. *Plant Dis.* **93**, 993–998 (2009).
81. Almeida-Trapp, M., De Souza, G. D., Rodrigues-Filho, E., Boland, W. & Mithöfer, A. Validated method for phytohormone quantification in plants. *Front. Plant Sci.* **5**, 417 (2014).
82. Pommerrenig, B., Eggert, K. & Bienert, G. P. Boron deficiency effects on sugar, ionome phytohormone profiles of vascular and non-vascular leaf tissues of common plantain (*Plantago major* L.). *Intern. J. Mol. Sci.* **20**(16), 3882 (2019).

Acknowledgments
We gratefully acknowledge financial support from a Capes-Humboldt Research Fellowship for Marilia Almeida-Trapp and the European Union's Programme 'Erasmus+ for Traineeship' for Valeria De Rosa. The authors thank Professor Domenico Bosco (University of Torino, Italy) for making available the CY phytoplasma strain and for his advice on insect rearing. We are also grateful to Dr. Laurence Cantrill (Out of Site English, Sydney, Australia), for the accurate English revision.

Author contributions
R.M. and L.P. conceived the project. C.B., V.D.R. grew the plants and A.L. and N.L. collected the samples. C.B., F.C. reared the vector insects and A.L. prepared the inoculum. C.B. and S.B., with the support of M.M., carried out phytoplasma quantification. V.D.R. and M.A.T. carried out the phytohormone analyses with the supervision of A.M. C.B., S.S. and R.M. prepared the samples and performed TEM analyses. R.M. and A.J.E.v.B. wrote the manuscript with the support of C.B. and A.M. All authors provided critical feedback.

Funding
This work was funded by the University of Udine, through the Department of Agriculture, Food, Environment and Animal Sciences (Di4A), Project Start-up 2018.

Competing interests
The authors declare no competing interests.

Additional information
Supplementary information is available for this paper at https://doi.org/10.1038/s41598-020-71660-0.

Correspondence and requests for materials should be addressed to R.M.

Reprints and permissions information is available at www.nature.com/reprints.

Publisher's note Springer Nature remains neutral with regard to jurisdictional claims in published maps and institutional affiliations.

3.3 PROTEIN-PROTEIN INTERACTION NETWORKS GIVE SUGGESTIONS ON THE POSSIBLE PHYTOPLASMA-EFFECTOR-MEDIATED INTERACTION OF ATSEOR2 WITH PLASMA MEMBRANE RECEPTORS IN ARABIDOPSIS.

COMMENTARY BY CHIARA BERNARDINI, RITA MUSETTI

Phytoplasma-associated diseases cause several damages concerning yield losses or quality losses in many economically important crops (Musetti and Pagliari, 2019). Right now, phytoplasma disease epidemics can be handled mainly by insect vector control using pesticides, or by the removal of inoculum sources. However, the efficacy of these approaches is limited because chemical control is often inadequate (Firrao *et al.*, 2007) and phytoplasma reservoirs are sometimes unknown or constituted by wild plants (Bertaccini and Duduk, 2009).

The study of the interaction with the plants at the molecular level could provide important information on the plant defense mechanism, giving opportunity to actuate more efficient and sustainable control strategies. The aggregation capability of the filamentous phloem proteins, named sieve-element occlusion related (SEOR) proteins in Arabidopsis, was considered as a fast and efficient strategy to plug the sieve plates in case of wound, pathogen attack and other injuries (van Bel, 2006). Moreover, we recently reported that AtSEOR2 protein may have a role in the slow-down of phytoplasma multiplication in *Arabidopsis thaliana* (Pagliari *et al.*, 2017), being involved, in some way, in plant immune processes (Pagliari *et al.*, 2018) or interfering with the hormone-mediated signaling pathways (Bernardini *et al.*, 2020).

Network-based analysis offers a holistic approach that can enable a detailed understanding of the relationships between phytopathogens and plants (Pritchard and Birch, 2011). A part the possible relationship of AtSEOR2 protein with hormone-related defense pathways (discussed in Bernardini *et al.*, 2020), STRING and Bio-grid databases (Szklarczyk *et al.* 2019), report that in Arabidopsis AtSEOR2 protein interacts with RPM1-interacting protein (AtRIN4) *in silico* (Afzal *et al.*, 2013; Mukhtar et al 2011; Arabidopsis Interactome Mapping Consortium, 2011).

Pagliari *et al.*, (2018) noticed that in *Atseor1ko* line, expressing AtSEOR2 protein not linked to its homolog AtSEOR1, the level of *AtRIN4*, *AtRPM1* and *AtRPS2* transcripts is constitutively higher in 75-day-old plants. Such as level was not affected by phytoplasma infection at that stage, when the typical disease symptoms were fully developed. As the effectiveness of defense processes is dependent on the precocity of

plant response (de Wit, 2007), we also evaluated the expression levels of the same genes, in wild type and *Atseor1ko* plants, at the onset of infection, i.e. 5 days after the end of the inoculation access period (IAP). Results evidenced that the expression levels of *AtRIN4* was increased in phytoplasma-infected *Atseor1ko* line at a pre-symptomatic stage (while *AtRPS2* was down-regulated and *AtRPM1* expression level was not affected), further supporting a possible interaction (Figure 3.5).

Table 3.1 ***Table of the primer used in this study****, with relative encoded proteins and function of the gene.*

GENE	nM	Forward primer 5'-3'	Reverse primer 5'-3'	Function and reference
AtRIN4	500	TTCAAGAACGCCGACTCATCA	AAAGCCAAAGCAGCAACATGAG	Part of the complex of pathogen recognition and involved with the activation of defense processes (Pagliari et al., 2018)
AtRPS2	500	GGGATCTGAAAGCGGCATGT	TGCCATCCACAATGCAAAGC	
AtRPM1	500	ACATGGAAGAGACTTGTGCGA	TGCAGTTGCGATCAGGTCAT	
AtUBC9	300	TCACAATTTCCAAGGTGCTGC	CGAGCAGTGGACTCGTACTT	In this study used as reference gene as reported by (Pagliari et al., 2017)

Here are some key aspects, taken from the literature, about AtSEOR2 and AtRIN4 interaction, which could offer new interesting possibility of investigation.

Since RIN4 is an important regulator of both pattern- and effector-triggered immunity (PTI or ETI, Mackey *et al.*, 2002; 2003; Afzal *et al.*, 2013), it is expected that pathogens will try to modify RIN4 not only using various effectors (i.e. the *Pseudomonas syringae* effectors AvrB, AvrRpm1, and AvrRpt2), but also

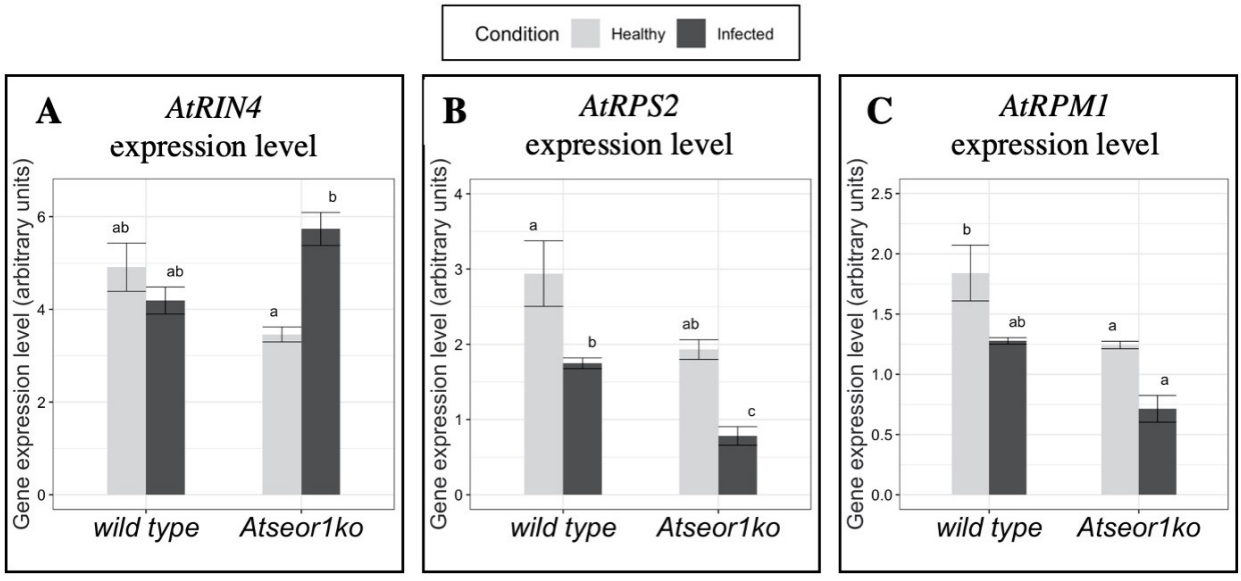

Figure 3.4 ***Expression levels of AtRIN4 (A), AtRPS2 (B) and AtRPM1 (C)at the early (5 days after IAP) stage of infection.*** *The expression is presented as the mean normalized expression (MNE) against the reference gene (AtUBC9) expression. In the bar charts, different letters (A; B; C, D) indicate significant differences of the MNE values according to the post hoc test Holm-Sidak, P<0.05. Error bars indicate Standard Error of the Mean.*

evolving new molecules that interfere with other effector-mediated RIN4 modifications. Ray *et al.*, (2019) reported a list of AtRIN4-associated proteins (among which AtSEOR2 protein) that target AtRIN4 to promote plant defense process, upon pathogen-effector activation.

Table 3.2 Features of the gene expression analysis.

Analysis step	Features
RNA extraction	As reported (Pagliari et al., 2017)
DNAse treatment and cDNA synthesis	As reported (Pagliari et al., 2017)
Real-time RT-PCR	Reaction volume: 10µl SsoFast EvaGreen Supermix (Bio-Rad Laboratories Inc., Hercules, CA, USA) cDNA obtained from 10 ng of RNA and primers following the concentration indicated in Tab.2
Cycling conditions	95°C for 3 min 95°C for 5 s and 58°C for 5 s (40 cycles) Melting curve analysis from 65°C to 95°C

The mechanism through which AtSEOR2 interacts with AtRIN4 is probably mediated by the characteristic NOI motif present in the latter. NOI domain interacts with proteins belonging to the Cys/His-rich. It has been reported that SEOR proteins are characterized by a conserved C-terminal M1 motif, containing several conserved cysteine residues (Rüping *et al.*, 2010) characteristic of the peptide ligands (Olson *et al.*, 2019), which are involved in different developmental and defence-related processes. Furthermore, Afzal *et al.*, (2011) raised the hypothesis that RIN4 might be involved in defense-associated vesicle trafficking, guiding or activating the polarized secretion of defense-related vesicles toward the pathogen infection site. Alternatively, vesicular complexes might recognize newly synthesized RIN4 proteins, driving RIN4 movement toward plasma membranes under pathogen attack. Interestingly, Anstead *et al.*, (2012) observed the presence of large numbers of parietal globular vesicular bodies in *Atseor1ko* plants expressing GFP-tagged AtSEOR2, whose function remained to be investigated.

Phytoplasma effectors could promote ETI directly or indirectly. It is reported that a phytoplasma effector (SAP44, MacLean, unpublished data) may interact with a plant NB-LRR (Nuclear Binding domain-

Leucine Rich Repeat) protein, suggesting that phytoplasma effectors may potentially be recognized by plant R-genes.

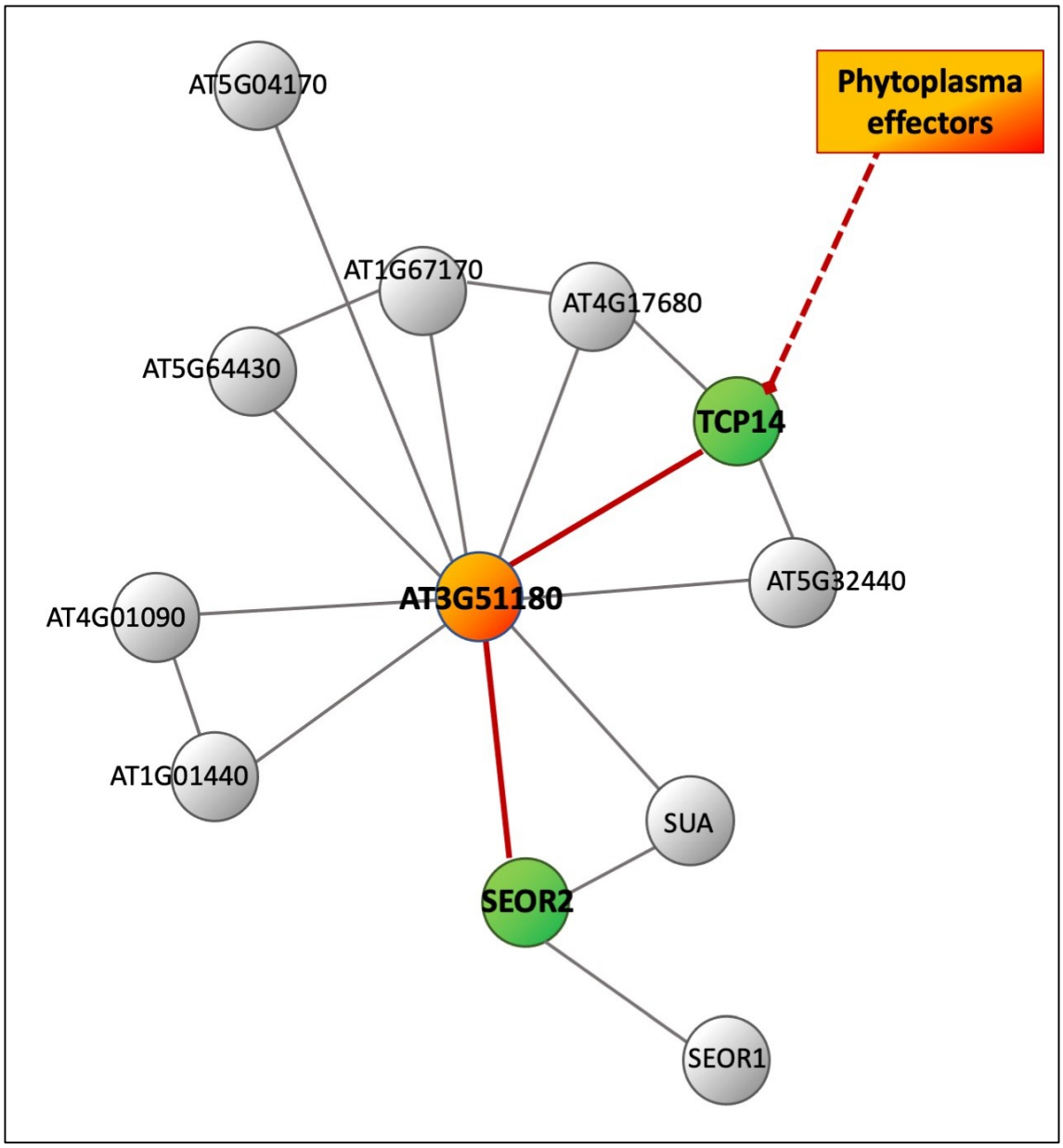

Figure 3.6 ***STRING interaction visualization of the genes taken in consideration****. Red line indicates the predicted link between gene responsible of the signalling cascade from the phytoplama effectors to the SEOR proteins. Orange circle is the possible link between the SEORs and the TCPs.*

According to network-based analyses (Szklarczyk *et al.* 2019; Takáč *et al.*, 2019) phytoplasma effectors could indirectly stimulate AtSEOR2-AtRIN4 interaction *via* the TEOSINTE BRANCHED, cycloidea and PCF (TCP) transcription factors. In fact, it is largely reported that phytoplasma effectors, belonging to the SAP class, interact with plant proteins belonging to the class of TCP (McLean *et al.*, 2011; Sugio *et al.*, 2011; Marrero *et al.*, 2020), and in particular with TCP14, which is the most targeted host protein by pathogen effectors. TCP14 is reported as a resistance promoter: in case of *Pseudomonas syringae* infection, it is able to

promote the disease resistance (Yang *et al.*, 2017) and it has the same localization of the effectors in case of infection (Weßling *et al.*, 2014). Further studies have demonstrated that the TCPs are involved in the regulation of immunity processes, in particular in the plant defense against biotrophs: experiments on mutant line unable to produce one TCPs, revealed the more susceptibility of the plants, further supporting the hypothesis that they are regulators of the defense processes (Kim *et al.*, 2014). TCP14 interacts with a transcription factors, encoded by the At3g51180 gene, which belongs to the CCCH zinc finger family, largely described by Wang *et al.*, (2008) as having important roles in the RNA processing. The expression profile indicated that most members of plant CCCH genes are regulated by abiotic or biotic stresses, suggesting that they could have an effective role in stress tolerance. At3g51180 is able to directly interact with AtSEOR2 protein (Figure 3.6). The whole cascade results in the activation of the SEOR2 expression and the consequent probable activation of RIN4 and the associated R proteins.

In conclusion, with this short commentary we wanted highlight the great potentiality of AtSEOR2 to interact with a number of proteins involved in pathogen perception and in defence processes. The roles of SEOR proteins in sieve-element biology is still largely unknow, but we can surely assume that they are not only related with the sieve-element sealing mechanism.

References

Afzal, A.J., da Cunha, L., Mackey, D., 2011. Separable Fragments and Membrane Tethering of *Arabidopsis* RIN4 Regulate Its Suppression of PAMP-Triggered Immunity. Plant Cell 23, 3798–3811. https://doi.org/10.1105/tpc.111.088708

Afzal, A.J., Kim, J.H., Mackey, D., 2013. The role of NOI-domain containing proteins in plant immune signaling. BMC Genomics 14, 327. https://doi.org/10.1186/1471-2164-14-327

Anstead, J.A., Froelich, D.R., Knoblauch, M., Thompson, G.A., 2012. Arabidopsis P-Protein Filament Formation Requires Both AtSEOR1 and AtSEOR2. Plant Cell Physiol. 53, 1033–1042. https://doi.org/10.1093/pcp/pcs046

Arabidopsis Interactome Mapping Consortium, 2011. Evidence for network evolution in an Arabidopsis interactome map. Science 333, 601–607.

Bernardini, C., Pagliari, L., De Rosa, V., Almeida-Trapp, M., Santi, S., Martini, M., Buoso, S., Loschi, A., Loi, N., Chiesa, F., Mithöfer, A., van Bel, A.J.E., Musetti, R., 2020. Pre-symptomatic modified phytohormone profile is associated with lower phytoplasma titres in an Arabidopsis seor1ko line. Sci. Rep. 10, 14770. https://doi.org/10.1038/s41598-020-71660-0

Bertaccini, A., Duduk, B., 2009. Phytoplasma and phytoplasma diseases: a review of recent research. Phytopathol. Mediterr. 48, 355–378.

de Wit, P.J., 2007. How plants recognize pathogens and defend themselves. Cell. Mol. Life Sci. 64, 2726–2732.

Firrao, G., Garcia-Chapa, M., Marzachì, C., 2007. Phytoplasmas: genetics, diagnosis and relationships with the plant and insect host. Front. Biosci. J. Virtual Libr. 12, 1353–1375.

Kim, S.H., Son, G.H., Bhattacharjee, S., Kim, H.J., Nam, J.C., Nguyen, P.D.T., Hong, J.C., Gassmann, W., 2014. The Arabidopsis immune adaptor SRFR1 interacts with TCP transcription factors that redundantly contribute to effector-triggered immunity. Plant J. 78, 978–989. https://doi.org/10.1111/tpj.12527

Mackey, D., Belkhadir, Y., Alonso, J.M., Ecker, J.R., Dangl, J.L., 2003. Arabidopsis RIN4 Is a Target of the Type III Virulence Effector AvrRpt2 and Modulates RPS2-Mediated Resistance. Cell 112, 379–389. https://doi.org/10.1016/S0092-8674(03)00040-0

Mackey, D., Holt, B.F., Wiig, A., Dangl, J.L., 2002. RIN4 Interacts with Pseudomonas syringae Type III Effector Molecules and Is Required for RPM1-Mediated Resistance in Arabidopsis. Cell 108, 743–754. https://doi.org/10.1016/S0092-8674(02)00661-X

MacLean, A.M., Sugio, A., Makarova, O.V., Findlay, K.C., Grieve, V.M., Tóth, R., Nicolaisen, M., Hogenhout, S.A., 2011. Phytoplasma Effector SAP54 Induces Indeterminate Leaf-Like Flower Development in Arabidopsis Plants. Plant Physiol. 157, 831–841. https://doi.org/10.1104/pp.111.181586

Marrero, M.C., Capdevielle, S., Huang, W., Busscher, M., Busscher-Lange, J., de Ridder, D., van Dijk, A.D., Hogenhout, S.A., Immink, R.G., 2020. Widespread targeting of development-related host transcription factors by phytoplasma effectors. bioRxiv.

Mukhtar, M.S., Carvunis, A.-R., Dreze, M., Epple, P., Steinbrenner, J., Moore, J., Tasan, M., Galli, M., Hao, T., Nishimura, M.T., 2011. Independently evolved virulence effectors converge onto hubs in a plant immune system network. science 333, 596–601.

Musetti, R., Pagliari, L. (Eds.), 2019. Phytoplasmas: Methods and Protocols, Methods in Molecular Biology. Springer New York, New York, NY. https://doi.org/10.1007/978-1-4939-8837-2

Olsson, V., Joos, L., Zhu, S., Gevaert, K., Butenko, M.A., De Smet, I., 2019. Look closely, the beautiful may be small: Precursor-derived peptides in plants. Annu. Rev. Plant Biol. 70, 153–186.

Pagliari, L., Buoso, S., Santi, S., Furch, A.C.U., Martini, M., Degola, F., Loschi, A., van Bel, A.J.E., Musetti, R., 2017.

Filamentous sieve element proteins are able to limit phloem mass flow, but not phytoplasma spread. J. Exp. Bot. 68, 3673–3688. https://doi.org/10.1093/jxb/erx199

Pagliari, L., Buoso, S., Santi, S., Van Bel, A.J.E., Musetti, R., 2018. What slows down phytoplasma proliferation? Speculations on the involvement of AtSEOR2 protein in plant defence signalling. Plant Signal. Behav. 13, e1473666.

Pritchard, L., Birch, P., 2011. A systems biology perspective on plant–microbe interactions: biochemical and structural targets of pathogen effectors. Plant Sci. 180, 584–603.

Ray, S.K., Macoy, D.M., Kim, W.-Y., Lee, S.Y., Kim, M.G., 2019. Role of RIN4 in Regulating PAMP-Triggered Immunity and Effector-Triggered Immunity: Current Status and Future Perspectives. Mol. Cells 42. https://doi.org/10.14348/MOLCELLS.2019.2433

Rüping, B., Ernst, A.M., Jekat, S.B., Nordzieke, S., Reineke, A.R., Müller, B., Bornberg-Bauer, E., Prüfer, D., Noll, G.A., 2010. Molecular and phylogenetic characterization of the sieve element occlusion gene family in Fabaceae and non-Fabaceae plants. BMC Plant Biol. 10, 219. https://doi.org/10.1186/1471-2229-10-219

Sugio, A., MacLean, A.M., Kingdom, H.N., Grieve, V.M., Manimekalai, R., Hogenhout, S.A., 2011. Diverse Targets of Phytoplasma Effectors: From Plant Development to Defense Against Insects. Annu. Rev. Phytopathol. 49, 175–195. https://doi.org/10.1146/annurev-phyto-072910-095323

Szklarczyk, D., Gable, A.L., Lyon, D., Junge, A., Wyder, S., Huerta-Cepas, J., Simonovic, M., Doncheva, N.T., Morris, J.H., Bork, P., 2019. STRING v11: protein–protein association networks with increased coverage, supporting functional discovery in genome-wide experimental datasets. Nucleic Acids Res. 47, D607–D613.

Takáč, T., Novák, D., Šamaj, J., 2019. Recent advances in the cellular and developmental biology of phospholipases in plants. Front. Plant Sci. 10, 362.

van Bel, A.J., 2006. Sieve-pore plugging mechanisms, in: Cell-Cell Channels. Springer, pp. 113–118.

Wang, D., Guo, Y., Wu, C., Yang, G., Li, Y., Zheng, C., 2008. Genome-wide analysis of CCCH zinc finger family in Arabidopsis and rice. BMC Genomics 20.

Weßling, R., Epple, P., Altmann, S., He, Y., Yang, L., Henz, S.R., McDonald, N., Wiley, K., Bader, K.C., Gläßer, C., Mukhtar, M.S., Haigis, S., Ghamsari, L., Stephens, A.E., Ecker, J.R., Vidal, M., Jones, J.D.G., Mayer, K.F.X., Ver Loren van Themaat, E., Weigel, D., Schulze-Lefert, P., Dangl, J.L., Panstruga, R., Braun, P., 2014. Convergent Targeting of a Common Host Protein-Network by Pathogen Effectors from Three Kingdoms of Life. Cell Host Microbe 16, 364–375. https://doi.org/10.1016/j.chom.2014.08.004

Yang, L., Teixeira, P.J.P.L., Biswas, S., Finkel, O.M., He, Y., Salas-Gonzalez, I., English, M.E., Epple, P., Mieczkowski, P., Dangl, J.L., 2017. Pseudomonas syringae Type III Effector HopBB1 Promotes Host Transcriptional Repressor Degradation to Regulate Phytohormone Responses and Virulence. Cell Host Microbe 21, 156–168. https://doi.org/10.1016/j.chom.2017.01.003

4. MANIPULATION OF CALLOSE-RELATED METABOLISM AS AN IDEAL BATTLEFIELD DURING PLANT-PHYTOPLASMA INTERACTION

Phytoplasmas cause big amount of changes in the plant host and plants face them with different responses. Considering the phytoplasma habitat (i.e. the phloem sieve elements) we studied, at first, the responses related to the Sieve-Element Occlusion (SEO) proteins (see chapter 3).

The purpose of the present chapter is focusing on the possible roles of sieve-plate callose in phytoplasma-infected plants, which range from physical occlusion of the sieve-pores to the activation of defense signaling.

4.1 THE CALLOSE METABOLISM AND THE IMPORTANCE OF SUGAR SIGNALING: AN INTRODUCTION

Callose and its synthesis

B 1,3-D glucan, commonly known as callose, is one of the most important glucans inside the plants. It is estimated to be 0.3% of the total sugar content in Arabidopsis thaliana (Falter 2015). Callose is a linear chain of glucose linked by 1-3 glycosidic bounds and assembled by the callose synthase (CalS) called also glucan synthase like enzyme (GSL). Callose linkage 1-3 gives it the helical shape. Inside the chain, 1-4 and 1-6 linkage might be present, but always in small quantities (Waldron and Faulds, 2007). This linkage between monomers is the sole difference that takes place between callose and cellulose: cellulose is in fact unbranched polymer consisting of (1-4)-linked b-D-Glcp (Waldron and Faulds, 2007). Callose plays a pivotal role in maintenance

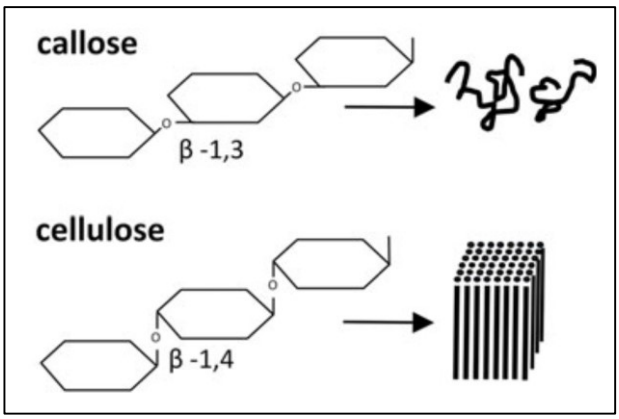

Figure 4.1 ***Structure of callose and cellulose.*** *Image from Piršelová and Matušíková (2013)*

of the structure of cell wall plate and plasmodesmata (Ellinger and Voigt, 2014), it is one of the defense mechanism of the plant and it is deposed during the cytochinesis and pollen formation and germination.

For long time cellulose synthase and callose synthase were considered the same enzyme (Jacob and Northcote 1985). Quite recently, thanks to further studies, the pathways have divided in two distinct complexes, even it is well known that they share the basilar steps.

Callose synthase gene family in Arabidopsis encodes for twelve enzymes, similar in the function, but different for localization (Ellinger and Voigt, 2014). They were studied independently by two research groups and were named as "glucan synthase like" or "callose synthase". In the Table 4. the conversion between the two different nomenclatures is given, as the biological functions of the different enzymes. CalS1, CalS2, CalS5, CalS8 and CalS10 have an important role during pollen development; CalS1 and CalS5 during pollen maturation; CalS6 and CalS8 in the formation of the premature cell wall; CalS5 in defence-related papillae.

Table 4.1 ***GSL and CalS nomenclature, functions and subcellular localization****. Image from Ellinger and Voigt*

GSL[1]	CalS[2]	Gene ID[3]	Subcellular localization (experimental)	Biological function
Biological role in fertility and cell division				
GSL1	CalS11	AT4G04970	MS/MS: plasma membrane (Benschop *et al.*, 2007)	Pollen development and fertility (Enns *et al.*, 2005)
GSL2	CalS5	AT2G13680	GFP-tagged protein in cultured tobacco BY-2 cells: plasma membrane and Golgi-related endo-membranes (Xie *et al.*, 2012)	Found in mature pollen grains (Grobei *et al.*, 2009); involved in late stages of pollen development and pollen tube (Dong *et al.*, 2005; Xie *et al.*, 2010)
GSL6	CalS1	AT1G05570	GFP-tagged protein: cytosol and plasma membrane (Hong *et al.*, 2001*a*); MS/MS: plasma (Alexandersson *et al.*, 2004; Keinath *et al.*, 2010; Benschop *et al.*, 2007; Zhang and Peck, 2011)	Required for callose depositions during cell plate formation (Hong *et al.*, 2001*a*, *b*)
GSL8	CalS10	AT2G36850	MS/MS: plasma membrane (Alexandersson *et al.*, 2004; Mitra *et al.*, 2009; Benschop *et al.*, 2007; Marmagne *et al.*, 2007; Zhang and Peck, 2011)	Required for male gametophyte development and plant growth (Töller *et al.*, 2008); entry of microspores into mitosis (Chen *et al.*, 2009; De Storme *et al.*, 2013); required for callose biosynthesis at the cell plate (Thiele *et al.*, 2009), involved in stomatal pattering and deposition at the plasmodesmata (Guseman *et al.*, 2010; Han *et al.*, 2014)
GSL10	CalS9	AT3G07160	MS/MS: plasma membrane (Alexandersson *et al.*, 2004; Dunkley *et al.*, 2006; Benschop *et al.*, 2007; Marmagne *et al.*, 2007; Mitra *et al.*, 2009; Keinath *et al.*, 2010; Zhang and Peck, 2011)	Required for male gametophyte development and plant growth (Töller *et al.*, 2008); together with GSL8, involved in entry of microspores into mitosis (De Storme *et al.*, 2013)
Structural reinforcement				
GSL5 (PMR4)	CalS12	AT4G03550	GFP-tagged protein: plasma membrane (Drakakaki *et al.*, 2012; Ellinger *et al.*, 2013); MS/MS: plasma membrane (Alexandersson *et al.*, 2004; Dunkley *et al.*, 2006; Benschop *et al.*, 2007; Mitra *et al.*, 2009; Keinath *et al.*, 2010; Zhang and Peck, 2011)	Required for wound and papillary callose formation in response to fungal pathogens (Jacobs *et al.*, 2003; Nishimura *et al.*, 2003; Ellinger *et al.*, 2013; Naumann *et al.*, 2013); important for exine formation and pollen wall patterning (Enns *et al.*, 2005)
GSL7	CalS7	AT1G06490	No experimental data	Responsible for callose deposition in the phloem (Barratt *et al.*, 2011; Xie *et al.*, 2011)
GSL12	CalS3	AT5G13000	MS/MS: plasma membrane (Benschop *et al.*, 2007; Keinath *et al.*, 2010; Zhang and Peck, 2011)	Required for callose deposition at plasmodesmata (Sevilem *et al.*, 2013)
Unknown function				
GSL3	CalS2	AT2G31960	MS/MS: plasma membrane (Alexandersson *et al.*, 2004; Benschop *et al.*, 2007; Kierszniowska *et al.*, 2009)	Unknown function
GSL4	CalS8	AT3G14570	No experimental data	Unknown function, found in roots (Lan *et al.*, 2011)
GSL9	CalS4	AT5G36870	No experimental data	Unknown function, found in leaf membranes (Mitra *et al.*, 2007)
GSL11	CalS6	AT3G59100	No experimental data	Unknown function
GSL1	CalS2	Gene ID3	Subcellular localization (experimental)	Biological function

Ellinger and Voigt classified the CalSs in two groups: the first one involved in pollen development and cell wall (CalS1, CalS2, CalS6, CalS8 and CalS10) while the second one involved in the callose plugging or reinforcement (CalS5, CalS7 and CalS12). There are two types of CalS in the plants (Nedukha, 2015): one is regulated by Calcium ions, and the second one that does not need calcium. The ones that do not need calcium are typically related with the formation of the pollen and stimulated by trypsin (Schlüpmann *et al.*, 1993).

The callose synthesis is catalyzed by a multisubunit enzyme complex (Verma and Hong, 2001). In this complex several components take part: sucrose synthase (SuSs), UDP-glucose transferase (UGT1) and, indeed, Callose Synthase.

Callose synthase and Cellulose synthase have a similar transmembrane topology (Nedukha, 2015): they have a multiple transmembrane domains clustered in two regions and a large hydrophilic central loop facing with cytoplasm. The hydrophilic loop comprises the UDP-glucose binding domain and the glycosyltransferase domain Figure 4.2. It seems that the entire complex is assembled inside di endoplasmic reticulum, then moved to the membrane with vesicle trafficking (Schneider *et al.*, 2016).

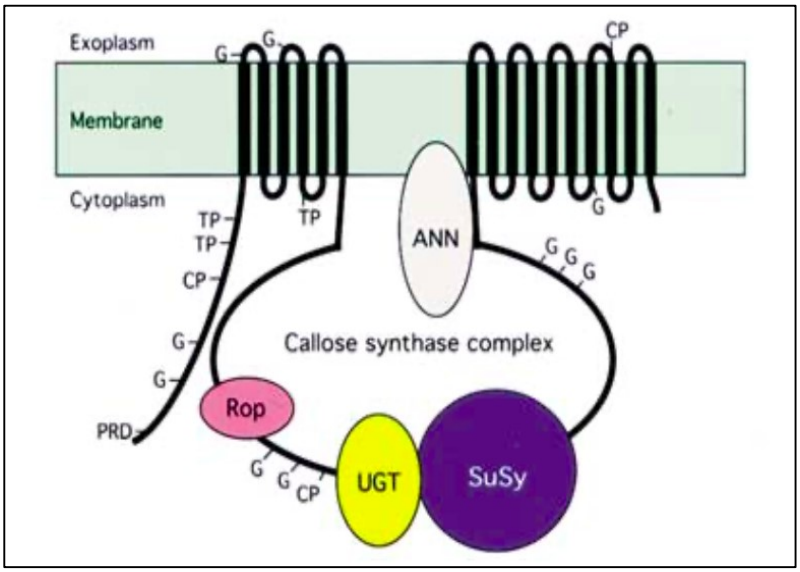

Figure 4.2 ***Hypothetical model of the callose synthase complex*** *showing transmembrane do mains and hydrophilic loop interacting with Rop1, annexin, UGT1 and SuSy. G, potential N-linked glycosylation sites; CP, cAMP- and cGMP-dependent phosphorylation sites; TP, potential tyrosine phosphorylation sites; PRD, proline-rich domain. Image and caption from Verma and Hong 2001.*

Callose synthase in the phloem

The sole CalS7 is peculiar of the phloem and involved in the production of callose at the sieve plate level (Barratt *et al.*, 2011; Xie *et al.*, 2011). Mutant of Arabidopsis (*Atcals7* knock-out line) obtained with tDNA insertion (Xie *et al.*, 2011) shows the absence of callose at the sieve plate but not in the xylem. This loss seems to affect also the phloem transport, that is impaired in comparison to the wild type condition. In case of mutation, the sieve pores appear smaller than those in wild type even if their number and the total diameter of the plate is similar (Barratt *et al.*, 2011). Experiments carried on with ^{14}C, have revealed that wild type plants transfer 26% of assimilates to the top of the stem while mutant line of callose only about 3.5% (Barratt *et al.*,

2011) confirming the hypothesis of reduced transport in the mutants. The two lines differ moreover for the content in sugars that seems to be significantly reduced in callose mutant.

Starting from sucrose, SuSs provide UDP-glucose that is moved to the active site of CalS by the UDP-glucose transferase (UGT1) (Verma and Hong, 2001). It seems that the CalSs are unable to bind UDP-glucose without the intervention of UGT1 that has a domain interacting with the CalS. UGT1 is bounded with Rop1 and annexin: both the proteins seem to be involved in the regulation of the activity of the entire complex. It seems that the annexin, similar to synaptotagmin (Nedukha, 2015), could act in the switch between callose and cellulose synthase in response to Ca^{2+} and Mg^{2+}. Rop1, instead, may be a spatial regulator of the Cals. Phragmoplastin, protein associated with cell plate, may activate the enzyme during the formation of cell plate. Several other proteins could be associated with the complex with minor functions.

The callose deposition at the sieve plate seems to be enhanced by increase of cytosolic Ca^{2+}. After mechanical injury, the concentration of Ca^{2+} ions increase rapidly and the callose deposition starts in about 20 min in *Vicia faba* (Furch *et al.*, 2007). After this the degradation occurs when the Ca^{2+} reaches again the basal level. The Ca^{2+} that acts ad signal, seems to be already stored inside the cells: studies on different metals and species demonstrate that also in case of Al toxicity, acting as suppressor of activity of the Ca^{2+}pump, the callose deposition is Ca^{2+}-mediated (Stass and Horst, 2009).

At the transcriptional level GSL5 and GSL8 are regulated by the salicylic acid receptor NPR1, for GLS8 also by ARF7 (auxin response factor), suggesting that the enhancement happens in case of stress of the plant (Ellinger and Voigt, 2014). A possible mechanism involved in the callose biosynthesis is related with the phosphorylation: studies attested the enhancement of the GSL10 and GSL12 operated by flg22 and xylanase. Except of biotic stresses, the callose pathway seems to be related with the presence inside the plant of reactive oxygen species (ROS, (Luna *et al.*, 2011) and salicylic acid (Nishimura *et al.*, 2003).

Glycolysis

The ß -1,3-glucanases are the enzymes responsible for the cleavage of 1,3 b glycosidic linkage (Hrmova and Fincher, 2009) and so for the hydrolysis of callose. The family of Arabidopsis ß -1,3-glucanases has been amply studied by Doxey (Doxey *et al.*, 2007) who classified all the 50 enzymes present in Arabidopsis in clusters. Some glucanases, ascribable to the class of PR2 genes, are responsible for the response to fungal pathogen (see below). Callose is a transitory material that could be found in the cell wall, but it is also present in many other organs of the plant: seeds, pollen and flowers are some examples. In these organs three major clades were identified: alfa, beta and gamma. Every cluster was the result of the same function acted by the enzyme. Essentially the ß -1,3-glucanase are ascribable to three functions: the cell wall morphogenesis and cell division (glucanases with low response to phytohormones and stresses in general), the flower specific glucanases and the glucanases present in root and leaves. Levy et. al (Levy *et al.*, 2007b, 2007a) revealed that,

in Arabidopsis, one of these glucanases is exclusively associated to plasmodesmata, in which it is responsible of the callose turnover and so indirectly of symplasmic communication.

Callose functions and localization

Functions of callose are strictly linked with its localization.

At first, callose plays an important role at the phragmoplast level. During the cytochinesis, there is the reorganization of the actin filaments and the increase of the vesicle trafficking. At this level the cell plate starts to be formed. At first there is the deposition of callose and the other polysaccharides that acts as matrix of the plate, probably to avoid the disorganized deposition of the cellulose, a more durable polysaccharide (Levy *et al.*, 2007a). In a second moment, gradually, the callose is removed through hydrolysis and substituted by the cellulose. The callose completely disappears from cell plate composition except from plasmodesmata in which is the major compound to give the shape and the resistance (Brown and Lemmon, 2009). Moreover, callose is one of the primary compounds found inside the cell wall and in the pollen tubes in which is responsible for the cell flexibility having tenseness and contraction during mechanical pressures.

Second important localization of the callose is at the plasmodesmata. Plasmodesmata are channels that, crossing the cell wall, provide a connection cell-to-cell (symplast connection, (Levy *et al.*, 2007a). Here callose helps the movement of water inside the plant, giving the structure to plasmodesmata (20-40 nm) and to the pore (200-400nm) of the sieve element plates. The movement across plasmodesmata is related with the balance between biosynthesis and hydrolysis of callose. Viral action acts at this level: some viruses unbalance this equilibrium. A movement protein, in fact, enhances the release of vesicle containing glucanase from the endoplasmic reticulum (ER) body. Hydrolyzing the callose at the plasmodesmata level, the plasmodesmata become larger promoting the virus spread.

Another particular kind of callose is the definitive callose: this is deposed (Levy and Epel, 2009) in old sieve elements to be used by the plant.

Finally callose is one of the plant defenses in case of injuries both biotic, with a sort of “leak sealant”, than abiotic (Nedukha, 2015). During fungal penetration, callose has been deposed in correspondence of austoria forming a papillae (Voigt and Somerville, 2009).

Bacteria normally colonize the intercellular spaces secreting flagellin. Plants perceive the pathogen flagellin with the FLS2 gene (flagellin sensitive 2), a transmembrane receptor chinase. In the same moment, xanthan secreted by pathogen binds the Ca^{2+} ions preventing the enhancement of callose biosynthesis.

Callose synthesis can be, also, inducted during abiotic stresses like cold, drought or metals (Luna *et al.*, 2011).

During abiotic stress both algae and plants produce callose, this suggests that the signaling related to callose deposition has been strongly maintained during the evolution (Stass and Horst, 2009). Metal toxicity, depending on the ion concentration and species tolerance, implicates callose deposition. As well as metals, anoxia of the roots (other prove of the presence of Ca^{2+} storage inside the cells) and temperature stress are other reasons of deposition. The most common abiotic stress cause of callose plugging is the wounding injury. After mechanical damage, in fact, the plant reacts with the callose deposition, initially on the cell wall of the surviving cells, then in the surrounding regions (Stass and Horst, 2009).

Interplay with hormones

Callose, as stress response, interplays in some way with phytohormones. Luna and coworkers demonstrated the role of ABA in the callose increase, interplaying, in particular, with PMR4 (Cals12 or GSL5) (Luna *et al.*, 2011). The hypotheses about the mechanism of regulation are two (Flors *et al.*, 2005): ABA could act at the level of PAL (phenylalanine-ammonia-lyase) and mediate the accumulation of callose interfering with nitric oxide, or the whole mechanism could involve the ROS and the consequent increase of Ca^{2+} ions. Mutant laking IBS3 (zeaxanthin epoxidase, involved in the ABA biosynthesis) is unable of deposing callose, and the same thing happens in ABA1 mutant line (ethilene responsive factor). The key for understand this mechanism could be found in the SNAREs (soluble N-ethyl-maleimide-sensitive proteins) that act on the $[K^+]$ and $[Cl^-]$ in the guard cells: their encoding gene PEN1 (arabidiol synthase) is responsible for the vesicle trafficking to the site of penetration of the pathogen. Moreover the study on the mutant line lacking the gene OCP3 (overexpressor of cationic peroxidase3, it mediates the JA-mediated COI1-dependent and ABA-mediated-PMR4 dependent resistance) shows a linkage between callose deposition and the phytohormone JA and ABA (García-Andrade *et al.*, 2011): callose deposition seems to be blocked when ABA biosynthesis is impaired.

Other studies have showed the link between SA and the callose production (Nishimura *et al.*, 2003). The lack of PRM4 (=Cals12) gene provokes cell hypersensitive response and so resistance to the pathogens. The blockage of the SA pathway restored the susceptibility suggesting the mutual regulation in the defense response of SA and callose synthase. It seems that the linkage callose-salicylic acid depends on a mitogen activated protein kinase 4 (Voigt and Somerville, 2009).

At last, auxin could influence the callose deposition interfering with activity of GSL8 (= Cals 10) or causing the rise of cytosolic Ca^{2+} or enhancing the production of ROS (Han *et al.*, 2014).

The substrate for callose synthesis: sucrose

The transport of sucrose in plants

As previously reported, the primary substrate for the callose synthesis is the sucrose.

Sucrose is the most important sugar present in the plant. It is transferred through phloem to the cells sink both via plasmodesmata than transporters (Wind *et al.*, 2010). AtSWEETs are transporters responsible for the upload of the sucrose in the phloem and so the long-distance transport (Chandran, 2015). Among SWEETs, the ones related with the phloem parenchyma in Arabidopsis are AtSWEET11 and AtSWEET12. The family of SUC transporter genes works together with SWEETs: SUC transporters are symporter of sucrose and H+ responsible for the entrance in the cell: the most expressed in the phloem are AtSUC2 and AtSUC3, they act at the level of tonoplast (Doidy *et al.*, 2012).

The catabolism of sucrose: invertases

Once that the sucrose reaches the sink tissues, it could be hydrolyzed by cell wall invertase and moved inside the cell as hexoses, it can enter for diffusion or via SUCs and follows different pathways. Invertases can be classified in three groups:

- **Cell wall invertase**: responsible of the cleavage of the callose at the apoplastic level are normally expressed in the sink tissue (Ruan, 2014); they can play a pivotal role in case of infection (Tauzin and Giardina, 2014). Once the sucrose has been hydrolized by cell wall invertase, the hexoses can be moved inside the cell by a transporter. Among the hexose transporter, the most important family is STP (Büttner, 2010, 2007; Reuscher *et al.*, 2014; Yamada *et al.*, 2016, 2011);
- **Alkaline/neutral invertases**: responsible for the control of the homeostasis in the plant cell (Ruan, 2014). They are located in the cytosol and in some organelles such as mithocondria and plastids (Tauzin and Giardina, 2014);
- **Vacuolar invertases**: responsible for the accumulation of the sugars in the organs (Ruan, 2014).

Cell wall invertase and vacuolar invertase expression is modulated by proteinaceous inhibitors (INHs): these seem to not be related with the pathogenicity condition that can indirectly guarantee the sucrose: hexose ratio, central point in which the sugar signaling is based on.

The catabolism of sucrose: sucrose synthases

Sucrose synthases (SuSs) are belonging to the class of glycosil transferase and they catalyze the reversible cleavage of callose into fructose and UDP-glucose or ADP-glucose. SuSs are localized to the plasma membrane and associated with other enzymes belonging to the complexes of callose synthase or cellulose

synthase (Stein and Granot, 2019). Normally they are mostly expressed in the sink tissue (Wind *et al.*, 2010). For all of them the structure is similar and consists of N-terminal and C-terminal GT-B.

SuSs can play a general role inside the phloem maybe concerning the equilibrium of sucrose and its products and phloem unloading. SuSs are the primary active enzyme involved in the growth. They supply the substrate for the synthesis of callose, cellulose and starch and they act in case of hypoxia, heat stress or in the shoot apical meristem. They could have a role in the signaling operated by sugars (Stein and Granot, 2019). There are six isoforms of SuSs in Arabidopsis with similar kinetic properties (Bieniawska *et al.*, 2007). Some of them are expressed in all the tissues of the plant as SUS1, SUS2 and SUS3. SUS4 seems to be expressed mostly in roots and siliques. SUS5 and SUS6 are less expressed than the others in all the organs of the plant and are peculiar of the phloem (Barratt *et al.*, 2009; Bieniawska *et al.*, 2007).

While the other SuSs do not influence the equilibrium of compounds inside Arabidopsis (Barratt *et al.*, 2009) AtSUS5 and AtSUS6 are required by the plants for the correct functioning of the phloem; these two genes are responsible for the cleavage of the sucrose inside the phloem where they provide the substrate to CALS7. Studies on the knockout mutants of these genes has showed plants with damaged sieve plates and reduced deposition of callose in correspondence of the sieve pores (Barratt *et al.*, 2009).

Sugars and signaling

The function of signaling of sucrose and sugars in general, in planta, is known from a long time (Koch, 2004) and at the beginning it was reported concerning chlorophyll. Sucrose is responsible for the defense against biotic and abiotic stresses (Morkunas and Ratajczak, 2014). It seems that the sugar signal is transmitted through calcium ions and calcium dependent kinases (Sakr *et al.*, 2018). Both hexoses and sucrose can be considered ad signal molecules of pattern triggered immunity and/or effector triggered immunity. There are several methods of activation of pathways by sugars:

- Phytohormones: it has been demonstrated that the interplay sugar-hormone can cause the activation of the PR proteins (Bolouri Moghaddam and Van den Ende, 2012); moreover sucrose is responsible for the enhancement of the anthocyanin production for which also ABA plays an important role: in the interaction sugars-signaling-phytohormones, ABA seems to be one of the most important signaling hormone with a particular relation with JA and increase of sucrose: ABA, in fact, is able to increase the expression level of the invertase genes, in case of stress, changing the ratio between the sucrose and its cleavage products (Bolouri Moghaddam and Van den Ende, 2012);
- Activation of phenil-propanoid metabolism is stimulated by high concentration of sugars in case of infection: the accumulation of sugars causes the production of ROS (Sakr *et al.*, 2018);

- Hexochinase is upregulated in case of high glucose level (consequence of an high activity of invertase enzymes): hexochinase associated with phytohormones has different roles in the development, growth and physiology (Morkunas and Ratajczak, 2014);

The interaction of sucrose with bZIP and non-fermentating-1-related SnRKs could be the major role of signaling of sucrose itself. The ZIP family gene in Arabidopsis is modulated in a positive, for some, or in a negative way, for other, by sucrose (Morkunas and Ratajczak, 2014). Under pathogen attack the dephosphorilation of SnRK1 can control almost one thousand of genes involved in several pathways. Moreover the interplay of ABA with the PP2C phosphatase, demonstrated that the ABA and SnRK1 are strictly related, while the relation with HXK1 has never been demonstrated leading to the hypothesis that the two sugar-dependent signal are independent from the other one (Sakr *et al.*, 2018).

Other sugars in the plants

In exception of the most common sugars as sucrose, glucose and fructose, several other sugars can take part to the defense mechanism. Myo-inositol, a sugar of raffinose family oligosaccharides (RFO) has a role in case of stress: it can intervene, with the other sugars belonging to the same family, to maintain the osmolarity during water stresses, or acting as a signal during abiotic stresses in general. (ElSayed *et al.*, 2014). The decrease of the sorbitol concentration regulates R genes causing an increase of susceptibility to *Alternaria* in apple (Meng *et al.*, 2018). Moreover sorbitol could also have a role in the osmotic balance of the cells: it has been demonstrated that the sorbitol level after infection increases with the increase of salicylic acid in order to face saline stresses; the same behavior has been demonstrated in case of drought stresses (Tari *et al.*, 2010).

Sugars and phytoplasmas

'*Candidatus* Phytoplasma asteris' genome, is composed by one bigger chromosome and two smaller. The dimension of the genome do not allow to have gene encoding for key metabolic pathways as the amino acid and fatty acid biosynthesis, the tricarboxylic acid cycle and the oxidative phosphorylation (Oshima *et al.*, 2004). For this conformation Oshima *et al.,* supposed that phytoplasmas have a unique sugar intake and metabolic system and that they have evolved retrogressively in order to lose genes and have a smaller genome. Phytoplasma genome has an inactive sucrose phosphorylase, but they are lacking of the pentose phosphates pathway and several other genes: this suggest us that they catch the necessary compounds directly from the host cell colonized. This hypothesis is supported by the presence of a large number of transporters, necessary to import metabolites from the host (Oshima *et al.*, 2004). The metabolite requirement is the mechanism which the pathogenicity based on.

Little is still known about the modified metabolism of sugars in case of infection by phytoplasmas even if could be the central node to understand the pathogenicity of them. Santi *et al.* demonstrated that the metabolism of grapevine following stolbur infection is moved and the pathogen induces a switch in the source-sink location (Santi *et al.*, 2013a, 2013b). The reduction of phloem loading, in fact, suggests an induction od carbohydrates sink caused by phytoplasma infection. Studies in other pathosystems have underlined the same accumulation of sugars in leaves and the consequent decrease of them in the original sink tissue (Lepka *et al.*, 1999; Maust *et al.*, 2003).

References

Barratt, D.H.P., Derbyshire, P., Findlay, K., Pike, M., Wellner, N., Lunn, J., Feil, R., Simpson, C., Maule, A.J., Smith, A.M., 2009. Normal growth of Arabidopsis requires cytosolic invertase but not sucrose synthase. Proc. Natl. Acad. Sci. 106, 13124–13129.

Barratt, D.H.P., Kölling, K., Graf, A., Pike, M., Calder, G., Findlay, K., Zeeman, S.C., Smith, A.M., 2011. Callose Synthase GSL7 Is Necessary for Normal Phloem Transport and Inflorescence Growth in Arabidopsis. Plant Physiol. 155, 328–341.

Bieniawska, Z., Paul Barratt, D.H., Garlick, A.P., Thole, V., Kruger, N.J., Martin, C., Zrenner, R., Smith, A.M., 2007. Analysis of the sucrose synthase gene family in Arabidopsis: The sucrose synthase gene family in Arabidopsis. Plant J. 49, 810–828.

Bolouri Moghaddam, M.R., Van den Ende, W., 2012. Sugars and plant innate immunity. J. Exp. Bot. 63, 3989–3998

Brown, R.C., Lemmon, B.E., 2009. Callose in Cell Division, in: Chemistry, Biochemistry, and Biology of 1-3 Beta Glucans and Related Polysaccharides. Elsevier, pp. 425–437.

Büttner, M., 2010. The Arabidopsis sugar transporter (AtSTP) family: an update: Arabidopsis sugar transporter family. Plant Biol. 12, 35–41.

Büttner, M., 2007. The monosaccharide transporter(-like) gene family in *Arabidopsis*. FEBS Lett. 581, 2318–2324.

Chandran, D., 2015. Co-option of developmentally regulated plant SWEET transporters for pathogen nutrition and abiotic stress tolerance: ROLE OF SWEET IN PATHOGEN NUTRITION AND STRESS TOLERANCE. IUBMB Life 67, 461–471.

Doidy, J., Grace, E., Kühn, C., Simon-Plas, F., Casieri, L., Wipf, D., 2012. Sugar transporters in plants and in their interactions with fungi. Trends Plant Sci. 17, 413–422.

Doxey, A.C., Yaish, M.W.F., Moffatt, B.A., Griffith, M., McConkey, B.J., 2007. Functional Divergence in the Arabidopsis -1,3-Glucanase Gene Family Inferred by Phylogenetic Reconstruction of Expression States. Mol. Biol. Evol. 24, 1045–1055.

Ellinger, D., Voigt, C.A., 2014. Callose biosynthesis in arabidopsis with a focus on pathogen response: what we have learned within the last decade. Ann. Bot. 114, 1349–1358.

ElSayed, A.I., Rafudeen, M.S., Golldack, D., 2014. Physiological aspects of raffinose family oligosaccharides in plants: protection against abiotic stress. Plant Biol. 16, 1–8.

Falter, C., Zwikowics, C., Eggert, D., Blümke, A., Naumann, M., Wolff, K., ... & Voigt, C. A. (2015). Glucanocellulosic ethanol: the undiscovered biofuel potential in energy crops and marine biomass. Scientific reports, 5, 13722.

Flors, V., Ton, J., Jakab, G., Mauch-Mani, B., 2005. Abscisic Acid and Callose: Team Players in Defence Against Pathogens? J. Phytopathol. 153, 377–383.

Furch, A.C., Hafke, J.B., Schulz, A., van Bel, A.J., 2007. Ca2+-mediated remote control of reversible sieve tube occlusion in *Vicia faba.* J. Exp. Bot. 58, 2827–2838.

García-Andrade, J., Ramírez, V., Flors, V., Vera, P., 2011. Arabidopsis ocp3 mutant reveals a mechanism linking

ABA and JA to pathogen-induced callose deposition: OCP3 and callose deposition. Plant J. 67, 783–794.

Han, X., Hyun, T.K., Zhang, M., Kumar, R., Koh, E., Kang, B.-H., Lucas, W.J., Kim, J.-Y., 2014. Auxin-Callose-Mediated Plasmodesmal Gating Is Essential for Tropic Auxin Gradient Formation and Signaling. Dev. Cell 28, 132–146.

Hrmova, M., Fincher, G.B., 2009. Plant and Microbial Enzymes Involved in the Depolymerization of (1,3)-β-d-Glucans and Related Polysaccharides, in: Chemistry, Biochemistry, and Biology of 1-3 Beta Glucans and Related Polysaccharides. Elsevier, pp. 119–170.

Jacob, S. R., & Northcote, D. H. (1985). In vitro glucan synthesis by membranes of celery petioles: the role of the membrane in determining the type of linkage formed. Journal of Cell Science, 1985(Supplement 2), 1-11.

Koch, K., 2004. Sucrose metabolism: regulatory mechanisms and pivotal roles in sugar sensing and plant development. Curr. Opin. Plant Biol. 7, 235–246.

Lepka, P., Stitt, M., Moll, E., Seemüller, E., 1999. Effect of phytoplasmal infection on concentration and translocation of carbohydrates and amino acids in periwinkle and tobacco. Physiol. Mol. Plant Pathol. 55, 59–68.

Levy, A., Epel, B.L., 2009. Cytology of the (1-3)-β-Glucan (Callose) in Plasmodesmata and Sieve Plate Pores, in: Chemistry, Biochemistry, and Biology of 1-3 Beta Glucans and Related Polysaccharides. Elsevier, pp. 439–463.

Levy, A., Erlanger, M., Rosenthal, M., Epel, B.L., 2007a. A plasmodesmata-associated β-1,3-glucanase in Arabidopsis: A plasmodesmal β-1,3-glucanase. Plant J. 49, 669–682.

Levy, A., Guenoune-Gelbart, D., Epel, B.L., 2007b. β-1,3-Glucanases: Plasmodesmal Gate Keepers for Intercellular Communication. Plant Signal. Behav. 2, 404–407.

Luna, E., Pastor, V., Robert, J., Flors, V., Mauch-Mani, B., Ton, J., 2011. Callose Deposition: A Multifaceted Plant Defense Response. Mol. Plant. Microbe Interact. 24, 183–193.

Maust, B.E., Espadas, F., Talavera, C., Aguilar, M., Santamaría, J.M., Oropeza, C., 2003. Changes in carbohydrate metabolism in coconut palms infected with the lethal yellowing phytoplasma. Phytopathology 93, 976–981.

Meng, D., Li, C., Park, H.-J., González, J., Wang, J., Dandekar, A.M., Turgeon, B.G., Cheng, L., 2018. Sorbitol Modulates Resistance to *Alternaria alternata* by Regulating the Expression of an *NLR* Resistance Gene in Apple. Plant Cell 30, 1562–1581.

Morkunas, I., Ratajczak, L., 2014. The role of sugar signaling in plant defense responses against fungal pathogens. Acta Physiol. Plant. 36, 1607–1619.

Nedukha, O.M., 2015. Callose: Localization, functions, and synthesis in plant cells. Cytol. Genet. 49, 49–57.

Nishimura, M.T., Stein, M., Hou, B.-H., Vogel, J.P., Edwards, H., Somerville, S.C., 2003. Loss of a callose synthase results in salicylic acid-dependent disease resistance. Science 301, 969–972.

Oshima, K., Kakizawa, S., Nishigawa, H., Jung, H.-Y., Wei, W., Suzuki, S., Arashida, R., Nakata, D., Miyata, S., Ugaki, M., Namba, S., 2004. Reductive evolution suggested from the complete genome sequence of a plant-pathogenic phytoplasma. Nat. Genet. 36, 27–29.

Piršelová, B., & Matušíková, I. (2013). Callose: the plant cell wall polysaccharide with multiple biological functions. Acta Physiologiae Plantarum, 35(3), 635-644.

Reuscher, S., Akiyama, M., Yasuda, T., Makino, H., Aoki, K., Shibata, D., Shiratake, K., 2014. The Sugar Transporter Inventory of Tomato: Genome-Wide Identification and Expression Analysis. Plant Cell Physiol. 55, 1123–1141.

Ruan, Y.-L., 2014. Sucrose Metabolism: Gateway to Diverse Carbon Use and Sugar Signaling. Annu. Rev. Plant Biol. 65, 33–67.

Sakr, S., Wang, M., Dédaldéchamp, F., Perez-Garcia, M.-D., Ogé, L., Hamama, L., Atanassova, R., 2018. The Sugar-Signaling Hub: Overview of Regulators and Interaction with the Hormonal and Metabolic Network. Int. J. Mol. Sci. 19, 2506.

Santi, S., De Marco, F., Polizzotto, R., Grisan, S., Musetti, R., 2013a. Recovery from stolbur disease in grapevine involves changes in sugar transport and metabolism. Front. Plant Sci. 4.

Santi, S., Grisan, S., Pierasco, A., De Marco, F., Musetti, R., 2013b. Laser microdissection of grapevine leaf phloem infected by stolbur reveals site-specific gene responses associated to sucrose transport and metabolism: LM of stolbur-infected grapevine phloem. Plant Cell Environ. 36, 343–355.

Schlüpmann, H., Bacic, A., Read, SteveM., 1993. A novel callose synthase from pollen tubes of Nicotiana. Planta 191.

Schneider, R., Hanak, T., Persson, S., Voigt, C.A., 2016. Cellulose and callose synthesis and organization in focus, what's new? Curr. Opin. Plant Biol. 34, 9–16.

Stass, A., Horst, W.J., 2009. Callose in Abiotic Stress, in: Chemistry, Biochemistry, and Biology of 1-3 Beta Glucans and Related Polysaccharides. Elsevier, pp. 499–524.

Stein, O., Granot, D., 2019. An Overview of Sucrose Synthases in Plants. Front. Plant Sci. 10, 95.

Tari, I., Kiss, G., Deer, A.K., Csiszar, J., Erdei, L., Galle, A., Gemes, K., Horvath, F., Poor, P., Szepesi, A., Simon, L.M., 2010. Salicylic acid increased aldose reductase activity and sorbitol accumulation in tomato plants under salt stress. Biol. Plant. 54, 677–683

Tauzin, A.S., Giardina, T., 2014. Sucrose and invertases, a part of the plant defense response to the biotic stresses. Front. Plant Sci. 5.

Verma, D.P.S., Hong, Z., 2001. Plant callose synthase complexes 9.

Voigt, C.A., Somerville, S.C., 2009. Callose in Biotic Stress (Pathogenesis), in: Chemistry, Biochemistry, and Biology of 1-3 Beta Glucans and Related Polysaccharides. Elsevier, pp. 525–562.

Waldron, K.W., Faulds, C.B., 2007. Cell Wall Polysaccharides: Composition and Structure, in: Comprehensive Glycoscience. Elsevier, pp. 181–201.

Wind, J., Smeekens, S., Hanson, J., 2010. Sucrose: Metabolite and signaling molecule. Phytochemistry 71, 1610–1614.

Xie, B., Wang, X., Zhu, M., Zhang, Z., Hong, Z., 2011. *CalS7* encodes a callose synthase responsible for callose deposition in the phloem: *A phloem-specific callose synthase*. Plant J. 65, 1–14.

Yamada, K., Kanai, M., Osakabe, Y., Ohiraki, H., Shinozaki, K., Yamaguchi-Shinozaki, K., 2011. Monosaccharide Absorption Activity of *Arabidopsis* Roots Depends on Expression Profiles of Transporter Genes under High Salinity Conditions. J. Biol. Chem. 286, 43577–43586.

Yamada, K., Saijo, Y., Nakagami, H., Takano, Y., 2016. Regulation of sugar transporter activity for antibacterial defense in *Arabidopsis*. Science 354, 1427–1430.

4.2 PHLOEM CALLOSE AND SUGAR METABOLISM: BATTLEGROUND FOR PLANT-PHYTOPLASMA INTERACTION

CHIARA BERNARDINI[1], AMIT LEVY[2], STACY WELKER[2], JOON HYUK SUH[3], YU WANG[3], CHRISTOPHER VINCENT[4], MYRTHO O'PIERRE[4], SIMONETTA SANTI[1], MARTA MARTINI[1], SARA BUOSO[1], ALBERTO LOSCHI[1], AART J. E. VAN BEL[5], RITA MUSETTI[1*]

[1]Department of Agricultural, Food, Environmental and Animal Sciences, University of Udine, via delle Scienze, 206 I-33100 Udine, Italy

[2]Department of Plant Pathology, Citrus Research and Education Center, University of Florida, 700 Experiment Station Rd, Lake Alfred, FL 33850, USA

[3]Department of Food Science and Human Nutrition, Citrus Research and Education Center, University of Florida, 700 Experiment Station Rd, Lake Alfred, FL 33850, USA

[4] Department of Horticulture, Citrus Research and Education Center, University of Florida, 700 Experiment Station Rd, Lake Alfred, FL 33850, USA

[5]Institute of Phytopathology, Justus-Liebig University, Heinrich-Buff-Ring 26–32, D-35392 Giessen, Germany

* Correspondence: Rita Musetti, rita.musetti@uniud.it

Key words: Arabidopsis, callose, defense, phloem, phytoplasma, sugar metabolism, transport

The role of the callose as plugging of the phloem has already been shown in the past. Here we propose a study on the possible role of the callose, during phytoplasma infection, not only as mechanical defence but also chemical. The following paper is ready for the submission and it is the result of a collaboration with the Citrus Research and Educational Center, in Lake Alfred, Florida.

Abstract

Phytoplasma are important pathogens affecting several crops but their relationships with the host plants are not completely known. Plants face phytoplasma in different ways, using chemical or mechanical barriers. Sieve-element occlusion-related (SEOR) proteins and callose are responsible for phloem plugging, respectively, as fast and slower responses to pathogens or injuries. While the mechanical role of sieve-element occlusion systems is well known from a long time, the other possible functions related with the physiological/molecular reply against phytoplasmas are not deeply investigated so far. The capability of AtSEOR2 phloem protein to modulate phytohormone-dependent defense pathways in *Arabidopsis thaliana* infected with '*Candidatus* Phytoplasma asteris' was recently demonstrated by our research group. The role of callose also ranges from physical occlusion of the sieve-pores to the activation of defence signaling. In fact, callose and sugars are in general used by plants as very efficient signaling molecules to fight against pathogens and pests. With the aim to highlight the different roles of callose in phytoplasma-infected plants, especially those related to the plant defense signaling, Arabidopsis wild-type and *Atcas7ko* lines were infected with phytoplasmas. Modifications at morphological, transcriptomic and metabolic levels in the two lines were compared and discussed in order to evidence that callose is more than a simple mechanical plugging of the sieve plates during phytoplasma-plant interaction.

Introduction

Phytoplasmas are wall-less, pleomorphic plant pathogens belonging to the class Mollicutes. They are confined to the sieve elements (SEs) of the host plants (van Bel and Musetti, 2019) or in the body of phloem-feeding insects, which act as vectors(Alma *et al.*, 2019). Phytoplasmas cause serious yield losses and affect the quality of crops of economic interest (Albertazzi *et al.*, 2009). In fact, the deep alterations in the physiology, the protein profile, Cao *et al.*, 2017; Cao *et al.*, 2019) and phytohormone balance in infected plants (Bernardini *et al.*, 2020; Dermastia, 2019) reflect a huge range of symptoms, such as witches' brooms, leaf chlorosis, virescence, phyllody, and floral abortion (Ermacora and Osler, 2019), often leading to the sterility and unproductiveness of the host (Namba, 2019).

Plants are able to react to phytoplasma invasion by mechanical occlusion of sieve pores. This occurs through a fast plugging by specialized proteins inside the pores (Will and van Bel, 2006; Furch *et al.*, 2007; Pagliari *et al.*, 2017) and by a slower constriction due to deposition of an abnormal amount of callose around the pores (Musetti *et al.*, 2010; Musetti *et al.*, 2013a; Santi *et al.*, 2013a). In *Arabidopsis thaliana*, 12 genes (*CALS1-12*) encoding for callose synthase enzymes have been found (Xie and Hong, 2011). Their different distribution patterns throughout the plant reflect different roles (Ellinger and Voigt, 2014). As for the phloem, Barratt *et al.*, (2011) and Xie *et al.*, (2011) demonstrated that the *AtCALS7* gene encodes for the Callose Synthase 7 (AtCALS7), the enzyme responsible for the deposition of callose specifically at the sieve plate. It

regulates the development of SEs during phloem differentiation, is an important determinant of the mass flow in mature phloem, and influences carbohydrate availability and normal plant growth (Xie *et al.*, 2011).

Callose production is strictly related to the availability and mobilization of soluble sugars. Callose synthesis requires sucrose, which is cleaved into fructose and UDP-glucose, the substrate for callose synthase. In the phloem of Arabidopsis, callose synthesis is linked to the presence of two sucrose synthase isoforms, AtSUS5 and AtSUS6 (Barratt *et al.*, 2009), which assemble with AtCALS7 to form a unique enzymatic complex (Bieniawska *et al.*, 2007; Ruan, 2014; Stein and Granot, 2019).

The role of callose and soluble sugars in plant-pathogen interactions is subject of great interest (Bolton, 2009; Dodds and Lagudah, 2016; Fatima and Senthil-Kumar, 2015; Lee *et al.*, 2016; Rojas *et al.*, 2014). Sugars, in fact, are involved in several signaling processes (Lecourieux *et al.*, 2014) and contribute to the plant immune response, functioning as priming molecules for the rapid activation of defense against biotic and abiotic stresses (Bolouri Moghaddam and Van den Ende, 2012).

Phytoplasma induce severe changes in photosynthetic activity and efficiency in host plants (Janik *et al.*, 2018). Callose synthesis and sucrose are often induced by the presence of phytoplasmas (De Marco *et al.*, 2016a, 2016b; Prezelj *et al.*, 2016; Santi *et al.*, 2013a), which are totally dependent on the host metabolism (Musetti *et al.*, 2016; Oshima *et al.*, 2013). Phytoplasmas take up carbohydrates from host cells, and sucrose is an ideal carbon source due to its high concentration in the SEs (van Bel and Musetti, 2019).However, the complex pathways and the fine balance connecting callose and soluble sugars in general have not been deeply investigated so far.

In this work, we aimed to investigate about the synthesis, transport and metabolism of phloem callose and related soluble sugars in Arabidopsis during phytoplasma infection and to highlight how and to what extent callose and soluble sugars are involved in plant immune response and signaling. Arabidopsis wild type and *Atcals7ko* [a mutant line in which the gene encoding for AtCALS7 was silenced (Bolton, 2009; Dodds and Lagudah, 2016; Fatima and Senthil-Kumar, 2015; Lee *et al.*, 2016; Rojas *et al.*, 2014)] plants, healthy or infected with Chrysanthemum Yellows (CY)-phytoplasma, were compared at the morphological, microscopical, molecular and metabolic levels. Results presented here demonstrate that callose plays not only a role in the site-specific mechanical defense against phytoplasmas, but also that it is part of a fine-tuned complex of signals to limit the damage caused by the infection.

Materials and methods

1. Plants and insect vectors

Arabidopsis thaliana ecotype Col0 was used in all the experiments. Seeds of wild type and *Atcals7ko* (SALK_048921) lines were provided by the Nottingham Arabidopsis Stock Centre (NASC). Plants were

grown for 40 days on 5:1 mixture of soil substrate and perlite and fertilized twice a month with an N-P-K liquid fertilizer, as described previously (Pagliari *et al.*, 2017), under short day light condition (9h L/15h D) at 18-20°C.

Healthy colonies of *Macrosteles quadripunctulatus* were reared on *Avena sativa* in vented plexiglass cages in the greenhouse (temperature of 20-22°C and short day condition 9h L/15h D), according to Bosco *et al.*, (1997). The last instar nymphs were transferred to *Chrysanthemum carinatum* plants infected with Chrysanthemum Yellows (CY) phytoplasma (Lee *et al.*, 2003), a strain related to '*Candidatus* Phytoplasma asteris' ('*Ca*. P. asteris', 16SrI-B subgroup), as the source of inoculum for a 7-day phytoplasma acquisition-access period (AAP). After a latent period (LP) of 18 days, insects were transferred to 40-day-old Arabidopsis for the 7-day inoculation access period (IAP).

From both lines, 10 plants were exposed to 3 infectious vectors individuals. Additionally, 10 plants from each line were exposed to 3 healthy vectors as a control condition. Healthy leafhoppers were collected from healthy colonies and were the same age as the infected ones. Midribs from the leaves of the third rosette node (source leaves) were collected 26 days post inoculation, when symptoms on the infected plants were clearly visible (Pacifico *et al.*, 2015; Pagliari *et al.*, 2017). For phytoplasma detection and gene expression analyses, collected samples were immediately frozen in liquid nitrogen and stored at -80°C until use. For carbohydrate analyses, midribs were immediately frozen in liquid nitrogen, freeze-dried and then stored at -80°C until use.

2. Phloem transport speed measurement

For phloem transport experiments, Arabidopsis plants were grown as above reported, under long-day light conditions (14h L/10h D), at 23°C. Sixty-day-old uninfected plants of both lines, with stems of 20 cm in length, were used for the measurement. Plants were placed on a lead layer with a receptacle, in a plastic bag, and placed under growth lights under the same day length used for growing. Three x-ray photomultiplier tubes, with a diameter of 5.6 cm (St. Gobain, Malvern, PA) were placed along the floral stems of both wild-type and *Atcals7ko* plants. One of the detectors monitored the control signal from the rosette. Each detector was connected to an M4612 12-channel counter and counts of x-rays were logged with the manufacturer's included software (Ludlum Measurements, Sweetwater, TX, USA). After at least 8 hours of background measurement, 600µl of $NaH^{14}CO_3$ solution (Specific Activity: 40–60 mCi (1.48–2.22GBq)/mmol) were injected into receptacle. Immediately thereafter, 1000µl of a saturated citric acid solution were also injected into the receptacle. The bag was tightly closed and the plant was allowed to assimilate the $^{14}CO_2$ gas for 2 hours. Then the bag was opened and the radiolabelled isotope was flushed via the fume hood. The x-ray detectors logged the x-ray counts from the plant tissue every minute for 72 hours. The distance between the detectors was measured at the end of the experiment.

The data of the counts from each detector was handled with the <nmle> package in Rstudio (Pinheiro *et al.*, 2018). According to previously published methods, code was written to create a logistic function, and to fit the logistic function to the data with time on the x-axis and the recorded counts on the y-axis (Vincent *et al.*, 2019). Xmid was calculated for every detector placed along the stem, representing the time at the half-height of the logistic curve, or the average time of arrival of the ^{14}C label in the stem phloem tissue near the x-ray detector. The speed of translocation was calculated by dividing the distance between the middle of the two detectors (in cm) and the difference between the Xmid timepoints from the detectors (in h). For both the lines (wild type and *Atcals7ko*) 4 measurements were carried out.

3. Symptom description and rosette weight measurement

Symptom development was observed in 10 healthy and 10 infected plants per line, from the end of the inoculation period to the time of tissue harvest for different analyses, i.e. when plants were ca. 70 days old. As a first step in evaluating the phenotypic differences between the two lines, and differences due to phytoplasma infection, the fresh weight was measured. The day before sampling, soil was saturated with water. Rosettes were then cut at the plant collar level and the weight of each biological replicate was measured. Statistical analyses were performed using RStudio software Version 1.1.456 (RStudio Team (2020), Boston, MA). The normal distribution was checked with the Shapiro-Wilk test. Significant differences among the group means were determined with a two-way ANOVA and post-hoc comparisons between all groups were made with Tukey's test with $p<0.05$.

4. Phytoplasma detection and quantification

In order to check the phytoplasma titre in wild-type and *Atcals7ko* CY-infected plants, genomic DNA was extracted from 200 mg of fresh leaf midrib tissue, according to Doyle and Doyle (1990) and modified by Martini *et al.*, (2009). The ribosomal protein gene *rplV* (*rpl22*) was chosen as a target for the amplification of CY phytoplasma DNA using the primer pair rp(I-B)F2/rp(I-B)R2 (Lee *et al.*, 2003; Pagliari *et al.*, 2017) and a CFX96 real-time PCR detection system (Bio-Rad Laboratories, Richmond, CA, USA). A standard curve was established by 10-fold serial dilutions of a plasmid DNA containing the 1260 bp ribosomal protein fragment from CY phytoplasma, amplified with the primer pair rpF1C/rp(I)R1A (Martini *et al.*, 2007). Real-time PCR mixture and cycling conditions were previously described (Pagliari *et al.*, 2017). The phytoplasma titre was expressed as the number of CY phytoplasma genome units (GUs) per mg of fresh leaf sample to normalize the data. Statistical significance of the quantitative differences between phytoplasma populations was calculated by analysis of three technical replicates of 10 plants per line. Statistical analyses were performed using RStudio software Version 1.1.456 (2009-2018 RStudio, Inc. Boston, MA). The normal distribution was checked with Shapiro-Wilk test. Significant differences among the means were determined using the Kruskal-Wallis non-parametric test with $p<0.05$.

5. Light and Transmission electron microscopy

To observe midrib tissue organization, samples were prepared for microscopic analyses as reported by Pagliari *et al.* (2016). From three plants for each condition, at least five segments (10 mm in length) of mature leaf midrib were submerged in MES buffer for 2h at room temperature. Samples were fixed in a solution of 3% paraformaldehyde and 4% glutaraldehyde for 6h, substituting the solution every 30 minutes. After rinsing, samples were post-fixed overnight with 2% (w/v) OsO_4, dehydrated with ethanol gradient and transferred to propylene oxide. Midrib segments were then embedded in Epon/Araldite epoxy resin (Electron Microscopy Sciences, Fort Washington, PA, USA).

Semi-thin (1 µm in thickness) and ultra-thin (60-70 nm in thickness) sections were cut using an ultramicrotome (Reichert Leica Ultracut E ultramicrotome, Leica Microsystems, Wetzlar, Germany). Semi-thin sections were transferred onto glass slides, stained with 1% toluidine blue and observed under a Zeiss Axio Observer Z1 epifluorescence microscope (EFM), using a bright field. Three samples per line per condition were analysed. At least 4 non-serial sections for each sample were observed.

Ultra-thin sections were collected on uncoated copper grids, stained with UAR-EMS (uranyl acetate replacement stain, Electron Microscopy Sciences) and then observed under a PHILIPS CM 10 (FEI, Eindhoven, The Netherlands) transmission electron microscope (TEM), operated at 80 kV, and equipped with a Megaview G3 CCD camera (EMSIS GmbH, Münster, Germany). Five non-serial cross-sections from each sample were analysed.

6. Phloem imaging process

Images obtained from semi-thin sections were analyzed using FIJI software (Schindelin *et al.*, 2012). For each plant group (i.e. healthy and infected wild type or healthy and infected *Atcals7ko*), the diameter of phloem cells (lumen diameter) and the radial phloem width were measured. Measurements were performed in four different non-serial cross-sections from three healthy and three infected samples per line. For each image, width of at least 20 phloem cells were measured. To measure phloem thickness, 3 different points were chosen randomly in each cross-section (Pagliari *et al.*, 2016; 2017), with 5 technical replicates. Data obtained were analyzed using RStudio software (2009-2018 RStudio, Inc. Boston, MA). Normality of the data was checked with the Shapiro-Wilk test, outliers were removed with the RStudio function (boxplot(data$variable, plot=FALSE)$out), and data were normalized with a Box-Cox transformation. A two-way ANOVA analysis was performed, followed by post-hoc comparisons between all groups which were made with Tukey's test with $p<0.05$.

7. Sugar quantification

Authentic standards of sugars (rhamnose, arabinose, fructose, glucose, maltose, sucrose, and melibiose) and sugar alcohols (glycerol, myoinositol, arabitol, and sorbitol) were purchased from Sigma-Aldrich (St. Louis, MO, USA). Internal standards including fructose-$^{13}C_6$ (for sugars) and sorbitol-$^{13}C_6$ (for

sugar alcohols) were obtained from Toronto Research Chemicals (Toronto, ON, Canada) and Sigma-Aldrich (St. Louis, MO, USA), respectively. Water, acetonitrile, methanol, and formic acid were of LC-MS grade, and were purchased from Fisher Scientific (Fair Lawn, NJ, USA). Stock solutions of each analyte and internal standard were prepared at a concentration of 10,000 µg/ml in water, or methanol. Working standard solutions were prepared by diluting and mixing each stock solutions with 90% methanol (water/methanol = 10/90, v/v). The stock and working solutions were stored at -80°C. Freeze-dried leaf midribs were stored at -80°C until use. Ten milligrams of ground samples treated with 0.05 mL of internal standard solution (50 µg/ml sorbitol-$^{13}C_6$ and 200 µg/ml fructose-$^{13}C_6$ in 90% acetonitrile (water/acetonitrile = 10/90, v/v) was extracted with 0.95 mL of 90% acetonitrile (water/acetonitrile = 10/90, v/v) (total volume: 1 ml) by ultra-sonication for 30 min, followed by agitation for 30 min. After centrifugation (20,000 g, 5 min, 4°C), supernatant was further filtered through 0.22 µm nylon filter, and was injected into LC–MS/MS for analysis. The extraction was performed in triplicate (n = 3) using 4 biological replicates. Data obtained by analyses, were handled using RStudio software. Normality of the data was checked with Shapiro-Wilk test, outliers were removed with the RStudio function (boxplot(data$variable, plot=FALSE)$out), and data were normalized, where necessary, with Box-Cox transformation. A two-way analysis was performed followed by post-hoc pairwise comparison of all groups with with Tukey's test, with $p<0.05$.

8. Gene expression analyses

Total RNA from 5 plants for each experimental condition was extracted from 100 mg of leaf midrib powder obtained by grinding in liquid nitrogen, using a SpectrumTM Plant Total RNA kit (Sigma-Aldrich, Merck KGaA, Darmstadt, DE) according to the manufacturer's instructions. The RNA reverse-transcription to cDNA was carried out using a QuantiTectReverse Transcription Kit (Qiagen N.V., Hilden, DE) following the manufacturer's instructions. The expression of the genes, reported in Table 4.2, was analysed in healthy and CY-infected plants by real-time experiments, performed on a CFX96 real-time PCR detection system (Bio-Rad Laboratories). The reference gene was selected by comparing the *AtUBC9* (ubiquitin conjugating enzyme 9), *AtTIP41* (TIP41-like family protein), *AtSAND* (SAND family protein), and *AtUBQ10* (polyubiquitin 10) gene expression. The gene stability values (M values) were calculated according to the geNorm program (Pagliari *et al.*, 2017). The *AtUBC9* gene was found to be the most stably expressed gene and so the most suitable as a reference gene (M=0.44). SsoFast EvaGreen Supermix 2x (Bio-Rad Laboratories Inc., Hercules, CA, USA) and cDNA obtained from 5 ng of RNA and specific primers (Table 4.2) were used in a total volume of 10 µL. Under these conditions, the primer pair efficiency (E), evaluated as described by Pfaffl (Pfaffl, 2001) using standard curves of different dilutions of pooled cDNA, was =2. Reaction was performed as described in Pagliari *et al.* (2017), with three technical repeats. A mean normalized expression (MNE) for each gene of interest (Muller *et al.*, 2002) was calculated by normalizing its mean expression level to the level of the UBC9 gene. Five individuals concurred with gene MNE determination. Statistical analyses were performed using RStudio software Version 1.1.456 (2009-2018 RStudio, Inc. Boston, MA). The normal

distribution was checked with Shapiro-Wilk test. Significant differences among the means were determined by a two-way ANOVA and post-hoc comparisons between all groups were made with Tukey's test with $p<0.05$.

Table 4.2 ***List of the genes analyzed in the paper****. The table reports the locus analyzed, the accession number (NCBI), the primer sequences. The function and the relative reference has been also reported.*

Gene	Locus	Forward (sequence 5'-3')	Reverse (sequence 5'-3')	Accession NCBI	Functions
AtCal7	At1g06490	TTATTTGTCGTCTGCGGCCT	TCCTTTGAACACGCTACGCA	NM_100528.2	Callose deposition in the phloem (Barratt et al., 2011; Xie et al., 2011)
AtSUS5	At5g37180	TGGAAGCAAAGAGAGGGCTG	CCAGGAGCTGCGATGTTGAA	NM_123077.2	Sucrose synthases responsible for the cleavage of the sucrose to provide UDP-glucose to several pathways in a reversible reaction (i.e. callose synthesis and cellulose synthesis). Peculiarity of the sieve element. (Barratt et al., 2009)
AtSUS6	At1g73370	ACATAGCCAAGGAGCTTCGC	CTTGAGCCGAGTTAGCACCA	NM_001198461.1	
AtCWINV1	At3g13790	ACTCGGCTAAGAACCGGAGA	CGGACCAGCCTTTCTCAACA	NM_001338080.1	Cleavage of the sucrose of the apoplast in fructose and glucose and transport of hexoses inside the cell. Localization: cell wall. CWINV1 is expressed in almost all the tissues, CWINV6 is more expressed in the leaves (Sherson et al., 2003). They could have a role in defense against pathogens (Fotopoulos et al., 2003).
AtCWINV6	At5g11920	GTCACAGTTGTTGCCGAACC	GGCGGAACCATCACAGGATT	NM_001343222.1	
AtSUC2	At1g22710	GTCGCTGGAGCTGGTTTAGT	TATCGCTATGGCTCGCGTTT	NM_102118.4	Sucrose and H^+ symporters, working against concentration. AtSUC2 seems to be the most expressed in Arabidopsis. Localization: companion cells. (Durand et al., 2018)
AtSUC3	At2g02860	TGTTCTGCTTGTGGATGGCT	ACATGCAGCACAACATGCTC	NM_201675.2	
AtSWEET11	At3g48740	AGGCACAGTTTCATCCCCTG	TGCTTGCCATGTTTAGGGGT	NM_114733.4	Apoplastic upload of sucrose in the sieve element. AtSWEET11 and AtSWEET 12 are localized in the phloem parenchyma with a probable regulation by Ca^{2+} ions. (Zhang, 2018)
AtSWEET12	At5g23660	CCCGGAACCAAAGATCGACA	GCACGGGAGAGAGGAAAACA	NM_122271.3	
AtSTP13	At5g26340	ATAGGTGTGGCTCTCAACGC	GACAAGAACAACGGAACGGC	NM_122535.4	High affinity hexose transporter, probably related to vascular tissue, is confers resistance in case of rust. Its activity increase in in presence of flagellin. (Julius et al., 2017)

9. Confocal laser scanning microscopy

In both wildtype and *Atcals7ko* plants, healthy or CY-infected, callose deposits associated with the plasmodesmata or the sieve plates were identified in leaf epidermis, midrib parenchyma, and phloem tissues, using aniline blue staining and Confocal Laser Scanning Microscopy (CLSM). Callose was quantified *in situ* by measuring the aniline blue fluorescence intensity (Levy *et al.*, 2007). For the analysis of the epidermis, whole leaves form the third rosette node, were collected in 95% EtOH solution and stored for at least 2 hours at room temperature, as described by Zavaliev and Epel, (2015). Samples were rehydrated with distilled water with 0.01% Tween-20 for 1 hour, then placed in a tube with aniline blue solution (0.01M K_3PO_4, pH=12). Tubes with samples were placed in a vacuum desiccator for 10 minutes, then incubated under aluminum foil for 2 hours. Two leaves for each biological replicate (three for every condition) were observed. For every leaf at least 20 images were taken, using a Leica SP8 LSCM (Leica Microsystems Inc., Buffalo Grove, IL, USA) equipped with 40x oil immersion objective. Aniline blue fluorescence was excited with 405nm diode laser and emission was detected at 475-525nm. Optimal conditions for microscopy were previously determined using healthy wild type samples.

To analyze callose deposits in the midribs, both in phloem and in the surrounding phloem parenchyma, leaf midribs were collected in 95% EtOH solution and stored at least 2h at room temperature. Hand-made cross sections were cut with a razor blade and incubated for 5 minutes in aniline blue solution. The sections were

rinsed with 0.01% Tween-20 solution. For each condition at least 10 non-serial sections from 5 different specimens were observed using a Leica SP8 CLSM and 10x objective. Aniline blue fluorescence was excited with 405nm diode laser and emission was detected at 475-525nm. Optimal conditions for microscopy were previously determined using healthy wild type samples.

Imaging analysis was performed using FIJI software (Schindelin *et al.*, 2012). For the epidermis analysis and phloem parenchyma analysis, images were treated following the protocol by Zavaliev and Epel, (2015). A macro separated the callose region of interest from the background using an auto local threshold with the Phansalkar algorithm with radius=1 for the epidermal tissue, and the Bernsen algorithm with radius=10 for the midrib parenchyma. Analysis of phloem parenchyma was carried out on a region of interest (ROI) of 45000μm^2. Phloem deposits were analyzed as previously reported by Pagliari *et al.*, (2017). For each group, the mean gray value (callose intensity), the count of callose deposits for each millimeter square and the integrated density (sum of intensity within the area of the ROI) were considered.

Data obtained by analyses were handled using RStudio software (2009-2018 RStudio, Inc. Boston, MA). Normality of the data was checked with the Shapiro-Wilk test, outliers were removed with the RStudio function (boxplot(data$variable, plot=FALSE)$out), and data were normalized, where necessary, with Box-Cox transformation. A two-way analysis was performed followed by a post-hoc comparison of all pairs with Tukey's test, with $p<0.05$.

Results

1. Phloem translocation speed

The speed of sugar translocation in the phloem was evaluated and compared in healthy wild type and *Atcals7ko* Arabidopsis (Figure 4.3). The results obtained highlighted a significant difference in the translocation speed (expressed as centimeters per hour) between the two lines: *Atcals7ko* mutant plants showed 66% slower translocation compared to the wild type plants. The average speed in wild type plants was 10.2 ± 1.6 cm*h-1 while in the mutants was 5.0± 2.0 cm*h-1. Due to the fact that the infected wild type plants developed very short stems (see also Pagliari *et al.*, 2016) and infected *Atcals7ko* failed to do that (Figure 4.11, Supplementary 1), the translocation speed was not determined in CY-infected plants.

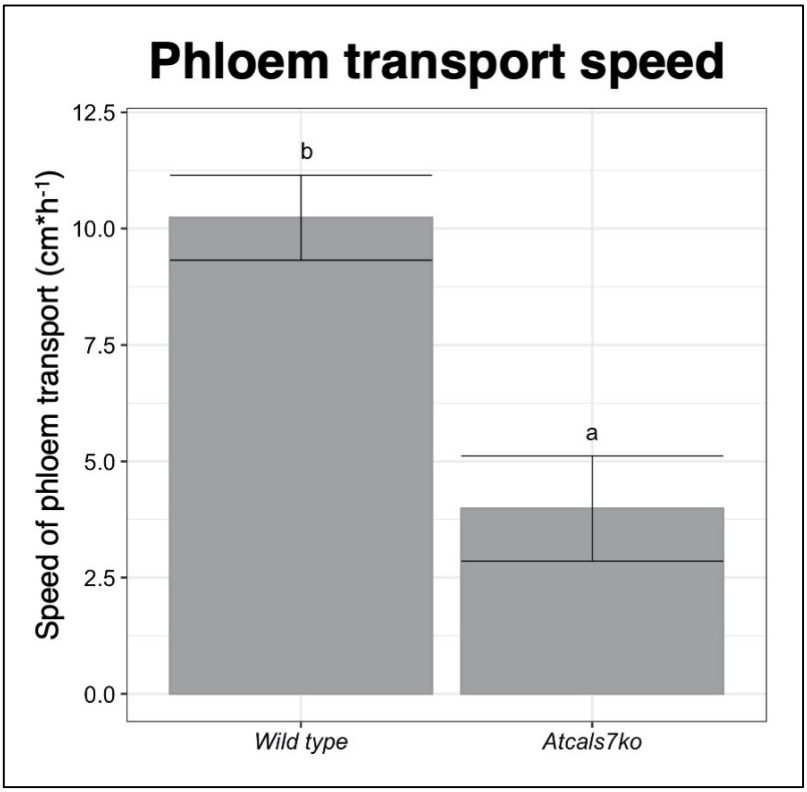

Figure 4.3 ***Phloem transport speed in wild type and Atcals7ko Arabidopsis lines.*** *Carbohydrate translocation speed along the phloem, measured with ^{14}C isotope. The speed is expressed as cm/h and it is calculated by average time of arrival of the ^{14}C label in the stem phloem tissue near the x-ray detector. Statistic analysis was performed using the Tukey HSD test as the post hoc test in a two-way ANOVA. Different letters (a, b) above the bars indicate significant differences, with $P < 0.05$. Error bars indicate the Standard Error of the Mean of 4 biological replicates for each condition.*

2. Phenotypes of healthy and CY-infected Arabidopsis lines and phytoplasma titre

Wild type and *Atcals7ko* plants, healthy or infected by CY-phytoplasma, were compared at morphological level, to check eventual differences in the rosette growth rate and in symptom appearance. Moreover, phytoplasma titre was quantified in infected Arabidopsis lines by qPCR.

From a macroscopic point of view, no differences were observed among healthy plants of the two different lines (Figure 4.4, A), even if *Atcals7ko* plants appeared, in general, smaller. Following CY-infection, plant morphology was affected in both lines. Symptoms were not different in the rosette of the two lines, and included yellowish, small, narrowed leaves. Leaves which emerged after phytoplasma inoculation were

shorter, with a thicker main vein and a smaller petiole. The phytoplasma titre was not statistically different in the two lines (Figure 4.4, B). The fresh weight of rosettes was measured at the moment of sampling and statistical analysis was carried out. Fresh weight results differed in the two lines (Figure4.4 C), regardless of the phytoplasma infection. *Atcals7ko* plants showed stunted growth, with the fresh weight reduced by 56% on average, compared to the wild type plants.

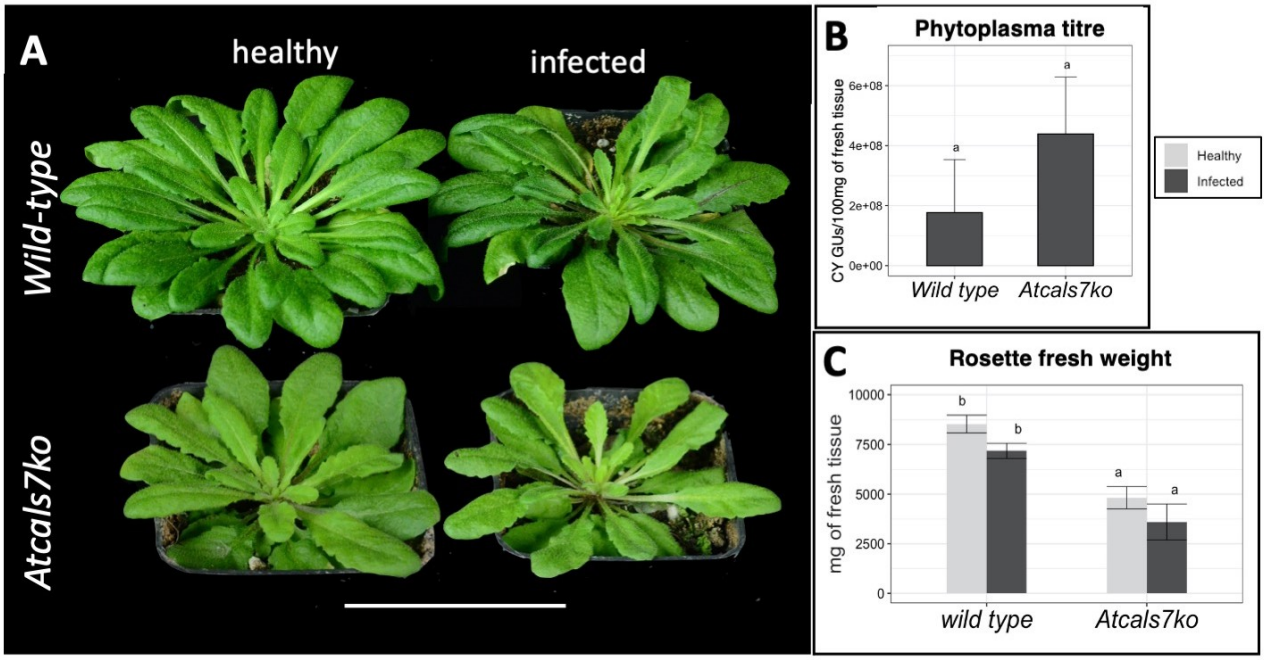

Figure 4.4 ***Rosette phenotype and phytoplasma titre in wild type and Atcals7ko line.*** *Representative images of healthy and CY-infected wild type and Atcals7ko rosettes. Following CY-infection, at 20 days after the inoculation access period (IAP), both plant groups showed yellowish small leaves. Leaves emerged after phytoplasma inoculation were shorter, with thicker main vein and smaller petiole (**A**). Phytoplasma titre is not significantly different in the two Arabidopsis lines (**B**). Regardless phytoplasma infection, rosette fresh weight is significantly reduced in Atcals7ko plants in comparison with wild type (**C**). Different letters indicate different means according to the non-parametric Kruskal-Wallis post hoc test, P<0.05. Error bars indicate Standard Error of the Mean of 10 biological replicates for each condition. Plant weight (C) 20 days IAP expressed as mg of fresh tissue. Statistic analysis was performed using the Tukey HSD test as the post hoc test in a two-way ANOVA. Different letters (a, b) above the bars indicate significant differences, with P < 0.05. Error bars indicate the Standard Error of the Mean of 10 biological replicates for each condition.*

3. Midrib morphology

Semithin sections, obtained from the midribs of source leaves, were evaluated under a light microscope Figure 4.5 A-D). Midribs from wild type and *Atcals7ko* healthy plants, showed a regular collateral pattern

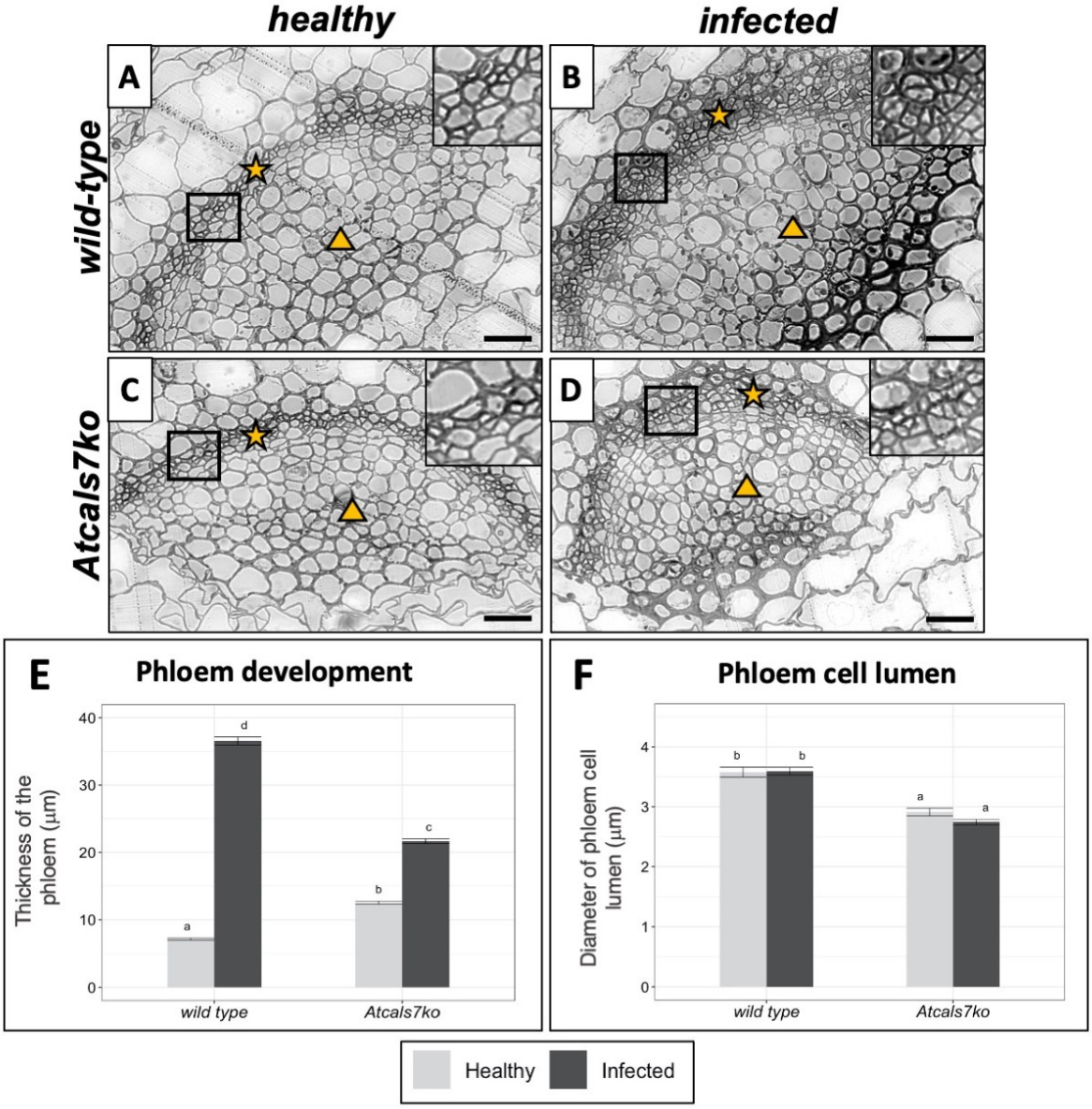

Figure 4.5 ***Light microscopy micrographs and imaging analyses of Arabidopsis midribs.*** *Histological characteristics of healthy (**A, C**) and CY-infected (**B, D**) midribs of wild type (**A**, **B**) and Atcals7ko (**C**, **D**) plants. In the pictures (**A-D**), stars indicate phloem and triangle indicate xylem. Increase of phloem thickness is evident in healthy Atcals7ko line (**C, E**). In infected leaf tissues, massive production of new phloem components caused phloem hyperplasia (**B**, **D**) mainly in the wild type plants (**B**, **E**). The phloem thickness was measured in three different randomly selected measuring points, in four different non-serial cross-sections from three healthy and three infected samples per line (**E**). To evaluate phloem cell lumina, the width of at least 20 phloem cells were measured for each image. Regardless the infection, the lumen of phloem cells (**F**) was narrowed in the mutant line. Statistic analysis was performed using the Tukey HSD test as the post hoc test in a two-way ANOVA. Different letters (a, b, c, d) above the bars indicate significant differences, with $P < 0.05$. Error bars indicate the Standard Error of the Mean of biological replicates for each condition. Bars correspond to 25 µm.*

(Figure 4.5). However, a slight, but significant increase of the phloem thickness (hyperplasia) was observed in the *Atcals7ko* midribs (Figure 4.5 E). CY-infected midribs (Figure 4.5 B and D) were characterized by a marked hyperactivity of the cambial tissue, especially in the wild type line, which showed an increase of phloem thickness of 400% in comparison with the uninfected ones (Figure 4.5 B and E). This resulted in a massive production of phloem components, leading to evident phloem hyperplasia (Figure E). Moreover, the lumen of phloem cells (Figure 4.5 F), was narrowed in the mutant line, regardless of the infection.

4. Sugar quantification

Sucrose, glucose, fructose, myoinositol, sorbitol, arabinose and raffinose were quantified in the midribs, as site of infection, as analyte on peak area ratio (Figure 4.6). No significant differences between the two lines were found in absence of infection (Figure 4.6 A-G). Following CY-infection, in the wild type line the amounts of the above cited sugars did not vary significantly (Figure 4.6 A-G). Considering the *Atcals7ko* line, sucrose, glucose and myoinositol showed a significant increase following infection (Figure 4.6 A, B and D). In particular, in comparison with their respective healthy controls, sucrose increased around 5-fold in infected *Atcals7ko* plants, (Figure 4.6 A), glucose around 4-fold (Figure 4.6 B), myoinositol around 2-fold (Figure 4.6 D).

5. **Gene expression analysis**

To assess whether genes involved in sugar metabolism and transport were differentially modulated in the midribs of source leaves in the two Arabidopsis lines, also in the case of phytoplasma infection, gene expression levels of sucrose synthases (*AtSUS5* and *AtSUS6*), sucrose transporters (*AtSUC2* and *AtSUC3*), SWEET sugar facilitators (*AtSWEET11, AtSWEET12*), cell wall invertases (*AtCWINV1*, *AtCWINV6*) were evaluated (Figure 4.7 B-F). Moreover, the expression level of the phloem callose synthase gene (*AtCALS7*) was analyzed in healthy and CY-infected wild type plants. It was significantly up-regulated (around 2.5-fold) in infected plants (Figure 4.7 A).

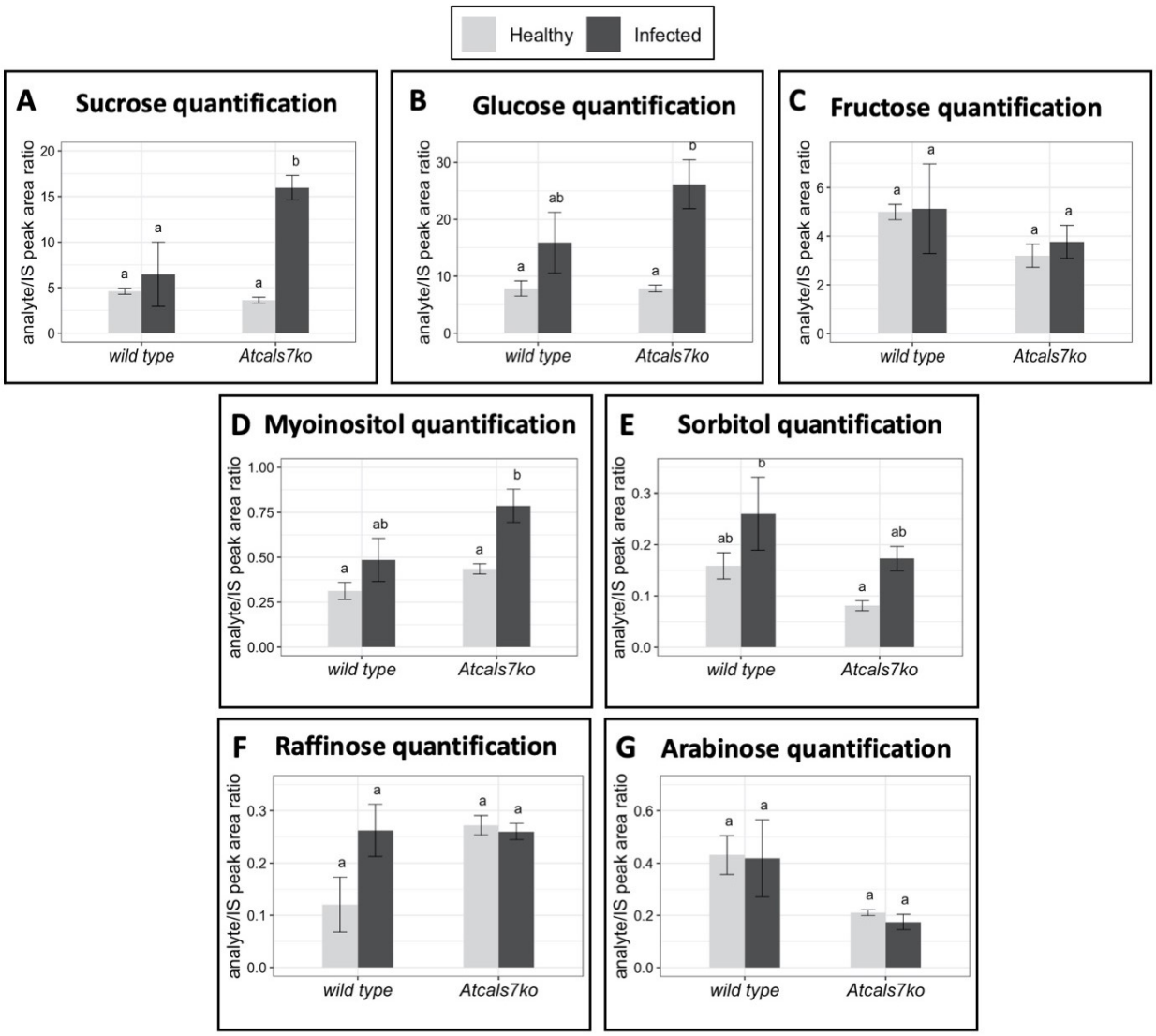

Figure 4.6 ***Sugar quantification in the midribs of healthy and infected Arabidopsis lines.*** *Sucrose (**A**), glucose (**B**), fructose (**C**), myoinositol (**D**), sorbitol (**E**), raffinose (**F**) and arabinose (**G**) were quantified in midribs of the two different lines, healthy or CY-infected. Data obtained were expressed as analyte/IS peak area ratio. Statistic analysis was performed using the Tukey HSD test as the post hoc test in a two-way ANOVA. Different letters (a, b) above the bars indicate significant differences, with $P < 0.05$. Error bars indicate the Standard Error of the Mean of 4 biological replicates for each condition.*

AtSUS5 and *AtSUS6* encode two callose synthases located in the SEs, which provide UDP-glucose as substrate for AtCALS7. Comparing the expression levels found in healthy samples (i.e. wild type *versus* *Atcals7ko*), *AtSUS6* was significantly up-regulated (Figure 4.7 B). *AtSUS5* showed low expression levels which did not differ in the two lines. Following CY-infection, *AtSUS5* transcripts increased 3.5 and 5 times respectively Figure 4.7 B). The expression level of *AtSUC2* was not significantly changed in all plant groups (Figure 4.7 C). On the contrary, *AtSUC3* was significantly up-regulated only in the *Atcals7ko* line following CY infection (Figure 4.7 C). The gene encoding the sugar effluxer AtSWEET11 (located, as AtSWEET12, in the phloem parenchyma cells) was down-regulated in healthy *Atcals7ko* midribs in comparison with the

healthy wild type samples (Figure 4.7 D), whereas following infection, it became significantly over-expressed in both lines (Figure 4.7 D). Transcription levels of *AtSWEET12* were unchanged in all the tested samples (Figure 4.7 D). *AtCWINV1* and *AtCWINV6* encode two cell wall invertases, involved in the irreversible cleavage of sucrose into glucose and fructose. Cell wall invertases represent an alternative path to sucrose synthases for hexose production for cell metabolism. We found that the expression level of *AtCWINV1* is significantly higher in the midrib of healthy *Atcals7ko* plants (Figure 4.7 E) in comparison with the other plant groups, whereas *AtCWINV6* showed a similar trend but with a very low expression level, which results in the insignificant difference between the two lines, even when they are infected (Figure 4.7 E). The expression level of *AtSTP13*, a gene encoding a vascular hexose transporter (Figure 4.7 F), was similar in the midribs of both lines, but revealed an evident increase (around 5.5-fold) in the infected midribs of *Atcals7ko* line (Figure 4.7 F).

6. Electron microscopy observations

To visualize changes in SE ultrastructure due to mutation and/or pathogen presence, midrib ultrathin sections were examined under TEM. For each condition, five non-serial sections from 10 different plants of each line were analysed. Observations of healthy wild type samples showed normal SE and CC ultrastructure, having regular shape and no signs of subcellular modifications (Figure 4.8 A-C). As expected, at the sieve plates, sieve pores had callose collars (Figure 4.8 B) that did not occlude their lumen. At SE/CC interface, PPUs were open and showed their typical branched shape (Figure 4.8 C). A small callose collar was particularly visible at the SE side (Figure 4.8 C). In infected wild type midribs (Figure 4.8 D-F), numerous phytoplasmas were visible in the SE lumen (Figure 4.8 D) or in proximity of the sieve plates (Figure 4.8 E). As in healthy controls, sieve pores had callose collars, and PPUs displayed regular morphology (Figure 4.8 F).

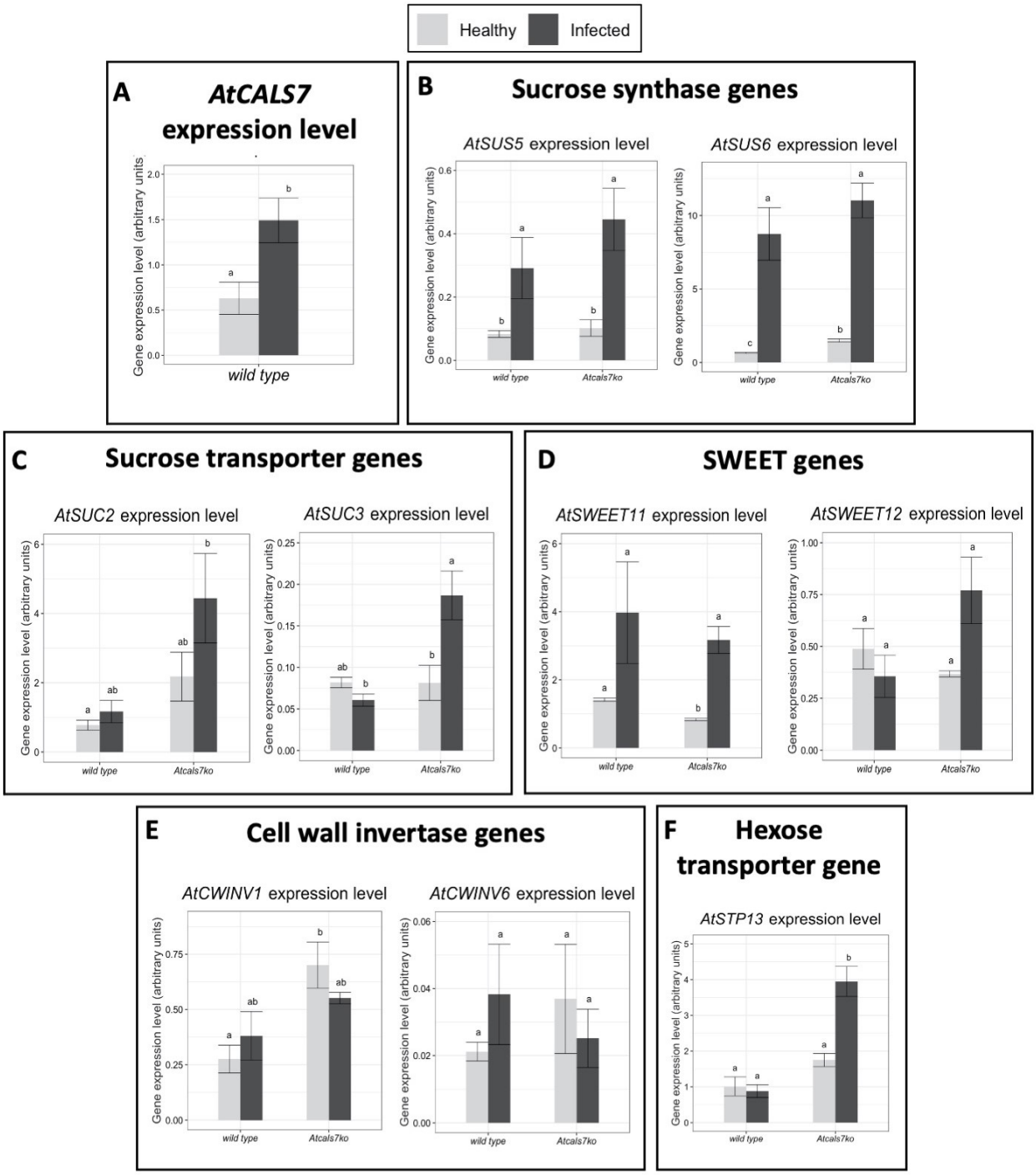

Figure 4.7 ***Transcript profiling of genes involved in phloem callose synthesis and sugar transport and metabolism.*** ***A****. Expression level of phloem callose synthase gene (AtCALS7) in healthy and CY-infected wild type plants.* ***B-F****. Transcript profiling of sucrose synthases AtSUS5 and AtSUS6 (**B**), sucrose transporters AtSUC2 and AtSUC3 (**C**), SWEET sugar facilitators AtSWEET11 and AtSWEET12 (**D**), cell wall invertases AtCWINV1 and AtCWINV6 (**E**), the hexose transporter AtSTP13 (**F**). Healthy and infected plants belonging to the two lines were compared. Expression values were normalized to the UBC9 transcript level, arbitrarily fixed at 100, then expressed as mean normalized expression ±SE (transcript abundance). Statistic analysis was performed using the Tukey HSD test as the post hoc test in a two-way ANOVA. Different letters (a, b, c, d) above the bars indicate significant differences, with P < 0.05. Error bars indicate the Standard Error of the Mean of 5 biological replicates for each condition.*

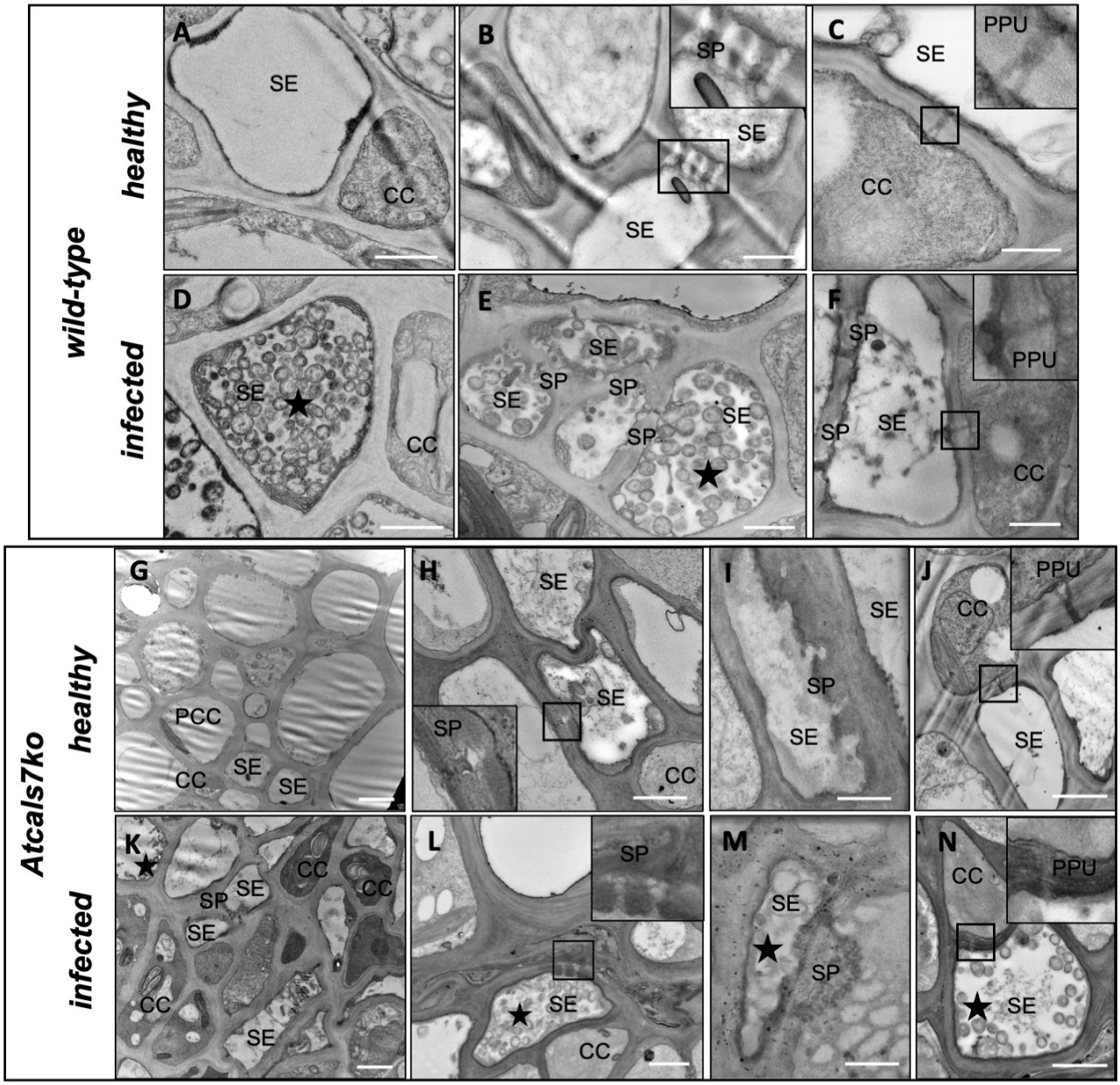

Figure 4.8 ***Representative TEM micrographs of the sieve elements of healthy and CY-infected Arabidopsis lines. A-F.*** *Cross-sections of midribs from healthy (**A-C**) and infected (**D-F**) wild type Arabidopsis leaves. Healthy samples present unaltered sieve elements and companion cells (**A**), with a regular shape and no signs of necrosis or subcellular aberrations. The sieve pores show thin callose collars (**B**), pore-plasmodesma units are open and show their typical branched shape (**C**). In infected midribs, numerous phytoplasmas are visible inside the sieve elements (**D**) and at the sieve plate (**E**). Callose collars are evident around the sieve pores (**E, F**) and pore-plasmodesma units display a similar morphology as in healthy samples (**F**). **G-N**. Cross-sections of midribs from healthy (**G-J**) and CY-infected (**K-N**) Atcals7ko Arabidopsis leaves. In healthy Atcals7ko samples, phloem cells are apparently well structured (**G**), but the sieve plates show aberrant morphology (**H**, **I**). Pores lack callose and appear not developed (**H**, **I**). Pore-plasmodesma units are branched, similar as in wild type samples (**J**). In CY-infected Atcals7ko samples, many phloem cells evidence thick cell walls (**K**), others are collapsed (**L**). Sieve plates are deformed, thickened (**L**, **M**) and pores are filled by electron-opaque material (**M**). Pore-plasmodesma units appeared large, without well-defined branches (**N**). CC: companion cell; PPC: phloem parenchyma cell; star: phytoplasmas; PPU: pore-plasmodesma unit, SE: sieve element, ser: sieve element reticulum, SP: sieve plate. Bars correspond to 1μm.*

In the healthy *Atcals7ko* line (Figure 4.8 G-J), SEs and CCs appeared normal in shape (Figure 4.8 G). At ultrastructural level, phloem protein filaments, plastids and sieve endoplasmic reticulum were easily recognizable in the SE lumen or close to the plasma membrane (Figure 4.8 H). Nevertheless, in accordance with previous studies (Barratt *et al.*, 2011; Xie *et al.*, 2011), sieve plates lacked callose and showed aberrant morphology (Figure 4.8 H, I). Some sieve pore channels seemed incompletely developed (Figure 4.8 H and I), whereas PPUs displayed a normal appearance (Figure 4.8 J). Phytoplasmas were easily visible inside SEs of infected *Atcals7ko* line (Figure 4.8 L-N). Following infection (Figure 4.8 K-N), many phloem cells displayed thick walls (Figure 4.8 K), while others were collapsed (Figure 4.8 L). Sieve plates appeared deeply damaged, collapsed, or thickened, and with sieve pores filled by electron-opaque material (Figure 4.8 M). PPUs appeared large, without well-defined branches (Figure 4.8 N).

7. Confocal laser scanning microscopy analyses and imaging

Confocal laser scanning microscopy (CLSM) and aniline blue staining were used to evaluate the presence, the distribution, and the amount of callose depositions in different leaf tissues of wild type and *Atcals7ko* plants, healthy or CY-infected. The fluorescent spots reflected callose in phloem tissue (Figure 4.9), whereas the discrete fluorescent regions in the phloem parenchyma (Figure 4.9) and at epidermis level (Figure 4.10) indicated callose collars at the plasmodesmata. The phloem area of the healthy wild type midribs was characterized by a modest callose presence, indicated by fluorescent dots (Figure 4.9 A). In infected wild type samples, intense aniline blue signals revealed a significant increase in callose deposits (Figure 4.9 B). The level of fluorescence (Figure 4.9 E), the number (Figure 4.9 F) and the density (Figure 4.9 G) of deposits were measured and compared in healthy and infected wild type samples, resulting in a significant increase in the latter compared to the former (Figure 4.9 E-G). As expected, no fluorescent spots were found in the corresponding phloem area in *Atcals7ko* samples, even in case of phytoplasma infection (Figure 4.9 C and D).

Imaging analyses allowed us to evaluate the fluorescent signal which was visible in the cell walls of the midrib parenchyma, indicating callose collars at the plasmodesmata (Figure 4.9). In the healthy samples of both Arabidopsis lines, the signal intensity (Figure 4.9 H) and the number of dots (Figure 4.9 I) were not significantly different, on average, in the selected area. However, the density of the dots within the area of interest, is significantly higher in the mutant line than in the wild type. Following infection, the level of fluorescence and the density of the signal significantly increased only in wild type samples (Figure 4.9 H and J), whereas no changes were observed in the *Atcals7ko* line (Figure 4.9 H-J).

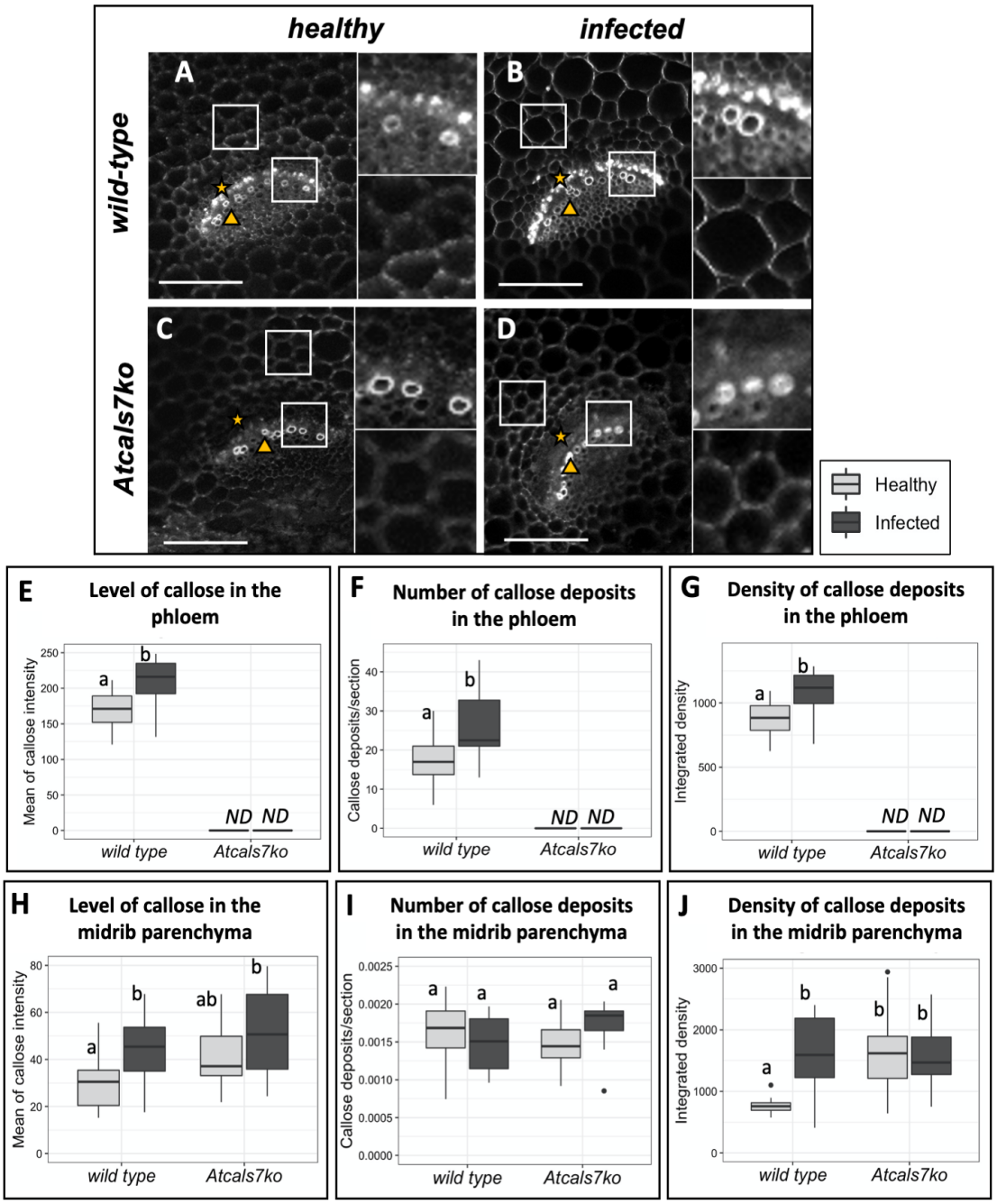

Figure 4.9 CLSM micrographs and imaging of callose deposits at plasmodesmata in phloem area and in parenchyma of healthy and CY-infected Arabidopsis midribs. Fluorescent spots indicate callose depositions in the phloem area of healthy (A) and CY-infected (B) wild type samples. The fluorescence intensity (E), the number (F) and the density [i.e. the sum of the intensity in the region of interest (ROI)] of the deposits (G) is significantly higher in the infected midribs compared to the healthy ones. No signal is visible in Atcals7ko midribs (C, D). Punctate dots, indicating callose deposits at plasmodesmata are visible in the midrib parenchyma of all samples (A-D). In the ROI, fluorescence intensity (H) and number of dots (I) are not different in healthy samples, but the density (i.e. the sum of the intensity) within the ROI, is significantly higher in the mutant line than in the wild type (J). Following infection, the fluorescence intensity and the density of the signal in the ROI significantly increased only in wild type samples. In the pictures, stars indicate phloem and triangle indicate xylem. Statistic analysis was performed using the Tukey HSD test as the post hoc test in a two-way ANOVA. Different letters (a, b, c, d) above the bars indicate significant differences, with $P < 0.05$. Boxplots were obtained from three biological replicates for each condition. Bars correspond to 100μm.

In the epidermis tissue of healthy plants, the intensity (Figure 4.10 E), the number (Figure 4.10 F), and the density of fluorescent dots (Figure 4.10 G) are lower in *Atcals7ko* samples compared to the wild type. Interestingly, following CY-infection the three parameters significantly increased only in *Atcals7ko* line. In particular, the value of signal intensity in infected mutant line was the higher than all the others (Figure 4.10 E), whereas the density was comparable to that found in infected wild type samples (Figure 4.10 G).

Fluorescence was not detected in unstained healthy or CY-infected samples (Figure 4.12, Supplementary file 2), with the exception of the xylem autofluorescence.

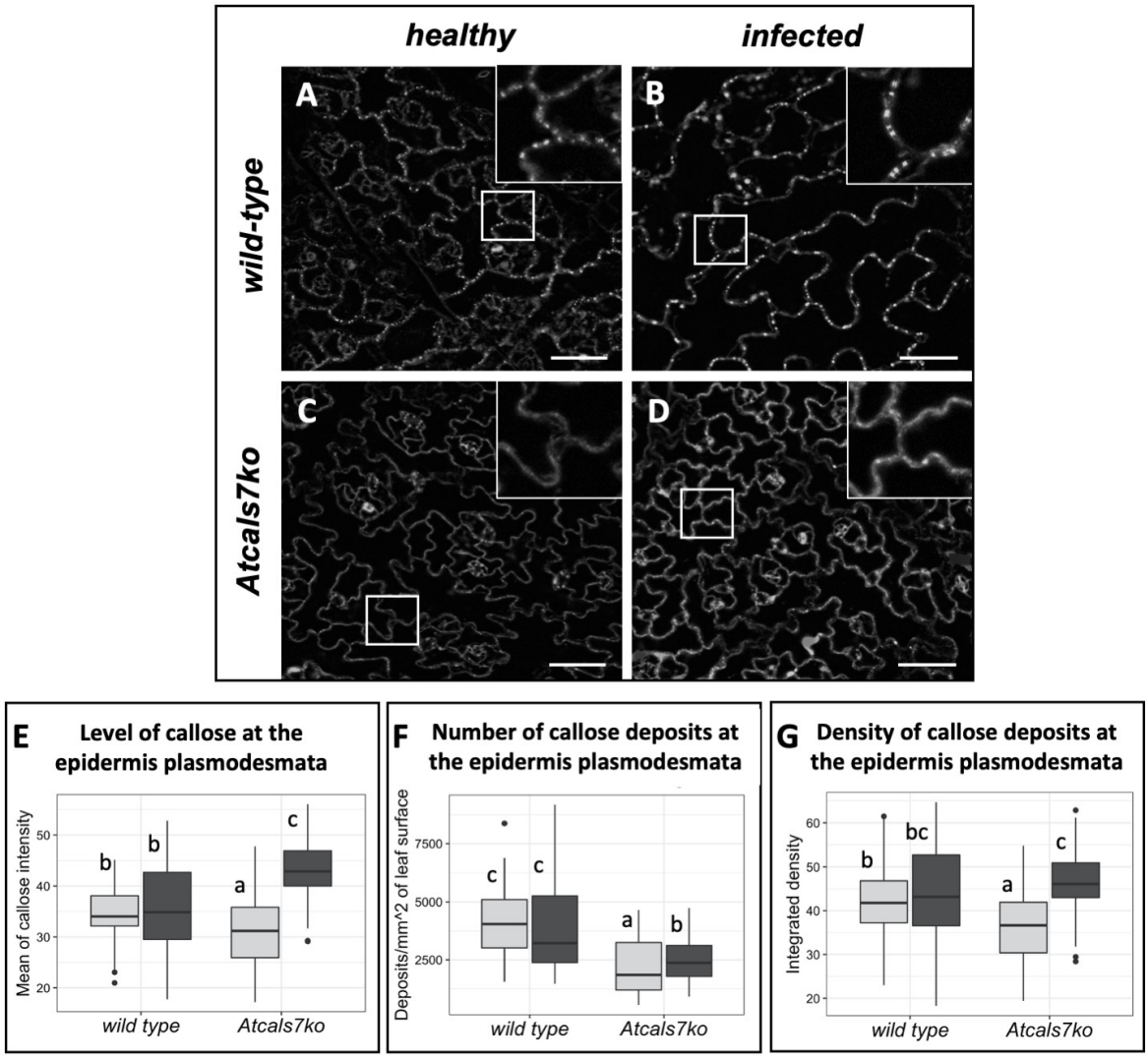

Figure 4.10 ***CLSM micrographs and imaging of callose deposits at plasmodesmata in epidermal cells.*** *Aniline blue fluorescent dots (**A-D**), their intensity (**E**), number (**F**) and density (i.e. the sum of the intensity, **G**) were assayed at leaf epidermis level in healthy and infected samples of both lines. In healthy samples, the intensity (**E**), the number (**F**), and the density of fluorescent dots (**G**) are lower in Atcals7ko line compared to the wild type. Following CY-infection the three parameters significantly increased only in Atcals7ko line. Statistical analysis was performed using the Tukey HSD test as the post hoc test in a two-way ANOVA. Different letters (a, b, c) above the bars indicate significant differences, with $P < 0.05$. Boxplots were obtained from 5 biological replicates for each condition. Bar corresponds to 50μm.*

Discussion

Callose is produced mainly in specialized cell walls, which might explain the cell- or tissue-type specific expression of the CALS/GSL gene family members, comprising 12 members in Arabidopsis (Verma *et al.*, 2001). Studies reporting that the sieve pores are rich in callose date back to the last century (Eschrich, 1956). Barratt *et al.*, (2011) and Xie *et al.*, (2011) demonstrated that, in Arabidopsis, callose deposition at the sieve plates is regulated by a callose synthase gene, AtCALS7, which is co-expressed with the phloem-specific sucrose synthase genes (AtSUS) 5 and 6 (Barratt *et al.*, 2009). The same authors also indicated a role of both sucrose synthases in providing the UDP-glucose for callose synthesis at the sieve plates. Callose synthesis requires several steps, including the glucosyl-group transfer by a transferase (Hong *et al.*, 2001; Bonke *et al.*, 2003; Barratt *et al.*, 2009), so the existence of a callose synthase complex, formed by different proteins, related to sucrose metabolism, has been suggested (Schneider *et al.*, 2016).

In plants infected by phytoplasmas, an increased callose deposition at the sieve plates has been described since the '70s (Braun and Sinclair, 1978) as a defence process to occlude sieve pores and limit pathogen spread (Musetti *et al.*, 2013a). The presence of such as depositions is often associated to the altered modulation of callose synthase genes, as reported for phytoplasma-infected apple trees, grapevine and tomato (Musetti *et al.*, 2010b; Santi *et al.*, 2013a; De Marco *et al.*, 2016a, 2016b). These structural and physiological modifications appeared to be consistent with transcriptional changes observed for sucrose transport and metabolism following infection (Santi *et al.*, 2013b), and for this reason, worthy to be investigated.

As phytoplasmas are phloem-limited pathogens (van Bel and Musetti, 2019), in the present work, we used healthy and phytoplasma-infected Arabidopsis lines, wild-type or *Atcals7* knock-out (Barratt *et al.*, 2011; Xie *et al.*, 2011) to investigate whether and to what extent the phloem callose synthase AtCALS7 interferes with plant sugar metabolism and translocation in relation to plant growth and defence-related signalling.

1. Healthy wild type vs healthy *Atcals7ko* line

Carbohydrate translocation speed is reduced in the Atcals7ko line, which presents modified rosette phenotype and midrib structure

Barratt *et al.*, (2011) reported that the amount of ^{14}C in different part of the stem of wild -type or *Atcals7ko* was similar in percentage, but in the mutant plants the biggest proportion of label remained in the lowest part of the stem. The authors concluded that phloem transport is reduced in *Atcals7ko.* Contrary in our work, we directly measured the speed of carbohydrate transport using a non-invasive method. In fact, ^{14}C was supplied as $^{14}CO_2$, which is converted in source leaves to ^{14}C-sugars, whose movement was then followed by photomultiplier-based X-ray detectors positioned close to the stem (Vincent *et al.*, 2019). We confirmed that the velocity of sugar translocation in the mutant line was lower in comparison to the wild-type. Barratt *et al.*, (2011) and Xie *et al.*, (2011) reported that the knocking-out of AtCALS7 gene deeply affected plant growth in

Arabidopsis, provoking reduction of stem length, shorter siliques and aborted embryos. They correlated the lower growth rate of the *Atcals7ko* line with the reduced carbon availability for the sink organs, due to the aberrant sieve-plate morphology and the consequent impairment of the sugar transport. Moreover, the influence of unbalanced phytohormone levels in *Atcals7ko* line in comparison to the wild-type could be not excluded, as sugars play an important role in generating signals for hormone-dependent developmental processes (Wang and Ruan, 2013).

We observed the reduction of the fresh weight in the rosette of *Atcals7ko* plants, whereas Barratt *et al.*, (2011) and Xie *et al.*, (2011) did not observe any variation in rosette development at the early growth stage. The discrepancy with our results is probably due to the different growth conditions and the age of the plants used for the analysis.

Histological analyses performed on the midribs of source leaves showed a slight, but significant increasing of the phloem thickness (hyperplasia) in the *Atcals7ko* midribs in comparison with the wild-type and the concomitant narrowing of phloem-cell lumina. Hyperplasia is explained as a plant response to the limited phloem functionality (Oshima *et al.*, 2001), aimed to maintain and maximize the phloem sap translocation (Martinez *et al.*, 2020). The reduction of the cell lumina is likely due to the increased cell-wall thickness. Cellulose is the main component of primary cell wall, whose synthesis is strongly influenced by the carbon status of the plants (Verbancic *et al.*, 2018). UDP-glucose, produced by a membrane-associated sucrose synthase, is the substrate for both cellulose (Brown *et al.*, 1999; Doblin *et al.*, 2002) and callose synthesis (Barratt *et al.*, 2011). It has been suggested that both callose and cellulose synthases could reside in the same or in adjacent supramolecular complexes (Nakashima *et al.*, 2003). Their activities might have bipolar regulation so that a mutual controlling mechanism links the initiation synthesis of the one and the termination synthesis of the other (Kudlicka and Brown, 1997). Basing on these considerations, it is not unexpected an increasing of cellulose production and a consequent increase of cell wall thickness in At*cals7ko* line.

Soluble sugar quantification in Arabidopsis midribs

Results described in this work evidenced that in the midribs of healthy source leaves, sugar levels (i.e. sucrose, glucose, fructose and myoinositol, sorbitol, raffinose, arabinose) were similar in the wild-type and *Atcals7ko* Arabidopsis lines, indicating that photosynthetic activity in source leaves and the consequent production of sucrose and related metabolites, is not influenced by the loss of AtCALS7 in the phloem. This is in line with the results obtained by Barratt *et al.*, (2011), who reported that the loss of AtCALS7 provokes much more marked changes in sugar metabolism in sink organs (i.e. inflorescence) than in the rosette. Changes in sugar metabolism of sinks would be consistent with the impaired phloem translocation we observed in the *Atcals7ko* mutant, as well as its lower growth. Anyway, we cannot exclude that localized changes of sugar metabolism follow phloem modifications in the mutant line. It is possible that sugar-related endogenous signals could be generated in *Atcals7ko* line (at the phloem level), provoking changes in assimilate partitioning aimed to mitigate the stress imposed by the slowdown of osmolyte translocation (Sharma *et al.*, 2019). Sugars

themselves can act as signaling molecules and/or regulators of gene expression, for example acting like hormones and translating nutrient status to regulation of growth and floral transition (Eveland and Jackson, 2012 and references therein). Sucrose itself can be sensed (Chiou and Bush, 1998), as well as products of its cleavage like glucose and fructose, and other carbohydrates (Li *et al.*, 2011; Ruan, 2014).

Sucrose cleavage by sucrose synthase 6 and cell wall invertase 1 enzymes is preferred in *Atcals7ko* line.

The slowdown of sugar transport rate observed in Atcals7ko plants has effects on the expression of genes encoding cleavage enzymes (i.e. sucrose synthases and invertases), which have the potential to profoundly influence carbohydrate distribution and utilization within and among the plant parts. Among the different sucrose synthase of Arabidopsis, AtSUS5 and 6 are localized in the phloem, in both sucrose loading and unloading zones of mature leaves (Barratt *et al.*, 2009) and control sucrose levels in the phloem (Claussen *et al.*, 1985). Barratt *et al.*, (2011) reported that AtSUS5 and AtSUS6 may have a specific role in the provision of the UDP-glucose substrate (as they reversibly cleave sucrose into UDP-glucose and fructose) for the synthesis of callose in the wall of sieve pores. As said before, UDP-glucose is also the substrate of cellulose synthase (Nakashima *et al.*, 2003). The activities of AtSUS are transcriptionally regulated (Martin *et al.*, 1993), so we evaluated the expression level of AtSUS5 and AtSUS6 in the two Arabidopsis lines. As the expression level of AtSUS6 is higher in the midrib of Atcals7ko line (whereas AtSUS5 showed very low expression levels not significantly different in the two lines), the loss of AtCALS7 could make available UDP-glucose to promote the activity of cellulose synthases (Nakashima *et al.*, 2003). Interestingly, as said above, in the *Atcals7ko* line, the lumina of the phloem cells are reduced in comparison to the wild-type, likely due to thicker cell walls.

The activities of enzymes responsible of sucrose cleavage in the apoplast, i.e. cell wall invertases (CWINV, Hothorn *et al.*, 2010) resulted also modulated in *Atcals7ko* line. The activities of CWINV are transcriptionally regulated (Veillet *et al.*, 2016; Cabello *et al.*, 2014). They irreversibly catalyze the cleavage of the extracellular sucrose into glucose and fructose (Roitsch and González, 2004; Hirose *et al.*, 2008). We found that the expression level of *AtCWINV1* is significantly higher in the midrib of *Atcals7ko* plants, whereas *AtCWINV6* showed a similar trend but without significant difference between the two lines. The increasing of *AtCWINV1* expression (and the consequent enzyme activation) alters the ratio of sucrose to hexoses in the apoplast, therefore modulating sugar signaling (Lastdrager *et al.*, 2014) and sugar partitioning. Overall, these results demonstrated that both intra- and extracellular sucrose cleavage contribute to the production of hexoses, which are able to act as energy source and signaling molecules in response to the osmotic stress (Janse van Rensburg *et al.*, 2017) imposed in Arabidopsis by the loss of AtCALS7.

The loss of *AtCALS7* impairs phloem loading.

To investigate if the different sugar partitioning in *Atcals7ko* line is related to modifications in phloem loading from the apoplasm, we investigated the transcription levels of genes encoding the main sugar transporters in Arabidopsis.

In the phloem parenchyma cells (PPCs) AtSWEET11 and AtSWEET12 are uniporters playing an important role in the efflux of sucrose, glucose and fructose (Le Hir *et al.*, 2015) from PPCs towards the apoplasmic space (Zhang, 2018): they are responsible for the step before phloem loading mediated by AtSUC2/H^+ symporter (Braun, 2012; Chen, 2014). In leaves, *AtSWEET11* and *AtSWEET12* genes were highly expressed when sucrose export was high and reduced during osmotic stress (Durand *et al.*, 2018). We found that *AtSWEET11* showed significant downregulation in *Atcals7ko* line. It is likely that, due to the impairment of the mass flow in the SEs of *Atcals7ko* line, high sucrose levels remain in the PPCs (Wei *et al.*, 2020). As a consequence, the expression levels of *AtSUC2* and *AtSUC3* result unchanged in *Atcals7ko* midribs compared to the wild-type. Among the genes encoding sucrose transporters, *AtSUC2* is the most expressed SUC gene in the rosette of Arabidopsis and displays a high and stable diurnal expression (Durand *et al.*, 2018). AtSUC2 is localized exclusively in the companion cells of Arabidopsis, it is highly expressed in mature leaves (Hafke *et al.*, 2013) and its function in phloem loading is well established (Giaquinta, 1977; Lalonde *et al.*, 2003). There is evidence that SUC2 activity is regulated at transcriptional, post-transcriptional and post-translational levels (Xu *et al.*, 2018; Wipf *et al.*, 2020). In fact, AtSUC2 expression and activity are regulated, both positively and negatively, by developmental (sink to source transition) and environmental cues, including light, sugar levels, turgor pressure, drought and osmotic stress, and hormones. However, Sakr *et al.*, (1997) reported that in Arabidopsis, the amount of AtSUC2 protein was not correlated with the sucrose transport rate because, in addition to protein amount, also the proton motive force might influence SUC activity (Khadilkar *et al.*, 2016). *AtSUC3* encodes for a transmembrane sucrose transporter, located in sieve elements (Meyer *et al.*, 2004) also indicated as a putative sucrose sensor (Meyer *et al.*, 2004). In the midribs of both Arabidopsis lines, *AtSUC3* has low expression level, as the transporter AtSUC3 is mainly expressed in sink tissues, where it delivers sucrose from the apoplasm (Meyer *et al.*, 2004). Similarly, the expression level of the monosaccharide transporter gene *AtSTP13*, which encodes a transporter active in the vascular tissues of Arabidopsis green leaves (Nørholm *et al.*, 2006) remains unchanged in the two lines.

Does the reduced phloem function in *Atcals7ko* line alter symplasmic cell communication?

Given the modification above described, we also investigated whether the loss of AtCALS7 in Arabidopsis and the subsequent reduced phloem function in *Atcals7ko* line (Barratt *et al.*, 2011; Xie *et al.*, 2011) may influence the symplasmic cell communication (i.e. *via* plasmodesmata) among different parts of the source leaf. In fact, it is widely established that plasmodesmata in a leaf form a special communication network between the mesophyll and the phloem (Lucas *et al.*, 1996).

TEM observations revealed the presence of aberrant callose-deficient sieve-plates in source leaves of *Atcals7ko* Arabidopsis, confirming what Barratt *et al.*, (2011) reported in Arabidopsis sink organs (stem and

root). At the CC/SE interface, PPUs appeared similar in morphology in the two Arabidopsis lines, but a thin callose layer is clearly visible only in the wild-type samples. This leads to the hypothesis that AtCALS7 could be responsible for the maintenance and regulation of the PPU gates beside the sieve pores. Nevertheless, whether the lack of phloematic callose could provoke changes in the regulation of CC/SE connectivity at PPUs remains to demonstrate.

To widely check the callose distribution and the eventual variations in callose-related signal intensity in different leaf areas of wild-type and *Atcals7ko* Arabidopsis plants, we used aniline-blue as fluorescent dye to detect callose depositions (Zavaliev and Epel 2015).

As expected, fluorescent dots appeared in correspondence of the phloem layer in the midribs of wild-type plants (De Marco *et al.*, 2016b; Pagliari *et al.*, 2016) but not in the *Atcals7ko* mutants. This is in agreement with TEM results commented above (Barratt *et al.*, 2011; Xie *et al.*, 2011).

In the adjacent parenchyma tissues, aniline-blue evidenced callose collars at the plasmodesmata, visible as numerous fluorescent punctate dots at the cell boundaries (Levy *et al.*, 2007). In the two Arabidopsis lines, the number of deposits and the fluorescence intensity was not significantly different, in average, in the selected area. But considering the density of the dots within the area of interest, this is significantly higher in the mutant line than in the wild-type, indicating changes in their morphology (*i.e.* from simple- to branched-shaped). Plasmodesmata have a dynamic structure, able to change in response to a number of stimuli (Fitzgibbon *et al.*, 2013; Sager and Lee, 2014). It has been reported that the appearance of complex, branched plasmodesmata may reduce intercellular communication (Lucas and Lee, 2004) and mark a shift from unselective to selective molecule transport, allowing increasing control of the substances passing between the cells (Oparka and Turgeon, 1999). Complex, branched plasmodesma formation is influenced by different stresses and quickly occurs in leaves following osmotic shocks (Schulz, 1995) and undergoing the sink-source transition (Roberts *et al.*, 2001).

As said before, the phloem mass flow is strongly impaired in the mutant line. This causes the increasing of sugar concentration and the subsequent increasing of turgor pressure inside the cells. In other words, the sieve tube damage, imposed by loss of *Atcals7ko* gene (Barratt *et al.*, 2011), perturbs the existing pressure conditions resulting in a turgor shift (Gould *et al.*, 2004), which influences the permeability (depending on the structure and the density) of plasmodesmata. We can state that symplasmic continuity is disrupted in the midrib parenchyma of *Atcals7ko* source leaves. In the epidermis tissue, the number of fluorescent dots, the signal intensity and the density are lower in *Atcals7ko* samples compared to the wild-type, indicating an attempt of mutant plants to establish the symplasmic continuity in tissues far from the phloem. The gating of plasmodesma orifice at distal level could be considered as a leaf response to the osmotic stress (Schulz, 1994) imposed by the impairment of sugar translocation at phloem level. Change in carbohydrate partitioning *via* symplast has the aim to reduce their water potential and prevent plasmolysis.

2. Phytoplasma effects on wild type vs *Atcals7ko* line

In CY-infected Arabidopsis, callose accumulation at the sieve plates is accompanied by the high expression level of the phloem specific *AtCALS7* gene. Moreover, using CY-infected *Atcals7ko* mutant plants, we suggest that AtCALS7 is involved in the regulation of the complex interactions established between plant host and phytoplasma, which deeply influencing sugar partitioning and homeostasis in plants during infection.

Morphological traits of CY-infected *Atcals7ko* midribs are indicative of heavily impaired phloem mass flow.

Lumen diameters in phloem cells are unchanged in both infected Arabidopsis lines in comparison with their respective healthy controls. This indicates that the loss of *AtCALS7* more than the infection, affects SE wall morphology. On the other hand, hyperplasia is a common characteristic of both CY-infected lines (Pagliari *et al.*, 2016), and it is particularly evident in the wild type. Phloem hyperplasia is reported as related to phloem-limited pathogens, such as viruses (Lv *et al.*, 2017) or phytoplasmas (Maejima *et al.*, 2014), which benefit for their infection processes. The great proliferation of invaded tissue in wild type line is not related to phytoplasma titre (this work and Christensen *et al.*, 2005) and might indicate a strong reaction of wild type plants to the stimuli imposed by phytoplasma effectors (Oshima *et al.*, 2001; Bai *et al.*, 2009; Sugio *et al.*, 2011).

Both infected lines do not show significant differences in the rosette fresh weight compared to their respective healthy controls, but failed to normally develop the stem. Stem stunting was previously reported in CY-infected wild type plants (Pagliari *et al.*, 2016) as indicative of the strong disturbance of phloem functions (Maust *et al.*, 2003): stem stunting is more accentuate in *Atcals7ko* infected individuals, which suffered of reduced growth even in healthy conditions (Figure 4.4 and supplementary 4.11). For these reasons it has not been possible to calculate and compare sugar translocation speed in the two infected Arabidopsis lines. Moreover, effects on carbohydrate translocation were reported in source leaves of many plants infected by phytoplasmas (Christensen *et al.*, 2005 and references therein). We might speculate that sugar translocation through the sieve elements is further compromised in infected *Atcals7ko* line in comparison to the other plant groups (i.e. infected wild type, healthy *Atcals7ko*, healthy wild type), given the aberrant structure of sieve plates and the concomitant presence of collapsed sieve elements observed by TEM (Figure 4.8 L).

To face phytoplasmas, wild type and *Atcals7ko* plants respond with a different sugar partitioning and metabolism at the site of infection.

As said before, it is often reported that following phytoplasma infection sugar, in particular sucrose, accumulate in source leaves (Maust *et al.*, 2003; Lee *et al.*, 2016; Xue *et al.*, 2018). In the midribs of wild type samples sugar contents are not significantly changed by infection. However high rate of sucrose metabolism is displayed at the infection site, as previously reported (Santi *et al.*, 2013b; Yao *et al.*, 2019), because *AtSUS5*

and *AtSUS6* transcripts show a significant increasing, in agreement with the high expression level of *AtCALS7* (Barratt *et al.*, 2011). This happens to provide precursors (i.e. UDP-glucose) for the synthesis of cellulose and/or callose (Tan *et al.*, 2015; De Marco *et al.*, 2020), or for the production of defense-related compounds (i.e. phenolics) (Bolouri-Moghaddam *et al.*, 2010; Musetti *et al.*, 2013b). In wild type plants, the expression levels of the sugar transporters *AtSWEET11*, *AtSWEET12*, *AtSUC2*, *AtSUC3* and *AtSTP13*, as well as the cell wall invertases *AtCWINV1* and *AtCWINV6* are not induced following infection, this being in accordance with the reduction of the mass flow (Dinant and Lemoine, 2010).

The enhancement of sucrose, glucose, and myoinositol levels in *Atcals7ko* infected plants, in comparison with those of the other plant groups, are indicative of a greater impairment of sugar translocation. Interestingly, *AtSUS5* and *AtSUS6* are up-regulated also in infected *Atcals7ko* plants (which lack of the phloem callose synthase), suggesting a greater involvement of phloem sucrose synthases in providing energy for sugar retrieval toward the infection site, to challenge phytoplasmas (Yao *et al.*, 2019). In fact, the significant increasing of *AtSWEET11*, *AtSTP13* and *AtSUC3*, transcripts in the midribs of the sole infected *Atcals7ko* plants, indicates that the sugar efflux to the apoplasmic space and its subsequent retrieval towards the SE/CC complex is highly activated (Meyer *et al.*, 2004), leading the infection site to a drastic shift toward sink-type environment (Santi *et al.*, 2013b) to fuel the host defense metabolism (Tadege *et al.*, 1998). Interestingly myoinositol can act as a signal to induce defense genes (Gebauer *et al.*, 2017; Bezrutczyk *et al.*, 2018) but it is also an excellent carbon source for cell wall constituents, such as pectin and hemicellulose (Loewus *et al.*,1962), which are, together with cellulose, the major types of polysaccharides in Arabidopsis cell wall (Bethke *et al.*, 2016). In absence of callose, the modulation of SE wall plasticity could be an important strategy to respond to the stress imposed by phytoplasmas, as demonstrated for other environmental cues (Wu *et al.*, 2018).

Consistent with the elevated expression levels of *AtSUC3* and *AtSUS5* and *6*, *AtCWINV1* and *6* transcripts are not changed in the infected *Atcals7ko* midribs, supporting the fact that intracellular sucrose cleavage is the major pathway for sucrose degradation in the CY-infected mutant plants.

Phytoplasma infection modifies symplasmic cell connectivity in the two Arabidopsis lines.

Plasmodesmal contacts (including sieve pores and PPUs) and their gating mechanisms seem to have great importance for the survival, dissemination and effector dispersal of phytoplasmas (van Bel and Musetti, 2019). CY infection does not alter PPU morphology in wild type Arabidopsis, nor callose accumulation is visible, similarly to what was previously reported in other phytoplasma-plant interactions (De Marco *et al.*, 2016b). This may indicate that in Arabidopsis the symplasmic connection and the possibility of metabolic exchange are maintained at CC/SE complex level (Musetti *et al.*, 2013a), regardless the infection.

In *Atcals7ko* line, it is interesting to underline that, beside the sieve plates, also PPUs seem affected in their morphology by the infection (Figure 4.8 N). However, it is not clear whether and how, this might influence CC/SE symplasmic communication.

Fluorescence microscopy imaging clearly confirmed the greater amount of callose in the phloem area of infected wild type plants in comparison to the healthy controls (Braun and Sinclair, 1978; Musetti *et al.*, 2010b; 2013a; Santi *et al.*, 2013a; De Marco *et al.*, 2016b), and the absence in the mutant line, even in case of biotic stress. This result is in accordance with the findings reported by Xie *et al.*, (2011), who noticed the lack of callose in *Atcals7ko* plants subjected to wounding stress of different intensity.

Following infection, wild type plants showed reduced symplasmic connectivity in the parenchyma cells of the midribs (similarly to what evidenced in healthy or infected *Atcals7ko* samples), because of the probable onset of complex plasmodesmata (see above). Changes in plasmodesma complexity may be a specific response to pathogens, allowing the plant to downregulate cell-to-cell communication rapidly in response to invasion, reducing the nonselective movement of pathogen-induced molecules between host cells (Benitez-Alonso *et al.*, 2010) and favoring apoplasmic transport. It is interesting to underline that H_2O_2 and other reactive oxygen species produced in tissues following infection (Musetti *et al.*, 2004), may accelerate the appearance of complex plasmodesmata (Fitzgibbon *et al.*, 2013).

In *Atcals7ko* line, cell connectivity at midrib parenchyma level (which already appeared compromised in healthy plants compared to wild-type) remains unchanged following CY-infection, but it appears reduced at epidermis level. Probably under sugar signaling, communication among cells, in the different tissues, is reduced to impede the spread of phytoplasma effectors from the sieve elements to the distal tissues (Tomczynska *et al.*, 2020). In fact, given that many effectors are small soluble proteins, it is possible that many phytoplasma-secreted proteins are mobile within the plant symplast (Bai *et al.*, 2009).

Concluding remarks

The results reported in this work demonstrated that the absence AtCALS7 affects both apoplasmic and symplasmic sugar partitioning in Arabidopsis, leading to the activation of sugar-mediated signaling to overcome plant osmotic stress, due to the impairment of sugar translocation in the SEs.

In case of phytoplasma infection, in presence of AtCALS7 (wild type plants), sugar metabolism increases at CC/SE level (infection site) to fuel pathogen metabolism (Kube *et al.*, 2012) and to promote plant-defence responses. Moreover, symplasmic connection in proximity of the infection site is reduced, indicating a source-sink translation. In absence of AtCALS7, sugar amount at the infection site increases significantly and sugar metabolism suffers a strong unbalance. The highly significant increasing of sugar apoplasmic transport seems counterbalanced by the decreasing of symplasmic connection among the cells of other leaf tissues.

Author contribution

CB and RM conceived the project. CB and SB grew the plants. CB and AL reared the insects and prepare the inoculum sources. CB and MM performed the molecular analysis on the phytoplasma titre. CB and SB performed the gene expression analysis. AL conceived the confocal analysis, the sugar quantification and the flow speed experiment. CB and SW performed the confocal analyses. CB, JHS and YW performed the sugar quantification. CB with the supervision of CV and the support of MOP performed the flow speed experiment. CB, RM wrote the manuscript with the help of SS and AJEVB. All the authors provided critical suggestions for the realization of the manuscript.

Acknowledgements

This work was funded by the University of Udine, through the Department of Agriculture, Food, Environment and Animal Sciences (Di4A), Project Start-up 2018. The authors thank Professor Domenico Bosco (University of Torino, Italy) for making available the CY phytoplasma strain and for his advice on insect rearing.

Supplementary materials

Here we provided some supplementary materials useful for the text comprehension. In the S1 we show the stem development in the Arabidopsis healthy plant both of the mutant line than the wild type line. In the S2 we show the control of the autofluorescence of the confocal analysis.

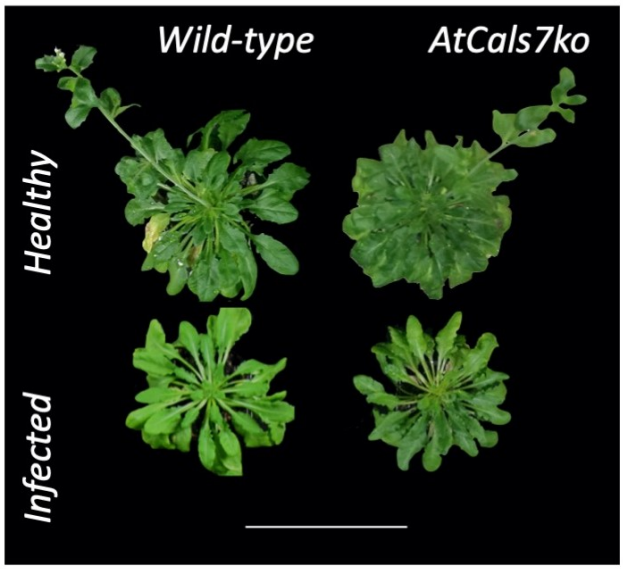

Figure 4.12 ***Sixty-day-old Arabidopsis plants grown under long day conditions.*** *Stem was well developed only in healthy plants (both wild type and Atcals7ko).*

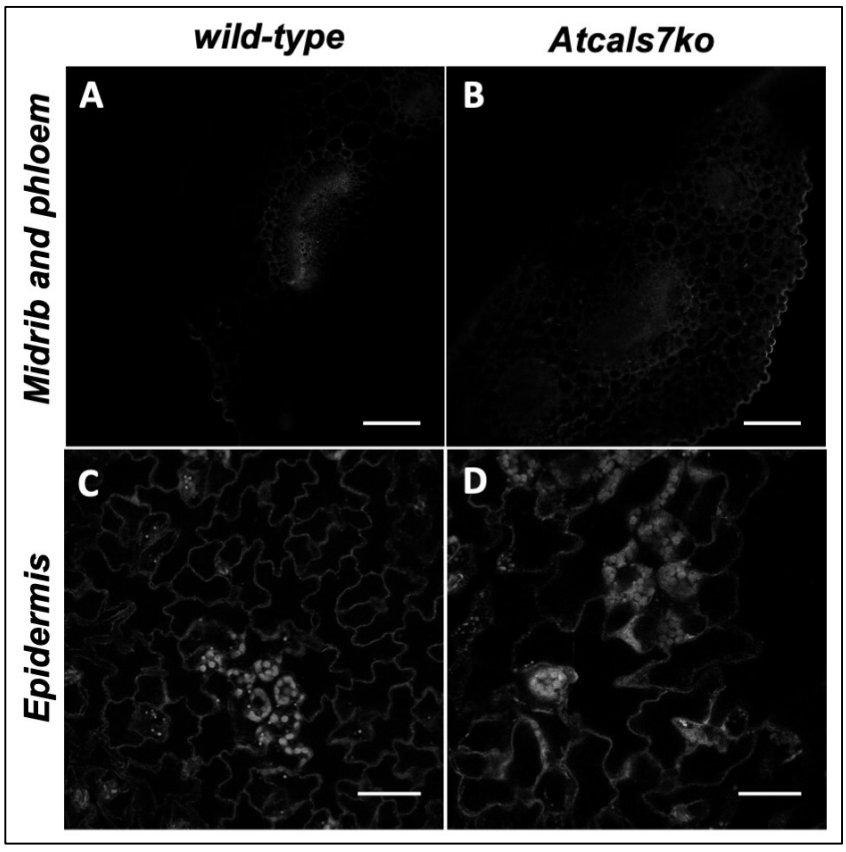

Figure 4.11 In ***unstained samples****, both midribs (A, B) and epidermis (C, D), the excitation wavelengths used for aniline blue fluorochrome (405 nm) did not elicit fluorescent signals. Fluorescence was not detected, with exception of autofluorescence of the xylem in midribs (A, B) and chloroplast in epidermis (C, D). Bars correspond to 50μm.*

References

Albertazzi, G., Milc, J., Caffagni, A., Francia, E., Roncaglia, E., Ferrari, F., Tagliafico, E., Stefani, E., Pecchioni, N., 2009. Gene expression in grapevine cultivars in response to Bois Noir phytoplasma infection. Plant Sci. 176, 792–804. https://doi.org/10.1016/j.plantsci.2009.03.001

Alma, A., Lessio, F., Nickel, H., 2019. Insects as phytoplasma vectors: ecological and epidemiological aspects, in: Phytoplasmas: Plant Pathogenic Bacteria-II. Springer, pp. 1–25.

Bai, X., Correa, V.R., Toruño, T.Y., Ammar, E.-D., Kamoun, S., Hogenhout, S.A., 2009. AY-WB Phytoplasma Secretes a Protein That Targets Plant Cell Nuclei. Mol. Plant-Microbe Interactions 22, 18–30. https://doi.org/10.1094/MPMI-22-1-0018

Barratt, D.H.P., Derbyshire, P., Findlay, K., Pike, M., Wellner, N., Lunn, J., Feil, R., Simpson, C., Maule, A.J., Smith, A.M., 2009. Normal growth of Arabidopsis requires cytosolic invertase but not sucrose synthase. Proc. Natl. Acad. Sci. 106, 13124–13129. https://doi.org/10.1073/pnas.0900689106

Barratt, D.H.P., Kölling, K., Graf, A., Pike, M., Calder, G., Findlay, K., Zeeman, S.C., Smith, A.M., 2011. Callose Synthase GSL7 Is Necessary for Normal Phloem Transport and Inflorescence Growth in Arabidopsis. Plant Physiol. 155, 328–341. https://doi.org/10.1104/pp.110.166330

Benitez-Alfonso, Y., Faulkner, C., Ritzenthaler, C., Maule, A.J., 2010. Plasmodesmata: gateways to local and systemic virus infection. Mol. Plant. Microbe Interact. 23, 1403–1412.

Bernardini, C., Pagliari, L., De Rosa, V., Almeida-Trapp, M., Santi, S., Martini, M., Buoso, S., Loschi, A., Loi, N., Chiesa, F., Mithöfer, A., van Bel, A.J.E., Musetti, R., 2020. Pre-symptomatic modified phytohormone profile is associated with lower phytoplasma titres in an Arabidopsis seor1ko line. Sci. Rep. 10, 14770. https://doi.org/10.1038/s41598-020-71660-0

Bethke, G., Thao, A., Xiong, G., Li, B., Soltis, N.E., Hatsugai, N., Hillmer, R.A., Katagiri, F., Kliebenstein, D.J., Pauly, M., 2016. Pectin biosynthesis is critical for cell wall integrity and immunity in Arabidopsis thaliana. Plant Cell 28, 537–556.

Bezrutczyk, M., Yang, J., Eom, J., Prior, M., Sosso, D., Hartwig, T., Szurek, B., Oliva, R., Vera-Cruz, C., White, F.F., 2018. Sugar flux and signaling in plant–microbe interactions. Plant J. 93, 675–685.

Bieniawska, Z., Paul Barratt, D.H., Garlick, A.P., Thole, V., Kruger, N.J., Martin, C., Zrenner, R., Smith, A.M., 2007. Analysis of the sucrose synthase gene family in Arabidopsis: The sucrose synthase gene family in Arabidopsis. Plant J. 49, 810–828. https://doi.org/10.1111/j.1365-313X.2006.03011.x

Bolouri-Moghaddam, M. R., Le Roy, K., Xiang, L., Rolland, F., & Van den Ende, W. (2010). Sugar signalling and antioxidant network connections in plant cells. The FEBS journal, 277(9), 2022-2037.

Bolouri Moghaddam, M.R., Van den Ende, W., 2012. Sugars and plant innate immunity. J. Exp. Bot. 63, 3989–3998.

Bolton, M.D., 2009. Primary metabolism and plant defense—fuel for the fire. Mol. Plant. Microbe Interact. 22, 487–497.

Bonke, M., Thitamadee, S., Mähönen, A.P., Hauser, M.-T., Helariutta, Y., 2003. APL regulates vascular tissue identity in Arabidopsis. Nature 426, 181–186.

Bosco, D., Minucci, C., Boccardo, G., Conti, M., 1997. Differential acquisition of chrysanthemum yellows phytoplasma by three leafhopper species. Entomol. Exp. Appl. 83, 219–224. https://doi.org/10.1046/j.1570-7458.1997.00175.x

Braun, D.M., 2012. SWEET! The pathway is complete. Science 335, 173–174.

Braun, E. J., & Sinclair, W. A. (1978). Translocation in phloem necrosis-diseased American elm seedlings. Phytopathology, 68(12), 1733-1737.

Brown, P.H., Hu, H., Roberts, W.G., 1999. Occurrence of sugar alcohols determines boron toxicity symptoms of ornamental species. J. Am. Soc. Hortic. Sci. 124, 347–352.

Buoso, S., Pagliari, L., Musetti, R., Martini, M., Marroni, F., Schmidt, W., Santi, S., 2019. ‘Candidatus Phytoplasma

solani' interferes with the distribution and uptake of iron in tomato. BMC Genomics 20, 703. https://doi.org/10.1186/s12864-019-6062-x

Cabello, S., Lorenz, C., Crespo, S., Cabrera, J., Ludwig, R., Escobar, C., Hofmann, J., 2014. Altered sucrose synthase and invertase expression affects the local and systemic sugar metabolism of nematode-infected Arabidopsis thaliana plants. J. Exp. Bot. 65, 201–212.

Cao, X.B., Fan, G.Q ., Dong, Y.P., Zhao, Z.L. , Deng, M.J., Wang, Z. and Liu, W. S., 2017. Proteome profiling of Paulownia seedlings infected with phytoplasma. Front. Plant. Sci. 8, 342

Cao, Y., Fan, G., Wang, Z., & Gu, Z. (2019). Phytoplasma-induced Changes in the Acetylome and Succinylome of Paulownia tomentosa Provide Evidence for Involvement of Acetylated Proteins in Witches' Broom Disease. Molecular & Cellular Proteomics, *18*(6), 1210-1226.

Chen, L., 2014. SWEET sugar transporters for phloem transport and pathogen nutrition. New Phytol. 201, 1150–1155.

Chiou, T.-J., Bush, D.R., 1998. Sucrose is a signal molecule in assimilate partitioning. Proc. Natl. Acad. Sci. 95, 4784–4788.

Christensen, N.M., Axelsen, K.B., Nicolaisen, M., Schulz, A., 2005. Phytoplasmas and their interactions with hosts. Trends Plant Sci. 10, 526–535. https://doi.org/10.1016/j.tplants.2005.09.008

Claussen, W., Hawker, J., Loveys, B., 1985. Sucrose synthase activity, invertase activity, net photosynthetic rates and carbohydrate content of detached leaves of eggplants as affected by attached stems and shoots (sinks). J. Plant Physiol. 119, 123–131.

De Marco, F., Eveillard, S., Batailler, B., Razan, F., Gilard, F., Le Hir, R., Vilaine, F., Dinant, S., 2016. Interactions between the stolbur phytoplasma infection and the phloem functions in tomato.

De Marco, F., Pagliari, L., Degola, F., Buxa, S.V., Loschi, A., Dinant, S., Hir, R.L., Morin, H., Santi, S., Musetti, R., 2016b. Combined microscopy and molecular analyses show phloem occlusions and cell wall modifications in tomato leaves in response to ' *Candidatus* Phytoplasma solani': RESPONSE OF TOMATO PHLOEM TO PHYTOPLASMA INFECTION. J. Microsc. 263, 212–225. https://doi.org/10.1111/jmi.12426

De Marco, F.D., Batailler, B., Thorpe, M.R., Razan, F., Hir, R.L., Vilaine, F., Bouchereau, A., Martin-Magniette, M.-L., Eveillard, S., Dinant, S., 2020. Role of the SUT1 and SUT2 sugar transporters during stolbur phytoplasma infection in tomato. Plant Biology. bioRxiv.

Dermastia, M., 2019. Plant Hormones in Phytoplasma Infected Plants. Front. Plant Sci. 10, 477. https://doi.org/10.3389/fpls.2019.00477

Dinant, S., Lemoine, R., 2010. The phloem pathway: new issues and old debates. C. R. Biol. 333, 307–319.

Doblin, M.S., Kurek, I., Jacob-Wilk, D., Delmer, D.P., 2002. Cellulose biosynthesis in plants: from genes to rosettes. Plant Cell Physiol. 43, 1407–1420.

Dodds, P.N., Lagudah, E.S., 2016. Starving the enemy. Science 354, 1377–1378.

Doyle, JJ, Doyle, JL, 1990. DNA extraction from Arabidopsis. Focus 12, 13–15.

Durand, M., Mainson, D., Porcheron, B., Maurousset, L., Lemoine, R., Pourtau, N., 2018. Carbon source–sink relationship in Arabidopsis thaliana: the role of sucrose transporters. Planta 247, 587–611. https://doi.org/10.1007/s00425-017-2807-4

Ellinger, D., Voigt, C.A., 2014. Callose biosynthesis in arabidopsis with a focus on pathogen response: what we have learned within the last decade. Ann. Bot. 114, 1349–1358. https://doi.org/10.1093/aob/mcu120

Ermacora, P., Osler, R., 2019. Symptoms of phytoplasma diseases, in: Phytoplasmas. Springer, pp. 53–67.

Eschrich, W., 1956. Kallose. Protoplasma 47, 487–530.

Eveland, A.L., Jackson, D.P., 2012. Sugars, signalling, and plant development. J. Exp. Bot. 63, 3367–3377.

Fatima, U., Senthil-Kumar, M., 2015. Plant and pathogen nutrient acquisition strategies. Front. Plant Sci. 6, 750.

Fitzgibbon, J., Beck, M., Zhou, J., Faulkner, C., Robatzek, S., Oparka, K., 2013. A developmental framework for complex plasmodesmata formation revealed by large-scale

imaging of the Arabidopsis leaf epidermis. Plant Cell 25, 57–70.

Furch, A.C., Hafke, J.B., Schulz, A., van Bel, A.J., 2007. Ca2+-mediated remote control of reversible sieve tube occlusion in Vicia faba. J. Exp. Bot. 58, 2827–2838.

Gebauer P, Korn M, Engelsdorf T, Sonnewald U, Koch C, Voll LM. 2017. Sugar accumulation in leaves of Arabidopsis sweet11/sweet12double mutants enhances priming of the salicylic acid-mediated defense response. Frontiers in Plant Science 8: e1378.

Giaquinta, R., 1977. Phloem loading of sucrose: pH dependence and selectivity. Plant Physiol. 59, 750–755.

Gould, N., Minchin, P.E., Thorpe, M.R., 2004. Direct measurements of sieve element hydrostatic pressure reveal strong regulation after pathway blockage. Funct. Plant Biol. 31, 987–993.

Hafke, J.B., Höll, S.-R., Kühn, C., van Bel, A.J.E., 2013. Electrophysiological approach to determine kinetic parameters of sucrose uptake by single sieve elements or phloem parenchyma cells in intact Vicia faba plants. Front. Plant Sci. 4. https://doi.org/10.3389/fpls.2013.00274

Hirose, T., Scofield, G.N., Terao, T., 2008. An expression analysis profile for the entire sucrose synthase gene family in rice. Plant Sci. 174, 534–543.

Hong, Z., Zhang, Z., Olson, J.M., Verma, D.P.S., 2001. A novel UDP-glucose transferase is part of the callose synthase complex and interacts with phragmoplastin at the forming cell plate. Plant Cell 13, 769–779.

Hothorn, M., Van den Ende, W., Lammens, W., Rybin, V., Scheffzek, K., 2010. Structural insights into the pH-controlled targeting of plant cell-wall invertase by a specific inhibitor protein. Proc. Natl. Acad. Sci. 107, 17427–17432.

Janik, K., Mittelberger, C., & Moser, M. (2018). Lights Out. The Chloroplast Under Attack During Phytoplasma Infection?. Annual Plant Reviews online, 399-426.

Janse van Rensburg, H.C., Van den Ende, W., 2018. UDP-Glucose: A Potential Signaling Molecule in Plants? Front. Plant Sci. 8, 2230. https://doi.org/10.3389/fpls.2017.02230

Khadilkar, A.S., Yadav, U.P., Salazar, C., Shulaev, V., Paez-Valencia, J., Pizzio, G.A., Gaxiola, R.A., Ayre, B.G., 2016. Constitutive and companion cell-specific overexpression of AVP1, encoding a proton-pumping pyrophosphatase, enhances biomass accumulation, phloem loading, and long-distance transport. Plant Physiol. 170, 401–414.

Kube, M., Mitrovic, J., Duduk, B., Rabus, R., & Seemüller, E. (2012). Current view on phytoplasma genomes and encoded metabolism. The Scientific World Journal, 2012.

Kudlicka, K., Brown Jr, R.M., 1997. Cellulose and callose biosynthesis in higher plants (I. Solubilization and separation of (1-> 3)-and (1-> 4)-[beta]-glucan synthase activities from mung bean). Plant Physiol. 115, 643–656.

Lalonde, S., Tegeder, M., Throne-Holst, M., Frommer, W.B., Patrick, J.W., 2003. Phloem loading and unloading of sugars and amino acids. Plant Cell Environ. 26, 37–56. https://doi.org/10.1046/j.1365-3040.2003.00847.x

Lastdrager, J., Hanson, J., Smeekens, S., 2014. Sugar signals and the control of plant growth and development. J. Exp. Bot. 65, 799–807.

Le Hir, R., Spinner, L., Klemens, P.A., Chakraborti, D., De Marco, F., Vilaine, F., Wolff, N., Lemoine, R., Porcheron, B., Géry, C., 2015. Disruption of the sugar transporters AtSWEET11 and AtSWEET12 affects vascular development and freezing tolerance in Arabidopsis. Mol. Plant 8, 1687–1690.

Lecourieux, F., Kappel, C., Lecourieux, D., Serrano, A., Torres, E., Arce-Johnson, P., Delrot, S., 2014. An update on sugar transport and signalling in grapevine. J. Exp. Bot. 65, 821–832.

Lee, D.-K., Ahn, S., Cho, H.Y., Yun, H.Y., Park, J.H., Lim, J., Lee, J., Kwon, S.W., 2016. Metabolic response induced by parasitic plant-fungus interactions hinder amino sugar and nucleotide sugar metabolism in the host. Sci. Rep. 6, 1–11.

Lee, I.-M., Martini, M., Bottner, K.D., Dane, R.A., Black, M.C., Troxclair, N., 2003. Ecological Implications from a Molecular Analysis of Phytoplasmas Involved in an Aster Yellows Epidemic in Various Crops in Texas. Phytopathology

93, 1368–1377. https://doi.org/10.1094/PHYTO.2003.93.11.1368

Levy, A., Erlanger, M., Rosenthal, M., Epel, B.L., 2007. A plasmodesmata-associated β-1,3-glucanase in Arabidopsis: A plasmodesmal β-1,3-glucanase. Plant J. 49, 669–682. https://doi.org/10.1111/j.1365-313X.2006.02986.x

Li, P., Wind, J. J., Shi, X., Zhang, H., Hanson, J., Smeekens, S. C., & Teng, S. (2011). Fructose sensitivity is suppressed in Arabidopsis by the transcription factor ANAC089 lacking the membrane-bound domain. Proceedings of the National Academy of Sciences, 108(8), 3436-3441.

Loewus, F.A., Kelly, S., Neufeld, E.F., 1962. Metabolism of myo-inositol in plants: conversion to pectin, hemicellulose, D-xylose, and sugar acids. Proc. Natl. Acad. Sci. U. S. A. 48, 421.

Lucas, W.J., Balachandran, S., Park, J., Wolf, S., 1996. Plasmodesmal companion cell-mesophyll communication in the control over carbon metabolism and phloem transport: insights gained from viral movement proteins. J. Exp. Bot. 1119–1128.

Lucas, W.J., Lee, J.-Y., 2004. Plasmodesmata as a supracellular control network in plants. Nat. Rev. Mol. Cell Biol. 5, 712–726.

Lv, M.-F., Xie, L., Song, X.-J., Hong, J., Mao, Q.-Z., Wei, T.-Y., Chen, J.-P., Zhang, H.-M., 2017. Phloem-limited reoviruses universally induce sieve element hyperplasia and more flexible gateways, providing more channels for their movement in plants. Sci. Rep. 7, 1–13.

Maejima, K., Oshima, K., Namba, S., 2014. Exploring the phytoplasmas, plant pathogenic bacteria. J Gen Plant Pathol 12.

Martin, T., Frommer, W.B., Salanoubat, M., Willmitzer, L., 1993. Expression of an Arabidopsis sucrose synthase gene indicates a role in metabolization of sucrose both during phloem loading and in sink organs. Plant J. 4, 367–377.

Martinez, H.E.P., Maia, J.T.L.S., Ventrela, M.C., Milagres, C. do C., Cecon, P.R., Clemente, J.M., Garbin, C.Z., 2020. Leaf and Stem Anatomy of Cherry Tomato Under Calcium and Magnesium Deficiencies. Braz. Arch. Biol. Technol. 63.

Martini, M., Loi, N., Ermacora, P., Carraro, L., Pastore, M., 2007. A real-time PCR method for detection and quantification of 'Candidatus Phytoplasma prunorum' in its natural hosts 2.

Martini, M., Musetti, R., Grisan, S., Polizzotto, R., Borselli, S., Pavan, F., Osler, R., 2009. DNA-Dependent Detection of the Grapevine Fungal Endophytes *Aureobasidium pullulans* and *Epicoccum nigrum*. Plant Dis. 93, 993–998. https://doi.org/10.1094/PDIS-93-10-0993

Maust, B.E., Espadas, F., Talavera, C., Aguilar, M., Santamaría, J.M., Oropeza, C., 2003. Changes in carbohydrate metabolism in coconut palms infected with the lethal yellowing phytoplasma. Phytopathology 93, 976–981.

Meyer, S., Lauterbach, C., Niedermeier, M., Barth, I., Sjolund, R.D., Sauer, N., 2004. Wounding enhances expression of AtSUC3, a sucrose transporter from Arabidopsis sieve elements and sink tissues. Plant Physiol. 134, 684–693.

Muller, P.Y., Janovjak, H., Miserez, A.R., Dobbie, Z., 2002. Short technical report processing of gene expression data generated by quantitative real-time RT-PCR. Biotechniques 32, 1372–1379.

Musetti, R., 2010a. Biochemical changes in plants infected by phytoplasmas. Phytoplasmas Genomes Plant Hosts Vectors 132–146.

Musetti, R., Paolacci, A., Ciaffi, M., Tanzarella, O. A., Polizzotto, R., Tubaro, F., ... & Osler, R. 2010b. Phloem cytochemical modification and gene expression following the recovery of apple plants from apple proliferation disease. Phytopathology, 100(4), 390-399.

Musetti, R., Buxa, S.V., De Marco, F., Loschi, A., Polizzotto, R., Kogel, K.-H., van Bel, A.J.E., 2013a. Phytoplasma-Triggered Ca^{2+} Influx Is Involved in Sieve-Tube Blockage. Mol. Plant-Microbe Interactions® 26, 379–386. https://doi.org/10.1094/MPMI-08-12-0207-R

Musetti, R., di Toppi, L.S., Ermacora, P., Favali, M.A., 2004. Recovery in Apple Trees Infected with the Apple Proliferation Phytoplasma: An Ultrastructural and Biochemical Study. Phytopathology 94, 203–208. https://doi.org/10.1094/PHYTO.2004.94.2.203

Musetti, R., Farhan, K., De Marco, F., Polizzotto, R., Paolacci, A., Ciaffi, M., Ermacora, P., Grisan, S., Santi, S.,

Osler, R., 2013b. Differentially-regulated defence genes in Malus domestica during phytoplasma infection and recovery. Eur. J. Plant Pathol. 136, 13–19. https://doi.org/10.1007/s10658-012-0147-6

Musetti, R., Pagliari, L., Buxa, S.V., Degola, F., De Marco, F., Loschi, A., Kogel, K.-H., van Bel, A.J., 2016. OHMS**: phytoplasmas dictate changes in sieve-element ultrastructure to accommodate their requirements for nutrition, multiplication and translocation. Plant Signal. Behav. 11, e1138191.

Nakashima, J., Laosinchai, W., Cui, X., Brown, R.M., 2003. New insight into the mechanism of cellulose and callose biosynthesis: proteases may regulate callose biosynthesis upon wounding. Cellulose 10, 369–389.

Namba, S., 2019. Molecular and biological properties of phytoplasmas. Proc. Jpn. Acad. Ser. B 95, 401–418.

Nørholm, M.H., Nour-Eldin, H.H., Brodersen, P., Mundy, J., Halkier, B.A., 2006. Expression of the Arabidopsis high-affinity hexose transporter STP13 correlates with programmed cell death. FEBS Lett. 580, 2381–2387.

Oparka, K.J., Turgeon, R., 1999. Sieve elements and companion cells—traffic control centers of the phloem. Plant Cell 11, 739–750.

Oshima, K., Maejima, K., Namba, S., 2013. Genomic and evolutionary aspects of phytoplasmas. Front. Microbiol. 4. https://doi.org/10.3389/fmicb.2013.00230

Oshima, K., Shiomi, T., Kuboyama, T., Sawayanagi, T., Nishigawa, H., Kakizawa, S., Miyata, S., Ugaki, M., Namba, S., 2001. Isolation and Characterization of Derivative Lines of the Onion Yellows Phytoplasma that Do Not Cause Stunting or Phloem Hyperplasia. Phytopathology® 91, 1024–1029. https://doi.org/10.1094/PHYTO.2001.91.11.1024

Pacifico, D., Galetto, L., Rashidi, M., Abbà, S., Palmano, S., Firrao, G., Bosco, D., Marzachì, C., 2015. Decreasing Global Transcript Levels over Time Suggest that Phytoplasma Cells Enter Stationary Phase during Plant and Insect Colonization. Appl. Environ. Microbiol. 81, 2591–2602. https://doi.org/10.1128/AEM.03096-14

Pagliari, L., Buoso, S., Santi, S., Furch, A.C.U., Martini, M., Degola, F., Loschi, A., van Bel, A.J.E., Musetti, R., 2017. Filamentous sieve element proteins are able to limit phloem mass flow, but not phytoplasma spread. J. Exp. Bot. 68, 3673–3688. https://doi.org/10.1093/jxb/erx199

Pagliari, L., Martini, M., Loschi, A., Musetti, R., 2016. Looking inside phytoplasma-infected sieve elements: A combined microscopy approach using Arabidopsis thaliana as a model plant. Micron 89, 87–97. https://doi.org/10.1016/j.micron.2016.07.007

Pfaffl, M.W., 2001. A new mathematical model for relative quantification in real-time RT–PCR. Nucleic Acids Res. 29, e45–e45.

Pinheiro, J., Bates, D., DebRoy, S., Sarkar, D., 2018. R Core Team. 2018. nlme: linear and nonlinear mixed effects models. R package version 3.1-137. R Found Stat Comput Retrieved HttpsCRAN R-Proj. Orgpackage Nlme Accessed 19 Jul 2018.

Prezelj, N., Covington, E., Roitsch, T., Gruden, K., Fragner, L., Weckwerth, W., Chersicola, M., Vodopivec, M., Dermastia, M., 2016. Metabolic consequences of infection of grapevine (Vitis vinifera L.) cv.“Modra frankinja” with Flavescence Dorée phytoplasma. Front. Plant Sci. 7, 711.

Roberts, I., Boevink, P., Roberts, A., Sauer, N., Reichel, C., Oparka, K., 2001. Dynamic changes in the frequency and architecture of plasmodesmata during the sink-source transition in tobacco leaves. Protoplasma 218, 31–44.

Roitsch, T., González, M.-C., 2004. Function and regulation of plant invertases: sweet sensations. Trends Plant Sci. 9, 606–613.

Rojas, C.M., Senthil-Kumar, M., Tzin, V., Mysore, K., 2014. Regulation of primary plant metabolism during plant-pathogen interactions and its contribution to plant defense. Front. Plant Sci. 5, 17.

Ruan, Y.-L., 2014. Sucrose Metabolism: Gateway to Diverse Carbon Use and Sugar Signaling. Annu. Rev. Plant Biol. 65, 33–67. https://doi.org/10.1146/annurev-arplant-050213-040251

Sager, R., Lee, J.-Y., 2014. Plasmodesmata in integrated cell signalling: insights from development and environmental signals and stresses. J. Exp. Bot. 65, 6337–6358.

Sakr, S., Noubahni, M., Bourbouloux, A., Riesmeier, J., Frommer, W.B., Sauer, N., Delrot, S., 1997. Cutting, ageing

and expression of plant membrane transporters. Biochim. Biophys. Acta BBA-Biomembr. 1330, 207–216.

Santi, S., De Marco, F., Polizzotto, R., Grisan, S., Musetti, R., 2013a. Recovery from stolbur disease in grapevine involves changes in sugar transport and metabolism. Front. Plant Sci. 4. https://doi.org/10.3389/fpls.2013.00171

Santi, S., Grisan, S., Pierasco, A., De Marco, F., Musetti, R., 2013b. Laser microdissection of grapevine leaf phloem infected by stolbur reveals site-specific gene responses associated to sucrose transport and metabolism: LM of stolbur-infected grapevine phloem. Plant Cell Environ. 36, 343–355. https://doi.org/10.1111/j.1365-3040.2012.02577.x

Schindelin, J., Arganda-Carreras, I., Frise, E., Kaynig, V., Longair, M., Pietzsch, T., Preibisch, S., Rueden, C., Saalfeld, S., Schmid, B., Tinevez, J.-Y., White, D.J., Hartenstein, V., Eliceiri, K., Tomancak, P., Cardona, A., 2012. Fiji: an open-source platform for biological-image analysis. Nat. Methods 9, 676–682. https://doi.org/10.1038/nmeth.2019

Schneider, R., Hanak, T., Persson, S., Voigt, C.A., 2016. Cellulose and callose synthesis and organization in focus, what's new? Curr. Opin. Plant Biol. 34, 9–16. https://doi.org/10.1016/j.pbi.2016.07.007

Schulz, A., 1995. Plasmodesmal widening accompanies the short-term increase in symplasmic phloem unloading in pea root tips under osmotic stress. Protoplasma 188, 22–37.

Schulz, A., 1994. Phloem transport and differential unloading in pea seedlings after source and sink manipulations. Planta 192, 239–248.

Sharma, A., Shahzad, B., Kumar, V., Kohli, S.K., Sidhu, G.P.S., Bali, A.S., Handa, N., Kapoor, D., Bhardwaj, R., Zheng, B., 2019. Phytohormones regulate accumulation of osmolytes under abiotic stress. Biomolecules 9, 285.

Stein, O., & Granot, D. (2019). An overview of sucrose synthases in plants. Frontiers in plant science, 10, 95.

Sugio, A., Kingdom, H.N., MacLean, A.M., Grieve, V.M., Hogenhout, S.A., 2011. Phytoplasma protein effector SAP11 enhances insect vector reproduction by manipulating plant development and defense hormone biosynthesis. Proc. Natl. Acad. Sci. 108, E1254–E1263. https://doi.org/10.1073/pnas.1105664108

Tadege, M., Bucher, M., Stähli, W., Suter, M., Dupuis, I., Kuhlemeier, C., 1998. Activation of plant defense responses and sugar efflux by expression of pyruvate decarboxylase in potato leaves. Plant J. 16, 661–671.

Tan, T.-C., Kracher, D., Gandini, R., Sygmund, C., Kittl, R., Haltrich, D., Hällberg, B.M., Ludwig, R., Divne, C., 2015. Structural basis for cellobiose dehydrogenase action during oxidative cellulose degradation. Nat. Commun. 6, 7542.

Tomczynska, I., Stumpe, M., Doan, T.G., Mauch, F., 2020. A Phytophthora effector protein promotes symplastic cell-to-cell trafficking by physical interaction with plasmodesmata-localised callose synthases. New Phytol.

van Bel, A.J.E., Musetti, R., 2019. Sieve element biology provides leads for research on phytoplasma lifestyle in plant hosts. J. Exp. Bot. 70, 3737–3755. https://doi.org/10.1093/jxb/erz172

Veillet, F., Gaillard, C., Coutos-Thévenot, P., La Camera, S., 2016. Targeting the AtCWIN1 Gene to Explore the Role of Invertases in Sucrose Transport in Roots and during Botrytis cinerea Infection. Front. Plant Sci. 7. https://doi.org/10.3389/fpls.2016.01899

Verbančič, J., Lunn, J.E., Stitt, M., Persson, S., 2018. Carbon supply and the regulation of cell wall synthesis. Mol. Plant 11, 75–94.

Verma, D.P.S., Hong, Z., 2001. Plant callose synthase complexes 9.

Vincent, C., Minchin, P.E.H., Liesche, J., 2019. Noninvasive Determination of Phloem Transport Speed with Carbon-14 (14C), in: Liesche, J. (Ed.), Phloem, Methods in Molecular Biology. Springer New York, New York, NY, pp. 153–162. https://doi.org/10.1007/978-1-4939-9562-2_13

Wang, L., Ruan, Y.-L., 2013. Regulation of cell division and expansion by sugar and auxin signaling. Front. Plant Sci. 4, 163.

Wei, X., Nguyen, S.T.T., Collings, D.A., McCurdy, D.W., 2020. Sucrose regulates wall ingrowth deposition in phloem parenchyma transfer cells in Arabidopsis via affecting phloem loading activity. J. Exp. Bot. 71, 4690–4702. https://doi.org/10.1093/jxb/eraa246

Will, T., van Bel, A.J., 2006. Physical and chemical interactions between aphids and plants. J. Exp. Bot. 57, 729–737.

Wipf, D., Pfister, C., Mounier, A., Leborgne-Castel, N., Frommer, W.B., Courty, P.-E., 2020. Identification of Putative Interactors of Arabidopsis Sugar Transporters. Trends Plant Sci.

Wu, S.-W., Kumar, R., Iswanto, A.B.B., Kim, J.-Y., 2018. Callose balancing at plasmodesmata. J. Exp. Bot. https://doi.org/10.1093/jxb/ery317

Xie, B., Hong, Z., 2011. Unplugging the callose plug from sieve pores. Plant Signal. Behav. 6, 491–493. https://doi.org/10.4161/psb.6.4.14653

Xie, B., Wang, X., Zhu, M., Zhang, Z., Hong, Z., 2011. *CalS7* encodes a callose synthase responsible for callose deposition in the phloem: *A phloem-specific callose synthase*. Plant J. 65, 1–14. https://doi.org/10.1111/j.1365-313X.2010.04399.x

Xu, Q., Chen, Siyuan, Yunjuan, R., Chen, Shaolin, Liesche, J., 2018. Regulation of Sucrose Transporters and Phloem Loading in Response to Environmental Cues. Plant Physiol. 176, 930–945. https://doi.org/10.1104/pp.17.01088

Xue, C., Liu, Z., Dai, L., Bu, J., Liu, M., Zhao, Z., Jiang, Z., Gao, W., Zhao, J., 2018. Changing Host Photosynthetic, Carbohydrate, and Energy Metabolisms Play Important Roles in Phytoplasma Infection. Phytopathology® 108, 1067–1077. https://doi.org/10.1094/PHYTO-02-18-0058-R

Yao, L., Yu, Q., Huang, M., Hung, W., Grosser, J., Chen, S., Wang, Y., Gmitter, F.G., 2019. Proteomic and metabolomic analyses provide insight into the off-flavour of fruits from citrus trees infected with 'Candidatus Liberibacter asiaticus.' Hortic. Res. 6, 1–13.

Zavaliev, R., Epel, B.L., 2015. Imaging Callose at Plasmodesmata Using Aniline Blue: Quantitative Confocal Microscopy, in: Heinlein, M. (Ed.), Plasmodesmata, Methods in Molecular Biology. Springer New York, New York, NY, pp. 105–119. https://doi.org/10.1007/978-1-4939-1523-1_7

Zhang, C., 2018. Mechanisms of phloem loading. Curr. Opin. Plant Biol. 5.

5. ON THE POSSIBLE ROLE(S) OF SYNAPTOTAGMIN1 IN PHYTOPLASMA-PLANT INTERACTION

CHIARA BERNARDINI AND RITA MUSETTI

As last (but not least) part of the doctorate project, we initiated investigation about Synaptotagmin 1 (SYTA), a protein involved in the establishment of endoplasmic reticulum-plasma membrane contact sites (ER-PM CS), which might play a role in the interaction of phytoplasmas with the sieve-element (SE) environment.

The research is developed in the frame of a collaboration with the University of Florida and the work is still in progress.

5.1 INTRODUCTION

Phloem-limited pathogens have a complex infection cycle in which host, vector and pathogen are involved. Inside the SEs, phytoplasma are observed floating in the lumen but also attached to the plasma membrane (PM) or adhering to sieve endoplasmic reticulum (SER) (Buxa et al., 2015; Pagliari et al., 2016), provoking evident structural remodeling of PM and SER cisternae in the infected SEs (Buxa et al., 2015). The whole mechanism which regulates the relationship among phytoplasma and sieve-element endo-membranes is still unknown, so more knowledge about this issue is requested, also to provide information useful for the control of the phytoplasma-related diseases.

The plant SYTs and their ortholog counterparts, the mammalian Extended Synaptotagmins (E-SYTs) and the yeast Tricalbins (Tcbs) are part of the ER-PM contact site (CS) tethers and share a common modular structure, comprising a N-terminal transmembrane (TM) domain that anchors them to the ER, a synaptotagmin-like mitochondrial- lipid binding (SMP) domain, and a variable number of the Ca^{2+}- and phospholipid-binding C2 domains (Giordano et al., 2013; Manford et al., 2012; Perez Sancho et al., 2015). The modular structure of SYTs implies two likely inter-related functions, namely the establishment of Ca^{2+}-

regulated ER-PM tethering by their C2 domains (Giordano et al., 2013; Manford et al., 2012; Perez Sancho et al., 2015; Saheki et al., 2016), and the SMP-dependent transport of lipids between the PM and the ER (Saheki et al., 2016; Schauder et al., 2014). Studies have shown that Tcbs are necessary to maintain PM integrity in yeast and to allow extreme curvature of cortical ER membrane: these processes would be facilitated by the transport of lipids from the highly curved, less packaged, cortical ER to the PM (Collado et al., 2019). Similarly, SYTA-1 *in planta* could also be involved in the process of PM repair, mediating membrane trafficking to restore PM integrity (Schapire et al., 2008). Moreover, it was recently reported that Arabidopsis mutants lacking SYTA-1 exhibited decreased plasma membrane integrity under multiple abiotic stresses such as freezing, high salt, osmotic stress or mechanical damage (Lopez et al., 2020).

More interestingly, SYTA-1 was associated to plant-cell endocytosis and to the cell-to-cell movement and systemic spread of plant viruses (Uchiyama et al., 2014). Plant cells have demonstrated great dynamics in endocytic activity (Baluska et al., 2002) aimed at the uptake of plant- or pathogen-derived elicitors, such as oligogalacturonic acid, glycoproteins and exopolysaccharides, which are produced during plant defense (Romanenko et al., 2002).

These findings, together to the fact that SYTA is expressed and modulated in the phloem (Santi, unpublished data) suggest a possible role of SYTA also in plant/phytoplasma interaction.

In this work we conducted a preliminary study about the synaptotagmin A-1 and phytoplasmas.

We first evaluated the expression level of *AtSYTA-1* in *Arabidopsis thaliana* healthy or infected with Chrysanthemum Yellows (CY) phytoplasma. Then we used the mutant line *Atsyta-1* to assess whether the lack of the protein affects plant growth and CY-symptom expression. An ultrastructural analysis was finally carried out to evaluate phytoplasma distribution inside SEs, to compare the morphology of PM and SER and the respective phytoplasma attachments in both Arabidopsis lines.

5.2 MATERIAL AND METHODS

Arabidopsis thaliana ecotype Col-0, wild type line was provided by NASC. The mutant line Sail 775A08 (*syta-1*, ecotype Col-0, Lewis and Lazarowitz, 2010) was kindly provided by Prof. Amit Levy, University of Florida.

30 plants for each line were grown in short day conditions (10L/14D) in a growth chamber with a controlled temperature of 18-20°C. Healthy colony of the leafhopper *Macrosteles quadripunctulatus* was maintained on *Avena sativa*. Insects of the last instar nymph were selected from the colony and put transferred to *Chrysanthemum carinatum* (daisy) plants, infected with Chrysanthemum Yellows (CY) phytoplasma, a strain belonging to the Aster Yellows group (16sIB). Insects were kept on daisy plants for a 7-day phytoplasma acquisition-access period (AAP). After a latency period of 20 days on *Avena sativa*, three infective insects per plants were placed on 40-days-old Arabidopsis, for a 7-days inoculation access period (IAP). After 7 days, the insect vectors were mechanically removed. Three healthy insects equal in age were transferred on Arabidopsis as control condition for seven days and then mechanically removed.

Samples for the analysis were collected 26 days after the end of IAP. For each condition at least 5 plants were collected.

The chlorophyll content was indirectly determined in each plant using a portable chlorophyll meter (SPAD-502, Minolta, Osaka, Japan). Given that the analysis is not invasive, SPAD measurement were performed on plants every 7 days on all the plants.

26 days after the end of IAP, plants were sampled: from the same plant, a part was used for the gene expression analysis, a part for the phytoplasma quantification, a part for the electron microscopy and a part for the fluorescence microscopy. The material for the molecular analyses were immediately frozen in liquid nitrogen.

Statistical analyses on the SPAD index measurement were performed using RStudio software Version 1.1.456 (RStudio Team (2020), Boston, MA). The normal distribution was checked with the Shapiro-Wilk test. Significant differences among the group means were determined with a two-way ANOVA and post-hoc comparisons between all groups were made with Tukey's test with $p<0.05$.

Phytoplasma detection

Around 1g of whole leaf tissue was used for DNA extraction following the Doyle and Doyle protocol (Doyle and Doyle, 1990), modified by Martini *et al.* (Martini *et al.*, 2009). Total genomic DNA quality and concentration was checked using NanoDrop 1000 Spectrophotometer (Thermo Fisher Scientific, Wilmington, DE, USA). The presence of phytoplasmas in the plants has been checked with the primer pair rp(I-B)F2/rp(I-

B)R2 following the protocol described by Bernardini *et al.*, (2020). For the quantification, the ribosomal gene rpl22 was choosen as target and amplified with the primer pair rp(I-B)F2/rp(I-B)R2 following the protocol described by Bernardini (Bernardini et al., 2020). Each sample has been run in three technical replicates and the titre of phytoplasma has been reported as CY phytoplasma genome units normalized with the weight of fresh tissue used for the extraction.

Statistical analysis was performed using RStudio. The normal distribution was checked with the Shapiro-Wilk test. Significant differences among the group means were determined with a two-way ANOVA and post-hoc comparisons between all groups were made with Tukey's test with $p<0.05$.

Electron microscopy and light microscopy

Midribs of mature leaf tissue were collected, chopped in section of 5mm and fixed for the TEM preparation. The inclusion was performed following the well-tuned protocol described in the previous studies (Bernardini *et al.*, 2020).

Ultra-thin (60-70nm in thickness) sections were cut with ultramicrotome (Reichert Leica Ultracut E ultramicrotome, Leica Microsystems, Wetzlar, Germany). Three samples per line per condition were analysed. At least 4 non-serial sections for each sample were observed. Ultra-thin sections were collected on uncoated copper grids, stained with UAR-EMS (uranyl acetate replacement stain, Electron Microscopy Sciences) and then observed under a PHILIPS CM 10 (FEI, Eindhoven, The Netherlands) transmission electron microscope (TEM), operated at 80 kV, and equipped with a Megaview G3 CCD camera (EMSIS GmbH, Münster, Germany). Five non-serial cross-sections from each sample were analyzed.

Gene expression analysis

Gene expression analysis was carried out for the *AtSYTA*, one of the gene involved in the production of the filament (see above), on healthy and infected wild type. RNA of five samples for each condition was extracted from 100mg of fresh tissue grinded in liquid nitrogen, using a SpectrumTM Plant Total RNA kit

(Sigma-Aldrich, Merck KGaA, Darmstadt, DE) according to the manufacturer's instructions.The RNA reverse-transcription to cDNA was carried out using a QuantiTectReverse Transcription Kit (Qiagen N.V., Hilden, DE) following the manufacturer's instructions. According to previous analysis, the *AtUBC9* (ubiquitin conjugating enzyme 9) was chosen as reference gene. Gene expression analysis was performed using SsoFast EvaGreen Supermix 2x (Bio-Rad Laboratories Inc., Hercules, CA, USA) and cDNA obtained from 5 ng of RNA and specific primers (Table 5.1) were used in a total volume of 10 µL. For each couple of primers, a standard curve has been defined, using CFX96 real-time PCR detection system (Bio-Rad Laboratories): the efficiency of the couple of primer has been evaluated by the software CFX Maestro (BioRad Laboratories). Function of the proteins and primer sequences are reported in Table 5.2. The mean normalized expression was calculated through the normalization of the target gene with the expression of the reference gene as reported by Muller (Muller *et al.*, 2002). Statistical analyses were performed using RStudio software Version 1.1.456 (2009-2018 RStudio, Inc. Boston, MA). The normal distribution was checked with Shapiro-Wilk test. Significant differences among the means were determined by a two-way ANOVA and post-hoc comparisons between all groups were made with Tukey's test with $p<0.05$.

Table 5.1 ***Table of the features of gene expression analysis.***

Analysis step	Features
RNA extraction	As reported (Pagliari et al., 2017)
DNAse treatment and cDNA synthesis	As reported (Pagliari et al., 2017)
Real-time RT-PCR	Reaction volume: 10µl SsoFast EvaGreen Supermix (Bio-Rad Laboratories Inc., Hercules, CA, USA) cDNA obtained from 10 ng of RNA and primers following the concentration indicated in Tab.2
Cycling conditions	95°C for 3 min 95°C for 5 s and 58°C for 5 s (40 cycles) Melting curve analysis from 65°C to 95°C

Table 5.2 ***Table of the primers used in this study and the function of the encoded protein***.

GENE	nM	Forward primer 5'-3'	Reverse primer 5'-3'	Function and reference
AtSYTA	500	CGGTCAGAGATCCCCAGACT	TCTCGGGATTCCCAACCTGT	Concurring in the formation of the anchoring net. (Wang, 2017)
AtUBC9	300	TCACAATTTCCAAGGTGCTGC	CGAGCAGTGGACTCGTACTT	In this study used as reference gene as reported by (Pagliari *et al.*, 2017)

Fluorescence microscopy

Midribs from each Arabidopsis line (healthy or CY-infected) were fixed in sugar gradient in order to preserve the structure of the tissues following freezing. Chopped midribs, were used for the fluorescence microscopy analysis following the protocol described by Pagliari *et al.*, (2016). For each midrib at least 5 sections were collected and fixed overnight in a solution containing 4% paraformaldehyde and 0.2% glutaraldehyde, diluted in Sorenson's phosphate buffer 0.2M, pH 7.2. Then, samples were placed in a graded sucrose series diluted in Sorenson's phosphate buffer 0.1M as follow: 0.7M for 4h at 4°C, 1.5M for 4h at 4°C and 2.3M overnight at 4°C. After the last sucrose solution, samples were infiltrated with Jung Tissue Freezing Medium embedding matrix (Leica Instruments GmbH, Nussloch, Germany), overnight at 4°C. Transversal slices 40 µm in thickness were obtained with a cryostat at -20°C (Jung CM 1500, Leica instruments, GmbH, Nussloch, Germany). Sections were collected, rinsed with PBS1x and coloured with DAPI staining (Thermo Fisher Scientific, Wilmington, DE, USA) diluted in PBS 300 nM, for 10 minutes, in the darkness and at room temperature. After the incubation, sections were rinsed in PBS and observed under a Zeiss Axio Observer Z1 microscope (Carl Zeiss GmbH, Munich, Germany) using an excitation filter at 405nm and emission at 435-490 nm. The exposure time was set up basing on the conditions used for the infected samples of both lines. For each condition, at least 4 non serial sections from 3 different biological replicates were observed. Unstained sections were observed with the same settings used for the stained ones, as controls. Images obtained from fluorescence microscopy were analysed using FIJI software (Schindelin *et al.*, 2012). Fluorescence intensity was evaluated adapting the protocol (Fontenete *et al.*, 2016) to the images of the infected samples, in order to create a mask suitable for the all the observed samples. The mask was created as follows: every fluorescence picture was acquired as two-channel-composite image, merging

```
// folder selection and list creation
dir = getDirectory("Select A folder");
fileList = getFileList(dir);
// output folder
output_dir = dir + File.separator + " output" + File.separator ;
File.makeDirectory(output_dir);
//activation of the batch mode
setBatchMode(true);
for (i = 0; i < lengthOf(fileList); i++) {
current_imagePath = dir+fileList[i];
if (!File.isDirectory(current_imagePath)){
// Split the pictures
open(current_imagePath);
getDimensions(width, height, channels, slices, frames);
if (channels > 1) run("Split Channels");
ch_nbr = nImages ;
for ( c = 1 ; c <= ch_nbr ; c++){
selectImage(c);
currentImage_name = getTitle();
saveAs("tiff", output_dir+currentImage_name);}
run("Close All");
}
```

Figure 5.1 ***Code used to split the composites****. In the code channel 1 is the brightfield, channel 2 is the fluorescence image. The code has been written in a macro, run in all the pictures.*

fluorescence and transmitted light brightfield images. Using the tools of FIJI the pictures have been divided in batch using the script reported in the Fig. 5.1. Each fluorescent picture was transformed in an 8-bit image. The background noise has been removed (radius= 80pixels) and the brightness and contrast has been adjusted using a minimum value of 50 (value able to exclude the autofluorescence). On the adjusted images a Laplacian of Gaussian filter (9x9 kernel) was applied, the resulting mask was transformed in a binary image (Fig. 5.2). On the mask, the analysis of the particles was performed. Data collected in table, were managed with RStudio software Version 1.1.456 (RStudio Team (2020), Boston, MA). On the count and on the area of fluorescent dots data, the normal distribution was checked with the Shapiro-Wilk test. Significant differences among the group means were determined with a two-way ANOVA and post-hoc comparisons between all groups were made with Tukey's test with $p<0.05$. Data were summarized with bar graphs. The codes used for the split of the composite pictures and for the particle analysis are reported in Fig. 5.1 and 5.2 respectively.

```
dir1 = getDirectory("Get Directory");
list = getFileList(dir1);
setBatchMode(true);
for (i = 0; i < list.length; i++) {
showProgress(i + 1, list.length);
open(dir1 + list[i]);
original_file_name = "C2-"+File.name;
duplicated_file_name=File.nameWithoutExtension+"-1";
run("Duplicate...", "title=&duplicated_file_name");
close("two")
setOption("ScaleConversions", true);
run("8-bit");
run("Subtract Background...", "rolling=80");
run("Brightness/Contrast...");
setMinAndMax(50, 255);
call("ij.ImagePlus.setDefault16bitRange", 8);
run("Apply LUT");
run("Convolve...", "text1=[0 0 0 -1 -1 -1 0 0 0\n0 -1 -1 -3 -3 -3 -1 -1 0\n0 -1 -3 -3 -1 -3 -3 -1 0\n-1 -3 -3 6 13 6 -3 -3 -1\n-1 -3 -1 13 24 13 -1 -3 -1\n-1 -3 -3 6 13 6 -3 -3 -1\n0 -1 -3 -3 -1 -3 -3 -1 0\n0 -1 -1 -3 -3 -3 -1 -1 0\n0 0 0 -1 -1 -1 0 0 0] normalize");
setOption("BlackBackground", true);
run("Make Binary");
run("Fill Holes");
run("Analyze Particles...", "display exclude summarize");
close();
```

Figure 5.2 ***Code used in the particles analysis****. A mask has been created following the Fontenete et al., 2016 code, modified by Bernardini. A Laplacian of Gaussian (LoG) filter 9x9 has been applied on the images.*

5.3 RESULT AND DISCUSSION

Plant phenotypes, symptom expression and phytoplasma detection

From a macroscopic point of view, the two Arabidopsis lines showed similar phenotypes (Fig. 5.3 A). Following phytoplasma infection, 26 days after the end of IAP, both wild type and mutant plants showed reduced growth, stunting, yellowish and chlorotic leaves, general decay. Leaf light transmittance, measured

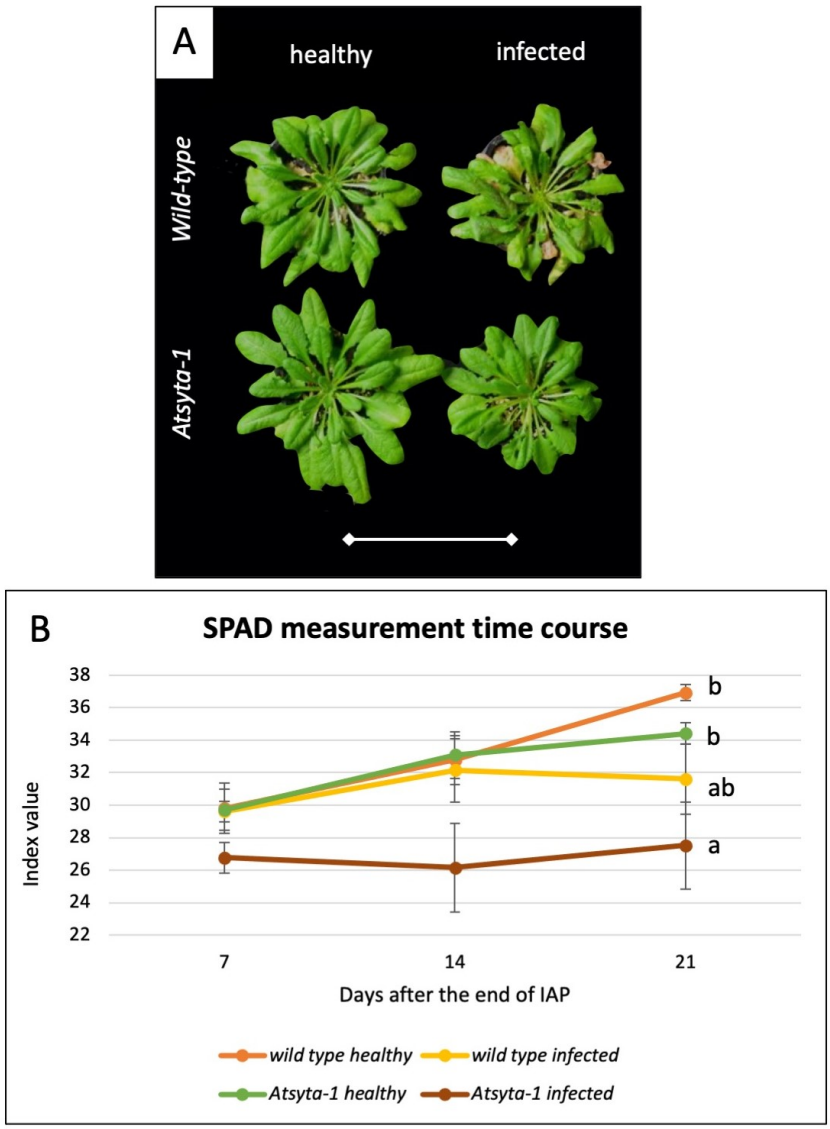

Figure 5.3 ***Biometric analyses on the wild type and Atsyta-1 mutant line healthy and infected.*** *The morphology of both the lines (**A**) appears similar among healthy samples belonging the two different lines and among the two conditions. Infected plants seem to be weakly smaller than healthy. SPAD measurement (**B**) shows a lower value of index for infected mutant line 21 after the end of IAP. The scatterplot express the means of at least 7 samples for each condition replicates ±SE of the mean. Different letters near the last point of the scatterplot express different mean according to two-way ANOVA followed by Tukey's test as post hoc test with $p<0.05$. Statistical analysis was carried out for the third measurement point.*

through SPAD index, which indirectly indicated chlorophyll content, decreased in both Arabidopsis lines following CY-phytoplasma infection (Fig. 5.3 B), but it is significantly lower only in *Atsyta-1* plants.

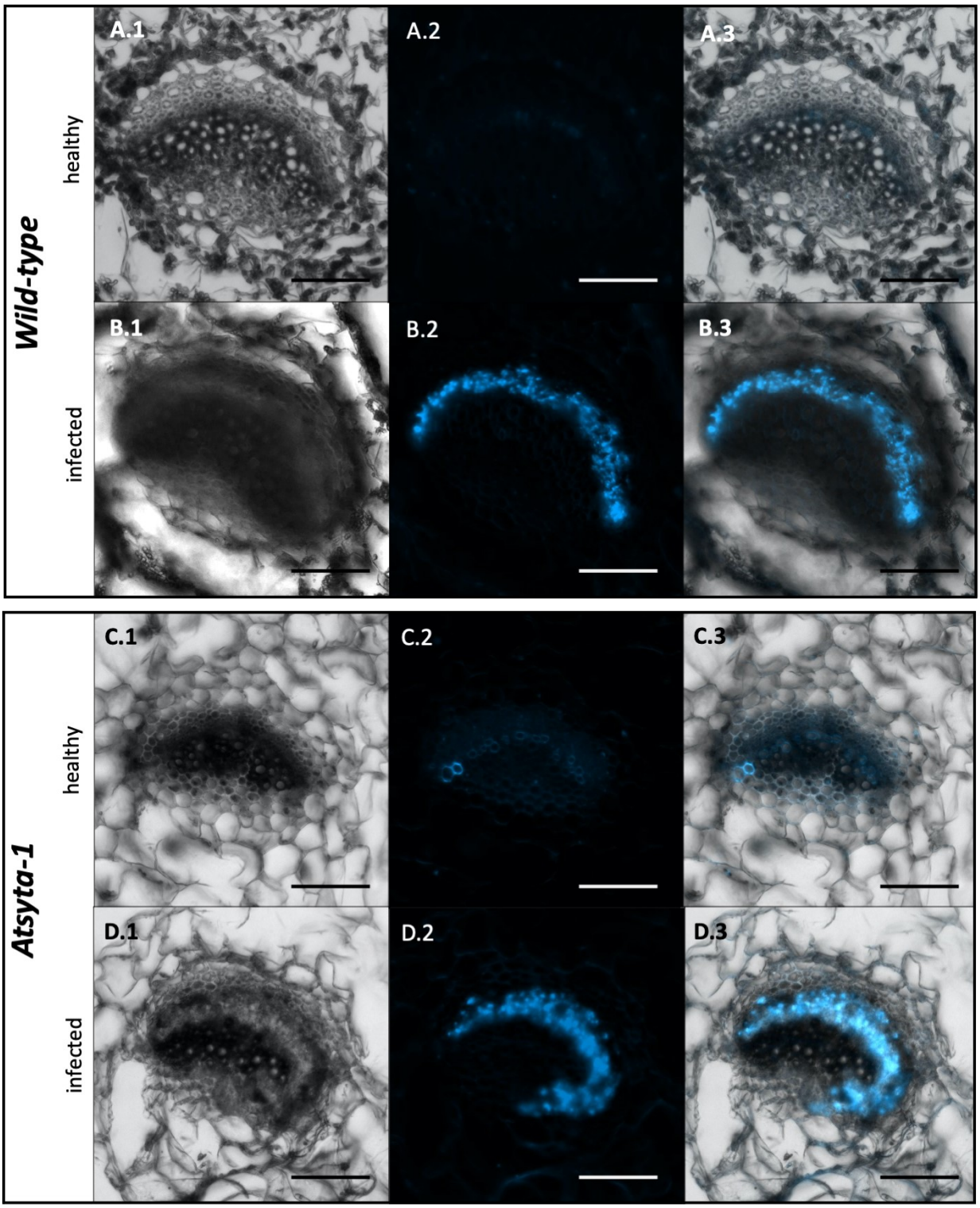

Figure 5.4 ***EFM representative micrograph of healthy (A and C) and infected (B and D) sections of wild type (A-B) and Atsyta-1 (C-D) plant****s. In the picture, column 1 is the brightfield picture, column 2 the DAPI stained sections observed with 5 seconds of exposure, while column 3 is the merge of the previous channels. In the stained pictures, the fluorescence is evident only in infected samples (C2 and D2) while a weak autofluorescence-related signal comes frome the healhty controls (A2 and C2). The signal, as shown in the merge (column 3) is localized to the phloem, habitat of the phytoplasmas. In the pictures, bars correspond to 100um.*

To assess phytoplasma presence molecular and fluorescence microscopy analyses were performed. both confirming phytoplasma presence in symptomatic Arabidopsis plants (Fig. 5.4 and 5.5). Phytoplasma titre and distribution in the vascular area did not differ in both infected lines (Fig. 5.5). DAPI fluorescence signal did not reveal substantial differences between infected samples belonging to the two different lines, as shown in the picture (Fig. 5.4). Imaging analysis revealed that the number of fluorescent dots and the distribution of fluorescent signal in the phloem tissue were similar in both wild type and *Atsyta-1* infected samples.

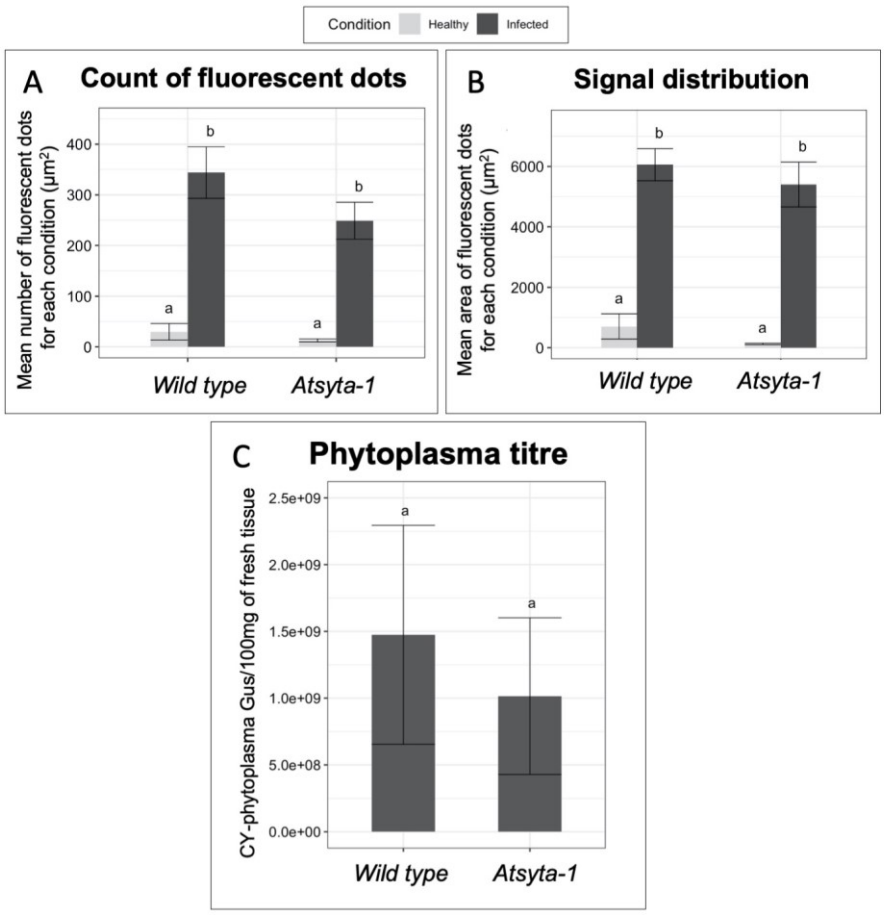

Figure 5.5 ***Fluorescence analysis imaging results and phytoplasma titre.*** *In thepictures: average count of fluorescent dots for each section (**A**) and average signal distribution of fluorescent dots for each section (**B**) in healthy and infected wild type and Atsyta-1 mutant line. Barplots indicate the mean value of at least 4 non serial sections from 3 different biological replicates have been analyzed ±SE of the mean. Phytoplasma titre in wild-type and Atsyta-1 mutant line (**C**): barplot indicates the mean value of phytoplasma titre ±SE of the mean. Different letter (a,b) over the bars indiate different mean according to the statistic analysis. Statistic analysis was performed using the Tukey HSD test as the post hoc test in a two-way ANOVA. Different letters (a, b) above the bars indicate significant differences, with P < 0.05. Error bars indicate the Standard Error of the Mean of 10 biological replicates for each condition.*

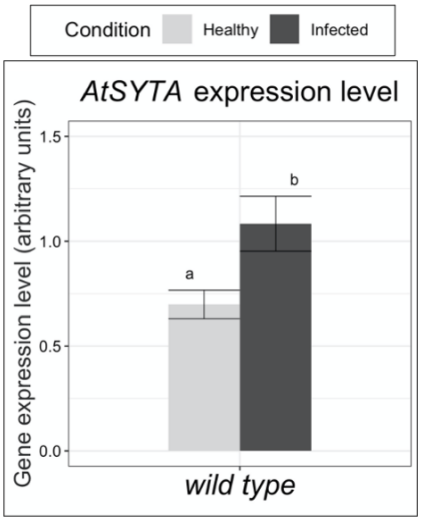

Figure 5.6 ***Expression level of the AtSYTA gene****. Expression values were normalized to the UBC9 transcript level, arbitrarily fixed at 100, then expressed as mean normalized expression ±SE (transcript abundance). Statistic analysis was performed using the Tukey HSD test as the post hoc test in a two-way ANOVA. Different letters (a, b) above the bars indicate significant differences, with P < 0.05. Error bars indicate the Standard Error of the Mean of 5 biological replicates for each condition.*

AtSYTA expression analysis in Arabidopsis following CY-infection

To assess whether AtSYTA could be subjected to modulation during phytoplasma infection, the expression analysis of *AtSYTA* was carried out and compared in healthy and CY-infected plants. Result showed that the gene was significantly overexpressed (ca. + 30%) in case of phytoplasma infection (Fig. 5.6).

Transmission electron microscopy investigations

Observations of healthy wild type samples showed normal sieve element and companion cell ultrastructure, which displayed regular shape and no signs of subcellular modifications (Figs. 5.7 A). In healthy plants, SER had a regular morphology: stacks were firmly pressed to the cell periphery (Figs. 5.7 B, D) and mostly oriented parallel to the plasma membrane. At the sieve plates, sieve pores had callose collars (Fig. 5.7 C) that did not occlude their lumen (Fig. 5.7 D).

Phytoplasmas lead to significant alteration of SER organization (Fig. 5.7). In fact, phytoplasma infection induced dramatic conformational alterations at SER level, which mainly relied on the increasing of the number of ER stacks, the slackening and the swelling of reticular cisternae (Figs. 5.7 G, I, J). Phytoplasmas were observed to adhere to the deformed ER membranes through a protrusion structure (Figs. 5.7). Endoplasmic reticulum in companion cells reveal any structural abnormality as demonstrated in the Fig. 5.7, suggesting a site-specific response of the organelle to the infection.

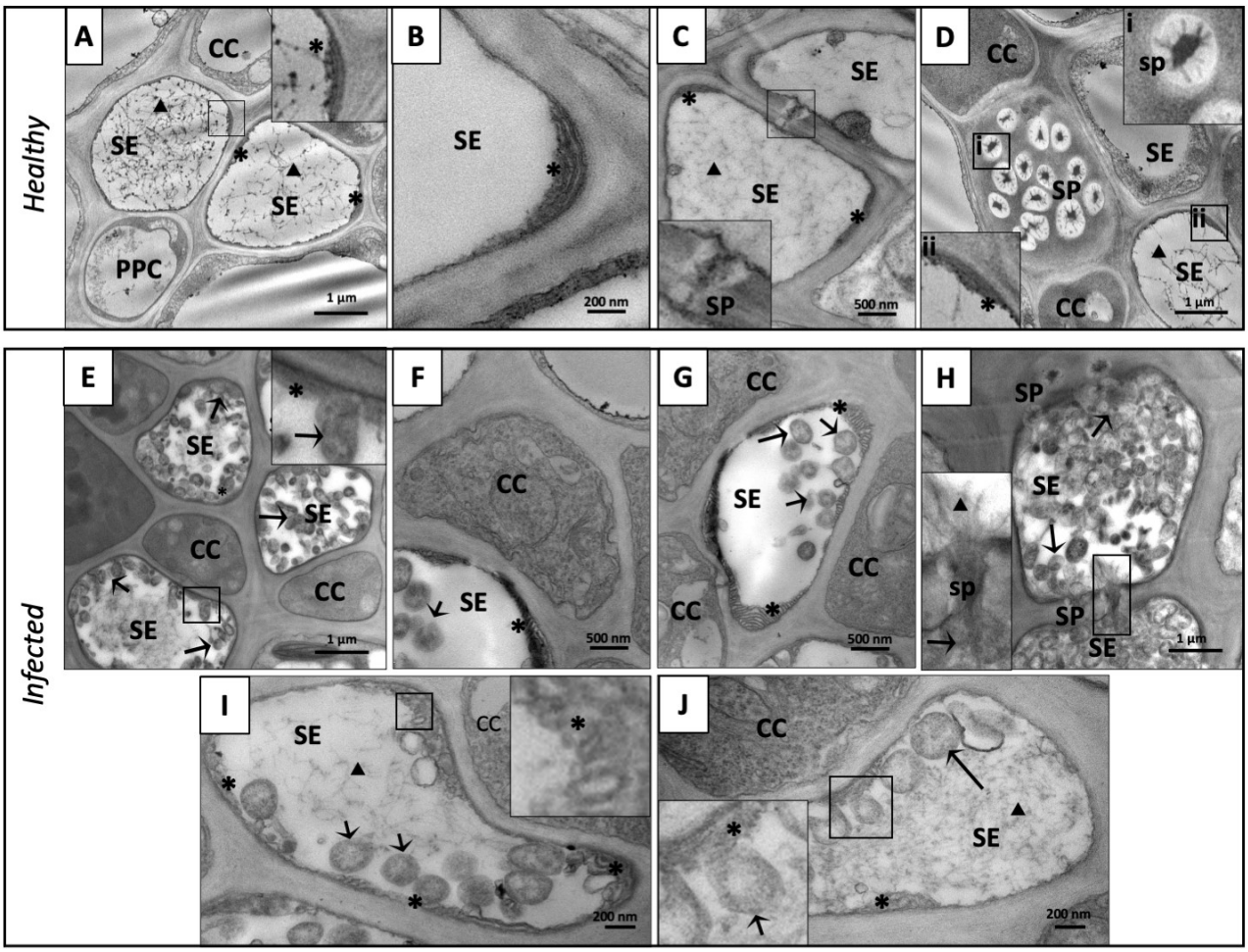

Figure 5.7 ***Representative TEM micrographs of the sieve elements of healthy and CY-infected Arabidopsis lines (A-J).*** *Cross-sections of midribs from healthy (**A-D**) and infected (**E-J**) wild type Arabidopsis leaves. In the pictures the phloem tissue organization in healthy (**A**) and infected (**E**) plants is shown. Healthy plant reticula are shown in picture **B**; sieve plates in healthy plants show a collare of callose around the sieve pore (**C-D**). In infected plants, phytoplasmas are uniformely spreaded in the sieve element lumina (**E-J**). Reticula of infected plants sometimes appear damaged (**I-J**), while other times are similar to the control condition (**F-G**). Infected sieve plates have the collar of callose as in the healthy plants (**H**). In the pictures SE=sieve element, CC= companion cell, PPC=phloem parenchyma cell, SP=sieve plates, sp=sieve pore, triangles= phloem protein, asterisk=sieve element reticulum, arrows=phytoplasmas. Bar length is indicated in each pictures.*

In healthy *Atsyta-1* plants, sieve-element structure was preserved and similar to that observed in wild-type samples (Figs. 5.8). In some cases, often when stricly associated to mitichondria (Fig. 5.8 C), SER showed modified morphology, showing enlarged and deformed cisternae (Fig. 5.8).

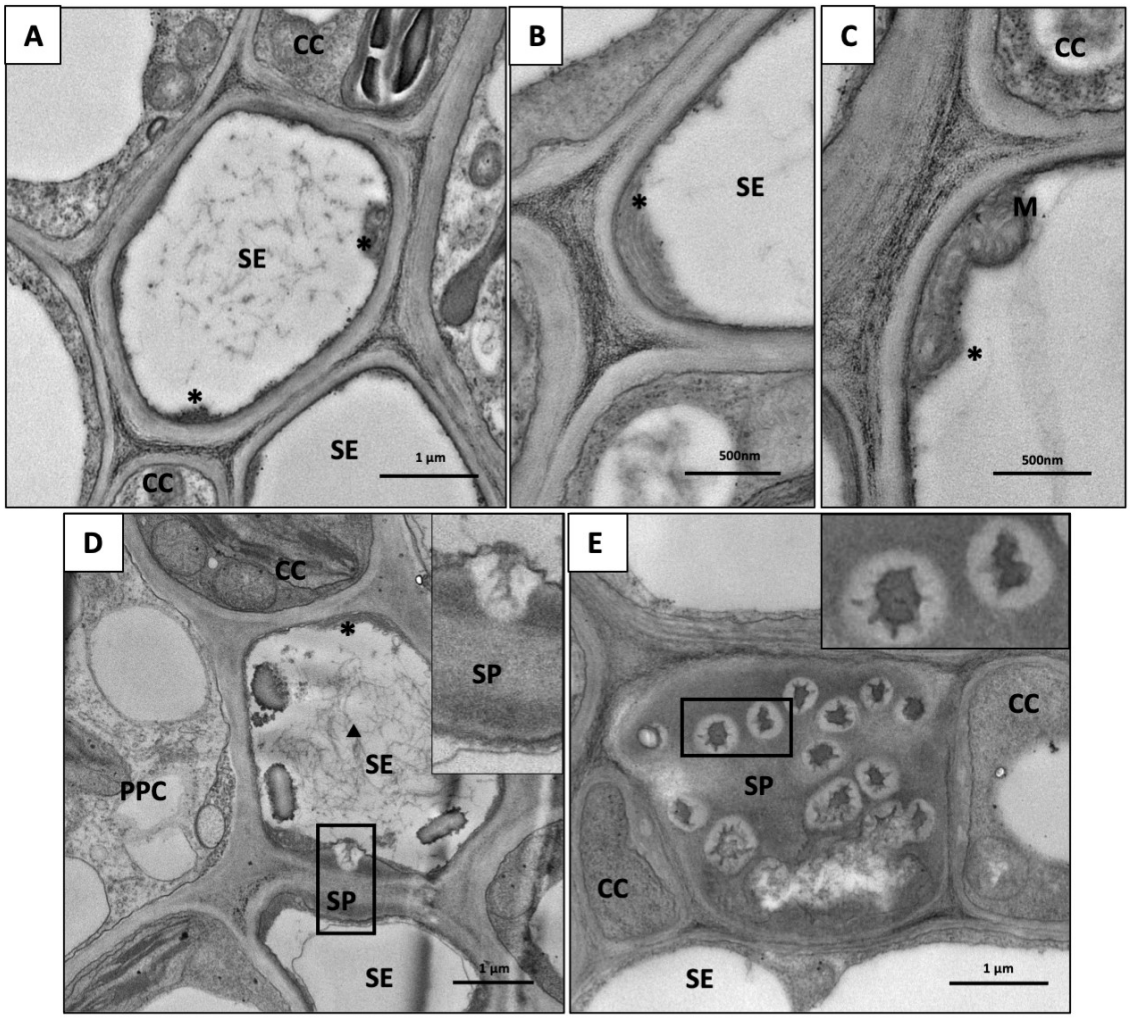

Figure 5.8 ***Representative TEM micrographs of the sieve elements of healthy Atsyta-1 line (A-E).*** *In the pictures the phloem tissue organization in healthy (**A**) mutant line is shown. Healthy plant reticula are shown in picture (**B**); sieve element reticula appear similar to wild-type condition (**B**) when not associated with another organelle (**C**); sieve plates in healthy plants show a collare of callose around the sieve pore (**D-E**). In the pictures SE=sieve element, CC= companion cell, PPC=phloem parenchyma cell, SP=sieve plates, sp=sieve pore, triangles= phloem protein, asterisk=sieve element reticulum, M=mitochondria. Bar length is indicated in each pictures.*

In infected *Atsyta-1* plants numerous phytoplasmas were found inside the sieve elements, making sometimes difficult to well distinguish the sieve element substructures (Fig. 5.9). Nevertheless, the connection of phytoplasmas to SER seemed to be maintained in *Atsyta-1* line. SER appeared deformed and with cisternae detached each from the others, as observed in infected wild-type samples. Interstingly, in *Atsyta-1* the structure jointing phytoplasmas with SER was apparently absent or, at least, not well defined in shape (Fig. 5.10).

Sieve-plate morphology seemed affected in some cases in infected mutant line, but the high level of phytoplasma cells appressed to the sieve pores made difficult a clear evaluation of sieve plate ultrastructure.

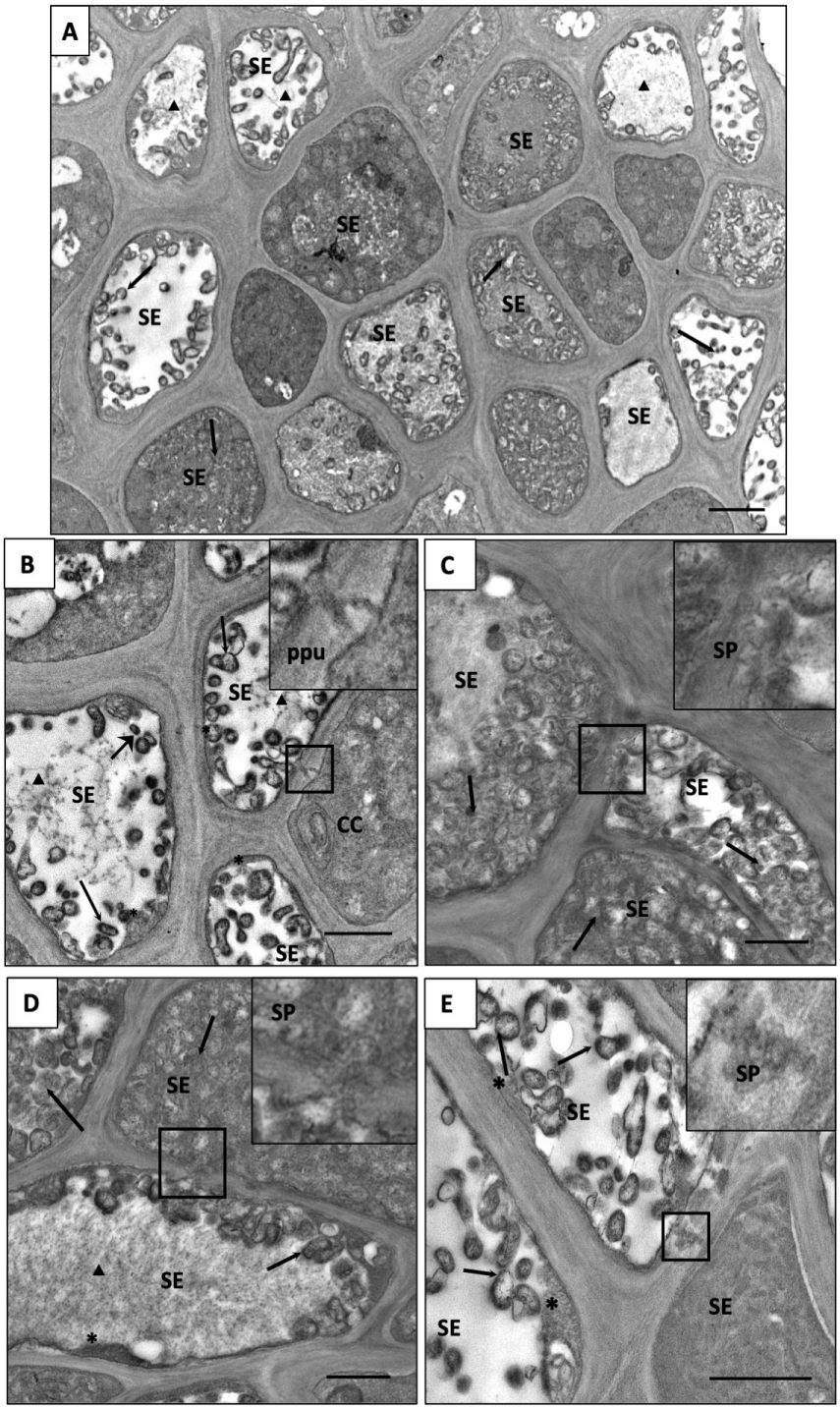

Figure 5.9 ***Representative TEM micrographs of infected Atsyta-1 line (A-E).*** *In the pictures spread of phytoplasmas in the phloem tissue is shown (**A**). The colonized cells show a regular PPU (**B**), while sieve plates seem damaged (**C-E**) In the pictures SE=sieve element, CC= companion cell, PPC=phloem parenchyma cell, ppu= pore plasmodesmata unit, SP=sieve plates, sp=sieve pore, triangles= phloem protein, asterisk=sieve element reticulum, arrows=phytoplasmas. Bar length is indicated in each pictures.*

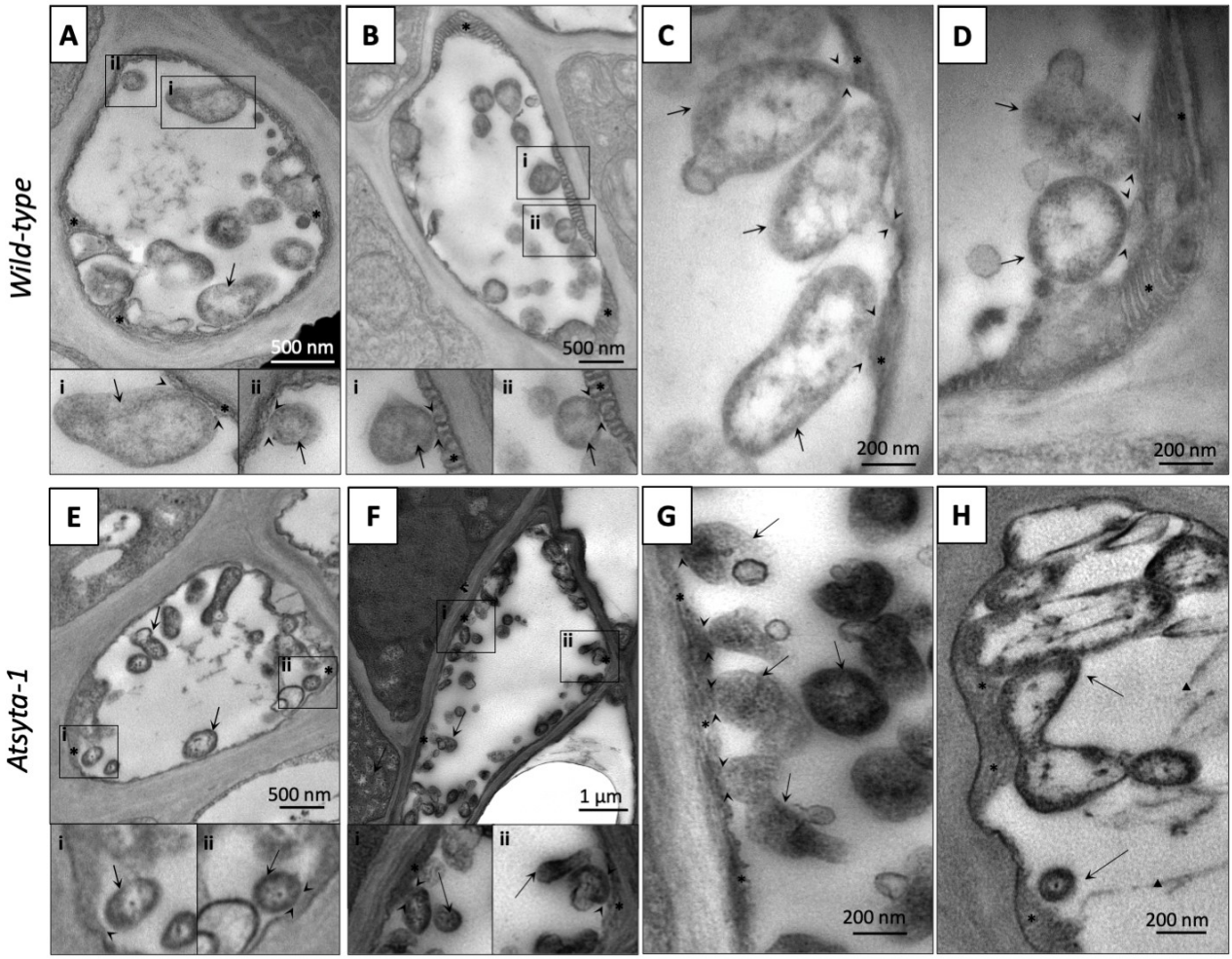

Figure 5.10 ***Representative TEM micrographs of sieve element endoplasmic reticula in infected wild type (A-D) amd Atsyta-1 line (E-H).*** *In the wild type plants, endoplasmic reticulum has a shape similar to the healthy samples: cisternae are visible and the shape clear. Phytoplasma attachment is in correspondence of reticula, where sometimes a tubular connction structure is visible (**A-D**). In mutant line, reticula are highly damaged: phytoplasmas seem to interact with the reticula, but the tubular structure is not visible (**E-H**). In the picture: arrows=phytoplasmas, ticks= contact sites with the reticula, triangles=phloem protein, asterisks=sieve element reticula.*

5.4 DISCUSSION AND FUTURE PERSPECTIVES

The role(s) of SYT proteins during phytoplasma infection is totally unexplored. We will try to perform some speculations, basing also on results obtained about other pathosystems.

From a macroscopic point of view, the lack of SYTA in Arabidopsis did not affect plant morphology, as previously described (Lewis and Lazarowitz, 2010). Even in case of infection, wild type and mutant plants

showed equal phenotype. Nevertheless, leaf light transmittance resulted significantly decreased in the mutant line following CY-phytoplasma infection. This confirms numerous studies reporting that phytoplasmas affect the photosynthetic machinery in the host plants (Buoso *et al.*, 2019 and literature within). Moreover, it has been suggested that AtSYTA might have a role in lipid homeostasis and transfer from ER to the diverse organelles (Michaud and Jouhet, 2019). As lipids have specific roles in biogenesis and maintenance of thylakoid membranes and photosynthesis (Kobayashi and Wada, 2016), it is possible that the lack of *AtSYTA* could affect lipid metabolism in the chloroplasts, contributing to the impairment of the chloroplast functionality, also imposed by phytoplasma infection (Janik *et al.*, 2018).

The fact that the expression level of *AtSYTA-1* significantly increases following phytoplasma infection, suggests other interesting speculations, worthy to be investigate in the next future.

As said below, it was reported that AtSYTA could be involved in plant-cell endocytosis processes, which are related to the defence responses (Romanenko *et al.*, 2002). Regarding animal endobacteria, it has been demonstrated that a SYT protein (SYT XI), localized into recycling endosomes and lysosomes, has antimicrobial activity, showing a direct effect on the establishment of the immune response *in vitro* (Duque *et al.*, 2013), and that SYT XI knockdown ensued in enhanced bacterial survival. We found inaltered level on phytoplasma genome units in both infected lines: this gave information about pathogen titre but not about its viability/activity inside the SEs (Pacifico *et al.*, 2015), so the evaluation of some phytoplasma transcripts in both lines should be helpful to have insight about a possible role of SYTA during phytoplasma infection.

From a structural point of view, samples from mutant line (both healthy and CY-infected) often showed SER with altered morphology, while in the wild-type line, SER modifications were present only following infection (Buxa *et al.*, 2015; Pagliari *et al.*, 2016). CY phytoplasmas appeared connected with SE also in *Atsyta-1* plants, but the ultrastructure of the connections appeared affected.

SYTA-1 was indicated as essential for maintaining the polygonal network of the endoplasmic reticulum and the stability/dynamics of proteins functioning as tethers on the ER-PM contact sites. As it is reported for many ER-PM tethering proteins (Eisenberg- Bord *et al.*, 2016), overexpression of SYT genes (as observed in Arabidopsis following phytoplasma infection) causes a drastic expansion of ER-PM contact sites (Lopez *et al.*, 2020). As said below, in tomato and Arabidopsis plants infected with phytoplasmas SER showed deformation of the stacks, which resulted in expansion of the cisternae, development of lobes and fragmentation into vesicles (Buxa *et al.*, 2016; Musetti *et al.*, 2016; Pagliari *et al.*, 2016). All these ultrastructural changes support an increased regulation of protein and lipid trafficking among the different subcellular compartments of the secretory and endocytic pathway in the infected SEs. In this context, the increasing of *AtSYTA-1* expression level could be related to the increased endocytic activity in host cell under phytoplasma attack and/or to the adaptation of PM and SER to the stress imposed by phytoplasmas, as demonstrated in Arabidopsis following infection by *Golovinomyces orontii* (Kim *et al.*, 2016).

On the other hand, in many plant-virus interactions, Arabidopsis SYTA showed great importance in the movement protein (MP)-mediated trafficking of viral genomes through plasmodesmata, favouring cell-to-cell viral invasion (Lewis and Lazarowitz, 2010). *SYTA-1* knockdown provoked the inhibition of the cell-to-cell movement proteins and the consequent delay in viral systemic infection, as reported for Cabbage leaf curl virus (CaLCuV) CaLCuV and Tobacco mosaic virus (TMV) (Lewis and Lazarowitz, 2010) and for Turnip Mosaic Virus (TuMV) and the Turnip Vein Clearing Virus (TVCV) (Uchiyama 2014; Levy 2015).

Phytoplasmas do not possess genes encoding movement proteins (Kube *et al.*, 2012). Their movement inside the sieve elements and the spread along the phloem through the sieve pores is likely mediated by plant actin filaments (Boonrod *et al.*, 2012; Buxa *et al.*, 2015; Musetti *et al.*, 2016). Even if the possibility of SYT proteins to interact with plant actin has been reported at plasmodesma level to regulate virus movement (Levy *et al.*, 2015; Yuan *et al.*, 2018), a similar interaction in the mature sieve pores, to favour phytoplasma spread through the sieve elements, appear unlikely, given the absence of desmotubular structure in the latter (Kalmbach and Helariutta, 2019).

5.5 CONCLUDING REMARKS

With this preliminary report, we give indication, for the first time, about a possible role of synaptotagmin in phytoplasma infection. Our report highlighted some interesting issues:

- Synaptotagmin A gene is significantly up-regulated following phytoplasma infection in Arabidopsis.
- The absence of Synaptotagmin A could affect the structure of the SER, in healthy sieve elements of Arabidopsis, in particular in case of association with the mitochondria.
- Synaptotagmin A could interfere with actin and movement capability of phytoplasmas inside the sieve element, maybe regulating the passage from a stationary to a motile phase. This issue is worthy to be deeply investigated.

Further investigation about the regulation of other proteins of endoplasmic-reticulum net (i.e. VAP27 and NET3C) are requested to have a more comprehensive picture of the relationship occurring between phytoplasma SER.

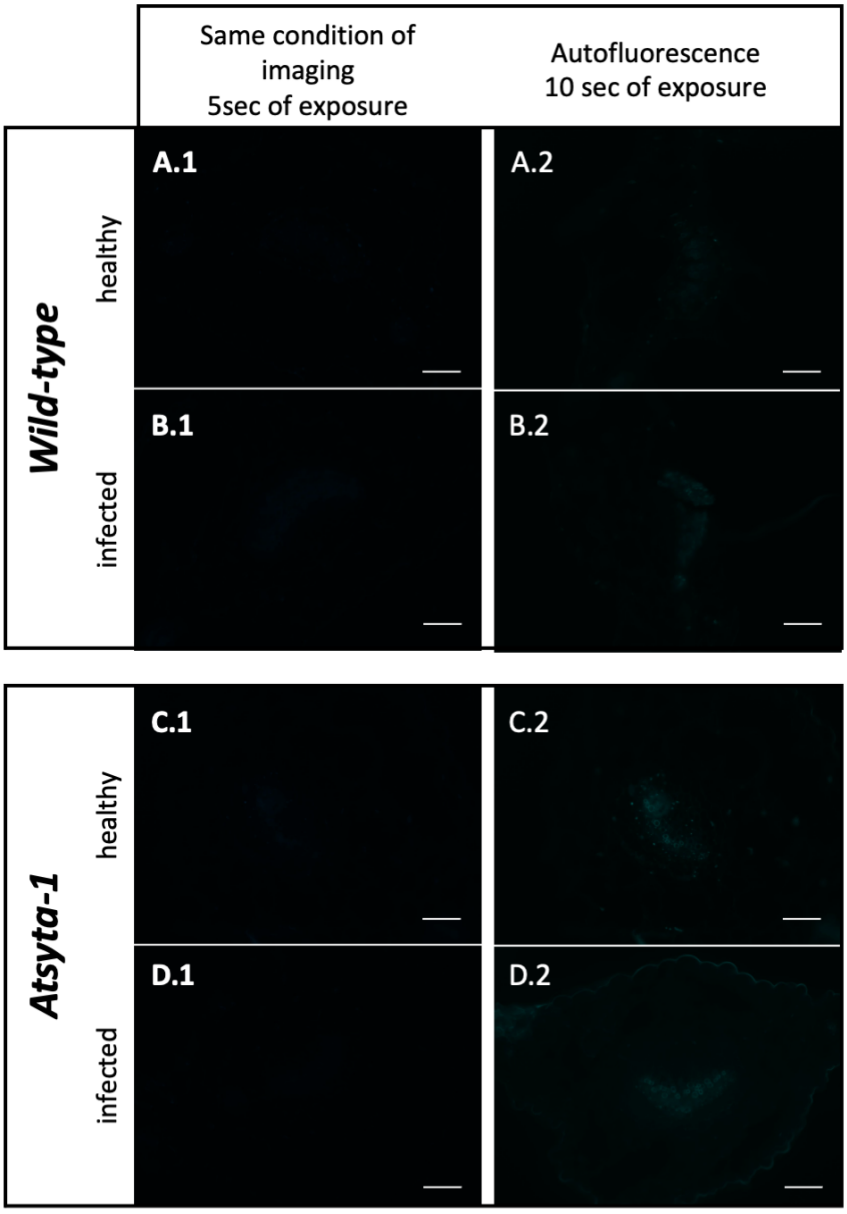

Figure 5.11 ***EFM unstained sections micrograph of healthy (A) and infected (B) wild type ad healthy (C) and infected (D) Atsyta-1 mutant line****. The pictures were collected with an exposure time equal (column 1) to the one used for the staining section, 5 seconds, or with an exposure time equal to the autofluorescence detection (column 2), 10 seconds. Only a weak signal were detected at the both conditions. Bars=100 um.*

5.6 REFERENCES

Baluška, F., Hlavacka, A., Šamaj, J., Palme, K., Robinson, D.G., Matoh, T., McCurdy, D.W., Menzel, D., Volkmann, D., 2002. F-actin-dependent endocytosis of cell wall pectins in meristematic root cells. Insights from brefeldin A-induced compartments. Plant Physiol. 130, 422–431.

Bernardini, C., Pagliari, L., De Rosa, V., Almeida-Trapp, M., Santi, S., Martini, M., Buoso, S., Loschi, A., Loi, N., Chiesa, F., Mithöfer, A., van Bel, A.J.E., Musetti, R., 2020. Pre-symptomatic modified phytohormone profile is associated with lower phytoplasma titres in an Arabidopsis seor1ko line. Sci. Rep. 10, 14770. https://doi.org/10.1038/s41598-020-71660-0

Boonrod, K., Munteanu, B., Jarausch, B., Jarausch, W., Krczal, G., 2012. An Immunodominant Membrane Protein (Imp) of ' *Candidatus* Phytoplasma mali' Binds to Plant Actin. Mol. Plant-Microbe Interactions® 25, 889–895. https://doi.org/10.1094/MPMI-11-11-0303

Buoso, S., Pagliari, L., Musetti, R., Martini, M., Marroni, F., Schmidt, W., Santi, S., 2019. 'Candidatus Phytoplasma solani' interferes with the distribution and uptake of iron in tomato. BMC Genomics 20, 703. https://doi.org/10.1186/s12864-019-6062-x

Buxa, S., Pagliari, L., Musetti, R., 2016. Epifluorescence microscopy imaging of phytoplasmas in embedded leaf tissues using DAPI and SYTO13 fluorochromes. Microscopie 25, 49–56.

Buxa, S.V., Degola, F., Polizzotto, R., De Marco, F., Loschi, A., Kogel, K.-H., di Toppi, L.S., van Bel, A.J.E., Musetti, R., 2015. Phytoplasma infection in tomato is associated with re-organization of plasma membrane, ER stacks, and actin filaments in sieve elements. Front. Plant Sci. 6. https://doi.org/10.3389/fpls.2015.00650

Collado, J., Kalemanov, M., Campelo, F., Bourgoint, C., Thomas, F., Loewith, R., Martínez-Sánchez, A., Baumeister, W., Stefan, C.J., Fernández-Busnadiego, R., 2019. Tricalbin-mediated contact sites control ER curvature to maintain plasma membrane integrity. Dev. Cell 51, 476–487.

Doyle, JJ, Doyle, JL, 1990. DNA extraction from Arabidopsis. Focus 12, 13–15.

Duque, G.A., Fukuda, M., Descoteaux, A., 2013. Synaptotagmin XI regulates phagocytosis and cytokine secretion in macrophages. J. Immunol. 190, 1737–1745.

Eisenberg-Bord, M., Shai, N., Schuldiner, M., Bohnert, M., 2016. A tether is a tether is a tether: tethering at membrane contact sites. Dev. Cell 39, 395–409.

Fontenete, S., Carvalho, D., Lourenço, A., Guimarães, N., Madureira, P., Figueiredo, C., Azevedo, N.F., 2016. FISHji: New ImageJ macros for the quantification of fluorescence in epifluorescence images. Biochem. Eng. J. 112, 61–69. https://doi.org/10.1016/j.bej.2016.04.001

Giordano, F., Saheki, Y., Idevall-Hagren, O., Colombo, S.F., Pirruccello, M., Milosevic, I., Gracheva, E.O., Bagriantsev, S.N., Borgese, N., De Camilli, P., 2013. PI(4,5)P2-Dependent and Ca2+-Regulated ER-PM Interactions Mediated by the Extended Synaptotagmins. Cell 153, 1494–1509. https://doi.org/10.1016/j.cell.2013.05.026

Janik, K., Mittelberger, C., Moser, M., 2018. Lights Out. The Chloroplast Under Attack During Phytoplasma Infection? Annu. Plant Rev. Online 399–426.

Kalmbach, L., Helariutta, Y., 2019. Sieve Plate Pores in the Phloem and the Unknowns of Their Formation. Plants 8, 25. https://doi.org/10.3390/plants8020025

Kim, H., Kwon, H., Kim, S., Kim, M.K., Botella, M.A., Yun, H.S., Kwon, C., 2016. Synaptotagmin 1 Negatively Controls the Two Distinct Immune Secretory Pathways to Powdery Mildew Fungi in Arabidopsis. Plant Cell Physiol. 57, 1133–1141. https://doi.org/10.1093/pcp/pcw061

Kobayashi, K., Wada, H., 2016. Role of lipids in chloroplast biogenesis, in: Lipids in Plant and Algae Development. Springer, pp. 103–125.

Levy, A., Zheng, J.Y., Lazarowitz, S.G., 2015. Synaptotagmin SYTA Forms ER-Plasma Membrane Junctions that Are Recruited to Plasmodesmata for Plant Virus Movement. Curr. Biol. 25, 2018–2025. https://doi.org/10.1016/j.cub.2015.06.015

Lewis, J.D., Lazarowitz, S.G., 2010. Arabidopsis synaptotagmin SYTA regulates endocytosis and virus movement protein cell-to-cell transport. Proc. Natl. Acad. Sci. 107, 2491–2496. https://doi.org/10.1073/pnas.0909080107

Manford, A.G., Stefan, C.J., Yuan, H.L., MacGurn, J.A., Emr, S.D., 2012. ER-to-plasma membrane tethering proteins regulate cell signaling and ER morphology. Dev. Cell 23, 1129–1140.

Martini, M., Musetti, R., Grisan, S., Polizzotto, R., Borselli, S., Pavan, F., Osler, R., 2009. DNA-Dependent Detection of the Grapevine Fungal Endophytes *Aureobasidium pullulans* and *Epicoccum nigrum*. Plant Dis. 93, 993–998. https://doi.org/10.1094/PDIS-93-10-0993

Michaud, M., Jouhet, J., 2019. Lipid trafficking at membrane contact sites during plant development and stress response. Front. Plant Sci. 10, 2.

Musetti, R., Pagliari, L., Buxa, S.V., Degola, F., De Marco, F., Loschi, A., Kogel, K.-H., van Bel, A.J., 2016. OHMS**: phytoplasmas dictate changes in sieve-element ultrastructure to accommodate their requirements for nutrition, multiplication and translocation. Plant Signal. Behav. 11, e1138191.

Pacifico, D., Galetto, L., Rashidi, M., Abbà, S., Palmano, S., Firrao, G., Bosco, D., Marzachì, C., 2015. Decreasing Global Transcript Levels over Time Suggest that Phytoplasma Cells Enter Stationary Phase during Plant and Insect Colonization. Appl. Environ. Microbiol. 81, 2591–2602. https://doi.org/10.1128/AEM.03096-14

Pagliari, L., Martini, M., Loschi, A., Musetti, R., 2016. Looking inside phytoplasma-infected sieve elements: A combined microscopy approach using Arabidopsis thaliana as a model plant. Micron 89, 87–97. https://doi.org/10.1016/j.micron.2016.07.007

Pérez-Sancho, J., Tilsner, J., Samuels, A.L., Botella, M.A., Bayer, E.M., Rosado, A., 2016. Stitching Organelles: Organization and Function of Specialized Membrane Contact Sites in Plants. Trends Cell Biol. 26, 705–717. https://doi.org/10.1016/j.tcb.2016.05.007

Romanenko, A., 2002. Endocytosis of exopolysaccharides of the potato ring rot causal agent by host-plant cells. Presented at the Doklady Biological Sciences, Springer, pp. 451–453.

Ruiz-Lopez, N., Perez-Sancho, J., del Valle, A.E., Haslam, R.P., Vanneste, S., Catala, R., Perea-Resa, C., Van Damme, D., Garcia-Hernandez, S., Albert, A., 2020. Synaptotagmins Maintain Diacylglycerol Homeostasis at Endoplasmic Reticulum-Plasma Membrane Contact Sites during Abiotic Stress. bioRxiv.

Saheki, Y., Bian, X., Schauder, C.M., Sawaki, Y., Surma, M.A., Klose, C., Pincet, F., Reinisch, K.M., De Camilli, P., 2016. Control of plasma membrane lipid homeostasis by the extended synaptotagmins. Nat. Cell Biol. 18, 504–515.

Schapire, A.L., Voigt, B., Jasik, J., Rosado, A., Lopez-Cobollo, R., Menzel, D., Salinas, J., Mancuso, S., Valpuesta, V., Baluska, F., Botella, M.A., 2008. *Arabidopsis* Synaptotagmin 1 Is Required for the Maintenance of Plasma Membrane Integrity and Cell Viability. Plant Cell 20, 3374–3388. https://doi.org/10.1105/tpc.108.063859

Schauder, C.M., Wu, X., Saheki, Y., Narayanaswamy, P., Torta, F., Wenk, M.R., De Camilli, P., Reinisch, K.M., 2014. Structure of a lipid-bound extended synaptotagmin indicates a role in lipid transfer. Nature 510, 552–555.

Uchiyama, A., Shimada-Beltran, H., Levy, A., Zheng, J.Y., Javia, P.A., Lazarowitz, S.G., 2014. The Arabidopsis synaptotagmin SYTA regulates the cell-to-cell movement of diverse plant viruses. Front. Plant Sci. 5. https://doi.org/10.3389/fpls.2014.00584

Yuan, C., Lazarowitz, S.G., Citovsky, V., 2018. The Plasmodesmal Localization Signal of TMV MP Is Recognized by Plant Synaptotagmin SYTA. mBio 9, e01314-18, /mbio/9/4/mBio.01314-18.atom. https://doi.org/10.1128/mBio.01314-18

6. APPENDIX

During the time that I spent in the Levy's lab and in the Vincent's lab in the Citrus Research and Educational Center, in Lake Alfred, Florida, we performed the quantification of the labelled carbon in wild type and callose mutant line. Part of the data of this experiment has been already described in the chapter 4.2. Here we provide further data analysis on that results, underling the potential of ^{14}C analysis. In the following chapter we will show the methodology that we applied to analyze the 14C still incorporated in the labelled leaves.

6.1 THE EXPERIMENT

Using the same *Arabidopsis* plants analyzed in the work in chapter 4.2, we performed a quantification of the amount of ^{14}C incorporated by healthy wild type and mutant lines after allowing the plant to acquire it through photosynthesis. By "^{14}C incorporated," we mean the amount of radioactive carbon still present inside the plant at a certain time. We standardized the data (counts/minute) by declaring the background noise before the ^{14}C infusion to have the value of 0 and the count at the end of the infusion to have the value of 1 (i.e. 100%). Using the standardized counts of x-rays detected from the ^{14}C-infused plants, we obtained equations to calculate the amount of carbon incorporated into the plants in the 24 hours before and after the labeling period. The goal of this analysis was to understand a possible relationship

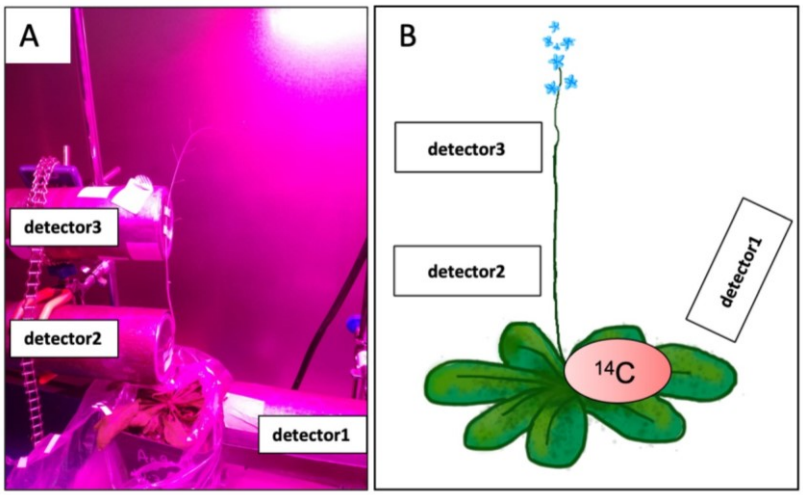

Figure 6.1 ***Real (A) and schematic representation (B) of the position of the x-ray detectors during the experiment****. Detector 1 measured the normal background signal from the rosette. Detectors 2 and 3 measured the mass flow of ^{14}C through the stem phloem (see chapter 4.2).*

```
#fitting the function on the plot
xsq<- x^2
xcub<- x^3
xquar<- x^4
xquin<-x^5
plot(y~x)
fit1<- lm(y~x)
anova(fit1)
fit2<- lm(y~x+xsq)
anova(fit2)
xv<- seq(min(x), max(x), 0.1)
yv<-predict(fit2,
list(x=xv,xsq=xv^2))
lines(xv,yv, col="green")
summary(fit2)

fit3<- lm(y~x+xsq+xcub)
anova(fit3)
xv<- seq(min(x), max(x), 0.01)
yv<-predict(fit3, list(x=xv,
xsq=xv^2, xcub=xv^3))
lines(xv,yv, col="red")
summary(fit3)
plot(fit3,which=1)
plot(fit3,which=2)

fit4<- lm(y~x+xsq+xcub+xquar)
anova(fit4)
xv<- seq(min(x), max(x), 0.001)
yv<-predict(fit3, list(x=xv,
xsq=xv^2, xcub=xv^3, xquar=x^4))
lines(xv,yv, col="blue")
summary(fit4)
plot(fit4,which=1)
plot(fit4,which=2)

fit5<-
lm(y~x+xsq+xcub+xquar+xquin)
anova(fit5)
summary(fit5)
xv<-seq(min(x), max(x), 0.0001)
yv<- predict(fit5,
list(x=xv,xsq=xv^2,xcub=xv^3,xqua
r=xv^4,xquin=xv^5))
plot(x,y)
lines(xv,yv, col="green")
plot(x,y)
model<-lm(y~x+I(x^2))
model2<-lm(y~poly(x, degree =
5,raw=T))
summary(model2)
```

Figure 6.2 ***Code used for the first method.*** *In the first method a plynomial function has been fitted on the data. The parameters were obtained with the reported code.*

between mutation and exportation from rosettes and understanding how much of the incorporated carbon is lost during a known range of time.

Plants were grown and a ^{14}C label was infused according to procedures previously explained in chapter 3.2. For each plant, two detectors were placed along the floral stem, and one detector was placed to catch the background signal from the rosette (Figure 4). Every detector measured a count of x-rays released from the phloem tissue every minute. For the analysis of the amount of ^{14}C incorporated, we subtracted the readings of the detectors placed on the rosette. Data were handled with RStudio (RStudio Team (2020). RStudio: Integrated Development for R. RStudio, PBC, Boston, MA). The data of the signal from the rosette were standardized as follows: it was given a value of 1 (100%) at the peak of the curve that corresponds to the maximum infusion of ^{14}C and a value of 0 at the background noise level, measured as the mean of the counts before the infusion of the radioactive source. This standardization procedure is illustrated in the code presented here (Figure 6.3).

```
#normalization of data channel_1
CH1= detector.readings %>%
filter(Channel==1)
CH1st<- CH1 %>%
mutate(baseline=mean(count[inoculation.start
.time<(begin_injection)]),label=(count-
baseline)/((mean(count[inoculation.start.tim
e>start_peak&inoculation.start.time<end_peak
]))-baseline))
y=C2$label x=C2$inoculation.start.time
plot(y~x)
```

Figure 6.3 ***Code used for the standardization process****. In the code begin injection=time in which the plants have been labelled, while end peak corresponds to the flushing of the labelled carbon*

First method

In order to calculate the y-value, once the plot of the points was obtained (Figure 6.2), a polynomial

function was fitted to the data, according to previously published code (Vincent *et al.*, 2019) adapted by Bernardini. All the polynomials from the second to the fifth degree were tested and fitted to the plot (Fig.6.4). The best fit for the dataset was the polynomial function to the fifth degree, which is written as:

$$y = a + bx + cx^2 + dx^3 + ex^4 + fx^5$$

The coefficients from a to f were provided as summary results of the fitting process by the software itself. The function was used to calculate the value of y at values of x with Microsoft Excel software (version 16.42, 20101102). As x, a late time in the infusion period was chosen, close to the end of the experiment: 24, 36 and 48 hours past the peak. For each biological replicate, we calculated the value of the radioactive carbon still incorporated in the plant. The results of the calculation were handled with RStudio, and a two-way ANOVA (considering mutation and time as factors) with a post-hoc T-test with a significance level at $P<0.05$ was performed on the means.

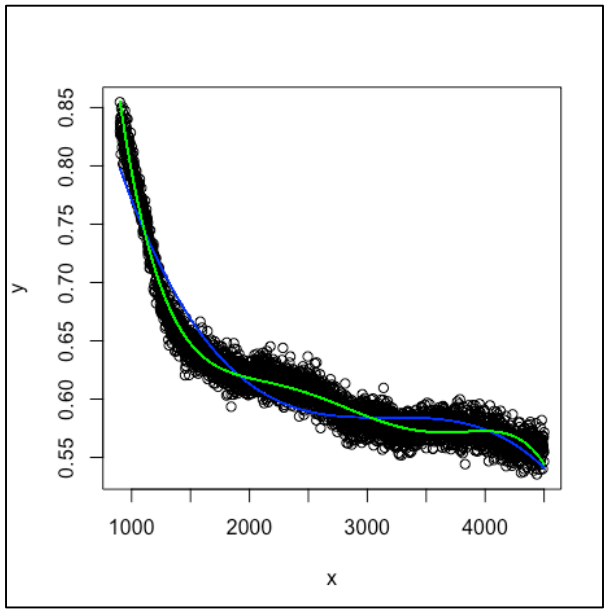

Figure 6.4 ***Plot of normalized data on which the function was fitted.*** *The x-axis represents the time over which the ^{14}C infusion elapsed. The y-axis represents the standardized counts, which vary from a maximum of 1 to a minimum of 0.*

Second method

Due to the low stability of the function in the first part of the fitting (for x <24hours), we proposed a second method to calculate the value of y at a certain x in the first part of the fitting. We choose as x three values at the beginning of the fitting: 8, 16 and 24 hours past the peak, which represents the end of infusion. For each selected time, we calculated the mean value of y for every x value in the range of 15 minutes before and 15 minutes after the selected x (for example, every x in the 15 minutes before the 8 hours post-infusion time and 15 minutes after the 8-hours post-infusion time). To do this, we applied to the data the code which is reported here (Fig. 6.5).

```
label.8hr=mean(label[inoculation.start.time>965&inoculation.start.time<995]

label.16hr=mean(label[inoculation.start.time>1445&inoculation.start.time<1475]

label.24hr=mean(label[inoculation.start.time>1925&inoculation.start.time<1955])
```

Figure 6.5 ***Code used for the second method****. The second method used for the data analysis was besed on the mean of a 30minutes period around the time choosen for the analysis.*

6.2 RESULTS

The final results of the analysis are presented as a scatterplot (Figure 6.6) and in Table 1. Although a trend is clear in the results, with a decrease in the percentage of the labelled carbon still incorporated in the

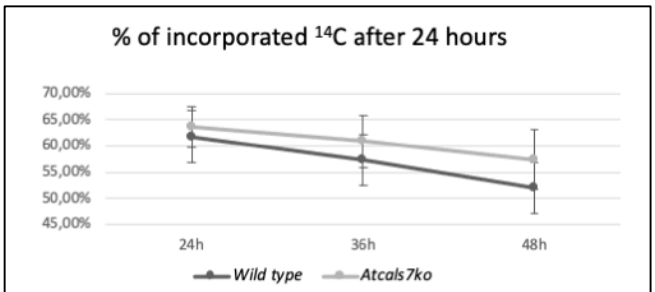

Time post injection	Wild type	Atcal7ko	st.dev WT	st.de Atcals7ko
24h	61,73%	63,63%	9,91%	7,70%
36h	57,34%	60,83%	9,55%	9,99%
48h	52,00%	57,40%	9,76%	11,51%

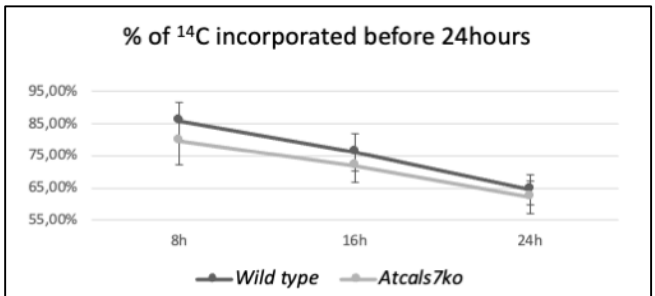

Time post injection	Wild type	Atcal7ko	st.dev WT	st.de Atcals7ko
8h	85,84%	79,49%	11,83%	14,48%
16h	76,21%	71,81%	11,55%	9,67%
24h	64,40%	62,00%	9,25%	10,04%

Figure 6.6 ***Labelled Carbon still present in the plants.*** *In the graph A data from the analysis of the first method are presented, in the graph B data analyzed with the second method are presented.*

plant, the high standard deviation did not allow for significant differences to appear between the time periods nor the mutation type. These preliminary results potentially indicate a higher ability of the mutant line to retain the labelled carbon, and so, as a consequence, a smaller transport capacity as previously reported by Barratt 2011 and our study (see chapter 4.2). The statistical analysis did not indicate significant differences among the results obtained, in particular no differences were shown between the two mutant lines. Comparing the two graphs obtained, it appears that the mutant line could have a slower decrease in the amount of the fixed carbon when compared to the wild type.

In conclusion this labelling method is useful to study *Arabidopsis* with the protocol that we previously described (materials and methods, chapter 4.2); the two applied methods for data analysis are suitable for our purposes, with the fitted function being more suitable for the end of the time course, while the method based on the mean is more suitable for the beginning of the analysis. The variability among the plants belonging to the same time and mutation groups was too high to have a significant result. In future experiments, more biological replicates will be necessary to obtain certain information about the decrease of the incorporated carbon over time.

7. CONCLUDING REMARKS

Despite the big progress obtained in the field, phloem tissue and in particular sieve-element biology still reserves many unclear traits. For example, actually it is not clear the function of many sieve-element structural components.

As reported before, sieve elements are unique cells, with features unshared with the cells belonging to the other tissues: they have not nucleus and lack in some vital functions, the organelle size is reduced and the shape modified. As in the case of mitochondria, the function is still object of study as well as the endoplasmic reticulum. For sure we know that sieve elements are a highway through which plants transfer chemical compounds, trophic substances and signaling-related molecules. This environment rich of sugars and poor in oxygen is the perfect habitat for phytoplasmas: phytoplasmas have, in fact, a high affinity with this tissue, in which they are able to replicate themselves and keep all the substances necessary for their life (as sugars). The difficulties related to the study of phytoplasmas are partially related with the lack of knowledge about the phloem: phytoplasmas are, in practice, unculturable (except some successful results) bacteria: in the future, more knowledge on the sieve element biology could provide important issues about this matter.

Among the sieve element structural components, filamentous phloem proteins are for many aspects, still mysterious. On the role of the phloem proteins, new insights have been reached in the last decades: the description of forisomes and the characterization of the sieve element occlusion (SEO) and sieve element occlusion-related (SEOR) genes lighted up them and allowed the creation of mutant lines suitable for *in vivo* functional study. Previous studies of our research group have demonstrated the possible role of the SEOR proteins in the phytoplasma-Arabidopsis interaction. With the experimental work described in this thesis we gave insight about the vast possibility of interaction of AtSEOR2 with the plant-defense system.

Another fundamental compound present in the sieve elements is callose: since a long time, callose has been considered as a key ‘product’ in the mechanical response of the infected plants against phytoplasmas, as long as some researchers, before the use of the molecular tools, proposed the aniline blue staining as suitable method to detect phytoplasma presence in the host sieve elements. The beginning of the molecular biology discarded this idea, but the role of the callose during phytoplasma infection remains uncontested. Sugars have a fundamental role in the stress-related signaling. Here we have investigated about the possible relations among callose and sugar metabolism during phytoplasma infection: little is still known about this topic and more study is required about the matter.

The last aspect that we took in consideration was about a possible role of synaptotagmin in phytoplasma infection, as already reported in other plant-pathogen interactions. Even if phytoplasmas are

"motile" inside the plant, the passive movement mechanism is pretty unknown: it has been reported about the role of the actin in the phytoplasma squeezing through the sieve pores, but, considering the role in the virus infection, a possible role following phytoplasma infection could be supposed.

With this thesis we attempted to give more knowledge about phytoplasma pathogens, focusing on their fine interaction with the sieve elements, their ideal habitat. The setting of novel experimental approaches, as the use of not-invasive techniques, the use of high-resolution microscopy integrated with the modern molecular biology tools, will be of fundamental importance in obtaining specific information about sieve-elements and the mechanisms regulating phytoplasma colonization. Knowledge will be surely useful also to approach other phloem-limited bacteria, which could represent further new threats for agricultural products worldwide.

8. ACKNOWLEDGMENT

To realize this study my major gratitude goes to my supervisor, Professor Rita Musetti that supported me, but even more, that pushed me when my motivation was coming down, giving me a reason to ask me always more and to reach my goals. Another important thank goes to P.A. Alberto Loschi: the big technical support that he gave me in obtaining plants and insects to start my experiments, is nothing compared to what he gave me from a human point of view. I am grate to PhDs Laura Pagliari and Sara Buoso: from them I learnt a lot concerning plant and insect rearing, infection and some of the techniques that I used during my PhD. With them I thank also all the Plant Pathology Research group of the University of Udine, for the help and for the time spent together in the lab, for the support and for the consideration that they always show in my regards.

Another part of my gratitude goes to my tutor in University of Florida, Professor Amit Levy and the whole Levy's Lab and my new friends: I was here during a pandemic: nevertheless the worst time choice, I felt like at home. They made everything possible to realize my experiments and to obtain the biggest amount of results.

At the end I want show my gratitude to my family my dad, my mom, Alessandro and Nora, that support me whatever bad idea I have, and to my new friends of the "Red wine night", something more of colleagues.

Finally, I want thank everyone that crossed my way, in each moment of my work because, even with negative answer, helped me to grow professionally a little bit more.

Everyone of the above-mentioned people contribute to me to realize in a different manner my work and I hope that, in a different manner, everyone will be proud of it.

9. List of abstracts presented at Conferences and Meetings

Jasmonates, salicylate and site-specific responses to phytoplasma infection in *Arabidopsis thaliana*

L. Pagliari[1], C. Bernardini[1], V. De Rosa[1], M. Martini[1], M. Almeida-Trapp[2], A. Mithöfer[2], R. Musetti[1]

[1]Department of Agricultural, Food, Environmental and Animal Sciences, University of Udine, via delle Scienze 206, I-33100 Udine, Italy; [2]Department of Bioorganic Chemistry, Max Planck Institute for Chemical Ecology, Hans-Knöll-Straße, 8 D-07745 Jena, Germany. E-mail: rita.musetti@uniud.it

Phytohormones are major actors in the sophisticated survival strategies developed in response to biotic and abiotic stresses. Several hormones take part to a complex signalling network, but jasmonate (JA) and salicylic acid (SA) play a crucial role. JA- and SA-mediated signalling pathways are mutually antagonistic. SA signalling is deemed to activate defences against biotrophic and hemibiotrophic pathogens, while JA is mainly though to induce resistance against necrotrophic pathogens. Phytoplasma are obligate biotrophic parasites associated with hundreds of diseases affecting many important crops. Considering the crude methods used to control phytoplasma diseases, a deeper knowledge on the defence mechanisms recruited by the plant to face phytoplasma invasion is required. In this work, phytohormone response was studied in *Arabidopsis thaliana* plants infected with '*Candidatus* Phytoplasma asteris' (strain Chrysantemum yellows, 16Sr-I). Phytohormone titre was measured in leaves of healthy and infected plants, in two tissues, the main-vein and the lamina. Differently from what was expected for biotrophic pathogens, phytohormone measurements on midrib tissue revealed an increase of JA and a decrease of SA levels. Since the veins are the sites where the direct interaction between phytoplasma and host occurs, this response could be interpreted as the "true" plant reaction to the infection. However, because separation of the midrib from the lamina might cause a wounding response, further experiments were performed to confirm a possible role of JA and/or SA upon phytoplasma infection and their ability to multiply. Thus, phytoplasma titre was measured in wild-type and Arabidopsis mutant lines, *dde2-2* and *sid2-2,* which are defective in JA and SA production, respectively.

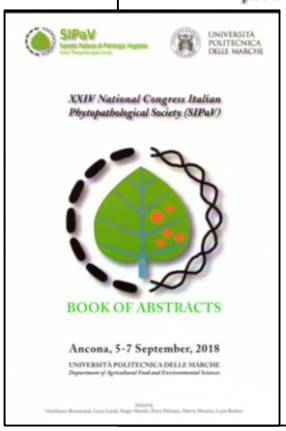

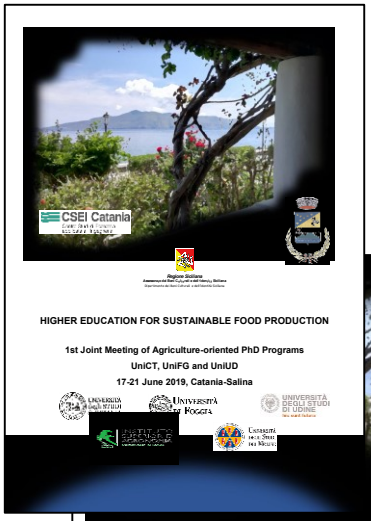

1st Joint Meeting of Agriculture-oriented PhD Programs

17-21 June 2019, Catania-Salina

...sponses in Arabidopsis sieve elements during phytoplasma infection

Chiara Bernardini - bernardini.chiara@spes.uniud.it

PhD in Agricultural Science and Biotechnology, University of Udine

Phytoplasmas are unculturable phloem-limited prokaryotes, discovered only 50 years ago and associated with numerous diseases affecting different crops. They are obligate pathogens with a very small genome, lacking many genes, indispensable for the autonomous life. The phytoplasma reliance on host metabolism causes severe alterations of plant cytology and physiology, resulting in the dramatic yield reduction. As direct methods to control phytoplasma diseases are not available so far, it is important to study in depth the strategies adopted by the plant to face phytoplasma infection. Sieve-elements are able to contrast the stress imposed by wounds or pathogen invasions, by the activation of Sieve Element Occlusion Related (SEOR) proteins or of callose, limiting the mass flow, and thus avoiding sugar losses or blocking pathogen spread. In *Arabidopsis thaliana* two SEOR genes concur to the formation of sieve-element protein filaments (*AtSEOR1* and *AtSEOR2*), through a heteromeric assemblage of the two proteins they encode. Our research group previously demonstrated that in the Arabidopsis line silencing Atseor1 gene (*Atseor1ko*), so expressing 'free' AtSEOR2 protein, phytoplasma titre is significantly lower in comparison with wild-type or *AtSeor2ko* plants. This led to speculate that AtSEOR2 protein, free from its bond with AtSEOR1, could act in plant-defence mechanism. Nevertheless, no explication of this phenomenon was provided. Aim of my research project is to investigate the possible involvement of AtSEOR2 protein in plant reactions against phytoplasmas. The effective defence responses occur precociously during plant-pathogen interaction, so we focused our investigations both in fully symptomatic plants at the late stage of infection and in plants yet asymptomatic, i.e. at an early stage of infection. As literature reports possible interferences of AtSEOR2 with the phytohormone signaling system, in particular with the indol-acetic acid (IAA) and abscisic acid (ABA) pathways, we quantify phytohormones in wild-type, *Atseor1ko*, *Atseor2ko* Arabidopsis lines following phytoplasma infection. Moreover, with the aim to evidence possible site-specific response we performed analyses using leaf laminae or midribs. Interestingly the amount of IAA and ABA are significantly higher in *Atseor1ko* plants compared to the other lines, starting from the first stage of infection, when macroscopical symptoms, sieve-element ultrastructural modifications and modulation of Atseor genes are not yet detectable in infected plants. The project will continue focusing on the second occlusion system activated in injuried sieve elements: the callose deposition at the sieve plates, regulated, in Arabidopsis, by the expression of the Callose synthase 7 (AtCas7) gene. The Arabidopsis mutant line *AtCas7ko* will be infected with phytoplasmas, with the aim to study not only the role of the long-term callose-mediated occlusion in infected Arabidopsis, but also to evidence variations in sugar metabolism, also related to the early plant defense signaling.

The author thanks Dr Axel Mithöfer and Dr Marilia Almeida-Trapp (Max Planck Institute for Chemical Ecology, Jena, Germany) for their collaboration in phytohormone quantification, Professor Domenico Bosco (University of Torino, Italy) for his advice on insect rearing and the transmission of CY phytoplasma. This work was supported by the Department of Agriculture, Food, Environment and Animal Sciences, University of Udine, Project Start up 2018.

IS-MPMI XVIII Congress
Abstracts of Poster Presentations

Abstracts submitted for presentation at IS-MPMI XVIII Congress in Glasgow, Scotland, July 14–18, 2019. The recommended format for citing congress abstracts, using the first abstract below as an example, is as follows:

Li, F., Upadhyaya, N., Schwessinger, B., Sperschneider, J., Matny, O., Raley, C., Miller, M. E., Silverstein, K., Nguyen-Phuc, H., Hirsch, C. D., Visser, B., Pretorius, Z. A., Steffenson, B., Dodds, P. N., and Figueroa, M. 2019. Contribution of a somatic hybridization event to the emergence of the Ug99 lineage of the wheat stem rust pathogen. (Abstr.) Molecular Plant-Microbe Interactions 32:S1.1. https://doi.org/10.1094/MPMI-32-10-S1.1

The abstracts are published as a supplement to *MPMI* for citation purposes. They were not reviewed by the *MPMI* Editorial Board and were not edited by the APS editorial staff.

https://doi.org/10.1094/MPMI-32-10-S1.1

Abscisic acid and auxin are early activated in Arabidopsis Atseor1ko mutants during phytoplasma infection

C. BERNARDINI (1), L. Pagliari (1), V. De Rosa (1), M. Almeida-Trapp (2), M. Martini (1), A. Mithofer (2), R. Musetti (1), (1) Dep. of Agricultural Food Environmental and Animal Sciences, University of Udine, Udine, Italy; (2) Dep. of Bioorganic Chemistry, Max Planck Institute for Chemical Ecology, Jena, Germany

Phytoplasmas are phloem-confined pathogens associated to several diseases of economically important plants. Plant response to the infection implies many physiological alterations, cytological modifications and modulation of global transcription and protein profile. We previously demonstrated that in Arabidopsis the absence of AtSEOR1 gene, involved in sieve-element filamentous protein formation in association with AtSEOR2, allowed the plant to face phytoplasma invasion more effectively. This led to speculate that AtSEOR2 protein, free from its bond with AtSEOR1, could act in defense mechanism. Nevertheless, no explication of this phenomenon was provided. In this study wild-type and *Atseor1ko* lines were analyzed at early and late infection stages, performing microscopic, molecular and physiological analyses to identify possible key aspects of phytoplasma-AtSEOR2-plant defense interactions. According to transmission electron microscope and gene expression analyses, at the first stage of the infection, sieve-element filamentous proteins are not involved in plant response to the phytoplasmas. On the other hand, stress-related phytohormones, measured in both leaf midribs and laminae through HPLC-MS/MS highlighted that site-specific auxin and abscisic acid response takes place precociously in the *Atseor1ko* plant infection site. Little is still known about the initial steps of the plant response against phytoplasma, but phytohormones seem to play a role in the first defense line.

Not only long-term sieve-element blockage against phytoplasmas: role(s) of callose in plant defence-mechanisms

C. Bernardini, L. Pagliari, S. Busso, A. Loschi, S. Santi, R. Musetti

Department of Agricultural, Food, Environmental and Animal Sciences, University of Udine, via delle Scienze, 206 I-33100 Udine, Italy. E-mail: rita.musetti@uniud.it

Phytoplasmas are uncultivable phloem-limited prokaryotes, affecting many crops of economic importance. Infection causes several modifications at cytological and physiological level, resulting in yield reduction. One of these modifications is the phloem plugging: several studies attested the importance of the sieve-element occlusion related (SEOR) proteins and callose, respectively in the brief- and long-term plugging of the sieve plates. Apart the role in the occlusion, callose has multiple biological functions: for example, it takes part in the processes of phloem maturation in intact plants, influencing the formation and development of the sieve-plate pores, so influencing the mass flow. The synthesis of callose requires several steps, so the existence of a callose synthase complex, interacting with different proteins, related to sucrose synthesis and metabolism, has been suggested. In a previous work, the anomalous deposition of callose in phytoplasma-infected phloem tissue and the altered modulation of two callose synthase genes have been described as only a small part of the all transcriptional modifications observed for the sucrose transport and metabolism following infection. With the aim to highlight the different roles of callose in phytoplasma-infected plants, especially those related to the plant early defense signaling, wild-type and AtCas7kn Arabidopsis plants were infected with phytoplasmas. Modifications at morphological and transcriptomic levels in the two lines were compared and discussed.

This work was founded by the University of Udine, Department of Agriculture, Food, Environment and Animal Sciences, Project Start-up PRID 2018.

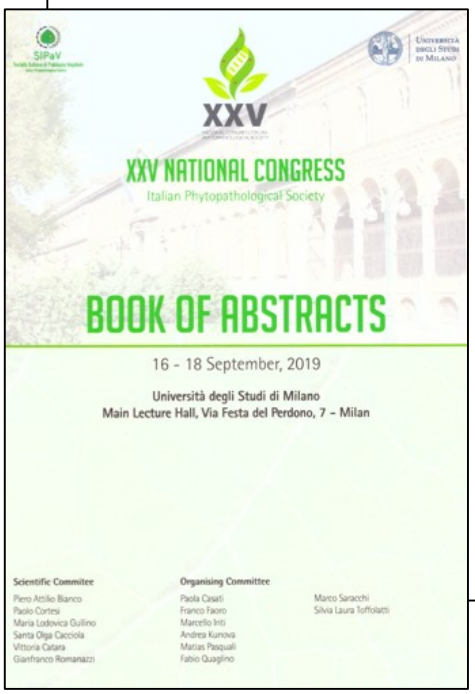

Callose response to phytoplasma infection: plugging at the sieve plate or something more?

CHIARA BERNARDINI, *RITA MUSETTI*

UNIVERSITY OF UDINE, BERNARDINI.CHIARA@SPES.UNIUD.IT

Phytoplasma are important pathogens affecting several crops but their relationships with the host plants are not completely known. Plants face phytoplasma in different ways, using chemical or mechanical barriers. Sieve-element occlusion-related (SEOR) proteins and callose are responsible for phloem plugging, respectively, as fast and slower responses to pathogens or injuries. While the mechanical role of sieve-element occlusion systems is well known from a long time, the other possible functions related with the physiological/molecular reply against phytoplasmas are not deeply investigated so far. The capability of AtSEOR2 phloem protein to modulate phytohormone-dependent defense pathways in *Arabidopsis thaliana* infected with "*Candidatus* Phytoplasma *asteris*" was recently demonstrated by our research group. The role of callose also ranges from physical occlusion of the sieve-pores to the activation of defence signaling. In fact, callose and sugars are in general used by plants as very efficient signaling molecules to fight against pathogens and pests. With the aim to highlight the different roles of callose in phytoplasma-infected plants, especially those related to the plant defense signaling, Arabidopsis wild-type and *Atcas7ko* lines were infected with phytoplasmas. Modifications at morphological, transcriptomic and metabolic levels in the two lines were compared and discussed in order to evidence that callose is more than a simple mechanical plugging of the sieve plates during phytoplasma-plant interaction.

2nd Joint meeting of Agriculture Oriented PhD programmes UniCT-UniFG-UniUD, 28th 30th September 2020, Udine, Italy